

# **The role of uncommon bacteria in catheter-associated urinary tract infections**

A Dissertation presented to the University of Porto for the degree of Doctor in Chemical and Biological Engineering by

Andreia Sofia Mateus Azevedo

Supervisor: Doctor Nuno F. Azevedo

Co-supervisor: Professor Luís F. Melo

Co-supervisor: Professor Jesper Wengel

Porto, July 2016



This work was financially supported by: Project POCI-01-0145-FEDER-006939 - Laboratory for Process Engineering, Environment, Biotechnology and Energy – LEPABE funded by FEDER funds through COMPETE2020 - Programa Operacional Competitividade e Internacionalização (POCI) – and by national funds through FCT - Fundação para a Ciência e a Tecnologia; DNA mimics Research Project PIC/IC/82815/2007 and PhD grant SFRH/BD/82663/2011.





*For my part I know nothing with any certainty,  
but the sight of the stars makes me dream.*



Vincent Van Gogh

---

*Ao meu pai, à minha mãe  
Aos meus avós*



## ACKNOWLEDGEMENTS

I would like to express my deepest thanks to all of those who gave me a constant scientific and personal cooperation, making possible the completion of this thesis.

Firstly, I am deeply grateful to my supervisor Professor Nuno Azevedo for his personal and scientific guidance, for his encouragement and kind advice throughout my PhD research. His suggestions and criticisms have been precious and beneficial to my future career.

I would also like to express my gratitude to my co-supervisor Professor Luís de Melo for giving me the opportunity of doing this PhD in his lab. I would also like to thank for the excellent guidance and support, as well as critical revisions of all my work.

Special thanks go to Carina Almeida for her patience and scientific support during these last four years. I will never forget your help and cheerfulness.

For their hospitality and support, I express my gratitude to Professor Jesper Wengel and Per Trolle Jorgensen. It was a pleasure to acquire some knowledge about nucleic acid chemistry in their lab at Nucleic Acid Center, University of Southern Denmark.

To all my BEL's colleagues for the all funny moments and friendly working atmosphere. In particular to Anabela for being always ready to help and to exchange ideas. Special thanks go to Joana Barros and Sílvia Fontenete for their friendship and their cheerfulness. I miss our happiness moments in the lab.

I would like to thank the support of the technicians Carla Ferreira, Sílvia Faia and Paula Pinheiro of the Department of Chemical Engineering at FEUP.

To my 'MS' friends, in particular to my girls, Andreia Bragança, Joana Marques and Raquel Queirós, for the all funny moments and good times that we always had together. Thank you for always being there. MS is like a family. You will always be in my heart!

I am deeply thankful to my family, especially to my mother, for supporting me in every way possible. Thanks for not letting me give up and for believing in me.

To you Filipe, my sweet love, thank you for your dedication, optimism and patience, even though large distances separated us at times. Thank you for being part of my life.

Last, but certainly not least, to my precious and bright star. I am thinking about you all the time.

*“I still get a lot of hugs, but none of them as warm as yours”. Dad, I miss you...*

*Andreia*



## ABSTRACT

Urinary tract infections (UTIs) account for more than 30% of nosocomial infections reported by acute care hospitals. Nearly all healthcare-associated UTIs are related to the insertion of a catheter in the urinary tract. Complications arising from catheter-associated urinary tract infections (CAUTIs) cause discomfort to the patient, prolong hospital stays, and increase costs and mortality.

CAUTIs originate from the colonization of urinary catheters by microorganisms. In fact, the surface of urinary catheter allows microorganisms to form intricate three-dimensional structures embedded in extracellular polymeric substances, commonly known as biofilm. Cells within biofilms are well-known for their increased resistance to antibiotic agents (when compared to planktonic cells) and also for their interactions with neighboring cells. While most studies have assessed single-species biofilms formation, it is now known that most biofilms involved in CAUTIs are polymicrobial communities, with pathogenic microorganisms (e.g. *Escherichia coli*, *Pseudomonas aeruginosa*, *Klebsiella pneumoniae*) and uncommon microorganisms (e.g. *Delftia tsuruhatensis*, *Achromobacter xylosoxidans*, *Burkholderia fungorum*) frequently co-inhabiting the same urinary catheter. However, little is known about the role that uncommon bacteria have on biofilm formation and infection outcome. This lack of knowledge affects CAUTIs management as uncommon bacteria action can, for instance, influence the rate at which pathogens adhere and grow, as well as, affect the overall biofilm resistance to antibiotics. Other relevant aspect is the understanding of factors that drive a single pathogenic bacterium to become prevalent in a polymicrobial community and subsequently cause infection.

Based on this evidence, understanding of polymicrobial biofilm dynamics in urinary catheters might be crucial to the development of novel strategies to manage CAUTIs. As such, this thesis had as the main objective to elucidate the role of uncommon bacteria in CAUTIs. To achieve this goal, single- and dual-species biofilms involving *E. coli*, the major cause of UTIs/CAUTIs, and two uncommon bacteria (*D. tsuruhatensis* and *A. xylosoxidans*) were formed and studied, in terms of the microbial composition and average fitness of *E. coli* over time, the spatial organization and the biofilm antimicrobial profile in conditions similar to those found on urinary catheters.

The experiments performed in 96-well plates revealed a greater ability of *E. coli* and uncommon bacteria to form biofilm communities in conditions mimicking the CAUTIs, whatever the pre-existing microbiota and the inoculum concentration (**Chapter 2**).

As the spatial localization of *E. coli* and uncommon bacteria when in polymicrobial biofilms might provide evidences on the type of interactions established, a new multiplex technique was developed and optimized for this purpose. This technique consisted on the coupling confocal microscopy with locked nucleic acid (LNA) and 2'-O-methyl RNA (2'OMe) fluorescence *in situ* hybridization (FISH). After development and optimization, LNA/2'OMe-FISH provided a clear discrimination of the species in three dimensions and the localization of the different biofilm populations. The transversal biofilm image showed that uncommon bacteria and *E. coli* were mixed, which is commonly associated with cooperation or synergetic interactions within biofilms (**Chapter 3**).

In silicone coupons, uncommon bacteria showed to have a positive impact on the fitness of *E. coli* and a greater tolerance to the antibiotic agents. In addition, after antibiotic treatment, *E. coli* was able to dominate the microbial consortia even being, in most cases, the most sensitive strain. These results might suggest that uncommon bacteria confer protection to the entire bacterial community (**Chapter 4**).

Finally, the co-culture of *E. coli* and *D. tsuruhatensis* in a flow cell reactor simulating the hydrodynamic conditions found in CAUTIs (shear strain rate of  $15 \text{ s}^{-1}$ ) suggested that *E. coli* and *D. tsuruhatensis* cooperate, when sharing the same environment, leading to the persistence of both bacteria in a stable and resistant microbial community (**Chapter 5**).

In summary, all these data show that, in fact, *E. coli* tendentially coexists with other bacteria instead of outcompeting and completely eliminating them. Uncommon bacteria were able to grow associated with the common pathogen *E. coli*, leading to a stable polymicrobial consortia that were in most situations more resistant to antibiotic agents. Therefore, it would be crucial to extend these types of studies to other pathogenic and uncommon bacteria in the context of CAUTIs. The ultimate goal is to encourage a personalized therapy to patients, targeting their individual microbiome, ensuring quality of care and minimizing the risk of mortality in patients with CAUTI.

## RESUMO

As infeções do trato urinário (UTIs) representam mais de 30% das infeções nosocomiais em unidades hospitalares. Praticamente todas as UTIs estão associadas à inserção de cateter no trato urinário. As complicações derivadas das infeções do trato urinário associadas a cateteres (CAUTIs) causam desconforto ao paciente, prolongam os períodos de hospitalização e aumentam os custos e a mortalidade.

As CAUTIs têm origem na colonização dos cateteres por microorganismos. De facto, a superfície dos cateteres permite que os microorganismos formem complexas estruturas tridimensionais envolvidas em substâncias poliméricas extracelulares, tipicamente chamadas de biofilmes. Está bem estabelecido que as células presentes nos biofilmes possuem uma maior resistência aos antibióticos (quando comparadas com as células em suspensão) e que também interagem com as células vizinhas. Embora a maioria dos estudos realizados se tenham debruçado no estudo de biofilmes formados por uma única espécie, é actualmente aceite que a maioria dos biofilmes envolvidos em CAUTIs são polimicrobianos, sendo que frequentemente microorganismos patogénicos (p.ex. *Escherichia coli*, *Pseudomonas aeruginosa*, *Klebsiella pneumoniae*) e microorganismos pouco comuns (p.ex. *Delftia tsuruhatensis*, *Achromobacter xylosoxidans*, *Burkholderia fungorum*) colonizem o mesmo cateter urinário. No entanto, pouco se sabe sobre o efeito que bactérias pouco comuns têm na formação do biofilme e na evolução da doença. Esta falta de informação afeta o tratamento das CAUTIs, uma vez que as bactérias pouco comuns podem, por exemplo, influenciar a taxa a que as bactérias patogénicas aderem e crescem, assim como influenciar a resistência dos biofilmes aos antibióticos. Outro aspecto relevante que pode influenciar o tratamento das CAUTIs prende-se com o conhecimento dos factores que levam uma espécie a predominar na comunidade polimicrobiana e a causar infeção.

Baseado nestas evidências, pensa-se que um melhor conhecimento da dinâmica de biofilmes polimicrobianos em cateteres urinários é crucial para desenvolver novas estratégias de controlo e tratamento de CAUTIs. Assim, a presente tese teve como principal objectivo elucidar o papel de bactérias pouco comuns nas CAUTIs. Para atingir este objectivo, biofilmes de uma única espécie e biofilmes polimicrobianos, constituídos tanto por *E. coli* (a principal causadora de UTIs/CAUTIs) como por

bactérias pouco comuns (*D. tsuruhatensis* and *A. xylosoxidans*), foram formados e estudados, em termos de composição microbiana e capacidade de adaptação da *E. coli* ao longo do tempo, organização espacial e perfil antimicrobiano do biofilme, em condições semelhantes às encontradas nos cateteres no interior do corpo humano.

Os ensaios experimentais realizados em microplacas de poliestireno de 96 poços demonstraram uma elevada capacidade da *E. coli* e das bactérias pouco comuns em formar biofilmes em condições semelhantes às encontradas nas CAUTIs, independentemente do microbioma pré-existente e da concentração inicial de inóculo (**Capítulo 2**).

Como a localização espacial da *E. coli* e das bactérias pouco comuns quando co-cultivadas pode fornecer evidências acerca das possíveis interações estabelecidas, uma nova técnica foi desenvolvida e otimizada para este propósito. Esta técnica consiste na combinação da análise de microscopia confocal com a hibridação *in situ* fluorescente (FISH) com sondas de *Locked nucleic acid* (LNA) e *2'-O-methyl RNA* (2'OMe). Após o desenvolvimento e otimização, a técnica de LNA/2'OMe-FISH permitiu uma discriminação tridimensional da localização das diferentes populações no biofilme. As imagens transversais mostraram que as bactérias pouco comuns e a *E. coli* se encontram co-agregadas que corresponde a uma organização espacial tipicamente associada a interações sinérgicas (**Capítulo 3**).

Em cupões de silicone, as bactérias pouco comuns mostraram ter um impacto positivo na capacidade de adaptação da *E. coli* e uma elevada tolerância a antibióticos. Adicionalmente, após o tratamento dos biofilmes com antibióticos, a *E. coli* predominou no consórcio microbiano apesar de ser na maioria dos casos a espécie mais sensível. Este resultado pode sugerir que as bactérias pouco comuns oferecem protecção à comunidade microbiana no seu todo (**Capítulo 4**).

Por último, o crescimento da *E. coli* e da *D. tsuruhatensis* numa célula escoamento que simulou as condições hidrodinâmicas encontradas nas CAUTIs (taxa de deformação com um valor de  $15 \text{ s}^{-1}$ ) sugeriu que ambas as bactérias cooperam metabolicamente quando partilham o mesmo espaço, havendo persistência de ambas numa comunidade microbiana estável e resistente (**Capítulo 5**).

Resumindo, os dados apresentados nesta tese mostram que, de facto, a *E. coli* tendencialmente coexiste com outras bactérias ao invés de competir e eliminá-las completamente. As bactérias pouco comuns foram capazes de crescer na presença da *E. coli*, levando à formação de consórcios polimicrobianos estáveis que na maioria das

situações apresentaram elevada resistência a antibióticos. Assim, poderá ser crucial expandir este estudo a outras bactérias patogénicas e pouco comuns no contexto das CAUTIs. O objectivo final é encorajar os clínicos a optarem por uma terapia personalizada tendo como alvo o microbioma individual de cada paciente, assegurando qualidade no tratamento e minimizando os riscos de mortalidade em pacientes com CAUTIs.



## STRUCTURE OF THE THESIS AND AIMS

The general aim of the work presented in this thesis is to investigate a potential role of uncommon bacteria over *E. coli* behavior in catheter-associated biofilm development, and hence understand how uncommon bacteria might affect catheter-associated urinary tract infections (CAUTIs).

This thesis is structured into six chapters. **Chapter 1** provides a state-of-the-art knowledge on basic and clinical aspects of CAUTIs, emphasizing the composition of microbial communities commonly found on the surface of urinary catheters, as well as aspects of biofilm formation. Also, a general outline of microbial interactions and how this might affect the outcome of CAUTIs is provided. To better study microbial interactions and spatial arrangement within biofilms a description of fluorescence *in situ* hybridization (FISH) is presented.

The potential interactions among *Escherichia coli* and two uncommon bacteria (*Delftia tsuruhatensis* and *Achromoabacter xylosoxidans*) found in catheter biofilm communities is undefined. Hence, in **Chapter 2** single- and dual-species biofilms encompassing uncommon bacteria and *E. coli* were evaluated under static conditions, in artificial urine medium (AUM), at 37° C, on the surface of 96-well microtiter plates. To better explain the potential interaction between *E. coli* and uncommon bacteria, additional features were analyzed, including growth rates of each bacterium in AUM, siderophore production by *E. coli* and uncommon bacteria, antimicrobial activity of biofilm supernatants and the influence of a pre-formed biofilm on the adhesion and biofilm formation of a second colonizer.

Afterwards, in order to study the spatial arrangement of the individual biofilm populations, a reliable alternative technique based on FISH was developed. Hence, in **Chapter 3**, a multiplex FISH procedure using locked nucleic acid and 2'-O-methyl RNA probes was developed, optimized and validated in a multiplex approach, for the *in situ* detection and localization of *E. coli* and uncommon bacteria within polymicrobial biofilms, without disturbing the biofilm structure.

In **Chapter 4**, studies on dual-species biofilms, involving *E. coli* and uncommon bacteria, were performed in silicone coupons. The other conditions were similar to those used in Chapter 2. Silicone was used in order to better mimic the surface of urinary catheters. The characterization of single- and dual-species biofilms in terms of the microbial composition over time, the average fitness of *E. coli*, the spatial organization and the biofilm antimicrobial profiles, was performed. In addition, the main focus of this Chapter was to evaluate the potential role of uncommon bacteria when antibacterial agents, commonly prescribed to treat CAUTIs, are used. For this, dual-species biofilms were quantified after exposure to an antibiotic concentration near or below the minimum biofilm eradication concentration to determine whether the exposure to these agents resulted in altered population balance.

The studies presented in Chapters 2 and 4 were performed under static conditions using microtiter plates or silicone coupons. While these biofilm systems allowed testing a large number of variables; inside the urinary catheter, biofilm formation is subjected to a flow of urine. As such, a flow cell reactor simulating the conditions found in a urinary catheter, where the biofilm was exposed to a shear rate of  $15 \text{ s}^{-1}$ , was used to investigate the microbial physiology of *E. coli* and *D. tsuruhatensis*, both in terms of the growth kinetics and the substrate uptake (lactic acid, urea, citric acid, creatinine and uric acid), individually and in consortium. These results will be presented in **Chapter 5**.

The last chapter, **Chapter 6**, presents the general conclusions of the work and proposes future research lines to improve knowledge in the field.

The present thesis reports the work performed at the BEL Group Lab at LEPABE (Laboratory for Process Engineering, Environment, Biotechnology and Energy), Faculty of Engineering (University of Porto) and at the Nucleic Acid Center at the Department of Physics, Chemistry and Pharmacy (University of Southern Denmark).



## TABLE OF CONTENTS

ACKNOWLEDGEMENTS.....	VII
ABSTRACT .....	IX
RESUMO.....	XI
STRUCTURE OF THE THESIS AND AIMS.....	XV
TABLE OF CONTENTS .....	XVII
LIST OF FIGURES .....	XXI
LIST OF TABLES.....	XXV
NOMENCLATURE.....	XXVII
SCIENTIFIC OUTPUTS .....	XXIX
<b>1 GENERAL INTRODUCTION .....</b>	<b>1</b>
<b>1.1 Biofilms on indwelling medical devices.....</b>	<b>3</b>
<b>1.2 Catheter-associated urinary tract infections.....</b>	<b>6</b>
1.2.1 Pathogenesis and virulence factors of uropathogenic biofilms.....	6
1.2.2 The microbiome diversity: traditional and uncommon microorganisms.....	9
1.2.3 Microbial ecology - interactions modes between microorganisms.....	12
1.2.4 Antibiotic resistance in CAUTI biofilms.....	19
<b>1.3 Relevance of spatial organization in microbial biofilms.....</b>	<b>21</b>
<b>1.4 Quantifying and locating biofilm populations in polymicrobial communities... </b>	<b>22</b>
1.4.1 Fluorescence in situ hybridization.....	25
<b>1.5 References.....</b>	<b>29</b>
<b>2 INTERACTIONS BETWEEN UNCOMMON BACTERIA AND <i>ESCHERICHIA COLI</i> IN</b>	
<b>CATHETER-ASSOCIATED URINARY TRACT BIOFILMS .....</b>	<b>45</b>
<b>2.1 Introduction.....</b>	<b>47</b>
<b>2.2 Material and methods.....</b>	<b>48</b>
2.2.1 Bacterial maintenance and inoculum preparation .....	48
2.2.2 Biofilm formation assays .....	49
2.2.3 Cultivability assesement.....	50
2.2.4 Biomass quantification by the CV assay.....	51
2.2.5 DAPI staining .....	52

2.2.6	<i>Determination of bacterial growth rates</i> .....	52
2.2.7	<i>Siderophores production</i> .....	52
2.2.8	<i>Antimicrobial activity of biofilm supernatants</i> .....	53
2.2.9	<i>Determination of the fitness and Malthusina parameter</i> .....	53
2.2.10	<i>Statistical analysis and data accommodation</i> .....	53
<b>2.3</b>	<b>Results and discussion</b> .....	<b>54</b>
2.3.1	<i>Single- and dual-species biofilm experiments</i> .....	54
2.3.2	<i>Antimicrobial activity of biofilm supernatants and siderophores production</i> .....	56
2.3.3	<i>Pre-colonization assays</i> .....	58
<b>2.4</b>	<b>Conclusions</b> .....	<b>60</b>
<b>2.5</b>	<b>References</b> .....	<b>63</b>
<b>2.6</b>	<b>Supplemental material</b> .....	<b>66</b>
<b>3</b>	<b>DETECTION AND DISCRIMINATION OF BIOFILM POPULATIONS USING LOCKED NUCLEIC ACID/2'-O-METHYL-RNA FLUORESCENCE <i>IN SITU</i> HYBRIDIZATION (LNA/2'OMe-FISH) .</b>	<b>77</b>
<b>3.1</b>	<b>Introduction</b> .....	<b>79</b>
<b>3.2</b>	<b>Material and methods</b> .....	<b>81</b>
3.2.1	<i>Culture of bacterial strains</i> .....	81
3.2.2	<i>Design and theoretical evaluation of oligonucleotide probes</i> .....	81
3.2.3	<i>Synthesis and purification of LNA/2'OMe oligonucleotide probes</i> .....	81
3.2.4	<i>Melting temperature analysis</i> .....	82
3.2.5	<i>FISH protocol development</i> .....	82
3.2.6	<i>Microscopic visualization and image quantification</i> .....	84
3.2.7	<i>LNA/2'OMe-FISH correlation with cultivability and PI staining</i> .....	84
3.2.8	<i>Spatial discrimination of biofilm population using LNA/2'OMe-FISH</i> .....	85
3.2.9	<i>Confocal laser scanning microscopy</i> .....	86
<b>3.3</b>	<b>Results and discussion</b> .....	<b>86</b>
3.3.1	<i>Analysis of LNA/2'OMe oligonucleotide probes</i> .....	87
3.3.2	<i>Thermodynamic parameters</i> .....	88
3.3.3	<i>Optimization of hybridization conditions</i> .....	90
3.3.4	<i>LNA/2'OMe-FISH validation</i> .....	94
<b>3.4</b>	<b>Conclusions</b> .....	<b>98</b>
<b>3.5</b>	<b>References</b> .....	<b>99</b>
<b>3.6</b>	<b>Supplemental material</b> .....	<b>103</b>
<b>4</b>	<b>IMPACT OF <i>DELFTIA TSURUHATENSIS</i> AND <i>ACHROMOBACTER XYLOSOXIDANS</i> ON <i>ESCHERICHIA COLI</i> DUAL-SPECIES BIOFILMS TREATED WITH ANTIBIOTIC AGENTS</b> .....	<b>105</b>
<b>4.1</b>	<b>Introduction</b> .....	<b>107</b>
<b>4.2</b>	<b>Material and methods</b> .....	<b>108</b>

4.2.1	<i>Culture conditions and preparation of inoculum</i> .....	108
4.2.2	<i>Single- and dual-species biofilm formation</i> .....	108
4.2.3	<i>CFU counts for quantification of biofilm cells</i> .....	109
4.2.4	<i>Antibiotic stock solutions</i> .....	109
4.2.5	<i>Antibiotic susceptibility testing</i> .....	110
4.2.6	<i>Determination of the species relative composition after antibiotic exposure</i> .....	110
4.2.7	<i>Effect of inoculum size on the species relative composition after antibiotic exposure</i> .....	111
4.2.8	<i>Spatial organization of biofilm populations</i> .....	111
4.2.9	<i>Statistical analysis</i> .....	111
<b>4.3</b>	<b>Results and discussion</b> .....	<b>111</b>
4.3.1	<i>Single- and dual-species biofilms growth and spatial organization of the species on silicone material</i> .....	112
4.3.2	<i>Antibiotic effects on the relative composition and spatial organization of biofilms formed by E. coli and uncommon bacteria</i> .....	114
<b>4.4</b>	<b>Conclusions</b> .....	<b>124</b>
<b>4.5</b>	<b>References</b> .....	<b>126</b>
<b>4.6</b>	<b>Supplemental material</b> .....	<b>129</b>
<b>5</b>	<b>AN IN VITRO MODEL OF CATHETER-ASSOCIATED URINARY TRACT INFECTIONS TO INVESTIGATE THE ROLE OF UNCOMMON BACTERIA ON THE <i>ESCHERICHIA COLI</i> MICROBIAL CONSORTIUM</b> .....	<b>133</b>
<b>5.1</b>	<b>Introduction</b> .....	<b>135</b>
<b>5.2</b>	<b>Material and methods</b> .....	<b>136</b>
5.2.1	<i>Strains and culture media</i> .....	136
5.2.2	<i>Determination of bacterial growth rates</i> .....	136
5.2.3	<i>Flow cell reactor setup</i> .....	136
5.2.4	<i>Flow cell reactor operation and biofilm formation</i> .....	138
5.2.5	<i>Sampling</i> .....	139
5.2.6	<i>Biofilm analysis</i> .....	139
5.2.7	<i>Fitness and Malthusian parameters calculation</i> .....	140
5.2.8	<i>Statistical analysis</i> .....	140
<b>5.3</b>	<b>Results and discussion</b> .....	<b>140</b>
5.3.1	<i>Characterization of E. coli and D. tsuruhatensis single-species biofilm growth under dynamic conditions</i> .....	141
5.3.2	<i>How uncommon bacterium might impact on E. coli population under dynamic conditions</i> 142	
5.3.3	<i>Substrate uptake by E. coli and D. tsuruhatensis in single- and dual-species biofilms</i> ....	145
<b>5.4</b>	<b>Conclusions</b> .....	<b>147</b>
<b>5.5</b>	<b>References</b> .....	<b>148</b>

5.6	Supplemental material .....	151
6	CONCLUDING REMARKS AND FUTURE PERSPECTIVES .....	153
6.1	Concluding remarks .....	155
6.2	Future perspectives.....	159
6.3	References.....	162

## LIST OF FIGURES

<b>Figure 1.1</b> - Pathogenesis of biofilm formation on urinary catheters during catheter-associated urinary tract infections development.....	8
<b>Figure 1.2</b> - Microbial diversity found in catheter biofilms. ....	11
<b>Figure 1.3</b> - Schematic illustration of potential bacterial interactions within biofilm communities.....	13
<b>Figure 1.4</b> - Steps of fluorescence <i>in situ</i> hybridization in a polymicrobial biofilm community. In the example presented in figure, two specific probes labeled with a different color allowed to identify and to distinguish the species involved in a mixed community after microscopy analysis.....	26
<b>Figure 1.5</b> - Structures of the monomers of some nucleic acid analogues. ....	27
<b>Figure 2.1</b> - Biofilm formation for single-species biofilms. Values for (a) total biomass and (b) cultivability .....	55
<b>Figure 2.2</b> - Relative fitness of <i>E. coli</i> in dual-species. Fitness of <i>E. coli</i> was determined in the presence of uncommon bacteria ( <i>D. tsuruhatensis</i> and <i>A. xylosoxidans</i> ) with simultaneous addition of the bacteria at the same initial concentration ( $10^8$ CFUs.ml <sup>-1</sup> ) .....	55
<b>Figure 2.3</b> - Screening for siderophores production using the chrome azurol S solid medium assay. ....	57
<b>Figure 2.4</b> - Values of the Malthusian parameter for pre-colonization experiments. The Malthusian parameter of the second microorganism added to a pre-formed biofilm was determined between time 0 and 48 hours.....	59
<b>Figure 2.5</b> - Schematic representation of the dual-species biofilm formation showing the main factors involved on the predominance and coexistence of <i>E. coli</i> with uncommon bacteria.....	62
<b>Figure S2.1</b> - Total cells and cultivability values for single-species biofilm of (a) <i>E. coli</i> , (b) <i>D. tsuruhatensis</i> and (c) <i>A. xylosoxidans</i> .....	66
<b>Figure S2.2</b> - Biofilm formation for dual-species biofilms, with simultaneous addition of the bacteria at the same concentration ( $10^8$ CFUs.ml <sup>-1</sup> ). For all combinations values for (a-b) total biomass and (c-f) cultivability, can be visualized .....	67
<b>Figure S2.3</b> - Total cells and cultivability values for (a) <i>E. coli</i> / <i>D. tsuruhatensis</i> and (b) <i>E. coli</i> / <i>A. xylosoxidans</i> dual-species biofilms (synchronized addition of both species).....	68

<b>Figure S2.4</b> - Effect of the initial inoculum concentration in single-species biofilms. Initial concentrations of $10^8$ CFUs.ml <sup>-1</sup> and $10^6$ CFUs.ml <sup>-1</sup> were evaluated for (a) <i>E. coli</i> , (b) <i>D. tsuruhatensis</i> and (c) <i>A. xylosoxidans</i> .....	69
<b>Figure S2.5</b> - Total biomass values for dual-species biofilms subjected to a pre-colonization step with the uncommon bacteria, followed by the addition of the <i>E. coli</i> . a) and b) present assays with inoculum concentrations of $10^8$ (uncommon bacteria) and $10^2$ ( <i>E. coli</i> ) CFUs.ml <sup>-1</sup> ; while c) and d) present inoculum concentrations of $10^2$ (uncommon bacteria) and $10^8$ ( <i>E. coli</i> ) CFUs.ml <sup>-1</sup> .....	70
<b>Figure S2.6</b> - Values for total biomass for dual-species pre-colonized with <i>E. coli</i> during 24h; followed by the addition of the uncommon bacteria. a) and b) present assays with inoculum concentrations of $10^8$ ( <i>E. coli</i> ) and $10^2$ (uncommon bacteria) CFUs.ml <sup>-1</sup> ; while c) and d) present inoculum concentrations of $10^2$ ( <i>E. coli</i> ) and $10^8$ (uncommon bacteria) CFUs.ml <sup>-1</sup> .....	71
<b>Figure S2.7</b> - Cultivability values for (a, c) <i>E. coli</i> / <i>D. tsuruhatensis</i> and (b, d) <i>E. coli</i> / <i>A. xylosoxidans</i> dual-species biofilms subjected to a pre-colonization step with uncommon bacteria ( $10^8$ CFUs.ml <sup>-1</sup> ), followed by the addition of the <i>E. coli</i> ( $10^2$ CFUs.ml <sup>-1</sup> ) .....	72
<b>Figure S2.8</b> - Cultivability values for (a, c) <i>E. coli</i> / <i>D. tsuruhatensis</i> and (b, d) <i>E. coli</i> / <i>A. xylosoxidans</i> dual-species biofilms pre-colonized with <i>E. coli</i> ( $10^8$ CFUs ml <sup>-1</sup> ) during 24h, followed by the addition of the uncommon bacteria ( $10^2$ CFUs ml <sup>-1</sup> ) .....	73
<b>Figure S2.9</b> - Cultivability values for (a, c) <i>E. coli</i> / <i>D. tsuruhatensis</i> and (b, d) <i>E. coli</i> / <i>A. xylosoxidans</i> dual-species biofilms subjected to a pre-colonization step by the uncommon bacteria ( $10^2$ CFUs ml <sup>-1</sup> ), followed by the addition of the <i>E. coli</i> ( $10^8$ CFUs ml <sup>-1</sup> ) .....	74
<b>Figure S2.10</b> - Cultivability values for (a, c) <i>E. coli</i> / <i>D. tsuruhatensis</i> and (b, d) <i>E. coli</i> / <i>A. xylosoxidans</i> dual-species biofilms pre-colonized with <i>E. coli</i> ( $10^2$ CFUs ml <sup>-1</sup> ) followed by the addition of the uncommon bacteria ( $10^8$ CFUs ml <sup>-1</sup> ) .....	75
<b>Figure 3.1</b> - Fluorescence intensity of <i>E. coli</i> , <i>D. tsuruhatensis</i> , <i>A. xylosoxidans</i> , and <i>B. fungorum</i> LNA/2'OMe probes .....	91
<b>Figure 3.2</b> - Epifluorescence microscopy images of a multiplex LNA/2'OMe-FISH assay for dual-species smears. ....	92
<b>Figure 3.3</b> - Comparison of the average fluorescence intensity of the selected LNA/2'OMe oligonucleotide probes obtained in standard smears (hybridization procedures performed in glass slides) and in suspension at 57 °C. ....	93
<b>Figure 3.4</b> - Evaluation of the <i>B. fungorum</i> growth curve by (a) CFU and LNA/2'OMe-FISH counts and by (b) O.D. and the resazurine assay.....	96
<b>Figure 3.5</b> - An example of LNA/2'OMe-FISH combined with CLSM analysis. CLSM images for (a) <i>B. fungorum</i> single-species biofilm and for (b) <i>E. coli</i> / <i>B. fungorum</i> dual-species biofilm,	

showing the localization of species in the biofilm formed in conditions mimicking the CAUTIs for 8 days on silicone coupons ..... 98

**Figure S3.1** - Representation of the linear regression equations and correlations values of theoretical melting temperature and RNA complement melting temperature for all LNA/2'OMe oligonucleotide probes. .... 103

**Figure S3.2** - Representation of the linear regression equations and correlations values of (a, c, e, g) LNA/2'OMe-FISH counts vs. CFU counts and (b, d, f, h) LNA/2'OMe-FISH counts vs. PI counts assessed in different physiological states for each species under study ..... 104

**Figure 4.1** - Single- and dual-species biofilm growth in silicone material. The three species were individually cultured or co-cultured at 37 °C, on silicone coupons, under static conditions ..... 113

**Figure 4.2** - Relative bacteria composition of the dual-species biofilms after antibiotic exposure. For each antibiotic, the (a) *E. coli* / *D. tsuruhatensis* and (b) *E. coli* / *A. xylosoxidans* 48 h dual-species biofilms were exposed to three different concentrations bellow the MBEC; then, the CFU counts were determined after 24 h of exposure. An initial inoculum concentration of  $10^5$  CFU.ml<sup>-1</sup> was used for these experiments ..... 117

**Figure 4.3** - Effect of a lower *D. tsuruhatensis* or *A. xylosoxidans* initial inoculum concentration ( $10^2$  CFU.ml<sup>-1</sup>) on the *E. coli* population after antibiotic exposure. For each antibiotic, the (a) *E. coli* / *D. tsuruhatensis* and (b) *E. coli* / *A. xylosoxidans* 48 h dual-species biofilms were exposed to three different concentrations bellow the MBEC, then, the CFU counts were determined after 24 h of exposure. An *E. coli* initial inoculum concentration of  $10^5$  CFU.ml<sup>-1</sup> was used for these experiments ..... 119

**Figure 4.4** - Effect of a lower *E. coli* initial inoculum concentration ( $10^2$  CFU.ml<sup>-1</sup>) on the relative bacteria composition of the dual-species biofilms after ampicillin and amoxocillin/alavulanic acid exposure. For each antibiotic, the (a) *E. coli* / *D. tsuruhatensis* and (b) *E. coli* / *A. xylosoxidans* 48 h dual-species biofilms were exposed to three different concentrations bellow the MBEC, then, the CFU counts were determined after 24 h of exposure. An initial inoculum concentration of  $10^5$  CFU.ml<sup>-1</sup> for *D. tsuruhatensis* and *A. xylosoxidans* was used for these experiments ..... 120

**Figure 4.5** - Spatial localization and structure of dual-species biofilms exposed to ampicillin. .... 121

**Figure 4.6** - Schematic representation of the hypothesis proposed in the present work to explain the predominance of a certain species when a dual-species biofilm is exposed to antibiotic ... 125

<b>Figure 5.1</b> - Schematic representation of the flow cell reactor.....	137
<b>Figure 5.2</b> - Formation of <i>E. coli</i> and <i>D. tsuruhatensis</i> single-species biofilms. (a) Cultivable cell values for biofilms in silicone coupons under dynamic conditions; (b) Comparison of....	142
<b>Figure 5.3</b> - Single- and dual-species biofilm growth in silicone material under dynamic conditions. (a) Cultivable cell values of each bacterium overtime; (b) Representation of the relative fitness of <i>E. coli</i> and <i>D. tsuruhatensis</i> ; (c) Images of LNA/2'OMe-FISH in combination with CLSM, showing the spatial organization of the <i>E. coli</i> / <i>D. tsuruhatensis</i> dual-species biofilm at (I) 16 h, (II) 48 h and (III) 72 h.....	144
<b>Figure 5.4</b> - The evolution of (a) lactic acid, (b) uric acid and (c) citric acid concentrations for <i>E. coli</i> , <i>D. tsuruhatensis</i> and <i>E. coli</i> / <i>D. tsuruhatensis</i> .....	146
<b>Figure 6.1</b> - Potential contribution of uncommon bacteria to a more stable polymicrobial biofilms development in CAUTIs .....	158



## LIST OF TABLES

<b>Table 1.1</b> - Microorganisms commonly found in indwelling medical devices-associated biofilm infections.....	4
<b>Table 1.2</b> - Type of ecological interactions in microbial communities based the effect on the fitness of the actor and recipient. ....	12
<b>Table 1.3</b> - Different types of potential microbial interactions occurring in the context of CAUTIs already described in the literature.....	18
<b>Table 3.1</b> - Sequence of LNA/2'OMe oligonucleotide probes synthesized in this study.....	81
<b>Table 3.2</b> - Theoretical sensitivity and specificity of each LNA/2'OMe oligonucleotide probe tested in this study. ....	88
<b>Table 3.3</b> - Theoretical melting temperature, Gibbs free energy and results of thermal denaturation experiments performed in urea buffer for each LNA/2'OMe oligonucleotide probe. ....	90
<b>Table 3.4</b> - Linear regression equations and Pearson correlations between LNA/2'OMe-FISH counts and CFU or PI counts for each species under study. ....	95
<b>Table 4.1</b> - MBEC values for <i>E. coli</i> , <i>D. tsuruhatensis</i> and <i>A. xylosoxidans</i> single- and dual-species biofilms, exposed to four relevant antibiotics. An initial inoculum concentration of $10^5$ CFU.ml <sup>-1</sup> was used for these experiments. ....	115
<b>Table 4.2</b> - Effect of a low <i>D. tsuruhatensis</i> or <i>A. xylosoxidans</i> initial inoculum concentration ( $10^2$ CFUs.ml <sup>-1</sup> ) on the <i>in vitro</i> susceptibility of the dual-species biofilms to four relevant antibiotics. ....	118
<b>Table S4.1</b> - CFU.cm <sup>-2</sup> counts for the <i>E. coli</i> / <i>D. tsuruhatensis</i> and <i>E. coli</i> / <i>A. xylosoxidans</i> 48 h dual-species biofilms exposed to three different concentrations bellow the MBEC. These counts were determined after 24 h of exposure. An initial inoculum concentration of $10^5$ CFU.ml <sup>-1</sup> for both species was used for these experiments.....	130
<b>Table S4.2</b> - The CFU.cm <sup>-2</sup> counts for the <i>E. coli</i> $10^5$ CFUs.ml <sup>-1</sup> / <i>D. tsuruhatensis</i> $10^2$ CFUs.ml <sup>-1</sup> and <i>E. coli</i> $10^5$ CFUs.ml <sup>-1</sup> / <i>A. xylosoxidans</i> $10^2$ CFUs.ml <sup>-1</sup> 48 h dual-species biofilms exposed to three different concentrations bellow the MBEC. These counts were determined after 24 h of exposure. ....	131

<b>Table S4.3</b> - The CFU.cm <sup>-2</sup> counts for the <i>E. coli</i> 10 <sup>2</sup> CFUs.ml <sup>-1</sup> / <i>D. tsuruhatensis</i> 10 <sup>5</sup> CFUs.ml <sup>-1</sup> and <i>E. coli</i> 10 <sup>2</sup> CFUs.ml <sup>-1</sup> / <i>A. xylosoxidans</i> 10 <sup>5</sup> CFUs.ml <sup>-1</sup> 48 h dual-species biofilms exposed to three different concentrations bellow the MBEC. These counts were determined after 24 h of exposure.....	132
<b>Table S4.4</b> - Effect of a low <i>E. coli</i> initial inoculum concentration (10 <sup>2</sup> CFUs.ml <sup>-1</sup> ) on the <i>in vitro</i> susceptibility of the dual-species biofilms to ampicillin and amoxicillin/clavulanic acid. ....	132
<b>Table S5.1</b> - Specifications of the flow cell reactor.....	151

## NOMENCLATURE

%	Percent
$\tau_w$	Shear stress (Pa)
°C	Celsius degrees
$\mu$	Fluid viscosity ( $\text{kg}\cdot\text{m}^{-1}\cdot\text{s}^{-1}$ )
$\mu\text{g}$	microgram
$\mu\text{l}$	microliter
$\mu\text{mol}$	micromol
2'OMe	2'-O-methyl RNA
$\dot{\gamma}$	Shear strain rate ( $\text{s}^{-1}$ )
$\Delta G^\circ$	Gibbs free energy change ( $\text{kcal}\cdot\text{mol}^{-1}$ )
$\lambda$	Wavelength (nm)
$\mu\text{m}$	micrometer
$\rho$	Fluid density ( $\text{kg}\cdot\text{m}^{-3}$ )
<b>AFU</b>	Arbitrary fluorescence units
<b>ANOVA</b>	One-Way analysis of variance
<b>AUM</b>	Artificial urine medium
<b>bp</b>	base pair
<b>CAUTIs</b>	Catheter-associated urinary tract infections
<b>CECT</b>	Spanish Type Culture Collection
<b>CFU</b>	Colony-forming units
<b>CLSM</b>	Confocal laser scanning microscopy
<b><math>\text{cm}^2</math></b>	square centimeter
<b>CTC</b>	5-cyano-2,3-ditolyt tetrazolium chloride
<b>CV</b>	Crystal violet
<b>CY3</b>	Cyanine 3
<b>DAPI</b>	4'-6-Diamidino-2-phenylindole
<b>DGGE</b>	Denaturant gradient gel electrophoresis
<b>DNA</b>	Deoxyribonucleic acid
<b>e.g.</b>	( <i>exempli gratia</i> ) for example
<b>EPS</b>	Extracellular polymeric substance
<b><i>et al.</i></b>	( <i>et alli</i> ) and others
<b>FAM</b>	6-FAM Fluorescein
<b>FISH</b>	Fluorescent <i>in situ</i> hybridization
<b>g</b>	gram
<b>g</b>	Relative centrifugal force
<b>GC</b>	Guanine-cytosine content
<b>GFP</b>	Green fluorescence protein

<b>h</b>	hour
<b>i.e.</b>	( <i>id est</i> ) That is
<b>IMDs</b>	Indwelling medical devices
<b>l</b>	liter
<b>LNA</b>	Locked nucleic acid
<b>Log</b>	logarithm with base 10
<b>LSU</b>	Large subunit
<b>M</b>	Molar
<b>MBEC</b>	Minimum biofilm eradication concentration
<b>mg</b>	milligram
<b>min</b>	minutes
<b>ml</b>	milliliter
<b>mM</b>	millimolar
<b>mm</b>	millimeter
<b>mmol</b>	millimole
<b>NaCl</b>	Sodium chloride
<b>nm</b>	nanometer
<b>nM</b>	nanomolar
<b>m</b>	Malthusian parameter
<b>O.D.</b>	Optical density
<b><i>p</i></b>	Statistical significance level
<b>PCR</b>	Polymerase chain reaction
<b>pH</b>	potential hydrogen
<b>PI</b>	Propidium iodide
<b>PNA</b>	Peptide nucleic acid
<b>PS</b>	Phosphorothioate
<b>Re</b>	Reynolds number
<b>RNA</b>	Ribonucleic acid
<b>rpm</b>	Revolutions per minute
<b>rRNA</b>	ribosomal ribonucleic acid
<b><i>Q</i></b>	Flow rate
<b>s</b>	seconds
<b>SPSS</b>	Statistical Package for the Social Sciences
<b>TCA</b>	Citric acid cycle
<b>Tm</b>	Melting temperature
<b>TRFP</b>	Terminal restriction fragment length polymerase
<b>TSA</b>	Tryptic Soy Agar
<b>TSB</b>	Tryptic Soy Broth
<b>UTIs</b>	Urinary tract infections
<b>UV</b>	Ultraviolet
<b>v/v</b>	volume/volume percent
<b>vs.</b>	versus
<b><i>W<sub>D.tsuruhatensis</sub></i></b>	<i>D. tsuruhatensis</i> fitness
<b><i>W<sub>E. coli</sub></i></b>	<i>E. coli</i> fitness

### **Papers in peer reviewed journals**

**Andreia S. Azevedo**, Carina Almeida, Luís F. Melo, Nuno F. Azevedo. *Impact of polymicrobial biofilms in catheter-associated urinary tract infections*. (submitted) **(Chapter 1)**

Anália Lourenço, Tom Coenye, Darla M. Goeres, Gianfranco Donelli, **Andreia S. Azevedo**, Howard Ceri, Filipa L. Coelho, Hans-Curt Flemming, Talis Juhna, Susana P. Lopes, Rosário Oliveira, Antonio Oliver, Mark E. Shirtliff, Ana M. Sousa, Paul Stoodley, Maria Olivia Pereira, Nuno F. Azevedo. *Minimum information about a biofilm experiment (MIABiE): standards for reporting experiments and data on sessile microbial communities living at interfaces*. *Pathog Dis.* (2014) Apr 70(3):250-6. doi: [10.1111/2049-632X.12146](https://doi.org/10.1111/2049-632X.12146). **(Chapter 1)**

**Andreia S. Azevedo**, Carina Almeida, Luís F. Melo, Nuno F. Azevedo. *Interaction between atypical microorganisms and E. coli in catheter-associated urinary tract biofilms*. *Biofouling*. (2014) Aug 22:893-902. doi: [10.1080/08927014.2014.944173](https://doi.org/10.1080/08927014.2014.944173). **(Chapter 2)**

**Andreia S. Azevedo**, Carina Almeida, Bruno Pereira, Pedro Madureira, Jesper Wengel, Nuno F. Azevedo. *Detection and discrimination of biofilm populations using Locked nucleic acid/2'-O-methyl-RNA fluorescence in situ hybridization (LNA/2'OMe-FISH)*. *Biochem Eng J.* (2015) Dec; 104:64-73. doi:[10.1016/j.bej.2015.04.024](https://doi.org/10.1016/j.bej.2015.04.024). **(Chapter 3)**

**Andreia S. Azevedo**, Carina Almeida, Bruno Pereira, Luís F. Melo, Nuno F. Azevedo. *Impact of Delftia tsuruhatensis and Achromobacter xylosoxidans on Escherichia coli dual-species biofilms treated with antibiotic agents*. *Biofouling*. (2016) Mar;32(3):227-41. doi: [10.1080/08927014.2015.1124096](https://doi.org/10.1080/08927014.2015.1124096). **(Chapter 4)**

**Andreia S. Azevedo**, Carina Almeida, Luciana C. Gomes, Filipe J. Mergulhão, Luís F. Melo, Nuno F. Azevedo. *An in vitro model of catheter-associated urinary tract infections to investigate the role of uncommon bacteria on the Escherichia coli microbial consortium.* (submitted) (**Chapter 5**)

### **Book chapters**

**Andreia S. Azevedo**, Carina Almeida, Luís F. Melo, Nuno F. Azevedo. *Chapter: Chapter 8 - Role of E. coli on Catheter-Associated Urinary Tract infections.* Cerca N (2015), Impact of biofilms in health: a transcriptomics prespective, Universidade do Minho – DEB, Braga, Portugal, ISBN: 978-989-97478-6-9. (**Chapter 1**)

### **Other publications (oral and poster communications in conferences)**

#### **Oral communications:**

**Andreia S. Azevedo**, Bruno Pereira, Carina Almeida, Luís F. Melo, Jesper Wengel, Nuno F. Azevedo. *Detection and Discrimination of Microorganisms Using Locked Nucleic Acid - Fluorescence In Situ Hybridization (LNA-FISH).* CHEMPOR 2014. 10-12 September (2014). Porto.

**Andreia S. Azevedo**, Carina Almeida, Bruno Pereira, Pedro Madureira, Jesper Wengel, Nuno F. Azevedo. *Detection and discrimination of biofilms populations using Locked Nucleic Acid - Fluorescence In Situ Hybridization (LNA-FISH).* ESGB Meeting "Biofilm-based Healthcare-associated Infections: from Microbiology to Clinics". 9-10 October (2014). Rome.

**Andreia S. Azevedo**, Carina Almeida, Luís F. Melo, Nuno F. Azevedo. *Interaction between non-disease causing microorganism and E. coli in catheter-associated urinary tract biofilms.* Eurobiofilms 2013. 09-12 September 2013. Ghent.

**Poster communications:**

Sílvia Fontenete, **Andreia S. Azevedo**, Rui Rocha, Rita Santos, Carina Almeida, Laura Cerqueira, Nuno Guimarães, Nuno F. Azevedo. *Application of nucleic acid mimics in fluorescence in situ hybridization for the visualization of naturally-occurring biofilms with minimal disruption*. Biofilms 6. 11-13 May (2014). Vienna.

**Andreia S. Azevedo**, Carina Almeida, Luís F. Melo, Nuno F. Azevedo. *Interaction between non-disease causing microorganism and E. coli in catheter-associated urinary tract biofilms*. Eurobiofilms 2013. 09-12 September (2013). Ghent.

Lourenço A, **Andreia S. Azevedo**, Coelho FB, Pereira MO, Azevedo NF. *Biofilms data standardisation and interchange: first year experience of the BioOmics platform*. Biofilms 5. 10-12 December (2012). Paris.

**Andreia S. Azevedo**, Carina Almeida, Luís F. Melo, Nuno F. Azevedo. *Biofilm formation on a microtiter-plate using artificial urine to mimic catheter-associated urinary tract infections*. Biofilms 5. 10-12 December (2012). Paris.





# Chapter 1

---

## General introduction

---

In this chapter, a general overview about the pathophysiology of catheter-associated urinary tract infections will be provided, emphasizing the microbiome composition commonly found on biofilms formed on the surface of urinary catheters. Also, the main mechanisms involved in bacteria-bacteria interactions will be discussed, and few suggestions about new research therapies targeted to these microbial communities will be approached. Lastly, a general outline of molecular techniques and their potential to localize the microorganisms within a biofilm community will be provided. This type of techniques might improve the knowledge about the microbiome ecology of biofilm communities. Hence, fluorescent *in situ* hybridization will be focused in more detail, due to its usefulness in providing a spatial characterization of the microbial biofilms.

### **Part of the work presented in this chapter was based on the following publications:**

**Andreia S. Azevedo**, Carina Almeida, Luís F. Melo, Nuno F. Azevedo. *Chapter: Chapter 8 - Role of E. coli on Catheter-Associated Urinary Tract infections*. Cerca N (2015), Impact of biofilms in health: a transcriptomics perspective, Universidade do Minho – DEB, Braga, Portugal, ISBN: 978-989-97478-6-9.

Anália Lourenço, Tom Coenye, Darla M. Goeres, Gianfranco Donelli, **Andreia S. Azevedo**, Howard Ceri, Filipa L. Coelho, Hans-Curt Flemming, Talis Juhna, Susana P. Lopes, Rosário Oliveira, Antonio Oliver, Mark E. Shirtliff, Ana M. Sousa, Paul Stoodley, Maria Olivia Pereira, Nuno F. Azevedo. *Minimum information about a biofilm experiment (MIABiE): standards for reporting experiments and data on sessile microbial communities living at interfaces*. *Pathog Dis.* (2014) Apr 70(3):250-6. doi: [10.1111/2049-632X.12146](https://doi.org/10.1111/2049-632X.12146).



## 1.1 Biofilms on indwelling medical devices

The microorganisms found in diverse environments, including aquatic, soil, industrial, and clinical settings, are able to alter their state between a planktonic and sessile mode of life. Typically, more than 90% of microorganisms live in the sessile state, which is induced when the microorganisms are exposed to changing environmental conditions<sup>1</sup>. This can result in a microbial community, known as microbial biofilm, that involves one or more species of microorganisms adhered to an inert or living surface, enclosed in an extracellular polymeric substance (EPS) matrix containing nucleic acids, proteins and polysaccharides<sup>2, 3</sup>. The ecological advantages of microorganisms in forming biofilms include protection from hostile environmental stimulus (e.g. pH, chemical exposure, radiation, and phagocytosis), acquisition of biofilm-specific antibiotic-resistant phenotypes and expanded metabolic cooperation<sup>1, 3</sup>. In addition, individual cells embedded in microbial biofilms display an altered phenotype, which is associated with a reduced growth rate, higher tolerance to antimicrobial agents or to host defenses, altered expression of specific genes and secretion of molecules and virulence factors<sup>1, 4-7</sup>.

Microbial biofilms play an important role in about 80% of human microbial infections<sup>8, 9</sup>. Common human infectious diseases involving biofilm formation in body tissues include chronic airway infections in cystic fibrosis patients<sup>10</sup>, chronic otitis<sup>11</sup>, chronic sinusitis<sup>12</sup>, chronic (diabetes) wound infection<sup>13</sup>, periodontitis<sup>14</sup> and urinary tract infection (UTI)<sup>15</sup>. In addition, due to recent advances in medical science, indwelling medical devices (IMDs) have been widely used in hospitals which may result in high incidence of IMD-related infections involving biofilms<sup>16</sup>, such as intravenous catheters<sup>17</sup>, prosthetic heart valves<sup>18</sup>, urinary catheters<sup>19</sup>, orthopedic devices<sup>20</sup>, cardiac pacemakers<sup>21</sup>, intrauterine devices<sup>22</sup>, biliary tract stents<sup>23</sup>, breast implants<sup>24</sup>, contact lenses<sup>25</sup> and voice prosthesis<sup>26</sup>.

The surface of IMDs offers a favorable environment for the colonization and growth of a large number of microorganisms, with a predominance of Gram-negative and Gram-positive bacterial species, as shown in Table 1.1. The source of these microorganisms might be the skin of hospitalized patients or health-care workers and the hospital environment<sup>27</sup>.

**Table 1.1** - Microorganisms commonly found in indwelling medical devices-associated biofilm infections.

Indwelling medical devices	Prevalent causative microorganisms	Refs.
Urinary catheters	<i>Escherichia coli</i> , <i>Proteus mirabilis</i> , <i>Enterococcus faecalis</i> , <i>Klebsiella pneumoniae</i> , <i>Pseudomonas aeruginosa</i>	19, 28, 29
Central venous catheter	Coagulase-negative <i>staphylococcus</i> , <i>Staphylococcus aureus</i> , <i>Enterococcus faecalis</i> , <i>P. aeruginosa</i> , <i>Candida albicans</i> , <i>K. pneumoniae</i>	2, 17, 30
Prosthetic heart valve	<i>S. aureus</i> , <i>Streptococcus</i> sp., coagulase-negative <i>staphylococcus</i> , <i>Enterococcus</i> sp.	18, 30
Orthopedic prosthesis	Staphylococci, <i>Streptococcus</i> sp., <i>Staphylococcus pneumoniae</i>	2, 20, 30
Contact lenses	<i>P. aeruginosa</i> , <i>S. aureus</i> , <i>Staphylococcus epidermidis</i> , <i>E. coli</i> , <i>Proteus</i> sp., <i>Candida</i> sp.	2, 25, 30, 31
Intrauterine devices	<i>S. epidermidis</i> , <i>S. aureus</i> , <i>C. albicans</i> , <i>Micrococcus</i> sp., <i>Lactobacillus plantarum</i> , <i>Enterococcus</i> sp., <i>Prevotella</i> sp., <i>E. coli</i>	22, 30, 32
Voice prosthesis	<i>C. albicans</i> , <i>Candida tropicalis</i> , <i>Candida glabrata</i> , <i>S. epidermidis</i> , <i>Streptococcus salivarius</i> , <i>P. aeruginosa</i> , <i>K. pneumoniae</i> , <i>S. aureus</i> , <i>Klebsiella oxytoca</i>	26, 33-35
Cardiac pacemakers	Coagulase-negative <i>staphylococcus</i> , <i>Streptococcus</i> sp., <i>S. aureus</i> , <i>S. epidermidis</i>	21, 36, 37
Biliary tract stents	<i>Enterococcus</i> sp., <i>E. coli</i> , <i>Klebsiella</i> sp., <i>Clostridium</i> sp., <i>Streptococcus</i> sp., <i>Candida</i> sp.	23, 38, 39
Breast implants	<i>E. coli</i> , <i>S. epidermidis</i> , <i>Propionibacterium acne</i> , coagulase-negative <i>staphylococcus</i>	24, 30, 40, 41

Biofilm-based infections have a great impact in public health. For instance, higher healthcare costs are related with these infections<sup>42</sup>, due to the prolonged stay in hospitals and the prolonged use of antimicrobials. Another worrying feature is that this type of infections are difficult to eradicate, due to the presence of polymicrobial communities involving multi-resistant pathogens<sup>43</sup>. In fact, polymicrobial biofilms are more resistant to antibiotic treatment than the corresponding single-species biofilms<sup>44-47</sup>

and corresponding planktonic cells<sup>48</sup>. In most cases, the only way to treat them is through the removal or substitution of the IMD<sup>42</sup>.

The European Center for Disease Prevention and Control reported that, annually, approximately 4.1 million patients are estimated to acquire a nosocomial infection (infections acquired in hospitals and other healthcare facilities) in European hospitals<sup>49</sup>. Among these infections, UTIs are a frequent nosocomial infection with approximately 150 million of new cases occurring each year worldwide<sup>50</sup>. The major risk factor for UTIs is the use of urinary catheters. It was reported that about 70-80 % of nosocomial infections are related with its use<sup>51, 52</sup>. The urinary catheter is inserted in patients through the urethra into the bladder to measure the urine output and to prevent/control urinary retention or incontinence<sup>53, 54</sup>. Despite careful aseptic management, the risk of developing catheter-associated urinary tract infection (CAUTI) increases 3-7 % with each day of catheterization<sup>28</sup>. Also, this risk is higher for women, older patients and diabetic patients<sup>28</sup>. It was estimated that approximately \$3790 is the minimum amount spent in treatment and diagnostic of each episode of CAUTI<sup>55</sup>, including antimicrobial therapy, increased length of hospitalization, physician visits and morbidity. In addition, it has been reported that patients with CAUTIs might develop other complications such as cystitis, pyelonephritis, Gram-negative bacteremia, prostatitis, epididymitis, endocarditis, vertebral osteomyelitis, septic arthritis, endophthalmitis and meningitis<sup>56</sup>.

The recent use of advanced molecular technologies has revealed the polymicrobial nature of UTIs/CAUTIs<sup>56-59</sup>. The microbial communities in CAUTIs can be shaped according to the host immune defenses of patient, prophylaxis and administered antibiotics. Additionally, the way how different microorganisms involved in a polymicrobial community interact (synergistically or antagonistically) will also have an impact on the microbial diversity, virulence and response to therapy. As such, more research about the microbiome composition, mechanisms of biofilm formation and of antimicrobial tolerance are required to better understand and treat these infections.

## 1.2 Catheter-associated urinary tract infections

### 1.2.1 Pathogenesis and virulence factors of uropathogenic biofilms

The presence of extensive microbial biofilms on the surface of urinary catheters removed from patients has long been documented (e.g.<sup>60</sup>). In fact, the constant replication of microorganisms with the continuous or intermittent flow of warm nutritious urine play a crucial role on establishment and development of a biofilm community on the surface of urinary catheters<sup>61</sup>. Additionally, the lumen of the urinary catheters is characterized by the absence of inherent defense mechanisms which makes the microorganism less prone, for example, to detachment by the urine flow, to phagocytosis and to the action of the antimicrobials agents<sup>62</sup>. Also, the normal defenses of the bladder might be weakened when the urinary catheter is used<sup>53</sup>.

As demonstrated in Figure 1.1-a, CAUTIs can develop in several ways. After the urinary catheter insertion, some urine components (proteins and other organic molecules, including magnesium and calcium ions) form a conditioning film along the urinary catheter surface. Such phenomenon alters the characteristics of the surface catheter and allows the adhesion of uropathogenic microorganisms<sup>63</sup> (microorganisms that colonize and persist in the urinary tract) (Figure 1.1-bI, II). The planktonic microorganisms adhere to the surface either by physical forces (e.g. van der Waals forces) or by specific adhesion molecules such as adhesins<sup>64, 65</sup> (Figure 1.1-bI). Flagella and pili are also a well-known group of virulence factors, expressed by uropathogenic microorganisms, which help the initial attachment of microorganisms to the uroepithelial cells and to the urinary catheter surface<sup>66, 67</sup>. Then, reversely attached microbial cells become strongly adhered to the surface (irreversible attachment)<sup>68</sup>. In the next stage, microorganisms firmly attached to the urinary catheter surface interact with each other<sup>65</sup> and start to produce polysaccharides<sup>61, 69, 70</sup> (Figure 1.1-bIII). EPS is mainly constituted by polysaccharides, proteins, lipids, nucleic acids (DNA and RNA); EPS protects the microorganisms within the biofilm, favors the mechanical stability of the biofilm and adhesion of the microorganisms to the surface<sup>71</sup> (Figure 1.1-bIII). The constant replication of microorganisms and EPS production results in the formation of three-dimensional structures with channels between them that are filled with urine and enable the transport of essential nutrients and oxygen to the microbial community<sup>61, 70, 72</sup> (Figure 1.1-bIV).

Lastly, microorganisms present within the biofilm community firmly adhered to the surface of urinary catheter can detach and return to the planktonic form<sup>68</sup>. At this stage, some microorganisms are able to produce enzymes that destabilize and breakdown the biofilm matrix; for example, *E. coli* produces *N*-acetyl-heparosan lyase<sup>73</sup>. In addition, if they are able to move against the urine flow, they colonize other sites of the urinary tract such as the bladder and the kidneys, and may even reach the bloodstream<sup>61, 70</sup> (Figure 1.1-bIV).

Once a mature biofilm is formed, the uropathogenic microorganisms have to further adapt to the conditions found on the urinary tract environment. For example, this is accomplished by the expression of genes responsible for the capsular polysaccharide and lipopolysaccharide synthesis, iron acquisition systems, antibiotics resistance mechanisms, nitrogen and oxygen levels adaptation<sup>74</sup>, and toxins production (e.g. hemolysins and cytotoxic necrotizing factor 1)<sup>70</sup>.

Nitrogen, iron and amino acids are essential nutrients for the survival of uropathogens during CAUTI development<sup>75, 76</sup>. However, iron concentration in urine is too low<sup>70, 77</sup>. To overcome this, uropathogens are able to upregulate genes encoding molecules capable to recruit the iron, called siderophores<sup>74, 78</sup>. According to this, the survival and growth of the uropathogenic microorganisms during the CAUTIs development, even at low iron concentrations, might be guaranteed when these microorganisms produce high concentrations of siderophores, or at least, when they are able to use the siderophores produced by neighboring microorganisms<sup>70, 77</sup>.

In addition, some bacteria including, *P. mirabilis*, *Proteus vulgaris* or *Providencia rettgeri*, convert urea, found at high concentrations in urine, to ammonia and carbon dioxide through the use of the urease enzyme<sup>5, 70</sup>. As an alternative, microorganisms such as the urease-negative *E. coli* use glutamine synthetase, an enzyme involved in glutamine synthesis and in ammonia metabolism<sup>74, 79</sup>. As a result of urea conversion into ammonia and carbon dioxide, the pH of the local environment becomes alkaline, which causes the precipitation of some minerals present in the urine, including calcium phosphate and magnesium ammonium phosphate<sup>80, 81</sup>. This represents a frequent problem associated with the formation of crystalline biofilms (as represented in Figure 1.1), which may have severe consequences, including trauma of the bladder and the urethral epithelia. Also, the deposition of the crystalline material on the surface of urinary catheters is frequently responsible for the blockage of the urine flow, which has consequences for patients such as incontinence problems<sup>61, 63, 82</sup>.

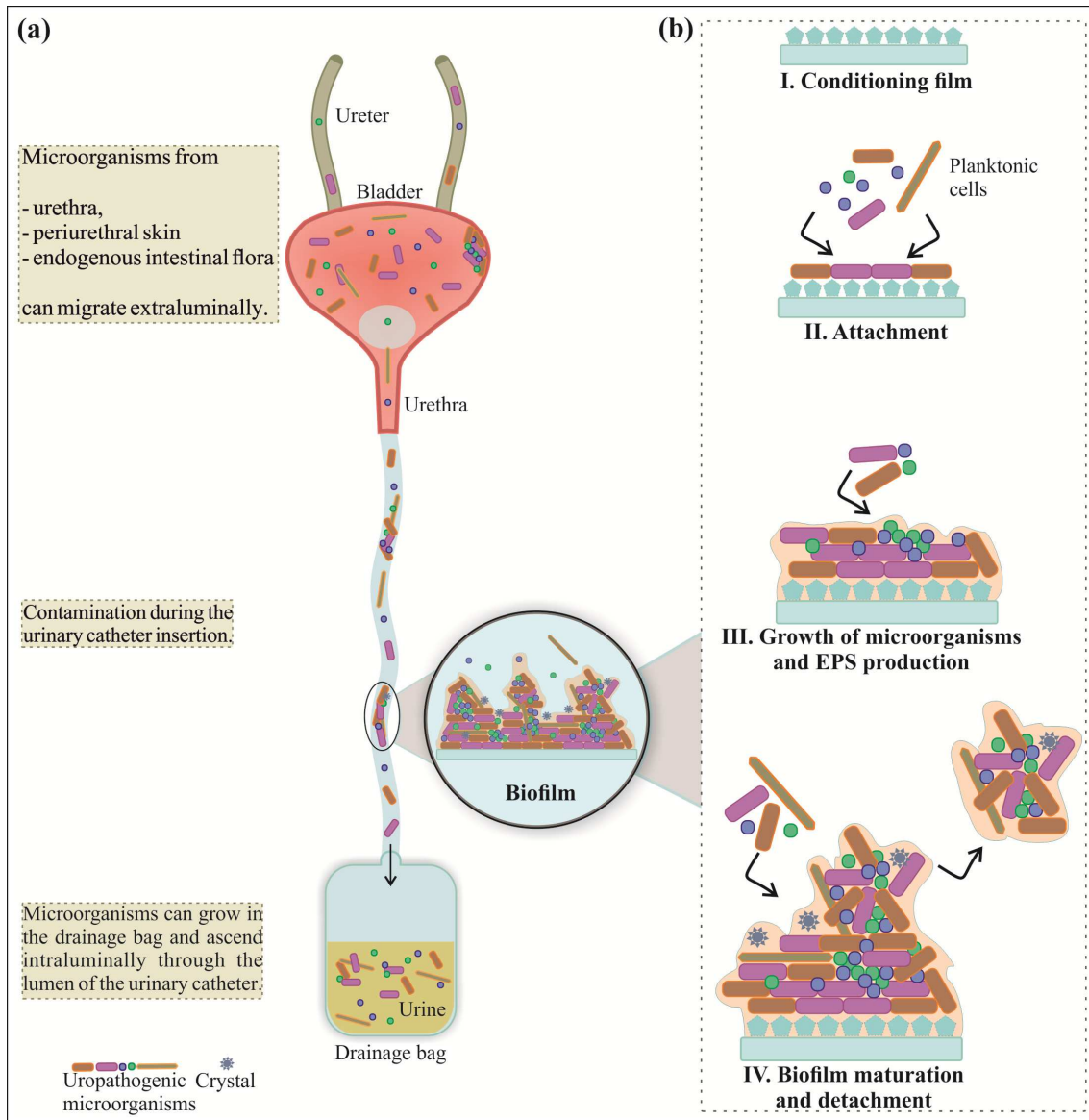


**Figure 1.1** - Pathogenesis of biofilm formation on urinary catheters during catheter-associated urinary tract infections development. (a) Catheter-associated urinary tract infections can develop in several ways: i) microorganisms present in the urethra, periurethral skin or endogenous intestinal flora can migrate around the catheter extraluminally; ii) microorganisms can grow in the interior of the drainage bag and ascend intraluminally through of the urinary catheter; iii) environmental and common skin microorganisms can be directly introduced at the time of the catheter insertion due to inadequately decontaminated equipment or improper practices of the healthcare workers<sup>83, 84</sup>; (b) Concerning CAUTIs, the first step involved in the formation of a catheter-associated biofilm is the deposition of a conditioning film on the surface of the urinary catheter which facilitate the binding of microorganisms (I, II). The next step involves the division of microorganisms and EPS production (III). Consequently, a developed biofilm with a 3-dimensional structure is formed, with spaces between the aggregates that are filled with fluid (urine).



**Figure 1.1 (continuation)** - Finally, microorganisms or aggregates of these microorganisms can detach from the mature biofilm, colonizing other sites (IV).

### ***1.2.2 The microbiome diversity: traditional and uncommon microorganisms***

In short-term catheterization (up to 7 days), the urinary catheter is frequently colonized by a single species. In long-term catheterization, the catheter is placed for several weeks and months in elderly and/or immunocompromised patients and, in this case, a polymicrobial infection is inevitable<sup>53, 70, 85, 86</sup>, with a dominance of Gram-negative bacteria<sup>87-89</sup>. Høla *et al.*<sup>90</sup> reported that approximately 30% of the biofilms in CAUTIs are colonized by three microorganisms, and, less frequently, two or four species are also found in these infections.

Traditionally, the diagnosis of CAUTIs is based on symptoms that patients present in combination with microbiological culture of urine. The urine collected from the catheter or from the bladder is subject to a culture on agar medium plates to detect the microorganisms involved in the infection<sup>88, 91</sup>. The infection is diagnosed when patients have a positive urine culture of  $\geq 10^5$  CFU.ml<sup>-1</sup> ( $\geq 10^4$  CFU.ml<sup>-1</sup> in children) in association with other symptoms (e.g. dysuria, urinary urgency, fever)<sup>92</sup>. However, the microbiological culture of urine from catheters might not reflect the microorganisms present in the biofilm formed on the surface of the catheter. In fact, microorganisms in biofilm have a different phenotype and behavior comparing with the planktonic microorganisms present in the urine. Typically, biofilm populations grow slowly or poorly on agar medium plates<sup>93</sup>. In addition, a viable but nonculturable state of some microorganisms and the antibiotic administration to prevent the infection might cause a false-negative result<sup>94</sup>. Thus, to improve the recovery and the quantification of the microorganisms attached to the urinary catheter, methodologies based on sonication have been recommended<sup>87</sup>. As the microorganisms attached extra- or intraluminally to the catheter can be different, a sonication step before the culture might allow the identification and quantification of microbial population located on both the outer and inner surface of the urinary catheter<sup>57</sup>. Then, the analysis of the microbial composition can be performed by microscopy, cultivation or culture-independent techniques<sup>95</sup>.

Recently, many culture-independent techniques have been widely used to identify and quantify the microbial diversity found on biofilm infection<sup>96</sup>. Previous studies<sup>97-104</sup> showed that some molecular techniques, including the denaturant gradient gel electrophoresis (DGGE), cloning, pyrosequencing, 16S ribosomal ribonucleic acid

(rRNA) gene polymerase chain reaction (PCR) for bacteria or 18S and 28S rRNA PCR for fungi and terminal restriction fragment length polymerase (TRFP) seem to be more reliable to assess the microbiota present in polymicrobial biofilms comparing with the conventional culture methods. Concerning microscopy analysis, there is a recent molecular approach known as fluorescent *in situ* hybridization (FISH) that has been a valuable technique to detect and quantify microorganisms (*in situ* or after a sonication step) (e.g.<sup>105-110</sup>). More details about this technique will be given below, in sub-section 1.4.1.

While each urinary catheter displays a unique biofilm community<sup>57</sup>, a list of the most prevalent microorganisms that are recurrently recovered from urinary catheters is presented in Figure 1.2. The European Centre for Disease Prevention and Control, in an annual epidemiological report from 2014, reported that the most frequently isolated microorganisms were *E. coli* (28%), *Candida* sp. (18%), *Enterococcus* sp. (17%), *P. aeruginosa* (14%) and *Klebsiella* sp. (8%) (Figure 1.2-a)<sup>111</sup>. Similar results were also reported by other studies, where a clear prevalence of *E. coli*, *P. aeruginosa*, *E. faecalis* and *P. mirabilis* was demonstrated<sup>90, 112, 113</sup>. The antimicrobial resistance of these microorganisms requires attention due to the continuous use of antimicrobial agents. In 2012, it was reported that the most common isolates from CAUTIs were resistant to, at least, one of the antimicrobial agents used in clinical practice<sup>111</sup>. Among the most prevalent microorganisms, 26.3% of *E. coli* isolates are resistant to third-generation cephalosporins; 26.6% of *P. aeruginosa* isolates are resistant to ceftazidime; and, 9.5% of *Enterococcus* sp. isolates are resistant to vancomycin<sup>111</sup>.

*E. coli*, the most well studied microorganism in CAUTIs, is a Gram-negative bacteria belonging to the family Enterobacteriaceae. The commensal *E. coli* strains normally inhabit the human intestine; while *E. coli* pathogenic strains are able to colonize and grow in the urinary tract (uropathogenic *E. coli*), causing UTIs<sup>70, 114</sup>. About 70-95% of UTIs are caused by *E. coli*<sup>115</sup>, and this microorganism is also present in the urine of 20-50% of catheterized patients<sup>89, 116</sup>. The proximity of the rectal area and the urinary tract facilitate *E. coli* dispersion<sup>70</sup>; but, it was reported that the presence of virulence factors such as  $\alpha$ -hemolysin, cytotoxic necrotizing factor I, lipopolysaccharide capsule, siderophore aerobactin and enterobactin, proteases and adhesive organelles are also responsible for the *E. coli* pathogenic nature during UTI and CAUTI development<sup>70, 117</sup>.

Other microorganisms, less commonly found on polymicrobial catheter biofilms, here designated as uncommon species, were also isolated and identified (Figure 1.2-b). The pathogenic potential of most of these microorganisms remains poorly studied. The presence of this type of microorganisms in biofilm-associated infections has been reported not only for CAUTIs (e.g.<sup>57, 87, 118</sup>) but also for cystic fibrosis (e.g.<sup>119, 120</sup>). For example, in a study performed by Franck and colleagues<sup>57</sup>, *Delftia tsuruhatensis* and *Achromobacter xylosoxidans* were found to be present in 25% of the urinary catheter-associated biofilms. For *Burkholderia fungorum* the prevalence value was 13%. These uncommon bacteria appear in CAUTIs in combination with well-established pathogenic bacteria such as *E. coli*, *K. pneumoniae* and *P. aeruginosa*<sup>57</sup>.

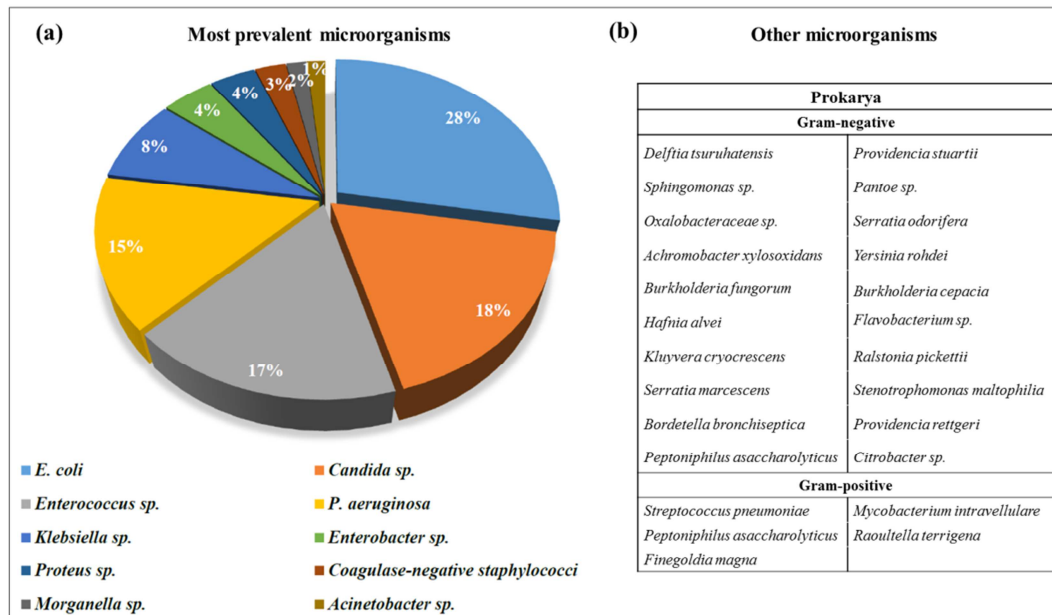


**Figure 1.2** - Microbial diversity found in catheter biofilms. (a) Percentages of the ten most frequently isolated microorganisms from catheter-associated urinary tract infections<sup>16</sup>; (b) List of some other microorganisms less frequently found in patients with catheter-associated urinary tract infections<sup>19, 90, 118, 121</sup>.

*B. fungorum*, a Gram-negative bacterium from Burkholderiaceae family, was firstly recovered in 2001 by Coeney *et al.*<sup>122</sup> from environmental, human and animal clinical samples. Concerning the human clinical samples, this bacterium was identified in the vaginal secretion of a pregnant woman<sup>122</sup>, the cerebrospinal fluid of a 66-year-old woman<sup>122</sup>, community-acquired bacteremia<sup>123</sup> and urinary catheter biofilms<sup>57</sup>.

*D. tsuruhatensis* is also a Gram-negative and rod-shaped bacterium from the Comamonadaceae family, isolated by Shigematsu *et al.*<sup>124</sup> from a domestic wastewater treatment plant. Human infections with *D. tsuruhatensis* have been reported in the medical literature, including a central venous catheter-related infection<sup>125</sup>, bacteremia in a patient with breast cancer<sup>126</sup>, and patients with CAUTIs<sup>57</sup>.

*A. xylosoxidans*, another Gram-negative bacteria, from the Alcaligenaceae family, was described in 1971 by Yabuuchi and Ohyama<sup>127</sup>, who had previously isolated it from patients with chronic, purulent otitis media. Human infections caused by *A. xylosoxidans* are frequently associated with hospital stays<sup>128</sup>, including UTIs<sup>129</sup>, CAUTIs<sup>57</sup>, bacteremia<sup>130-132</sup> and cystic fibrosis<sup>133, 134</sup>.

However, in all these cases, the microbial interactions between *B. fungorum*, *D. tsuruhatensis* and *A. xylosoxidans* and pathogenic bacteria, remain unclear. As little is known about the potential implication and contributions of these uncommon bacteria in nosocomial human infections, it would be crucial to investigate their behavior in the context of certain human infections, specifically in the context of CAUTIs.

### 1.2.3 Microbial ecology - interactions modes between microorganisms

Given that the outcome of a polymicrobial infection depends on how microbial communities interact, the research community rapidly recognized the urgency to study polymicrobial biofilms in order to understand the precise ways in which this interaction occurs. Based on the fitness consequences on the microorganisms, six different modes of interactions in microbial communities are presented in the literature: mutualism, commensalism, parasitism or predation, competition, amensalism and neutralism (Table 1.2)<sup>135</sup>.

**Table 1.2** - Type of ecological interactions in microbial communities based the effect on the fitness of the actor and recipient. Adapted from<sup>135</sup>.

		Species 2		
		+	-	0
Species 1	+	Mutualism +/+	Parasitism or predation +/-	Commensalism +/0
	-	Parasitism or predation -/+	Competition -/-	Amensalism -/0
	0	Commensalism 0/+	Amensalism 0/-	Neutralism 0/0

+ Positive (win); - Negative (loss); 0 Neutral.

When competitive or amensalistic, microbial interaction modes might be mediated by a large number of mechanisms including competition over nutrients and growth inhibition by toxins production (Figure 1.3-a); in case of mutualism, parasitism or predation and commensalism, interactions can be mediated by metabolic interactions, cell-cell signaling via quorum sensing, public good molecules secretion and increased antibiotic-resistance (Figure 1.3-b).

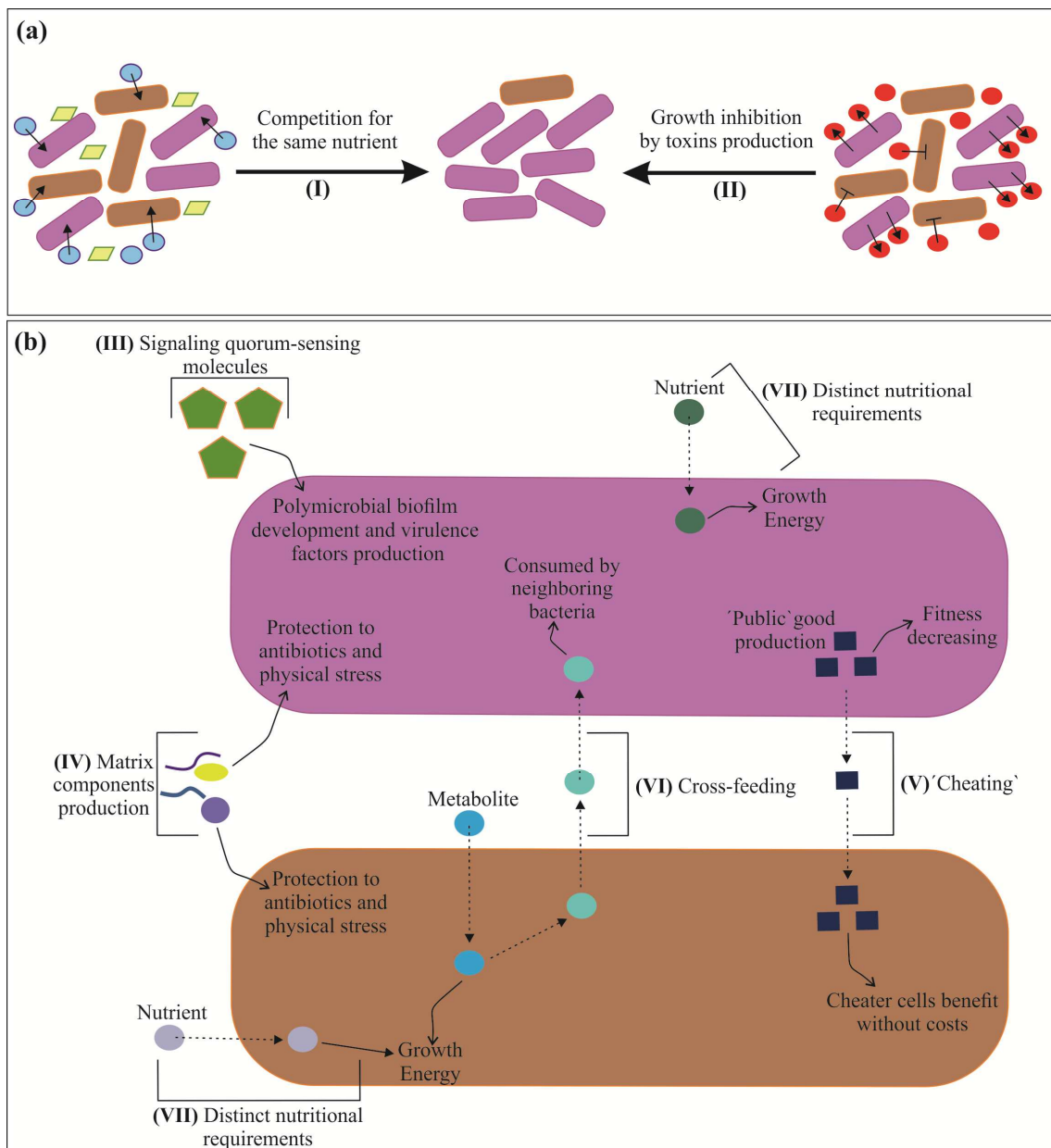


**Figure 1.3** - Schematic illustration of potential bacterial interactions within biofilm communities. (a) Competitive or amensalistic interactions among bacteria might involve a competition for nutrients (I) or production of toxins that kill the neighboring members (II),

respectively; (b) On the other hand, bacteria within biofilms might cooperate by producing cell-signaling molecules (III), matrix components (IV), public good metabolites (V) and cross-feeding metabolites (VI).

**Figure 1.3 (continuation)** - In addition, they might use different nutritional sources and in this case the fitness of one species is not affected by the other (VII). These interactions result in the growth of bacteria within biofilms and polymicrobial biofilm development with high resistance to stress conditions.

A behavior in which both microorganisms benefit from the presence of each other is designated by mutualism. This type of social behavior might occur when the microorganisms cooperate in order to increase the overall resistance to antimicrobial agents of all members involved in microbial community<sup>136</sup>. One example of mutualistic behavior might occur when two microorganisms exchange metabolic products, known as the cross-feeding phenomenon<sup>137</sup>. Metabolic cooperation is another example, observed when certain bacterial species modify the environmental conditions within biofilms (e.g. pH, oxygen concentration) to favor the growth of neighbors. For example, oxygen consumption by aerobic microorganisms could be beneficial for the growth of anaerobic microorganisms<sup>4</sup>.

In a commensalistic interaction, one microorganism benefits from the presence of other without affecting it. An example of commensalism happens when one microorganism metabolizes a compound produced by other member<sup>138</sup> or receives a plasmid carrying genes that might promote antibiotic resistance or virulence factors production<sup>139</sup>. On the other hand, in an amensalistic microbial interaction, a microorganism affects negatively the other without being affected by the interaction. An example of this microbial competition is bacteriocins production<sup>140</sup>. Bacteriocins are molecules that when secreted kill the other members of the microbial community<sup>141</sup>.

A competition relationship is a type of antagonistic interaction in which microorganisms occupy the same niche and compete for nutrients and physical resources<sup>135, 138, 142, 143</sup>. However, there are situations in which microorganisms co-inhabit the same environment without interaction (neutralism). For instance, microorganisms might share the same space, but have different nutritional requirements. Thus, the microorganisms live together without any beneficial or harmful effect from each other<sup>135</sup>.

The predation or parasitism are other type of microbial interactions, where an increase of fitness of one member occurs at a cost of others<sup>144</sup>. In particular, secondary metabolites produced with a cost to microorganisms might be used by neighboring members (cheaters) of the biofilm without any cost<sup>145</sup>. Examples of this type of molecules, commonly referred to as “public goods”, include quorum sensing signaling molecules<sup>146</sup>, iron-scavenging siderophores<sup>147-150</sup> and antibiotic-degradation enzymes<sup>151, 152</sup>. “Public goods” producers spend energy in its production and the cheaters exploit the “public good” without cooperating; hence, cheaters are able to outcompete the “public good” producers<sup>153</sup>. For example, a group of bacteria might be able to produce antibiotic-degrading enzymes that will help all microbial members resist to antibiotic agents. This phenomenon is crucial to the  $\beta$ -lactam antibiotics inactivation in which the presence of  $\beta$ -lactamases in the biofilms matrix might inactivate them<sup>151, 152, 154</sup>. On the other hand, the release of signaling molecules (autoinducers) *via* quorum sensing might be also considered another example of predation or parasitism, since its production involves a cost for cells that secrete the autoinducers<sup>153</sup>, and a benefit to the other members involved in the microbial community<sup>155-157</sup>. In polymicrobial biofilms, it has been demonstrated that a universal autoinducer of interspecies communication, AI2, used by Gram -negative and -positive bacteria, plays a crucial role on development of polymicrobial biofilms and production of certain virulence factors (e.g.<sup>158-161</sup>).

Briefly, considering that the polymicrobial biofilms exist in most human infections<sup>162</sup>, it is highly probable that the cooperation among microorganisms occur, enabling the coexistence of microorganisms<sup>163</sup>. In this way, inter-species cooperation increases the fitness and the resistance of overall biofilm community if any environmental conditions changes<sup>47, 164, 165</sup>.

Taking into account that the biofilms in urine and catheters of patients with CAUTIs are more commonly formed by polymicrobial communities, a better knowledge about the microbiome ecology and its implication on CAUTIs outcome will be crucial to a decreased mortality and morbidity associated with these infections. Few *in vivo* and *in vitro* studies have focused their research on microbial interactions in context of CAUTIs<sup>106, 116, 166-170</sup> (summarized in Table 1.3). The majority of the studies found in the literature have studied the microbial interactions between pathogenic bacteria (e.g. *E. coli*, *K. pneumoniae*, *P. mirabilis*, *P. aeruginosa*) in *in vitro* conditions similar to those found in CAUTIs. Those studies have used silicone coupons inserted in well tissue culture plates, 96-well microplates and flow cells at 37 °C to simulate the

body temperature. An important aspect in these studies is related with the use of artificial urine medium (AUM) that ensure the reproducibility of results. In fact, human urine varies significantly in terms of pH and composition according the type of food intake and the health of the individual<sup>171</sup>. *In vivo* studies using a rat model of CAUTI, in which urinary catheter were inserted in the bladder, have also been reported<sup>172-174</sup>. This approach reproduces the host environment and mimics the host immune system, but it depends on animal models and is not useful to high-throughput screening.

### 1.2.3.1 Reported interaction within CAUTI- associated mixed biofilms

As demonstrated in Table 1.3, in the context of CAUTIs, bacteria use different mechanisms to interact. These interactions are very diverse, as the same species present distinct behaviors when co-cultured with different bacteria. These experimental findings support the diversity of interactions described above.

For instance, the *in vitro* study performed by Cerqueira *et al.*<sup>106</sup> has shown that despite *E. coli* being the most prevalent causative agent of CAUTIs, it turned out to be the less well-adapted to dual-species biofilms, in contrast with *P. aeruginosa* that seemed to persist better within the microbial consortia. However, Croxall *et al.*<sup>167</sup> demonstrated that *E. coli* from polymicrobial UTI samples showed more resistance to antibiotics and are more invasive in *in vitro* epithelial cell infection studies. These are two good examples of *E. coli* populations being “shaped” by the complex consortium in which they are inserted.

The same happens for other common UTI-associated species. The virulence of *P. aeruginosa* and *S. aureus* is clearly stimulated when both bacteria are grown in a consortium<sup>166</sup>. But, when *P. aeruginosa* is observed together with *P. mirabilis* in urinary catheter biofilms, these two bacteria interact antagonistically<sup>116, 168</sup>.

The complexity of interactions is even higher when the factor “time” is taken into account. For instance, Macleod and Stickler<sup>116</sup> reported that any antagonistic effect of four other urinary tract pathogens (*E. cloacae*, *M. morgani*, *E. coli* and *K. pneumoniae*) against *P. mirabilis* in catheter biofilms is minimal and temporary. Also, co-infection of *P. mirabilis* with *E. cloacae* or *P. aeruginosa* significantly increased the time that catheters took to block<sup>116</sup>.

Recent data have also suggested the importance of studying bacterial metabolism during infection development to better characterize the microbial interactions<sup>76, 170</sup>. In fact, bacterial metabolism seems to contribute to the persistence



and pathogenesis of bacteria within biofilms as much as their virulence abilities<sup>76</sup>. For instance, the catabolism of amino acids present in urine generates tricarboxylic acid cycle (TCA; also known as citric acid cycle or Krebs cycle) intermediates and gluconeogenesis substrates, allowing uropathogenic *E. coli* to infect more efficiently the urinary tract<sup>76</sup>. The TCA cycle involves a series of chemical reactions used by all aerobic organisms to generate energy through the oxidation of acetyl-CoA derived from carbohydrates, fats and proteins into carbon dioxide and chemical energy in the form of guanosine triphosphate<sup>175</sup>. Gluconeogenesis is a metabolic pathway that results in the production of glucose from certain non-carbohydrate carbon substrates such as lactic acid, glycerol, glycine, serine, aspartate, and others<sup>176</sup>. Based on this, a recent study analyzed the central metabolism of *E. coli* and *P. mirabilis* to explain their ability of co-infect the same niche (urinary tract). Firstly, it could be assumed that both bacteria have the same nutritional preferences since they colonize the same environment; however, results showed that *E. coli* and *P. mirabilis* use different central metabolic pathways despite having access to the same nutrients in the urine (e.g. amino acids, peptides and urea). This suggests that co-infecting bacteria might not compete for nutrients, hence increasing their fitness during UTI development<sup>170</sup>.

The different behavior of complex communities associated to CAUTIs led scientists to speculate on their ability to control biofilm by interfering on their species composition; or on the possibility of anticipating the possible clinical outcome based on the biofilm composition. For instance, an *in vivo* study performed by Armbruster *et al.*<sup>169</sup> showed that the co-infection of *P. mirabilis* and *P. stuartii*, also a common colonizer of urinary catheters, resulted in a higher incidence of urolithiasis and bacteremia due to an increased activity of total urease<sup>169</sup>. This might indicate that the simultaneous presence of these species in CAUTI-associated biofilms represents an additional risk for the patient. If this proved to be true, those clinical situations should be handled with extra attention.

**Table 1.3** - Different types of potential microbial interactions occurring in the context of CAUTIs already described in the literature.

Pathogen	Experimental conditions	Microbial interaction	Explanation	Ref.
<i>E. coli</i> with <i>P. aeruginosa</i>	Six-well tissue culture plates containing silicone coupons immersed in AUM at 37 °C and 120 rpm	<i>P. aeruginosa</i> dominated over <i>E. coli</i> when co-cultured	<i>E. coli</i> presented lower growth rate (0.20 h <sup>-1</sup> ) when compared to <i>P. aeruginosa</i> (0.30 h <sup>-1</sup> ) The extracellular production of virulence factors by <i>P. aeruginosa</i> , such as N-acyl-L-homoserine lactones, can negatively regulate biofilm formation by <i>E. coli</i> in mixed biofilms.	106
<i>P. aeruginosa</i> with <i>S. aureus</i>	Glass flow cells supplied with a constant flow of AUM (30 ml.h <sup>-1</sup> ) at 37 °C	Virulence of <i>P. aeruginosa</i> and <i>S. aureus</i> was stimulated when both bacteria grown in consortium	Production of <i>P. aeruginosa</i> exotoxin A was increased nearly 2000-fold when <i>P. aeruginosa</i> and <i>S. aureus</i> were grown in a mixed biofilm.	166
<i>P. mirabilis</i> with <i>M. morgani</i> , <i>K. pneumoniae</i> , <i>E. coli</i> , <i>E. cloacae</i> or <i>P. aeruginosa</i>	Bladder model constituted by a glass chamber maintained at 37 °C. Silicone catheters were inserted into the chamber. The catheter retention balloons were inflated with 10 ml sterile water and the catheters were connected to drainage bags. Sterile AUM was pumped into the chambers	Impact on the ability of <i>P. mirabilis</i> to encrust and block urinary catheters	Co-infection of <i>P. mirabilis</i> with <i>M. morgani</i> , <i>K. pneumoniae</i> or <i>E. coli</i> had no effect on the ability of <i>P. mirabilis</i> to encrust and block catheters. Co-infection with <i>E. cloacae</i> or <i>P. aeruginosa</i> significantly increased the time that catheters took to block. A pre-inoculation with <i>E. cloacae</i> , <i>M. morgani</i> , <i>K. pneumoniae</i> or <i>E. coli</i> significantly delayed catheter blockage. However, <i>P. mirabilis</i> was able to colonize the biofilms and block the urinary catheters.	116
<i>P. mirabilis</i> with <i>P. stuartii</i>	Mice were inoculated with 50 µL of a 1:1 mixture of both bacteria	High incidence of urolithiasis and bacteremia	Total urease activity was increased during co-culture. A synergistic induction of urease activity might explain in part the high incidence of <i>P. mirabilis</i> and <i>P. stuartii</i> in polymicrobial CAUTIs.	169
<i>P. mirabilis</i> with <i>P. aeruginosa</i>	96-well microplates in human urine, at 37 °C with 100 rpm	Antagonistic interaction between <i>P. aeruginosa</i> and <i>P. mirabilis</i>	The elimination of <i>P. aeruginosa</i> at 72 h was probably due to the increase of pH between 48 and 72 h as a result of <i>P. mirabilis</i> urease activity.	168
<i>E. coli</i> with <i>P. mirabilis</i>	Mouse model of ascending UTI	<i>E. coli</i> and <i>P. mirabilis</i> do not directly compete for nutrients	<i>E. coli</i> and <i>P. mirabilis</i> have different central metabolic pathways despite have access to the same nutrients in the urine.	170

Altogether, these studies have focused on the ability of pathogenic bacteria commonly found on biofilm catheters to change their behavior when living in a consortium. While all these studies have revealed some aspects of interactions and persistence displayed by known CAUTIs pathogens, the role of uncommon bacteria on CAUTIs development or the interactions between uncommon bacteria and CAUTIs-associated pathogenic bacteria is yet to be described. In the literature, there are already some indications about the possible contributions of uncommon microorganisms on the pathophysiology and on the antimicrobial susceptibility pattern of biofilms associated with cystic fibrosis<sup>177, 178</sup>. Recently, Lopes *et al.*<sup>178</sup> reported that two uncommon bacteria, *Inquilinus limosus* and *Dolosigranulum pigrum*, interact synergistically with *P. aeruginosa*, forming stable dual-species biofilms with increased tolerance to antibiotics. These data suggested that uncommon bacteria might have a role on the physiology of pathogenic bacteria or even of the entire microbial community. As such, more studies are required to understand how the microorganisms adhered to a urinary catheter interact, and how these interactions influence the fitness of each individual species, the microbial community dynamics, the architecture and tolerance to antimicrobial agents.

#### **1.2.4 Antibiotic resistance in CAUTI biofilms**

Since antibiotic discovery, an abusive and inadequate use of antibiotics has dramatically increased the selective antibiotic pressure, leading to the appearance of multiple antibiotic-resistant bacteria<sup>179-181</sup>. Unfortunately, this substantially reduces the chance to treat a bacterial infection. Hence, the higher antibiotic resistance is a problematic concern of biofilm-associated infections in general. A variety of biofilm-associated resistance mechanisms are described in the literature. (1) The negative charge of EPS acts as a barrier that provide a slow or incomplete penetration of the antibiotic (with a positive charge)<sup>182, 183</sup>. Also, the presence of antibiotic degradative enzymes within the biofilm matrix can inactivate/or modify the antibiotic agents<sup>184</sup>. (2) Within biofilms there are gradients of nutrients and oxygen which are responsible for the existence of a heterogeneous population. The microorganisms that are subject to a depletion of oxygen and nutrients present a low metabolic activity (reduced growth rate) which is responsible to their higher resistance to antibiotics agents that are more efficient against actively-growing microorganisms<sup>183, 185</sup>. (3) Alterations in the biofilm phenotype, such as loss of viable bacteria and increase of biofilm biomass, might protect biofilm microorganisms against the action of  $\beta$ -lactam antibiotics<sup>186</sup>. (4)

Presence of “persister” cells that is defined as a sub population of biofilm cells that acquire a dormant and a highly protected state such as a spore-like form<sup>187, 188</sup>. (5) The horizontal gene transfer of antibiotic resistance genes also occurs within the biofilm community<sup>189-191</sup>. For instance,  $\beta$ -lactamase genes are localized on plasmids which can spread rapidly through the bacterial population. Also, *E. coli* can present efflux pump-coding genes on its plasmid, conferring a high-level resistance to various antimicrobial agents (e.g. tetracycline and ampicillin)<sup>189</sup>.

The antibiotic therapy directed to a particular bacterium can be unsuccessful if any of these mechanisms is activated, if recolonization occurs or if the elimination of one bacterium provides a favorable environment for other bacteria to recolonize<sup>142</sup>. Currently, the therapeutic strategies to prevent or treat CAUTIs involve the use of renally excreted antibiotics in combination with a periodic replacement of the urinary catheter. To minimize the chances of a new re-infection, it is recommended to replace the urinary catheter after 48 h of antibiotic treatment<sup>16</sup>.

Antibiotics (e.g. trimethoprim/sulfamethoxazole, nitrofurantoin, ciprofloxacin, gentamicin, amoxicillin/clavulanic acid) are administered during 7 days in patients who have relief of symptoms and 10-14 days for patients who do not respond to the antibiotic therapy<sup>88</sup>. However, it has been described that bacterial uropathogens isolated from patients with CAUTI or UTI revealed high resistance to some antibiotic agents used in clinical practice, such as ampicillin, trimethoprim-sulfamethoxazole, ciprofloxacin, amoxicillin/clavulanic acid, and others<sup>167, 192, 193</sup>. In addition, if the urinary catheter is not removed or replaced, re-infection can occur after the end of an antibiotic treatment. An alternative to antibiotic administration or urinary catheter removal could be the use of urinary catheters impregnated with antimicrobial agents (e.g. nitrofurazone, gentamicin, norfloxacin, nitrofur). However, the success of this new therapeutic strategy remains unclear<sup>194-196</sup>. Some studies have shown a reduced development of CAUTIs during short-term use, but other studies have not demonstrated an effective decrease in the incidence of CAUTIs<sup>197, 198</sup>. In fact, antimicrobial resistance might interfere with the success of this strategy<sup>199</sup>. Thus, new targets for the development or improvement of therapies or strategies to prevent CAUTIs should be investigated. In this respect, the polymicrobial nature of CAUTIs and the social interaction among microorganisms should be taken in consideration. These interactions may occur between pathogenic bacteria or even between pathogenic and uncommon bacteria by a range of mechanisms previously cited including quorum sensing signaling,

metabolite exchange, transfer of genetic material, etc. Consequently, these microbial interactions might impact biofilm formation and antibiotic resistance<sup>178, 200</sup>. In the context of CAUTIs, it should also be crucial to understand the mechanisms underlying the growth of uropathogenic and uncommon bacteria in urine. As referred above, *in vitro* studies have provided some insights about which metabolic pathways enable the microorganisms to adapt, survive and grow in human urine during a CAUTI or UTI development<sup>76, 170, 201-203</sup>. Afterwards, new ways to treat or prevent CAUTIs would be improved by disrupting the quorum-sensing, or even by using a urinary catheter able to scavenge essential nutrients within urine, or manipulating the composition of a microbial community through a non-pathogenic microorganism to prevent the adhesion of pathogens<sup>62, 70</sup>.

### 1.3 Relevance of spatial organization in microbial biofilms

The spatial distribution of microorganisms within biofilms has been shown to affect microbial interactions during biofilm development and virulence<sup>105, 106</sup>, particularly when microorganisms are in close proximity<sup>153, 204-206</sup>. In general, three forms of spatial structure of microbial biofilms have been described. (1) Each microorganism involved in microbial community forms separate microcolonies, side by side, which might be associated with noncommensal interactions among the microorganisms. For instance, the co-culture of *Burkholderia* sp. and *Pseudomonas* sp. in a flow cell showed that both bacteria form separate microcolonies, competing by the same nutrient resource<sup>207</sup>. (2) Microorganisms might be mixed together, showing a co-aggregation organization which is commonly associated with synergetic interactions<sup>162</sup>. (3) Lastly, a layered-biofilm structure might be found when one microorganism is found in the upper layers and the other(s) is found in the lower layer of the biofilm. This spatial organization might be: synergistic through a metabolic interaction, as seen when *Acinetobacter* sp. found in the upper layer converts the substrate into another compound to be used by *Pseudomonas putida* located in the lower layer<sup>208</sup>; or competitive as observed in a dual-species biofilm when *P. aeruginosa* was able to outgrow and cover *Agrobacterium tumefaciens*<sup>209</sup>.

Overall, the localization of microbial populations within biofilms depends on the environmental conditions and the function of each biofilm member, which in turn affects the way they interact. Hence, by analyzing the spatial localization of microorganisms, the microbial interactions of microorganisms and the possible mechanisms underlying the microbial ecology of communities might be partially elucidated.

## 1.4 Quantifying and locating biofilm populations in polymicrobial communities

*In vitro* (e.g. microtiter plate, Calgary biofilm device, flow cell, annular reactors, etc.) and *in vivo* (e.g. rats, rabbits and mice models) models have contributed to the current knowledge about biofilm physiology within biofilm-related infections. Microtiter plate-based systems are the most widely-used platforms to study bacterial attachment/biofilm development, biofilm antibiotic tolerance and resistance and efficiency of antibiofilm/antimicrobial products<sup>210</sup>. For instance, 96-well plates and silicone coupons placed in 6, 12 or 24-well plates have been used to mimic the conditions found in CAUTIs<sup>106, 168, 211</sup>. These systems offer several advantages: they are user-friendly methods<sup>212</sup>; cheap since they use small volume of reagents<sup>51, 213</sup>; allow the high throughput screening of several antibiotics (or other molecules) or the testing of large number of parameters simultaneously (e.g. multiple organisms, composition of growth medium, temperatures, shear stress, O<sub>2</sub> and CO<sub>2</sub>); coatings or impregnations of materials can also be evaluated<sup>214</sup>. However, during an experiment performed in a microtiter plate-based system, culture medium might have to be replaced at determined time points because nutrients become depleted and signaling molecules and toxins tend to accumulate over time<sup>212</sup>.

Another *in vitro* platform already used in CAUTIs studies is the flow cell system<sup>166</sup>. Flow cells are dynamic systems in which growth medium is (semi-) continuously added and waste-products are (semi-)continuously removed<sup>212</sup>. They are useful to evaluate biofilm formation, biofilm antibiotic tolerance and efficiency of antibiofilm/antimicrobial products over time<sup>210</sup>. An important advantage of this model is that it allows simulating the hydrodynamic (fluid flow) conditions found inside of

systems under study<sup>215</sup>. However, this model is costly, labor-intensive and expertise is needed<sup>210, 212</sup>. In this system, the biofilms are grown in coupons inserted inside of a flow cell and, consequently, only a single microorganism (or a community), antibiotic agent or other molecule, material or growth medium can be tested in an experiment<sup>212</sup>. In addition, these systems don't take into account the interplay among microorganisms and host defenses.

On the other hand, a variety of techniques can be used to evaluate the biofilm dynamics in *in vitro* or *in vivo* model systems. The conventional plate count is the most widely-used technique to determine the number of cultivable cells within biofilms after scraping and/or sonication (when biofilms are grown on the bottom and the walls of the microtiter plate) or after sonication or scraping and vortexing (when biofilms are grown on coupons)<sup>212, 216</sup>. Moreover, selective media for each microorganism might be used in order to assess the prevalence of the bacteria in mixed biofilms. The limitations of this method are related to the time it takes to perform an analysis, the existence of viable but nonculturable cells and to the need of biofilm cells detachment. The detachment process of the bacterial cells can be incomplete or can affect cell viability, compromising cells counts<sup>217, 218</sup>. Another technique extensively used in biofilms studies is the crystal violet staining that consists in staining the negatively charged bacteria (both living and dead cells) and polysaccharides of the EPS by the use of the crystal violet dye, allowing the quantification of total biofilm biomass<sup>219, 220</sup>. However, this method does not provide information about the number and diversity of living bacteria in the biofilm<sup>221</sup>.

In recent decades, the biofilm research field has been greatly revolutionized due to the improvement of the techniques used to locate or analyze the physiology of microorganisms in biofilms communities<sup>4</sup>. Most studies involve the use of Sanger sequencing, DGGE, PCR and real-time PCR to characterize the microbial composition and dynamics within biofilms directly in biofilm samples<sup>222-226</sup>. Other techniques based on the application of dyes or fluorochromes in combination with epifluorescence microscopy or confocal scanning laser microscopy (CLSM), including 5-cyano-2,3-ditolyt tetrazolium chloride (CTC) staining (for respiratory activity), 4',6-diamidino-2-phenylindole (DAPI), SYTO staining (for live and dead cells) and fluorescent lectin staining (for EPS biofilm), have been used to study the physiological activities in biofilms<sup>4, 105, 106, 227-230</sup>. However, it is important to mention that they might be inadequate techniques to spatially discriminate complex biofilm populations, due to their non-specific nature<sup>105</sup>.

Two molecular techniques, using bacterial fluorescent protein labeling and fluorescently-labeled nucleic acids, known as FISH, in combination with CLSM, have been used to study the spatial organization and changes of specific members of complex microbial populations (e.g.<sup>105, 106, 109, 231-234</sup>). The fluorescent protein labeling technique involves the development of strains engineered to be constitutively bioluminescent by the insertion of a gene coding for a fluorescent protein in the microorganism that is to be studied (e.g. green fluorescent protein)<sup>212, 235</sup>. This technique combined with epifluorescence microscopy or CLSM enables to observe the lab-grown biofilms at real time without destructing the biofilm (e.g.<sup>236-239</sup>). Also, it offers the possibility to label each microorganism involved in polymicrobial biofilms with a different colour<sup>233, 240-242</sup>, which is advantageous when the objective of research is to evaluate the type of interactions between populations<sup>234</sup>. However, this technique requires construction of genetically modified strains, and it is thus not applicable to natural biofilm samples<sup>109</sup>. In addition, the use of genetically modified organisms can affect the bacterial survival and metabolism and, consequently, the biofilm dynamics<sup>243</sup>. To overcome this, researchers have been using the FISH methodology that, despite the pre-fixation step, can be applied to natural biofilms without altering the microbial structure<sup>109, 244</sup>. Considering the importance of FISH in biofilm research, more details about this technique will be presented next.

Lastly, it should be mentioned that, as different methodology versions and biofilm growth devices are used in biofilm studies, data standardization and structuring is crucial to allow researchers to understand, replicate and assess studies at an inter-laboratory scale. This requires the definition of the minimum information that must be documented to ensure that an experiment on microbial biofilms is described unambiguously and comprehensively. Following this lead, a new standard initiative called the minimum information about a biofilm experiment (MIABiE, <http://miabie.org/index.php>) is preparing a set of guidelines for the documentation of biofilm experiments and data, namely the minimum information checklists. MIABiE does not intend to establish specific rules or provide standards on how biofilm experiments should be performed. Instead, MIABiE provides guidelines about the data to be recorded, considering the purpose of the study and the devices and techniques involved, in order for the procedure and the results to be easily reproducible and interpretable<sup>245</sup>. In addition, deposition of data on a common format is essential for sharing the results and permits other researchers to reproduce, analyze and compare



inter- or intra-laboratory biofilm experiments. At this moment, this is possible accessing the 'BiofOmics' on-line platform (<http://biofomics.org/>) where researchers are able to upload free-of-charge all the experimental details and/or download results obtained by other researchers<sup>246</sup>.

#### 1.4.1 Fluorescence *in situ* hybridization

FISH is a well-established molecular biology technique used for the identification/detection of microorganisms based on its phylogenetic markers at 16S or 23S rRNA sequences, particularly abundant and relatively stable in viable cells<sup>247</sup>. It is based on the hybridization of fluorescently-labeled oligonucleotides (commonly called probes) with a conserved rRNA sequence. These rRNA-directed oligonucleotide probes used in FISH are generally between 13-18 bp and are covalently labeled with a fluorescent dye molecule attached to the 3' or the 5'-end (e.g. cyanine, fluorescein, alexa fluor)<sup>244, 247</sup>. The design of probes can be performed *in silico* using public databases (Silva rRNA Database - <http://www.arb-silva.de/>; Ribosomal Database Project II - <http://rdp.cme.msu.edu/>) where the 16S or 23S ribosomal RNA sequences are available<sup>248, 249</sup>. During this step, it is important to take into account some criteria such as the GC content, the probe length, absence of self-complementary structures within the probe and high specificity (i.e., ensure that the probe will not detect other species) and sensitivity (i.e., ensure that the probe will detect all strains of the same species) for the target organism<sup>250, 251</sup>. In addition, the oligonucleotide probe affinity is defined as the overall Gibbs free energy change ( $\Delta G^\circ$ ) and is another important factor for the success of a FISH procedure. The  $\Delta G^\circ$  overall is a strong predictor of hybridization efficiency. A threshold  $\Delta G^\circ$  of  $-13 \text{ kcal.mol}^{-1}$  has been recommended for the design of DNA probes to guarantee an adequate hybridization efficiency<sup>252, 253</sup>.

To perform FISH in bacteria, four steps have to be performed: fixation/permeabilization, hybridization, washing and detection<sup>247</sup> (Figure 1.4). The fixation/permeabilization step is critical because it prevents cell lysis and nucleic acid degradation, and at the same time, it makes the cell wall permeable to the probes. For the permeabilization of bacterial cells, chemical fixatives including formalin, paraformaldehyde, methanol or ethanol<sup>254-257</sup> are frequently used; and, for Gram-positive bacteria a pre-treatment with lysozyme or other proteolytic enzymes is essential<sup>255, 256</sup>. During the hybridization step, at specific pH, temperature, ionic strength conditions and denaturing agents (formamide or urea) concentrations, the probe will

diffuse into the interior of the cell and hybridize with the target sequence<sup>258</sup>. The washing step allows to remove unbound probe, ensuring that the method will only detect the target bacteria<sup>257</sup>. Finally, if the hybridization has occurred, bacteria might be quantified by epifluorescence microscopy or fluorescence-activated flow cytometry (with a previous sonication step), or localized *in situ* by CLSM<sup>244</sup> (Figure 1.4).

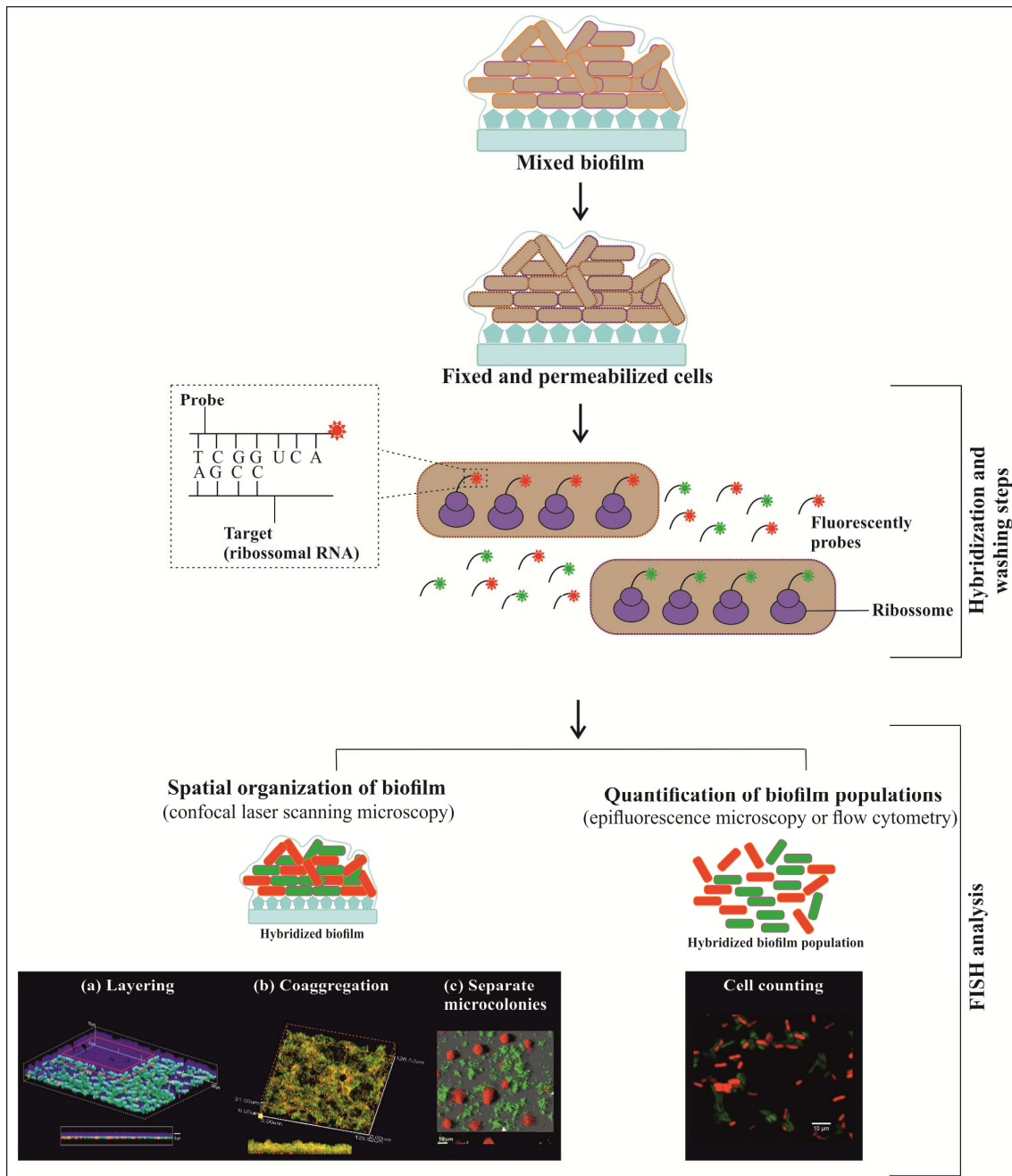


**Figure 1.4** - Steps of fluorescence *in situ* hybridization in a polymicrobial biofilm community. In the example presented in figure, two specific probes labeled with a different color allowed to identify and to distinguish the species involved in a mixed community after microscopy analysis.

**Figure 1.4 (continuation)** - First, the biofilm sample is fixed to stabilize the cells and permeabilize the cell membrane. Then, labelled probes are added and allowed to hybridize with the rRNA target. The excess probe is washed away. Finally, the sample is analyzed under epifluorescence microscopy or flow cytometry to quantify each member involving in the biofilm, or, under CLSM to determine the spatial distribution of biofilm populations. Species in polymicrobial biofilms can be organize in three different ways: (a) arranged in layers (confocal microscopy image reprinted with permission from<sup>105</sup>); (b) co-aggregation (confocal microscopy image reprinted with permission from<sup>259</sup>); (c) separate microcolonies (confocal microscopy image reprinted with permission from<sup>260</sup>).

#### 1.4.1.1 Nucleic acid mimics: locked nucleic acid and 2'-O-methyl-RNA

Labelled DNA probes were traditionally used in the FISH technique for the *in situ* identification of microorganisms. However, the use of DNA probes has some limitations related to cell permeability, toxicity, hybridization affinity and target site accessibility; consequently, a poor signal-to-noise ratio and a low specificity and sensitivity for target nucleic acids was observed<sup>244, 261-263</sup>. To overcome this, the scientific community started employing nucleic acid mimics. Nucleic acid mimics are expected to enhance affinity, selectivity and stability, to have increased resistance to nucleases and provide the ability to cross more rapidly biological membranes and the cell wall<sup>264</sup>. Nucleic acid mimics involve modifications or replacement of the nucleic acid base (e.g. C5-modified uridine nucleosides), phosphate backbones (when oxygen is replaced by sulfur in the backbone of analogues or derivatives which are called by phosphorothioates probes; PS probes) or the sugar-phosphate backbone. Some nucleic acid analogues with modifications in the sugar-phosphate backbone include the peptide nucleic acid (PNA), locked nucleic acid (LNA), and 2'-O-methyl-RNA (2'OMe) which have been known to improve the efficiency of the FISH technique (Figure 1.5)<sup>265-267</sup>.

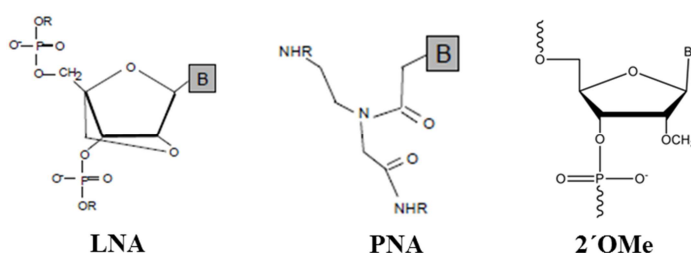


**Figure 1.5** - Structures of the monomers of some nucleic acid analogues.

LNA was first synthesized by the Imanishi (1997)<sup>268</sup> and Wengel groups (1998)<sup>269</sup>. LNA is a synthetic RNA derivative where the 2'-oxygen and the 4'-carbon atoms are connected via a methylene bridge<sup>268-271</sup>. Since then, this synthetic nucleic acid has been used in FISH methodology (e.g.<sup>107, 108, 263, 272, 273</sup>). Comparing with DNA probes, LNA monomers offers several advantages such as greater affinity toward DNA and RNA targets, higher biostability (resistance to nuclease degradation), better signal-to-noise ratio and better sensitivity and specificity<sup>274-277</sup>. Also, it has been reported that the application of LNA probes might be more advantageous than the use of PNA probes in FISH experiments due to higher solubility of LNA in water and its higher efficiency to hybridize with RNA or DNA<sup>278-280</sup>. Enhanced thermal stability has been shown in DNA duplexes containing LNA residues that have the ability to increase the melting temperature ( $T_m$ ), per single LNA nucleotide incorporation, between 1 °C and 8 °C against DNA and 2 °C to 10 °C against RNA<sup>277, 281, 282</sup>.

2'OMe is another RNA mimic which displays a C3'-endo furanose ring conformation, displaying a high nuclease resistant and a greater affinity for RNA targets than the LNA/DNA probes<sup>283-285</sup>. In FISH experiments, when short probes are used, 2'OMe has shown a high discrimination between matched and mismatched RNA targets and an increased  $T_m$  and ability to bind to targets<sup>283</sup>. Also, introducing LNA monomers at every third position of 2'OMe probes seems result in a better sensitivity in FISH experiments<sup>286, 287</sup>.

All these properties of LNA and 2'OMe make them a promising tool for therapeutic (e.g. gene silencing)<sup>270, 288, 289</sup> and diagnostic (e.g. detection of microRNAs, SNP genotyping, identification of bacteria)<sup>107, 290-294</sup> purposes. However, assessing of spatial organization of species in biofilm samples has been mostly limited to PNA probes. Sets of PNA probes, specifically designed for each bacteria, labelled with different fluorochromes and working at same temperature (multiplex FISH), in combination with CLSM analysis have been used to visualize/study the co-localization of each bacteria in the biofilm (e.g.<sup>105, 106, 109</sup>). The LNA and 2'OMe probes, despite their negative charge, offer higher design flexibility comparatively to the PNA and DNA probes, as mixed synthesis is possible. Hence, LNA/2'OMe-FISH holds great promise in biofilm research, allowing the analysis of microbial community composition and its dynamics without disturbing biofilm structure.

## 1.5 References

1. **J.W. Costerton, K.J. Cheng, G.G. Geesey, T.I. Ladd, J.C. Nickel, M. Dasgupta, T.J. Marrie.** Bacterial biofilms in nature and disease. *Annu Rev Microbiol* **41**, 435-464 (1987).
2. **J.W. Costerton, P.S. Stewart, E. Greenberg.** Bacterial biofilms: a common cause of persistent infections. *Science* **284**, 1318-1322 (1999).
3. **M.E. Davey, A. O'Toole G.** Microbial biofilms: from ecology to molecular genetics. *Microbiol Mol Biol Rev* **64**, 847-867 (2000).
4. **P.S. Stewart, M.J. Franklin.** Physiological heterogeneity in biofilms. *Nat Rev Microbiol* **6**, 199-210 (2008).
5. **R.M. Donlan, J.W. Costerton.** Biofilms: survival mechanisms of clinically relevant microorganisms. *Clin Microbiol Rev* **15**, 167-193 (2002).
6. **R.M. Donlan.** Biofilms: microbial life on surfaces. *Emerg Infect Dis* **8**, 881-890 (2002).
7. **L. Hall-Stoodley, P. Stoodley.** Evolving concepts in biofilm infections. *Cell Microbiol* **11**, 1034-1043 (2009).
8. **U. Römling, C. Balsalobre.** Biofilm infections, their resilience to therapy and innovative treatment strategies. *J Intern Med* **272**, 541-561 (2012).
9. **D. Davies.** Understanding biofilm resistance to antibacterial agents. *Nat Rev Drug Discov* **2**, 114-122 (2003).
10. **N. Høiby, O. Ciofu, T. Bjarnsholt.** *Pseudomonas aeruginosa* biofilms in cystic fibrosis. *Future Microbiol* **5**, 1663-1674 (2010).
11. **M. Wessman, T. Bjarnsholt, S.R. Eickhardt-Sørensen, H.K. Johansen, P. Homøe.** Mucosal biofilm detection in chronic otitis media: a study of middle ear biopsies from Greenlandic patients. *Eur Arch Otorhinolaryngol* **272**, 1079-1085 (2015).
12. **R. Jain, R. Douglas.** When and how should we treat biofilms in chronic sinusitis? *Curr Opin Otolaryngol Head Neck Surg* **22**, 16-21 (2014).
13. **G.A. James, E. Swogger, R. Wolcott, E. Pulcini, P. Secor, J. Sestrich, J.W. Costerton, P.S. Stewart.** Biofilms in chronic wounds. *Wound Repair Regen* **16**, 37-44 (2008).
14. **S. Socransky, A. Haffajee, M. Cugini, C. Smith, R. Kent.** Microbial complexes in subgingival plaque. *J Clin Periodontol* **25**, 134-144 (1998).
15. **S. Soto, A. Smithson, J. Horcajada, J. Martinez, J. Mensa, J. Vila.** Implication of biofilm formation in the persistence of urinary tract infection caused by uropathogenic *Escherichia coli*. *Clin Microbiol Infect* **12**, 1034-1036 (2006).
16. **H. Wu, C. Moser, H.-Z. Wang, N. Høiby, Z.-J. Song.** Strategies for combating bacterial biofilm infections. *Int J Oral Sci* **7**, 1-7 (2015).
17. **R.N. Smith, J.P. Nolan.** Central venous catheters. *BMJ* **347** (2013).
18. **D.R. Murdoch, G.R. Corey, B. Hoen, J.M. Miró, V.G. Fowler, A.S. Bayer, A.W. Karchmer, L. Olaison, P.A. Pappas, P. Moreillon, S.T. Chambers, V.H. Chu, V. Falcó, D.J. Holland, P. Jones, J.L. Klein, N.J. Raymond, K.M. Read, M.F. Tripodi, R. Utili, A. Wang, C.W. Woods, C.H. Cabell, I.C.E.I. The.** Clinical Presentation, Etiology and Outcome of Infective Endocarditis in the 21(st) Century: The International Collaboration on Endocarditis-Pro prospective Cohort Study. *Arch Intern Med* **169**, 463-473 (2009).
19. **V. Holá, F. Ruzicka, M. Horka.** Microbial diversity in biofilm infections of the urinary tract with the use of sonication techniques. *FEMS Immunol Med Microbiol* **59**, 525-528 (2010).
20. **D. Campoccia, L. Montanaro, C.R. Arciola.** The significance of infection related to orthopedic devices and issues of antibiotic resistance. *Biomaterials* **27**, 2331-2339 (2006).
21. **R.C. Inacio, G.B. Klautau, M.A.S. Murça, C.B.d. Silva, S. Nigro, L.A. Rivetti, W.L. Pereira, M.J.C. Salles.** Microbial diagnosis of infection and colonization of cardiac implantable electronic devices by use of sonication. *Int J Infect Dis* **38**, 54-59 (2015).
22. **M.E. Auler, D. Morreira, F.F.O. Rodrigues, M.S. Abr Ao, P.F.R. Margarido, F.E. Matsumoto, E.G. Silva, B.C.M. Silva, R.P. Schneider, C.R. Paula.** Biofilm formation on intrauterine devices in patients with recurrent vulvovaginal candidiasis. *Med Mycol* **48**, 211-216 (2010).

23. **J. Schneider, A. Hapfelmeier, J. Fremd, P. Schenk, A. Obermeier, R. Burgkart, S. Forkl, S. Feihl, N. Wantia, B. Neu, M. Bajbouj, S. von Delius, R.M. Schmid, H. Algül, A. Weber.** Biliary endoprosthesis: a prospective analysis of bacterial colonization and risk factors for sludge formation. *PLoS ONE* **9**, e110112 (2014).
24. **M.J. Karau, K.E. Greenwood-Quaintance, S.M. Schmidt, N.V. Tran, P.A. Convery, S.R. Jacobson, U. Bite, R.P. Clay, P.M. Petty, C.H. Johnson.** Microbial biofilms and breast tissue expanders. *Biomed Res Int* **2013** (2013).
25. **M.D. Willcox.** *Pseudomonas aeruginosa* infection and inflammation during contact lens wear: a review. *Optom Vis Sci* **84**, 273-278 (2007).
26. **H.C. van der Mei, K.J.D.A. Buijssen, B.F.A.M. van der Laan, E. Ovchinnikova, G.I. Geertsema-Doornbusch, J. Atema-Smit, B. van de Belt-Gritter, H.J. Busscher.** Voice prosthetic biofilm formation and *Candida* morphogenic conversions in absence and presence of different bacterial strains and species on silicone-rubber. *PLoS ONE* **9**, e104508 (2014).
27. **A. Prüss, E. Giroult, P. Rushbrook** Safe management of wastes from health-care activities, Edn. 2nd ed. (World Health Organization, Switzerland 1999).
28. **T.M. Hooton, S.F. Bradley, D.D. Cardenas, R. Colgan, S.E. Geerlings, J.C. Rice, S. Saint, A.J. Schaeffer, P.A. Tambayh, P. Tenke.** Diagnosis, prevention, and treatment of catheter-associated urinary tract infection in adults: 2009 International Clinical Practice Guidelines from the Infectious Diseases Society of America. *Clin Infect Dis* **50**, 625-663 (2010).
29. **L.E. Nicolle.** Catheter-related urinary tract infection. *Drugs Aging* **22**, 627-639 (2005).
30. **A.S. Lynch, G.T. Robertson.** Bacterial and fungal biofilm infections. *Annu Rev Med* **59**, 415-428 (2008).
31. **P.R. Sankaridurg, S. Sharma, M. Willcox, T.J. Naduvilath, D.F. Sweeney, B.A. Holden, G.N. Rao.** Bacterial colonization of disposable soft contact lenses is greater during corneal infiltrative events than during asymptomatic extended lens wear. *J Clin Microbiol* **38**, 4420-4424 (2000).
32. **Z. Pal, E. Urban, E. Dosa, A. Pal, E. Nagy.** Biofilm formation on intrauterine devices in relation to duration of use. *J Med Microbiol* **54**, 1199-1203 (2005).
33. **S.I. Sayed, R. Kazi, S. Sengupta, A. Chowdhari, M. Jagade.** Microbial colonization of Blom-Singer indwelling voice prostheses in laryngectomized patients: a perspective from India. *Ear Nose Throat J* **91** (2012).
34. **R.E. Kania, G.E. Lamers, N. van de Laar, M. Dijkhuizen, E. Lagendijk, P. Tran Ba Huy, P. Herman, P. Hiemstra, J.J. Grote, J. Frijns.** Biofilms on tracheoesophageal voice prostheses: a confocal laser scanning microscopy demonstration of mixed bacterial and yeast biofilms. *Biofouling* **26**, 519-526 (2010).
35. **B. Tićac, R. Tićac, T. Rukavina, P.G. Kesovija, D. Pedisić, B. Maljevac, R. Starčević.** Microbial colonization of tracheoesophageal voice prostheses (Provox2) following total laryngectomy. *Eur Arch Otorhinolaryngol* **267**, 1579-1586 (2010).
36. **X.-M. Chu, H. Yu, X.-X. Sun, Y. An, B. Li, X.-B. Li.** Identification of bacteriology and risk factor analysis of asymptomatic bacterial colonization in pacemaker replacement patients. *PLoS ONE* **10**, e0119232 (2015).
37. **A. Oliva, B.L. Nguyen, M.T. Mascellino, A. D'Abramo, M. Iannetta, A. Ciccaglioni, V. Vullo, C.M. Mastroianni.** Sonication of explanted cardiac implants improves microbial detection in cardiac device infections. *J Clin Microbiol* **51**, 496-502 (2013).
38. **G. Donelli, E. Guaglianone, R. Di Rosa, F. Fiocca, A. Basoli.** Plastic biliary stent occlusion: factors involved and possible preventive approaches. *Clin Med Res* **5**, 53-60 (2007).
39. **P. Basioukas, A. Vezakis, O. Zarkotou, G. Fragulidis, K. Themeli-Digalaki, S. Rizos, A. Polydorou.** Isolated microorganisms in plastic biliary stents placed for benign and malignant diseases. *Ann Gastroenterol* **27**, 399-403 (2014).
40. **J.L. Del Pozo, N.V. Tran, P.M. Petty, C.H. Johnson, M.F. Walsh, U. Bite, R.P. Clay, J.N. Mandrekar, K.E. Piper, J.M. Steckelberg.** Pilot study of association of bacteria on breast implants with capsular contracture. *J Clin Microbiol* **47**, 1333-1337 (2009).
41. **U.M. Rieger, J. Mesina, D.F. Kalbermatten, M. Haug, H.P. Frey, R. Pico, R. Frei, G. Pierer, N.J. Lüscher, A. Trampuz.** Bacterial biofilms and capsular contracture in patients with breast implants. *Br J Surg* **100**, 768-774 (2013).

42. **R.M. Donlan.** Biofilm formation: a clinically relevant microbiological process. *Clin Infect Dis* **33**, 1387-1392 (2001).
43. **I. Francolini, G. Donelli.** Prevention and control of biofilm-based medical-device-related infections. *FEMS Immunol Med Microbiol* **59**, 227-238 (2010).
44. **V. Leriche, R. Briandet, B. Carpentier.** Ecology of mixed biofilms subjected daily to a chlorinated alkaline solution: spatial distribution of bacterial species suggests a protective effect of one species to another. *Environ Microbiol* **5**, 64-71 (2003).
45. **A.G. Al-Bakri, P. Gilbert, D.G. Allison.** Influence of gentamicin and tobramycin on binary biofilm formation by co-cultures of *Burkholderia cepacia* and *Pseudomonas aeruginosa*. *J Basic Microbiol* **45**, 392-396 (2005).
46. **M. Burmølle, J.S. Webb, D. Rao, L.H. Hansen, S.J. Sørensen, S. Kjelleberg.** Enhanced biofilm formation and increased resistance to antimicrobial agents and bacterial invasion are caused by synergistic interactions in multispecies biofilms. *Appl Environ Microbiol* **72**, 3916-3923 (2006).
47. **D. Kara, S.B. Luppens, J.M. Cate.** Differences between single- and dual-species biofilms of *Streptococcus mutans* and *Veillonella parvula* in growth, acidogenicity and susceptibility to chlorhexidine. *Eur J Oral Sci* **114**, 58-63 (2006).
48. **H. Ceri, M. Olson, C. Stremick, R. Read, D. Morck, A. Buret.** The Calgary Biofilm Device: new technology for rapid determination of antibiotic susceptibilities of bacterial biofilms. *J Clin Microbiol* **37**, 1771-1776 (1999).
49. **European Centre for Disease Prevention and Control-Healthcare-associated infections.** [http://ecdc.europa.eu/en/healthtopics/Healthcare-associated\\_infections/Pages/index.aspx](http://ecdc.europa.eu/en/healthtopics/Healthcare-associated_infections/Pages/index.aspx) (last accession, April 2016).
50. **W.E. Stamm, S.R. Norrby.** Urinary tract infections: disease panorama and challenges. *J Infect Dis* **183**, 1-4 (2001).
51. **P. Zarb, B. Coignard, J. Griskeviciene, A. Muller, V. Vankerckhoven, K. Weist, M. Goossens, S. Vaerenberg, S. Hopkins, B. Catry, D. Monnet, H. Goossens, C. Suetens, E.p.p.p.s. National Contact Points for the, E.p.p.p.s. Hospital Contact Points for the.** The European Centre for Disease Prevention and Control (ECDC) pilot point prevalence survey of healthcare-associated infections and antimicrobial use. *Euro Surveill* **17** (2012).
52. **E. Lo, L.E. Nicolle, S.E. Coffin, C. Gould, L.L. Maragakis, J. Meddings, D.A. Pegues, A.M. Pettis, S. Saint, D.S. Yokoe.** Strategies to prevent catheter-associated urinary tract infections in acute care hospitals: 2014 update. *Infect Control Hosp Epidemiol* **35**, 32-47 (2014).
53. **J.W. Warren.** Catheter-associated urinary tract infections. *Int J Antimicrob Agents* **17**, 299-303 (2001).
54. **L. Hall-Stoodley, J.W. Costerton, P. Stoodley.** Bacterial biofilms: from the natural environment to infectious diseases. *Nat Rev Microbiol* **2**, 95-108 (2004).
55. **M. Friedman.** The inflation calculator. Retrieved from <http://www.westegg.com/inflation/> (2014).
56. **D.E. Fouts, R. Pieper, S. Szpakowski, H. Pohl, S. Knoblach, M.J. Suh, S.T. Huang, I. Ljungberg, B.M. Sprague, S.K. Lucas, M. Torralba, K.E. Nelson, S.L. Groah.** Integrated next-generation sequencing of 16S rDNA and metaproteomics differentiate the healthy urine microbiome from asymptomatic bacteriuria in neuropathic bladder associated with spinal cord injury. *J Transl Med* **10**, 174 (2012).
57. **D.N. Frank, S.S. Wilson, A.L. St Amand, N.R. Pace.** Culture-independent microbiological analysis of foley urinary catheter biofilms. *PLoS One* **4**, e7811 (2009).
58. **D.A. Lewis, R. Brown, J. Williams, P. White, S.K. Jacobson, J.R. Marchesi, M.J. Drake.** The human urinary microbiome; bacterial DNA in voided urine of asymptomatic adults. *Front Cell Infect Microbiol* **3**, 41 (2013).
59. **A.J. Wolfe, E. Toh, N. Shibata, R. Rong, K. Kenton, M. Fitzgerald, E.R. Mueller, P. Schreckenberger, Q. Dong, D.E. Nelson, L. Brubaker.** Evidence of uncultivated bacteria in the adult female bladder. *J Clin Microbiol* **50**, 1376-1383 (2012).

60. **L. Ganderton, J. Chawla, C. Winters, J. Wimpenny, D. Stickler.** Scanning electron microscopy of bacterial biofilms on indwelling bladder catheters. *Eur J Clin Microbiol Infect Dis* **11**, 789-796 (1992).
61. **P. Tenke, B. Kovacs, M. Jackel, E. Nagy.** The role of biofilm infection in urology. *World J Urol* **24**, 13-20 (2006).
62. **B.W. Trautner, R.O. Darouiche.** Role of biofilm in catheter-associated urinary tract infection. *Am J Infect Control* **32**, 177-183 (2004).
63. **J.K. Hatt, P.N. Rather.** Role of bacterial biofilms in urinary tract infections. *Curr Top Microbiol Immunol* **322**, 163-192 (2008).
64. **S. Marić, J. Vraneš.** Characteristics and significance of microbial biofilm formation. *Periodicum Bilogorum* **109**, 115-121 (2007).
65. **P. Gupta, S. Sarkar, B. Das, S. Bhattacharjee, P. Tribedi.** Biofilm, pathogenesis and prevention-a journey to break the wall: a review. *Arch Microbiol* **198**, 1-15 (2016).
66. **A.L. Flores-Mireles, J.N. Walker, M. Caparon, S.J. Hultgren.** Urinary tract infections: epidemiology, mechanisms of infection and treatment options. *Nat Rev Microbiol* **13**, 269-284 (2015).
67. **L.E. Nicolle.** Catheter associated urinary tract infections. *Antimicrob Resist Infect Control* **3**, 23 (2014).
68. **L. Hall-Stoodley, J.W. Costerton, P. Stoodley.** Bacterial biofilms: from the natural environment to infectious diseases. *Nat Rev Microbiol* **2**, 95-108 (2004).
69. **H.J. Busscher, W. Norde, H.C. van der Mei.** Specific molecular recognition and nonspecific contributions to bacterial interaction forces. *Appl Environ Microbiol* **74**, 2559-2564 (2008).
70. **S.M. Jacobsen, D.J. Stickler, H.L. Mobley, M.E. Shirliff.** Complicated catheter-associated urinary tract infections due to *Escherichia coli* and *Proteus mirabilis*. *Clin Microbiol Rev* **21**, 26-59 (2008).
71. **H.-C. Flemming, J. Wingender.** The biofilm matrix. *Nat Rev Microbiol* **8**, 623-633 (2010).
72. **J.D. Denstedt, G. Reid, M. Sofer.** Advances in ureteral stent technology. *World J Urol* **18**, 237-242 (2000).
73. **I.W. Sutherland.** Polysaccharases for microbial exopolysaccharides. *Carbohydrate Polymers* **38**, 319-328 (1999).
74. **J.A. Snyder, B.J. Haugen, E.L. Buckles, C.V. Lockatell, D.E. Johnson, M.S. Donnenberg, R.A. Welch, H.L. Mobley.** Transcriptome of uropathogenic *Escherichia coli* during urinary tract infection. *Infect Immun* **72**, 6373-6381 (2004).
75. **S. Subashchandrabose, H.L.T. Mobley.** Virulence and fitness determinants of uropathogenic *Escherichia coli*. *Microbiol Spectr* **3** (2015).
76. **C.J. Alteri, S.N. Smith, H.L. Mobley.** Fitness of *Escherichia coli* during urinary tract infection requires gluconeogenesis and the TCA cycle. *PLoS Pathog* **5**, e1000448 (2009).
77. **G.H. Shand, H. Anwar, J. Kadurugamuwa, M.R. Brown, S.H. Silverman, J. Melling.** *In vivo* evidence that bacteria in urinary tract infection grow under iron-restricted conditions. *Infect Immun* **48**, 35-39 (1985).
78. **M. Demir, I. Kaleli.** Production by *Escherichia coli* isolates of siderophore and other virulence factors and their pathogenic role in a cutaneous infection model. *Clin Microbiol Infect* **10**, 1011-1014 (2004).
79. **E.C. Hagan, A.L. Lloyd, D.A. Rasko, G.J. Faerber, H.L. Mobley.** *Escherichia coli* global gene expression in urine from women with urinary tract infection. *PLoS Pathog* **6**, e1001187 (2010).
80. **D.J. Stickler.** Clinical complications of urinary catheters caused by crystalline biofilms: something needs to be done. *J Intern Med* **276**, 120-129 (2014).
81. **R.J. Broomfield, S.D. Morgan, A. Khan, D.J. Stickler.** Crystalline bacterial biofilm formation on urinary catheters by urease-producing urinary tract pathogens: a simple method of control. *J Med Microbiol* **58**, 1367-1375 (2009).



82. **D.J. Stickler.** Bacterial biofilms in patients with indwelling urinary catheters. *Nat Clin Pract Urol* **5**, 598-608 (2008).
83. **W.E. Stamm.** Catheter-associated urinary tract infections: epidemiology, pathogenesis, and prevention. *Am J Med* **91**, 65S-71S (1991).
84. **P.A. Tambyah, K.T. Halvorson, D.G. Maki.** A prospective study of pathogenesis of catheter-associated urinary tract infections. *Mayo Clin Proc* **74**, 131-136 (1999).
85. **J.W. Warren.** The catheter and urinary tract infection. *Med Clin North Am* **75**, 481-493 (1991).
86. **L.E. Nicolle.** The chronic indwelling catheter and urinary infection in long-term-care facility residents. *Infect Control Hosp Epidemiol* **22**, 316-321 (2001).
87. **V. Hola, F. Ruzicka, M. Horka.** Microbial diversity in biofilm infections of the urinary tract with the use of sonication techniques. *FEMS Immunol Med Microbiol* **59**, 525-528 (2010).
88. **T.M. Hooton, S.F. Bradley, D.D. Cardenas, R. Colgan, S.E. Geerlings, J.C. Rice, S. Saint, A.J. Schaeffer, P.A. Tambayh, P. Tenke, L.E. Nicolle, A. Infectious Diseases Society of.** Diagnosis, prevention, and treatment of catheter-associated urinary tract infection in adults: 2009 International Clinical Practice Guidelines from the Infectious Diseases Society of America. *Clin Infect Dis* **50**, 625-663 (2010).
89. **L.E. Nicolle.** Catheter-related urinary tract infection. *Drugs Aging* **22**, 627-639 (2005).
90. **V. Hola, F. Ruzicka** The formation of poly-microbial biofilms on urinary catheters. (INTECH Open Access Publisher, Czech Republic 2011).
91. **L.E. Nicolle.** Catheter-related urinary tract infection: practical management in the elderly. *Drugs Aging* **31**, 1-10 (2014).
92. **I. Burckhardt, S. Zimmermann.** *Streptococcus pneumoniae* in urinary tracts of children with chronic kidney disease. *Emerg Infect Dis* **17**, 120-122 (2011).
93. **J.W. Costerton** The Biofilm Primer, Edn. 6th ed. (Springer Berlin Heidelberg, Berlin; 2007).
94. **W. Zimmerli, A. Trampuz, P.E. Ochsner.** Prosthetic-joint infections. *N Engl J Med* **351**, 1645-1654 (2004).
95. **N. Hoiby, T. Bjarnsholt, C. Moser, G.L. Bassi, T. Coenye, G. Donelli, L. Hall-Stoodley, V. Hola, C. Imbert, K. Kirketerp-Moller, D. Lebeaux, A. Oliver, A.J. Ullmann, C. Williams.** ESCMID guideline for the diagnosis and treatment of biofilm infections 2014. *Clin Microbiol Infect* **21**, 1-25.
96. **R. Wolcott, J.W. Costerton, D. Raoult, S.J. Cutler.** The polymicrobial nature of biofilm infection. *Clin Microbiol Infect* **19**, 107-112 (2013).
97. **M.S. Tuttle, E. Mostow, P. Mukherjee, F.Z. Hu, R. Melton-Kreft, G.D. Ehrlich, S.E. Dowd, M.A. Ghannoum.** Characterization of bacterial communities in venous insufficiency wounds by use of conventional culture and molecular diagnostic methods. *J Clin Microbiol* **49**, 3812-3819 (2011).
98. **S.E. Dowd, Y. Sun, P.R. Secor, D.D. Rhoads, B.M. Wolcott, G.A. James, R.D. Wolcott.** Survey of bacterial diversity in chronic wounds using pyrosequencing, DGGE, and full ribosome shotgun sequencing. *BMC Microbiol* **8**, 43 (2008).
99. **C.E. Davies, K.E. Hill, M.J. Wilson, P. Stephens, C.M. Hill, K.G. Harding, D.W. Thomas.** Use of 16S ribosomal DNA PCR and denaturing gradient gel electrophoresis for analysis of the microfloras of healing and nonhealing chronic venous leg ulcers. *J Clin Microbiol* **42**, 3549-3557 (2004).
100. **L.B. Price, C.M. Liu, J.H. Melendez, Y.M. Frankel, D. Engelthaler, M. Aziz, J. Bowers, R. Rattray, J. Ravel, C. Kingsley, P.S. Keim, G.S. Lazarus, J.M. Zenilman.** Community analysis of chronic wound bacteria using 16S rRNA gene-based pyrosequencing: impact of diabetes and antibiotics on chronic wound microbiota. *PLoS One* **4**, e6462 (2009).
101. **T.R. Thomsen, M.S. Aasholm, V.B. Rudkjobing, A.M. Saunders, T. Bjarnsholt, M. Givskov, K. Kirketerp-Moller, P.H. Nielsen.** The bacteriology of chronic venous leg ulcer examined by culture-independent molecular methods. *Wound Repair Regen* **18**, 38-49 (2010).
102. **M.S. Tuttle, E. Mostow, P. Mukherjee, F.Z. Hu, R. Melton-Kreft, G.D. Ehrlich, S.E. Dowd, M.A. Ghannoum.** Characterization of bacterial communities in venous insufficiency wounds by use of conventional culture and molecular diagnostic methods. *J Clin Microbiol* **49**, 3812-3819.

103. **M. Guembe, M. Marin, P. Martin-Rabadan, A. Echenagusia, F. Camúñez, G. Rodríguez-Rosales, G. Simó, M. Echenagusia, E. Bouza.** Use of Universal 16S rRNA gene PCR as a diagnostic tool for venous access port-related bloodstream infections. *J Clin Microbiol*, JCM. 02414-02412 (2012).
104. **P.D. Khot, D.L. Ko, D.N. Fredricks.** Sequencing and analysis of fungal rRNA operons for development of broad-range fungal PCR assays. *Appl Environ Microbiol* **75**, 1559-1565 (2009).
105. **C. Almeida, N.F. Azevedo, S. Santos, C.W. Keevil, M.J. Vieira.** Discriminating multi-species populations in biofilms with peptide nucleic acid fluorescence *in situ* hybridization (PNA FISH). *PLoS One* **6**, e14786 (2011).
106. **L. Cerqueira, J.A. Oliveira, A. Nicolau, N.F. Azevedo, M.J. Vieira.** Biofilm formation with mixed cultures of *Pseudomonas aeruginosa/Escherichia coli* on silicone using artificial urine to mimic urinary catheters. *Biofouling* **29**, 829-840 (2013).
107. **S. Fontenete, N. Guimaraes, M. Leite, C. Figueiredo, J. Wengel, N. Filipe Azevedo.** Hybridization-based detection of *Helicobacter pylori* at human body temperature using advanced locked nucleic acid (LNA) probes. *PLoS One* **8**, e81230 (2013).
108. **S. Fontenete, M. Leite, N. Guimaraes, P. Madureira, R.M. Ferreira, C. Figueiredo, J. Wengel, N.F. Azevedo.** Towards fluorescence *in vivo* hybridization (FIVH) detection of *H. pylori* in gastric mucosa using advanced LNA probes. *PLoS One* **10**, e0125494 (2015).
109. **S. Malic, K.E. Hill, A. Hayes, S.L. Percival, D.W. Thomas, D.W. Williams.** Detection and identification of specific bacteria in wound biofilms using peptide nucleic acid fluorescent *in situ* hybridization (PNA FISH). *Microbiology* **155**, 2603-2611 (2009).
110. **T. Bjarnsholt, X.C. Nielsen, U. Johansen, L. Nørgaard, N. Høiby** in *Cystic Fibrosis* 143-171 (Humana Press, New York; 2011).
111. **European Centre for Disease Prevention and Control. Antimicrobial resistance surveillance in Europe 2014.** Annual Report of the European Antimicrobial Resistance Surveillance Network (EARS-Net). (2015).
112. **M. Matsukawa, Y. Kunishima, S. Takahashi, K. Takeyama, T. Tsukamoto.** Bacterial colonization on intraluminal surface of urethral catheter. *Urology* **65**, 440-444 (2005).
113. **M. Ohkawa, T. Sugata, M. Sawaki, T. Nakashima, H. Fuse, H. Hisazumi.** Bacterial and crystal adherence to the surfaces of indwelling urethral catheters. *J Urol* **143**, 717-721 (1990).
114. **H.M. Probert, G.R. Gibson.** Bacterial biofilms in the human gastrointestinal tract. *Curr Issues Intest Microbiol* **3**, 23-27 (2002).
115. **R. Kucheria, P. Dasgupta, S.H. Sacks, M.S. Khan, N.S. Sheerin.** Urinary tract infections: new insights into a common problem. *Postgrad Med J* **81**, 83-86 (2005).
116. **S.M. Macleod, D.J. Stickler.** Species interactions in mixed-community crystalline biofilms on urinary catheters. *J Med Microbiol* **56**, 1549-1557 (2007).
117. **T.A. Oelschlaeger, U. Dobrindt, J. Hacker.** Virulence factors of uropathogens. *Curr Opin Urol* **12**, 33-38 (2002).
118. **Y. Xu, C. Moser, W.A. Al-Soud, S. Sorensen, N. Hoiby, P.H. Nielsen, T.R. Thomsen.** Culture-dependent and -independent investigations of microbial diversity on urinary catheters. *J Clin Microbiol* **50**, 3901-3908 (2012).
119. **F. Bittar, H. Richet, J.C. Dubus, M. Reynaud-Gaubert, N. Stremmer, J. Sarles, D. Raoult, J.M. Rolain.** Molecular detection of multiple emerging pathogens in sputa from cystic fibrosis patients. *PLoS One* **3**, e2908 (2008).
120. **T. Coenye, J. Goris, T. Spilker, P. Vandamme, J.J. LiPuma.** Characterization of unusual bacteria isolated from respiratory secretions of cystic fibrosis patients and description of *Inquilinus limosus* gen. nov., sp. nov. *J Clin Microbiol* **40**, 2062-2069 (2002).
121. **H.S. Choe, S.W. Son, H.A. Choi, H.J. Kim, S.G. Ahn, J.H. Bang, S.J. Lee, J.Y. Lee, Y.H. Cho, S.S. Lee.** Analysis of the distribution of bacteria within urinary catheter biofilms using four different molecular techniques. *Am J Infect Control* **40**, e249-254 (2012).
122. **T. Coenye, S. Laevens, A. Willems, M. Ohlen, W. Hannant, J.R. Govan, M. Gillis, E. Falsen, P. Vandamme.** *Burkholderia fungorum* sp. nov. and *Burkholderia caledonica* sp. nov., two new species isolated from the environment, animals and human clinical samples. *Int J Syst Evol Microbiol* **51**, 1099-1107 (2001).

123. **G.P. Gerrits, C. Klaassen, T. Coenye, P. Vandamme, J.F. Meis.** *Burkholderia fungorum* septicemia. *Emerg Infect Dis* **11**, 1115-1117 (2005).
124. **T. Shigematsu, K. Yumihara, Y. Ueda, M. Numaguchi, S. Morimura, K. Kida.** *Delftia tsuruhatensis* sp. nov., a terephthalate-assimilating bacterium isolated from activated sludge. *Int J Syst Evol Microbiol* **53**, 1479-1483 (2003).
125. **B. Preiswerk, S. Ullrich, R. Speich, G.V. Bloemberg, M. Hombach.** Human infection with *Delftia tsuruhatensis* isolated from a central venous catheter. *J Med Microbiol* **60**, 246-248 (2011).
126. **O. Tabak, B. Mete, S. Aydin, N.M. Mandel, B. Otlu, R. Ozaras, F. Tabak.** Port-related *Delftia tsuruhatensis* bacteremia in a patient with breast cancer. *New Microbiol* **36**, 199-201 (2013).
127. **E. Yabuuchi, A. Oyama.** *Achromobacter xylosoxidans* n. sp. from human ear discharge. *Jpn J Microbiol* **15**, 477-481 (1971).
128. **J. Gomez-Cerezo, I. Suarez, J.J. Rios, P. Pena, M.J. Garcia de Miguel, M. de Jose, O. Monteagudo, P. Linares, A. Barbado-Cano, J.J. Vazquez.** *Achromobacter xylosoxidans* bacteremia: a 10-year analysis of 54 cases. *Eur J Clin Microbiol Infect Dis* **22**, 360-363 (2003).
129. **D. Tena, A. Gonzalez-Praetorius, M. Perez-Balsalobre, O. Sancho, J. Bisquert.** Urinary tract infection due to *Achromobacter xylosoxidans*: report of 9 cases. *Scand J Infect Dis* **40**, 84-87 (2008).
130. **J.-H. Weitkamp, Y.-W. Tang, D.W. Haas, N.K. Midha, J.E. Crowe.** Recurrent *Achromobacter xylosoxidans* bacteremia associated with persistent lymph node infection in a patient with hyper-immunoglobulin M syndrome. *Clin Infect Dis* **31**, 1183-1187 (2000).
131. **O. Turel, S. Kavuncuoglu, E. Hosaf, S. Ozbek, E. Aldemir, T. Uygur, N. Hatipoglu, R. Siraneci.** Bacteremia due to *Achromobacter xylosoxidans* in neonates: clinical features and outcome. *Braz J Infect Dis* **17**, 450-454 (2013).
132. **G. Aisenberg, K.V. Rolston, A. Safdar.** Bacteremia caused by *Achromobacter* and *Alcaligenes* species in 46 patients with cancer (1989–2003). *Cancer* **101**, 2134-2140 (2004).
133. **A. Lambiase, M.R. Catania, M. Del Pezzo, F. Rossano, V. Terlizzi, A. Sepe, V. Raia.** *Achromobacter xylosoxidans* respiratory tract infection in cystic fibrosis patients. *Eur J Clin Microbiol Infect Dis* **30**, 973-980 (2011).
134. **L. Amoureux, J. Bador, E. Siebor, N. Taillefumier, A. Fanton, C. Neuwirth.** Epidemiology and resistance of *Achromobacter xylosoxidans* from cystic fibrosis patients in Dijon, Burgundy: first French data. *J Cyst Fibros* **12**, 170-176 (2013).
135. **H. Song, M.Z. Ding, X.Q. Jia, Q. Ma, Y.J. Yuan.** Synthetic microbial consortia: from systematic analysis to construction and applications. *Chem Soc Rev* **43**, 6954-6981 (2014).
136. **J.M. Rodríguez-Martínez, A. Pascual.** Antimicrobial resistance in bacterial biofilms. *Rev Med Microbiol* **17**, 65-75 (2006).
137. **T. Woyke, H. Teeling, N.N. Ivanova, M. Huntemann, M. Richter, F.O. Gloeckner, D. Boffelli, I.J. Anderson, K.W. Barry, H.J. Shapiro, E. Szeto, N.C. Kyrpides, M. Mussmann, R. Amann, C. Bergin, C. Ruehland, E.M. Rubin, N. Dubilier.** Symbiosis insights through metagenomic analysis of a microbial consortium. *Nature* **443**, 950-955 (2006).
138. **K. Faust, J. Raes.** Microbial interactions: from networks to models. *Nat Rev Microbiol* **10**, 538-550 (2012).
139. **J.M. Ghigo.** Natural conjugative plasmids induce bacterial biofilm development. *Nature* **412**, 442-445 (2001).
140. **Y. Michel-Briand, C. Baysse.** The pyocins of *Pseudomonas aeruginosa*. *Biochimie* **84**, 499-510 (2002).
141. **W. Chang, D.A. Small, F. Toghrol, W.E. Bentley.** Microarray analysis of *Pseudomonas aeruginosa* reveals induction of pyocin genes in response to hydrogen peroxide. *BMC Genomics* **6**, 115 (2005).
142. **F. Harrison.** Microbial ecology of the cystic fibrosis lung. *Microbiology* **153**, 917-923 (2007).
143. **R.A. Rastall, G.R. Gibson, H.S. Gill, F. Guarner, T.R. Klaenhammer, B. Pot, G. Reid, I.R. Rowland, M.E. Sanders.** Modulation of the microbial ecology of the human colon by

probiotics, prebiotics and synbiotics to enhance human health: an overview of enabling science and potential applications. *FEMS Microbiol Ecol* **52**, 145-152 (2005).

144. **S.A. West, A.S. Griffin, A. Gardner, S.P. Diggle.** Social evolution theory for microorganisms. *Nat Rev Microbiol* **4**, 597-607 (2006).

145. **J.B. Xavier.** Social interaction in synthetic and natural microbial communities. *Mol Syst Biol* **7**, 483 (2011).

146. **S.P. Diggle, A. Gardner, S.A. West, A.S. Griffin.** Evolutionary theory of bacterial quorum sensing: when is a signal not a signal? *Philos Trans R Soc Lond B Biol Sci* **362**, 1241-1249 (2007).

147. **N. Jiricny, S.P. Diggle, S.A. West, B.A. Evans, G. Ballantyne, A. Ross-Gillespie, A.S. Griffin.** Fitness correlates with the extent of cheating in a bacterium. *J Evol Biol* **23**, 738-747 (2010).

148. **O.X. Cordero, L.A. Ventouras, E.F. DeLong, M.F. Polz.** Public good dynamics drive evolution of iron acquisition strategies in natural bacterioplankton populations. *Proc Natl Acad Sci U S A* **109**, 20059-20064 (2012).

149. **M.A. Brockhurst, A. Buckling, D. Racey, A. Gardner.** Resource supply and the evolution of public-goods cooperation in bacteria. *BMC Biology* **6**, 1-6 (2008).

150. **F. Harrison, A. Buckling.** Siderophore production and biofilm formation as linked social traits. *ISME J* **3**, 632-634 (2009).

151. **O. Ciofu, T.J. Beveridge, J. Kadurugamuwa, J. Walther-Rasmussen, N. Hoiby.** Chromosomal beta-lactamase is packaged into membrane vesicles and secreted from *Pseudomonas aeruginosa*. *J Antimicrob Chemother* **45**, 9-13 (2000).

152. **L.A. Dugatkin, M. Perlin, J.S. Lucas, R. Atlas.** Group-beneficial traits, frequency-dependent selection and genotypic diversity: an antibiotic resistance paradigm. *Proc Biol Sci* **272**, 79-83 (2005).

153. **C.D. Nadell, J.B. Xavier, K.R. Foster.** The sociobiology of biofilms. *FEMS Microbiol Rev* **33**, 206-224 (2009).

154. **O. Ciofu, N. Høiby** in *Antibiotic Policies: Fighting Resistance*. (eds. I.M. Gould, J.W.M. Meer) 149-174 (Springer US, Boston, MA; 2008).

155. **S.P. Diggle, A.S. Griffin, G.S. Campbell, S.A. West.** Cooperation and conflict in quorum-sensing bacterial populations. *Nature* **450**, 411-414 (2007).

156. **K.P. Rumbaugh, S.P. Diggle, C.M. Watters, A. Ross-Gillespie, A.S. Griffin, S.A. West.** Quorum sensing and the social evolution of bacterial virulence. *Curr Biol* **19**, 341-345 (2009).

157. **S.E. Darch, S.A. West, K. Winzer, S.P. Diggle.** Density-dependent fitness benefits in quorum-sensing bacterial populations. *Proc Natl Acad Sci U S A* **109**, 8259-8263 (2012).

158. **C.S. Pereira, J.A. Thompson, K.B. Xavier.** AI-2-mediated signalling in bacteria. *FEMS Microbiol Rev* **37**, 156-181 (2013).

159. **C.E. Armbruster, W. Hong, B. Pang, K.E. Weimer, R.A. Juneau, J. Turner, W.E. Swords.** Indirect pathogenicity of *Haemophilus influenzae* and *Moraxella catarrhalis* in polymicrobial otitis media occurs via interspecies quorum signaling. *MBio* **1**, e00102-00110 (2010).

160. **A.C. Perez, B. Pang, L.B. King, L. Tan, K.A. Murrah, J.L. Reimche, J.T. Wren, S.H. Richardson, U. Ghandi, W.E. Swords.** Residence of *Streptococcus pneumoniae* and *Moraxella catarrhalis* within polymicrobial biofilm promotes antibiotic resistance and bacterial persistence *in vivo*. *Pathog Dis* **70**, 280-288 (2014).

161. **K. Duan, C. Dammel, J. Stein, H. Rabin, M.G. Surette.** Modulation of *Pseudomonas aeruginosa* gene expression by host microflora through interspecies communication. *Mol Microbiol* **50**, 1477-1491 (2003).

162. **S. Elias, E. Banin.** Multi-species biofilms: living with friendly neighbors. *FEMS Microbiol Rev* **36**, 990-1004 (2012).

163. **S. Periasamy, P.E. Kolenbrander.** *Aggregatibacter actinomycetemcomitans* builds mutualistic biofilm communities with *Fusobacterium nucleatum* and *Veillonella* species in saliva. *Infect Immun* **77**, 3542-3551 (2009).

164. **E. Giaouris, E. Heir, M. Desvaux, M. Hébraud, T. Møretrø, S. Langsrud, A. Doulgeraki, G.-J. Nychas, M. Kačaniová, K. Czaczyk, H. Ölmez, M. Simões.** Intra- and inter-species interactions within biofilms of important foodborne bacterial pathogens. *Front Microbiol* **6**, 841 (2015).
165. **S.B.I. Luppens, D. Kara, L. Bandounas, M.J. Jonker, F.R.A. Wittink, O. Bruning, T.M. Breit, J.M. Ten Cate, W. Crielaard.** Effect of *Veillonella parvula* on the antimicrobial resistance and gene expression of *Streptococcus mutans* grown in a dual-species biofilm. *Oral Microbiol Immunol* **23**, 183-189 (2008).
166. **M.J.H. Goldsworthy.** Gene expression of *Pseudomonas aeruginosa* and MRSA within a catheter-associated urinary tract infection biofilm model. *Bioscience Horizons* **1**, 28-37 (2008).
167. **G. Croxall, V. Weston, S. Joseph, G. Manning, P. Cheetham, A. McNally.** Increased human pathogenic potential of *Escherichia coli* from polymicrobial urinary tract infections in comparison to isolates from monomicrobial culture samples. *J Med Microbiol* **60**, 102-109 (2011).
168. **S.M. Lehman, R.M. Donlan.** Bacteriophage-mediated control of a two-species biofilm formed by microorganisms causing catheter-associated urinary tract infections in an *in vitro* urinary catheter model. *Antimicrob Agents Chemother* **59**, 1127-1137 (2015).
169. **C.E. Armbruster, S.N. Smith, A. Yep, H.L. Mobley.** Increased incidence of urolithiasis and bacteremia during *Proteus mirabilis* and *Providencia stuartii* coinfection due to synergistic induction of urease activity. *J Infect Dis* **209**, 1524-1532 (2014).
170. **C.J. Alteri, S.D. Himpsl, H.L. Mobley.** Preferential use of central metabolism *in vivo* reveals a nutritional basis for polymicrobial infection. *PLoS Pathog* **11**, e1004601 (2015).
171. **R. Siener, A. Jahnen, A. Hesse.** Influence of a mineral water rich in calcium, magnesium and bicarbonate on urine composition and the risk of calcium oxalate crystallization. *Eur J Clin Nutr* **58**, 270-276 (2004).
172. **M.S. Conover, A.L. Flores-Mireles, M.E. Hibbing, K. Dodson, S.J. Hultgren.** Establishment and characterization of UTI and CAUTI in a mouse model. *J Vis Exp* **23**, e52892 (2015).
173. **J.E. Nett, E.G. Brooks, J. Cabezas-Olcoz, H. Sanchez, R. Zarnowski, K. Marchillo, D.R. Andes.** Rat indwelling urinary catheter model of *Candida albicans* biofilm infection. *Infect Immun* **82**, 4931-4940 (2014).
174. **J.E. Nett, E.G. Brooks, J. Cabezas-Olcoz, H. Sanchez, R. Zarnowski, K. Marchillo, D.R. Andes.** Rat indwelling urinary catheter model of *Candida albicans* biofilm infection. *Infect Immun* **82**, 4931-4940 (2014).
175. **B.H. Kim, G.M. Gadd, B.H. Kim, G.M. Gadd.** 85-127 (Cambridge University Press, Cambridge; 2008).
176. **T.J. Berg JM, Stryer L. Biochemistry**, Edn. 5th edition. (ed. N.Y.W.H. Freeman) (Available from: <http://www.ncbi.nlm.nih.gov/books/NBK21150/>; 2002).
177. **S.P. Lopes, N.F. Azevedo, M.O. Pereira.** Microbiome in cystic fibrosis: Shaping polymicrobial interactions for advances in antibiotic therapy. *Crit Rev Microbiol* **41**, 353-365 (2015).
178. **S.P. Lopes, H. Ceri, N.F. Azevedo, M.O. Pereira.** Antibiotic resistance of mixed biofilms in cystic fibrosis: impact of emerging microorganisms on treatment of infection. *Int J Antimicrob Agents* **40**, 260-263 (2012).
179. **N. Woodford, D.M. Livermore.** Infections caused by Gram-positive bacteria: a review of the global challenge. *J Infect* **59**, 4-16 (2009).
180. **D.R. Guay.** Contemporary management of uncomplicated urinary tract infections. *Drugs* **68**, 1169-1205 (2008).
181. **D.I. Andersson, D. Hughes.** Antibiotic resistance and its cost: is it possible to reverse resistance? *Nat Rev Microbiol* **8**, 260-271 (2010).
182. **H.C. Flemming, J. Wingender.** The biofilm matrix. *Nat Rev Microbiol* **8**, 623-633 (2010).
183. **P.S. Stewart.** Mechanisms of antibiotic resistance in bacterial biofilms. *Int J Med Microbiol* **292**, 107-113 (2002).
184. **O. Ciofu, N. Høiby** in *Antibiotic Policies: Fighting Resistance*. (eds. I.M. Gould, J.W.M. Meer) 149-174 (Springer US, Boston, MA; 2008).

185. **I. Keren, N. Kaldalu, A. Spoering, Y. Wang, K. Lewis.** Persister cells and tolerance to antimicrobials. *FEMS Microbiol Lett* **230**, 13-18 (2004).
186. **S. Wu, X. Li, M. Gunawardana, K. Maguire, D. Guerrero-Given, C. Schaudinn, C. Wang, M.M. Baum, P. Webster.** Beta-lactam antibiotics stimulate biofilm formation in non-typeable *Haemophilus influenzae* by up-regulating carbohydrate metabolism. *PLoS One* **9**, e99204 (2014).
187. **K. Lewis.** Riddle of biofilm resistance. *Antimicrob Agents Chemother* **45**, 999-1007 (2001).
188. **P.S. Stewart, J.W. Costerton.** Antibiotic resistance of bacteria in biofilms. *Lancet* **358**, 135-138 (2001).
189. **T. May, A. Ito, S. Okabe.** Induction of multidrug resistance mechanism in *Escherichia coli* biofilms by interplay between tetracycline and ampicillin resistance genes. *Antimicrob Agents Chemother* **53**, 4628-4639 (2009).
190. **V.J. Savage, I. Chopra, A.J. O'Neill.** *Staphylococcus aureus* biofilms promote horizontal transfer of antibiotic resistance. *Antimicrob Agents Chemother* **57**, 1968-1970 (2013).
191. **M. Broszat, E. Grohmann** in *Antibiofilm Agents*, Vol. 8. (eds. K.P. Rumbaugh, I. Ahmad) 67-95 (Springer Berlin Heidelberg, 2014).
192. **G.G. Zhanel, J.A. Karlowsky, G.K. Harding, A. Carrie, T. Mazzulli, D.E. Low, D.J. Hoban.** A Canadian national surveillance study of urinary tract isolates from outpatients: comparison of the activities of trimethoprim-sulfamethoxazole, ampicillin, mecillinam, nitrofurantoin, and ciprofloxacin. The Canadian Urinary Isolate Study Group. *Antimicrob Agents Chemother* **44**, 1089-1092 (2000).
193. **H.A. Kazi MM, Sale H, Mane D, Yande M, et al.** Catheter associated urinary tract infections (CAUTI) and antibiotic sensitivity pattern from confirmed cases of CAUTI in a tertiary care hospital: a prospective study. *Clin Microbiol* **4:193** (2015).
194. **J.R. Johnson, M.A. Kuskowski, T.J. Wilt.** Systematic review: antimicrobial urinary catheters to prevent catheter-associated urinary tract infection in hospitalized patients. *Ann Intern Med* **144**, 116-126 (2006).
195. **Y.W. Cho, J.H. Park, S.H. Kim, Y.H. Cho, J.M. Choi, H.J. Shin, Y.H. Bae, H. Chung, S.Y. Jeong, I.C. Kwon.** Gentamicin-releasing urethral catheter for short-term catheterization. *J Biomater Sci Polym Ed* **14**, 963-972 (2003).
196. **J.H. Park, Y.W. Cho, Y.H. Cho, J.M. Choi, H.J. Shin, Y.H. Bae, H. Chung, S.Y. Jeong, I.C. Kwon.** Norfloxacin-releasing urethral catheter for long-term catheterization. *J Biomater Sci Polym Ed* **14**, 951-962 (2003).
197. **R. Pickard, T. Lam, G. MacLennan, K. Starr, M. Kilonzo, G. McPherson, K. Gillies, A. McDonald, K. Walton, B. Buckley, C. Glazener, C. Boachie, J. Burr, J. Norrie, L. Vale, A. Grant, J. N'Dow.** Types of urethral catheter for reducing symptomatic urinary tract infections in hospitalised adults requiring short-term catheterisation: multicentre randomised controlled trial and economic evaluation of antimicrobial- and antiseptic-impregnated urethral catheters (the CATHETER trial). *Health Technol Assess* **16**, 1-197 (2012).
198. **R. Pickard, T. Lam, G. MacLennan, K. Starr, M. Kilonzo, G. McPherson, K. Gillies, A. McDonald, K. Walton, B. Buckley, C. Glazener, C. Boachie, J. Burr, J. Norrie, L. Vale, A. Grant, J. N'Dow.** Antimicrobial catheters for reduction of symptomatic urinary tract infection in adults requiring short-term catheterisation in hospital: a multicentre randomised controlled trial. *Lancet* **380**, 1927-1935 (2012).
199. **S. Pereira, L. Nguyen, J.J. Stevermer.** PURLs: A simple way to reduce catheter-associated UTIs. *J Fam Pract* **63**, E10-E12 (2014).
200. **S.P. Lopes, N.F. Azevedo, M.O. Pereira.** Emergent bacteria in cystic fibrosis: *in vitro* biofilm formation and resilience under variable oxygen conditions. *Biomed Res Int* **2014**, 678301 (2014).
201. **H.C. Vebo, M. Solheim, L. Snipen, I.F. Nes, D.A. Brede.** Comparative genomic analysis of pathogenic and probiotic *Enterococcus faecalis* isolates, and their transcriptional responses to growth in human urine. *PLoS One* **5**, e12489 (2010).
202. **A. Berger, K. Dohnt, P. Tielen, D. Jahn, J. Becker, C. Wittmann.** Robustness and plasticity of metabolic pathway flux among uropathogenic isolates of *Pseudomonas aeruginosa*. *PLoS ONE* **9**, e88368 (2014).

203. **J. Zdziarski, E. Brzuszkiewicz, B. Wullt, H. Liesegang, D. Biran, B. Voigt, J. Grönberg-Hernandez, B. Ragnarsdottir, M. Hecker, E.Z. Ron, R. Daniel, G. Gottschalk, J. Hacker, C. Svanborg, U. Dobrindt.** Host imprints on bacterial genomes-Rapid, Divergent Evolution in individual patients. *PLoS Pathog* **6**, e1001078 (2010).
204. **C.D. Nadell, J.B. Xavier, S.A. Levin, K.R. Foster.** The evolution of quorum sensing in bacterial biofilms. *PLoS Biol* **6**, e14 (2008).
205. **J.B. Xavier, E. Martinez-Garcia, K.R. Foster.** Social evolution of spatial patterns in bacterial biofilms: when conflict drives disorder. *Am Nat* **174**, 1-12 (2009).
206. **P.G. Eglund, R.J. Palmer, Jr., P.E. Kolenbrander.** Interspecies communication in *Streptococcus gordonii*-*Veillonella atypica* biofilms: signaling in flow conditions requires juxtaposition. *Proc Natl Acad Sci U S A* **101**, 16917-16922 (2004).
207. **A.T. Nielsen, T. Tolker-Nielsen, K.B. Barken, S. Molin.** Role of commensal relationships on the spatial structure of a surface-attached microbial consortium. *Environ Microbiol* **2**, 59-68 (2000).
208. **B.B. Christensen, J.A. Haagensen, A. Heydorn, S. Molin.** Metabolic commensalism and competition in a two-species microbial consortium. *Appl Environ Microbiol* **68**, 2495-2502 (2002).
209. **D. An, T. Danhorn, C. Fuqua, M.R. Parsek.** Quorum sensing and motility mediate interactions between *Pseudomonas aeruginosa* and *Agrobacterium tumefaciens* in biofilm cocultures. *Proc Natl Acad Sci USA* **103**, 3828-3833 (2006).
210. **D. Lebeaux, A. Chauhan, O. Rendueles, C. Beloin.** From *in vitro* to *in vivo* models of bacterial biofilm-related infections. *Pathogens* **2**, 288-356 (2013).
211. **S. Silva, M. Negri, M. Henriques, R. Oliveira, D. Williams, J. Azeredo.** Silicone colonization by non-*Candida albicans* *Candida* species in the presence of urine. *J Med Microbiol* **59**, 747-754 (2010).
212. **T. Coenye, H.J. Nelis.** *In vitro* and *in vivo* model systems to study microbial biofilm formation. *J Microbiol Methods* **83**, 89-105 (2010).
213. **C. Niu, E. Gilbert.** Colorimetric method for identifying plant essential oil components that affect biofilm formation and structure. *Appl Environ Microbiol* **70**, 6951-6956 (2004).
214. **H. Nailis, D. Vandenbosch, D. Deforce, H.J. Nelis, T. Coenye.** Transcriptional response to fluconazole and amphotericin B in *Candida albicans* biofilms. *Res Microbiol* **161**, 284-292 (2010).
215. **M.O. Pereira, M.J. Vieira.** Effects of the interactions between glutaraldehyde and the polymeric matrix on the efficacy of the biocide against *Pseudomonas fluorescens* biofilms. *Biofouling* **17**, 93-101 (2001).
216. **M. Hamilton** The biofilm laboratory: step-by-step protocols for experimental design, analysis, and data interpretation, Edn. 1<sup>st</sup> ed. (Cytergy, Montana State Univ., Center for Biofilm Engineering; 2003).
217. **E. Bouza, N. Alvarado, L. Alcalá, M. Sánchez-Conde, M.J. Pérez, P. Muñoz, P. Martín-Rabadán, M. Rodríguez-Crèixems.** A prospective, randomized, and comparative study of 3 different methods for the diagnosis of intravascular catheter colonization. *Clin Infect Dis* **40**, 1096-1100 (2005).
218. **L. Slobbe, A. el Barzouhi, E. Boersma, B.J. Rijnders.** Comparison of the roll plate method to the sonication method to diagnose catheter colonization and bacteremia in patients with long-term tunnelled catheters: a randomized prospective study. *J Clin Microbiol* **47**, 885-888 (2009).
219. **G.D. Christensen, W. Simpson, J. Younger, L. Baddour, F. Barrett, D. Melton, E. Beachey.** Adherence of coagulase-negative staphylococci to plastic tissue culture plates: a quantitative model for the adherence of staphylococci to medical devices. *J Clin Microbiol* **22**, 996-1006 (1985).
220. **S. Stepanović, D. Vuković, I. Dakić, B. Savić, M. Švabić-Vlahović.** A modified microtiter-plate test for quantification of staphylococcal biofilm formation. *J Microbiol Methods* **40**, 175-179 (2000).
221. **B. Pitts, M.A. Hamilton, N. Zelver, P.S. Stewart.** A microtiter-plate screening method for biofilm disinfection and removal. *J Microbiol Methods* **54**, 269-276 (2003).
222. **L. Yang, Y. Liu, H. Wu, N. Hoiby, S. Molin, Z.J. Song.** Current understanding of multi-species biofilms. *Int J Oral Sci* **3**, 74-81 (2011).

223. **A.K. Welsh, R.J. McLean.** Characterization of bacteria in mixed biofilm communities using denaturing gradient gel electrophoresis (DGGE). *Curr Protoc Microbiol* **Chapter 1**, Unit 1E.1 (2007).
224. **M.H. Castonguay, S. van der Schaaf, W. Koester, J. Krooneman, W. van der Meer, H. Harmsen, P. Landini.** Biofilm formation by *Escherichia coli* is stimulated by synergistic interactions and co-adhesion mechanisms with adherence-proficient bacteria. *Res Microbiol* **157**, 471-478 (2006).
225. **S. Nagashima, A. Yoshida, N. Suzuki, T. Ansai, T. Takehara.** Use of the genomic subtractive hybridization technique to develop a real-time PCR assay for quantitative detection of *Prevotella* spp. in oral biofilm samples. *J Clin Microbiol* **43**, 2948-2951 (2005).
226. **E. Gaetti-Jardim, Jr., S.L. Marcelino, A.C. Feitosa, G.A. Romito, M.J. Avila-Campos.** Quantitative detection of periodontopathic bacteria in atherosclerotic plaques from coronary arteries. *J Med Microbiol* **58**, 1568-1575 (2009).
227. **T.R. Neu, B. Manz, F. Volke, J.J. Dynes, A.P. Hitchcock, J.R. Lawrence.** Advanced imaging techniques for assessment of structure, composition and function in biofilm systems. *FEMS Microbiol Ecol* **72**, 1-21 (2010).
228. **Y. Shen, S. Stojcic, M. Haapasalo.** Bacterial viability in starved and revitalized biofilms: comparison of viability staining and direct culture. *J Endod* **36**, 1820-1823 (2010).
229. **J. Barros, L. Grenho, C.M. Manuel, C. Ferreira, L. Melo, O.C. Nunes, F.J. Monteiro, M.P. Ferraz.** Influence of nanohydroxyapatite surface properties on *Staphylococcus epidermidis* biofilm formation. *J Biomater Appl* **28**, 1325-1335 (2014).
230. **J.R. Lawrence, G.D. Swerhone, U. Kuhlicke, T.R. Neu.** *In situ* evidence for microdomains in the polymer matrix of bacterial microcolonies. *Can J Microbiol* **53**, 450-458 (2007).
231. **A.C. Rodrigues, S. Wuertz, A.G. Brito, L.F. Melo.** Three-dimensional distribution of GFP-labeled *Pseudomonas putida* during biofilm formation on solid PAHs assessed by confocal laser scanning microscopy. *Water Sci Technol* **47**, 139-142 (2003).
232. **A. Bridier, R. Briandet, T. Bouchez, F. Jabot.** A model-based approach to detect interspecific interactions during biofilm development. *Biofouling* **30**, 761-771 (2014).
233. **S. Beaufort, T. Da Silva, C. Lafforgue, S. Alfenore.** Fluorescent proteins as *in vivo* and *in situ* reporters to study the development of a *Saccharomyces cerevisiae* yeast biofilm and its invasion by the bacteria *Escherichia coli*. *FEMS Microbiol Ecol* **80**, 342-351 (2012).
234. **J. van Gestel, F.J. Weissing, O.P. Kuipers, A.T. Kovacs.** Density of founder cells affects spatial pattern formation and cooperation in *Bacillus subtilis* biofilms. *ISME J* **8**, 2069-2079 (2014).
235. **J.K. Sanders, S.E. Jackson.** The discovery and development of the green fluorescent protein, GFP. *Chem Soc Rev* **38**, 2821-2822 (2009).
236. **P.K. Sharma, E. Engels, W. Van Oeveren, R.J. Ploeg, C.v.H. der Mei, H.J. Busscher, G.M. Van Dam, G. Rakhorst.** Spatiotemporal progression of localized bacterial peritonitis before and after open abdomen lavage monitored by *in vivo* bioluminescent imaging. *Surgery* **147**, 89-97 (2010).
237. **A.F. Engelsman, H.C. van der Mei, K.P. Francis, H.J. Busscher, R.J. Ploeg, G.M. van Dam.** Real time noninvasive monitoring of contaminating bacteria in a soft tissue implant infection model. *J Biomed Mater Res B Appl Biomater* **88**, 123-129 (2009).
238. **C. Vuong, S. Kocianova, J. Yu, J.L. Kadurugamuwa, M. Otto.** Development of real-time *in vivo* imaging of device-related *Staphylococcus epidermidis* infection in mice and influence of animal immune status on susceptibility to infection. *J Infect Dis* **198**, 258-261 (2008).
239. **A. Bridier, R. Briandet, T. Bouchez, F. Jabot.** A model-based approach to detect interspecific interactions during biofilm development. *Biofouling* **30**, 761-771 (2014).
240. **T. Tolker-Nielsen, U.C. Brinch, P.C. Ragas, J.B. Andersen, C.S. Jacobsen, S. Molin.** Development and dynamics of *Pseudomonas* sp. biofilms. *J Bacteriol* **182**, 6482-6489 (2000).
241. **L. Yang, Y. Liu, T. Markussen, N. Hoiby, T. Tolker-Nielsen, S. Molin.** Pattern differentiation in co-culture biofilms formed by *Staphylococcus aureus* and *Pseudomonas aeruginosa*. *FEMS Immunol Med Microbiol* **62**, 339-347 (2011).



242. **K. Wouters, E. Maes, J.A. Spitz, M.B. Roeffaers, P. Wattiau, J. Hofkens, D. Springael.** A non-invasive fluorescent staining procedure allows Confocal Laser Scanning Microscopy based imaging of *Mycobacterium* in multispecies biofilms colonizing and degrading polycyclic aromatic hydrocarbons. *J Microbiol Methods* **83**, 317-325 (2010).
243. **J.S. Teodosio, M. Simoes, F.J. Mergulhao.** The influence of nonconjugative *Escherichia coli* plasmids on biofilm formation and resistance. *J Appl Microbiol* **113**, 373-382 (2012).
244. **R. Amann, B.M. Fuchs.** Single-cell identification in microbial communities by improved fluorescence *in situ* hybridization techniques. *Nat Rev Microbiol* **6**, 339-348 (2008).
245. **A. Lourenço, T. Coenye, D.M. Goeres, G. Donelli, A.S. Azevedo, H. Ceri, F.L. Coelho, H.-C. Flemming, T. Juhna, S.P. Lopes.** Minimum information about a biofilm experiment (MIABiE): standards for reporting experiments and data on sessile microbial communities living at interfaces. *Pathog Dis* **70**, 250-256 (2014).
246. **A. Lourenço, A. Ferreira, N. Veiga, I. Machado, M.O. Pereira, N.F. Azevedo.** BioOmics: A web platform for the systematic and standardized collection of high-Throughput biofilm data. *PLoS ONE* **7**, e39960 (2012).
247. **R. Amann, B.M. Fuchs, S. Behrens.** The identification of microorganisms by fluorescence *in situ* hybridisation. *Curr Opin Biotechnol* **12**, 231-236 (2001).
248. **B.L. Maidak, J.R. Cole, T.G. Lilburn, C.T. Parker, Jr., P.R. Saxman, J.M. Stredwick, G.M. Garrity, B. Li, G.J. Olsen, S. Pramanik, T.M. Schmidt, J.M. Tiedje.** The RDP (Ribosomal Database Project) continues. *Nucleic Acids Res* **28**, 173-174 (2000).
249. **W. Ludwig, O. Strunk, R. Westram, L. Richter, H. Meier, Yadhukumar, A. Buchner, T. Lai, S. Steppi, G. Jobb, W. Forster, I. Brettske, S. Gerber, A.W. Ginhart, O. Gross, S. Grumann, S. Hermann, R. Jost, A. König, T. Liss, R. Lussmann, M. May, B. Nonhoff, B. Reichel, R. Strehlow, A. Stamatakis, N. Stuckmann, A. Vilbig, M. Lenke, T. Ludwig, A. Bode, K.H. Schleifer.** ARB: a software environment for sequence data. *Nucleic Acids Res* **32**, 1363-1371 (2004).
250. **N.F. Azevedo, T. Jardim, C. Almeida, L. Cerqueira, A.J. Almeida, F. Rodrigues, C.W. Keevil, M.J. Vieira.** Application of flow cytometry for the identification of *Staphylococcus epidermidis* by peptide nucleic acid fluorescence *in situ* hybridization (PNA FISH) in blood samples. *Antonie Van Leeuwenhoek* **100**, 463-470 (2011).
251. **C. Almeida, N.F. Azevedo, R.M. Fernandes, C.W. Keevil, M.J. Vieira.** Fluorescence *in situ* hybridization method using a peptide nucleic acid probe for identification of *Salmonella* spp. in a broad spectrum of samples. *Appl Environ Microbiol* **76**, 4476-4485 (2010).
252. **L.S. Yilmaz, D.R. Noguera.** Mechanistic approach to the problem of hybridization efficiency in fluorescent *in situ* hybridization. *Appl Environ Microbiol* **70**, 7126-7139 (2004).
253. **L.Ş. Yilmaz, H.E. Ökten, D.R. Noguera.** Making all parts of the 16S rRNA of *Escherichia coli* accessible *in situ* to single DNA oligonucleotides. *Appl Environ Microbiol* **72**, 733-744 (2006).
254. **N. Guimaraes, N.F. Azevedo, C. Figueiredo, C.W. Keevil, M.J. Vieira.** Development and application of a novel peptide nucleic acid probe for the specific detection of *Helicobacter pylori* in gastric biopsy specimens. *J Clin Microbiol* **45**, 3089-3094 (2007).
255. **A.P. Silverman, E.T. Kool.** Oligonucleotide probes for RNA-targeted fluorescence *in situ* hybridization. *Adv Clin Chem* **43**, 79-115 (2007).
256. **M. Wagner, M. Horn, H. Daims.** Fluorescence *in situ* hybridisation for the identification and characterisation of prokaryotes. *Curr Opin Microbiol* **6**, 302-309 (2003).
257. **A. Moter, U.B. Gobel.** Fluorescence *in situ* hybridization (FISH) for direct visualization of microorganisms. *J Microbiol Methods* **41**, 85-112 (2000).
258. **L. Cerqueira, N.F. Azevedo, C. Almeida, T. Jardim, C.W. Keevil, M.J. Vieira.** DNA mimics for the rapid identification of microorganisms by fluorescence *in situ* hybridization (FISH). *Int J Mol Sci* **9**, 1944-1960 (2008).
259. **A.S. Azevedo, C. Almeida, B. Pereira, L.F. Melo, N.F. Azevedo.** Impact of *Delfia tsuruhatensis* and *Achromobacter xylooxidans* on *Escherichia coli* dual-species biofilms treated with antibiotic agents. *Biofouling* **32**, 227-241 (2016).
260. **S.K. Hansen, P.B. Rainey, J.A. Haagensen, S. Molin.** Evolution of species interactions in a biofilm community. *Nature* **445**, 533-536 (2007).

261. **H. Daims, M. Wagner.** Quantification of uncultured microorganisms by fluorescence microscopy and digital image analysis. *Appl Microbiol Biotechnol* **75**, 237-248 (2007).
262. **S.A. Wilks, C.W. Keevil.** Targeting species-specific low-affinity 16S rRNA binding sites by using peptide nucleic acids for detection of *Legionellae* in biofilms. *Appl Environ Microbiol* **72**, 5453-5462 (2006).
263. **K. Kubota, A. Ohashi, H. Imachi, H. Harada.** Improved *in situ* hybridization efficiency with locked-nucleic-acid-incorporated DNA probes. *Appl Environ Microbiol* **72**, 5311-5317 (2006).
264. **R.R. Breaker.** Natural and engineered nucleic acids as tools to explore biology. *Nature* **432**, 838-845 (2004).
265. **C. Almeida, J.M. Sousa, R. Rocha, L. Cerqueira, S. Fanning, N.F. Azevedo, M.J. Vieira.** Detection of *Escherichia coli* O157 by peptide nucleic acid fluorescence *in situ* hybridization (PNA-FISH) and comparison to a standard culture method. *Appl Environ Microbiol* **79**, 6293-6300 (2013).
266. **S. Fontenete, N. Guimarães, M. Leite, C. Figueiredo, J. Wengel, N. Filipe Azevedo.** Hybridization-based detection of *Helicobacter pylori* at human body temperature using advanced Locked Nucleic Acid (LNA) Probes. *PLoS ONE* **8**, e81230 (2013).
267. **M.J. Soe, T. Moller, M. Dufva, K. Holmstrom.** A sensitive alternative for microRNA *in situ* hybridizations using probes of 2'-O-methyl RNA + LNA. *J Histochem Cytochem* **59**, 661-672 (2011).
268. **S. Obika, D. Nanbu, Y. Hari, K.-i. Morio, Y. In, T. Ishida, T. Imanishi.** Synthesis of 2'-O, 4'-C-methyleneuridine and-cytidine. Novel bicyclic nucleosides having a fixed C 3,-endo sugar puckering. *Tetrahedron Letters* **38**, 8735-8738 (1997).
269. **A.A. Koshkin, V.K. Rajwanshi, J. Wengel.** Novel convenient syntheses of LNA [2.2.1] bicyclo nucleosides. *Tetrahedron letters* **39**, 4381-4384 (1998).
270. **B. Vester, J. Wengel.** LNA (locked nucleic acid): high-affinity targeting of complementary RNA and DNA. *Biochemistry* **43**, 13233-13241 (2004).
271. **S. Singh, A. Koshkin.** LNA (locked nucleic acids): synthesis and high-affinity nucleic acid recognition. *Chem Commun*, 455-456 (1998).
272. **K.L. Robertson, D.C. Thach.** LNA flow-FISH: A flow cytometry-fluorescence *in situ* hybridization method to detect messenger RNA using locked nucleic acid probes. *Anal Biochem* **390**, 109-114 (2009).
273. **R. Maruo, H. Yamada, M. Watanabe, Y. Hidaka, Y. Iwatani, T. Takano.** mRNA quantification after fluorescence activated cell sorting using locked nucleic acid probes. *Mol Biotechnol* **49**, 42-47 (2011).
274. **R. Thomsen, P.S. Nielsen, T.H. Jensen.** Dramatically improved RNA *in situ* hybridization signals using LNA-modified probes. *RNA* **11**, 1745-1748 (2005).
275. **A. Silahatoglu, H. Pfundheller, A. Koshkin, N. Tommerup, S. Kauppinen.** LNA-modified oligonucleotides are highly efficient as FISH probes. *Cytogenet Genome Res* **107**, 32-37 (2004).
276. **R.N. Veedu, J. Wengel.** Locked nucleic acid as a novel class of therapeutic agents. *RNA Biol* **6**, 321-323 (2009).
277. **M. Petersen, J. Wengel.** LNA: a versatile tool for therapeutics and genomics. *Trends Biotechnol* **21**, 74-81 (2003).
278. **K.L. Robertson, D.C. Thach.** LNA flow-FISH: A flow cytometry-fluorescence *in situ* hybridization method to detect messenger RNA using locked nucleic acid probes. *Analytical Biochemistry* **390**, 109-114 (2009).
279. **A.N. Elayadi, D.A. Braasch, D.R. Corey.** Implications of high-affinity hybridization by locked nucleic acid oligomers for inhibition of human telomerase. *Biochemistry* **41**, 9973-9981 (2002).
280. **D.A. Braasch, D.R. Corey.** Locked nucleic acid (LNA): fine-tuning the recognition of DNA and RNA. *Chem Biol* **8**, 1-7 (2001).
281. **S. Obika, D. Nanbu, Y. Hari, J.-i. Andoh, K.-i. Morio, T. Doi, T. Imanishi.** Stability and structural features of the duplexes containing nucleoside analogues with a fixed N-type conformation, 2'-O, 4'-C-methylenribonucleosides. *Tetrahedron letters* **39**, 5401-5404 (1998).

282. **S. Singh.** Universality of LNA-mediated high-affinity nucleic acid recognition. *Chem Commun*, 1247-1248 (1998).
283. **M. Majlessi, N.C. Nelson, M.M. Becker.** Advantages of 2'-O-methyl oligoribonucleotide probes for detecting RNA targets. *Nucleic Acids Res* **26**, 2224-2229 (1998).
284. **H. Inoue, Y. Hayase, A. Imura, S. Iwai, K. Miura, E. Ohtsuka.** Synthesis and hybridization studies on two complementary nona (2'-O-methyl) ribonucleotides. *Nucleic Acids Res* **15**, 6131-6148 (1987).
285. **E. Kierzek, A. Ciesielska, K. Pasternak, D.H. Mathews, D.H. Turner, R. Kierzek.** The influence of locked nucleic acid residues on the thermodynamic properties of 2'-O-methyl RNA/RNA heteroduplexes. *Nucleic Acids Res* **33**, 5082-5093 (2005).
286. **S. Fontenete, J. Barros, P. Madureira, C. Figueiredo, J. Wengel, N.F. Azevedo.** Mismatch discrimination in fluorescent *in situ* hybridization using different types of nucleic acids. *Appl Microbiol Biotechnol* **99**, 3961-3969 (2015).
287. **M.J. Søre, T. Møller, M. Dufva, K. Holmstrøm.** A sensitive alternative for microRNA *in situ* hybridizations using probes of 2'-O-methyl RNA + LNA. *J Histochem Cytochem* **59**, 661-672 (2011).
288. **D.A. Braasch, Y. Liu, D.R. Corey.** Antisense inhibition of gene expression in cells by oligonucleotides incorporating locked nucleic acids: effect of mRNA target sequence and chimera design. *Nucleic Acids Res* **30**, 5160-5167 (2002).
289. **J. Kurreck, E. Wyszko, C. Gillen, V.A. Erdmann.** Design of antisense oligonucleotides stabilized by locked nucleic acids. *Nucleic Acids Res* **30**, 1911-1918 (2002).
290. **A.N. Silahatoglu, D. Nolting, L. Dyrskjøt, E. Berezikov, M. Møller, N. Tommerup, S. Kauppinen.** Detection of microRNAs in frozen tissue sections by fluorescence *in situ* hybridization using locked nucleic acid probes and tyramide signal amplification. *Nat Protoc* **2**, 2520-2528 (2007).
291. **A. Simeonov, T.T. Nikiforov.** Single nucleotide polymorphism genotyping using short, fluorescently labeled locked nucleic acid (LNA) probes and fluorescence polarization detection. *Nucleic Acids Res* **30**, e91-e91 (2002).
292. **S. Fontenete, M. Leite, D. Cappoen, R. Santos, C.V. Ginneken, C. Figueiredo, J. Wengel, P. Cos, N.F. Azevedo.** Fluorescence *In vivo* Hybridization (FIVH) for detection of *Helicobacter pylori* Infection in a C57BL/6 Mouse Model. *PLoS One* **11**, e0148353 (2016).
293. **W.P. Kloosterman, E. Wienholds, E. de Bruijn, S. Kauppinen, R.H. Plasterk.** *In situ* detection of miRNAs in animal embryos using LNA-modified oligonucleotide probes. *Nat Methods* **3**, 27-29 (2006).
294. **N.G. Priya, N. Pandey, R. Rajagopal.** LNA probes substantially improve the detection of bacterial endosymbionts in whole mount of insects by fluorescent *in situ* hybridization. *BMC Microbiol* **12**, 81 (2012).



## Chapter 2

---

### Interactions between uncommon bacteria and *Escherichia coli* in catheter-associated urinary tract biofilms

Andreia S. Azevedo, Carina Almeida, Luís F. Melo, Nuno F. Azevedo.

---

*Biofouling*. 2014. 30(8):893-902. doi: [10.1080/08927014.2014.944173](https://doi.org/10.1080/08927014.2014.944173).

#### Abstract

Most biofilms involved in CAUTIs are polymicrobial, with pathogenic (e.g. *E. coli*) and uncommon bacteria (e.g. *D. tsuruhatensis*) frequently co-inhabiting the same catheter. Nevertheless, there is a lack of knowledge about the role of uncommon bacteria in CAUTIs. Here, single- and dual-species biofilms consisting of *E. coli* and uncommon bacteria (*D. tsuruhatensis*, *A. xylosoxidans*), were evaluated. All species were good biofilm producers (Log 5.84-7.25 CFUs.cm<sup>-2</sup> at 192 h) in artificial urine. The ability of uncommon bacteria to form biofilm appears to be hampered by the presence of *E. coli*. Additionally, when *E. coli* was added to a pre-formed biofilm of the uncommon bacteria, it seemed to take advantage of the first colonizers to accelerate adhesion, even when added at lower concentrations. Results suggest a greater ability of *E. coli* to form biofilms in conditions mimicking the CAUTIs, whatever the pre-existing microbiota and the inoculum concentration.

**Keywords:** *Escherichia coli*, uncommon bacteria, polymicrobial biofilms, urinary tract infections, urinary catheters.



## 2.1 Introduction

Hospital-acquired (nosocomial) infections are frequently related with biofilms formed in medical devices, such as prosthetic heart valves, cardiac pacemakers, urinary catheters, contact lenses and orthopedic devices<sup>1-5</sup>. The higher economic costs associated with these diseases is due to long hospitalization periods for infected patients<sup>1, 6, 7</sup>. The most common nosocomial infections are UTIs<sup>8</sup> and about 80% of these infections, known as CAUTIs, are related to the insertion of catheters in the urinary tract<sup>7, 9</sup>. These medical devices are used in hospital and nursing home settings to relieve urinary retention and incontinence<sup>2</sup>. However, in patients with long-term urinary catheters, the infection is inevitable in most of the cases<sup>10</sup>.

CAUTIs originate from the colonization of the surface of catheters by microorganisms. Indeed, urinary catheters provide an attractive niche for bacterial colonization due to the intermittent flow of warm nutritious urine, leading to the formation and growth of a biofilm<sup>11</sup>. Biofilms have been described as microbial communities attached to a surface and embedded in EPS<sup>12, 13</sup>. In this mode of life, microorganisms can survive in hostile environments, and are protected against external aggressive factors encountered in host tissues (e.g. antibodies, phagocytes, etc.) or other environmentally-challenging conditions (e.g. UV light, extreme temperatures, shear forces, etc.)<sup>14</sup>. In contrast to their planktonic counterparts, cells in the biofilm microenvironment are typically resistant to antibiotics<sup>15</sup>. Consequently, infections on medical devices associated with biofilms are persistent and difficult to eradicate<sup>16</sup>.

Recent studies involving urinary catheters have shown that CAUTIs are mostly polymicrobial<sup>17-19</sup>. The potential pathogens involved in initial adhesion are usually *S. epidermidis*, *E. coli* or *E. faecalis*<sup>20</sup>; but several others species (such as *P. aeruginosa*, *P. mirabilis*, *P. stuartii* and *K. pneumoniae*) can appear in the later stages of infection, in conjugation with initial colonizers<sup>10, 20</sup>. Furthermore, it was recently observed that these pathogenic microorganisms can co-inhabit the catheter surface with other unusual microorganisms with unproven pathogenic potential (e.g. *D. tsuruhatensis*, *A. xylosoxidans*)<sup>18</sup>. While interactions of *E. coli* with other common causes of UTIs, have already been addressed<sup>6, 10, 20, 21</sup>; there is a lack of knowledge about the possible role that these uncommon bacteria have on the rate at which pathogenic microorganisms adhere and form biofilms and, consequently, their effect on the CAUTIs outcome. In fact, some

studies have demonstrated recently, for other pathologies, that the uncommon bacteria could have some important contributions in biofilm infections<sup>22, 23</sup>.

Both pathogenic and uncommon bacteria have in common the ability to form mono or multi-species biofilms on the surface of the urinary catheter<sup>18</sup>, which means that interactions between the different bacterial populations are possible, if not likely. For instance, some of these microorganisms are able to degrade certain components of plastics<sup>24, 25</sup>, which means that some products of their metabolism might feed other microorganisms (e.g. *Escherichia coli*) and, eventually, they could act as primary colonizers of the catheter. In opposition, it might be possible that the colonization by these uncommon bacteria can prevent the colonization by pathogenic bacteria. Hence, understanding the role that uncommon bacteria have on biofilm dynamics might be crucial to help in the development of novel strategies to prevent or minimize bacterial adhesion to catheters.

As such, in here we evaluated single-species (*E. coli*, *D. tsuruhatensis*, *A. xylosoxidans*) and dual-species (*E. coli* / *D. tsuruhatensis*, *E. coli* / *A. xylosoxidans*) biofilm formation in 96-well microtiter plates. To better mimic conditions found in urinary catheters, biofilms were formed in AUM<sup>26</sup> at 37 °C. In order to understand which type of interactions occurs between different species, we compared dual-species biofilms with individual biofilms fitness regarding: total biomass formed, total cells counts and cultivability values. Four additional features were also explored: the growth rates of each microorganism, the siderophore production by *E. coli* and uncommon bacteria, the antimicrobial activity of biofilm supernatants and the influence of a pre-formed biofilm on the adhesion and biofilm formation of a second colonizer.

## **2.2 Material and methods**

### **2.2.1 Bacterial maintenance and inoculum preparation**

For each experiment, *E. coli* CECT 434, *A. xylosoxidans* B3, *D. tsuruhatensis* BM90 were streaked from a frozen stock (-80 °C) on Tryptic Soy Agar (TSA) (Merck, Germany) and grown overnight at 37 °C. *E. coli* CECT 434 was originally isolated from a clinical sample in Seattle, Washington, and is often used in quality control testing; *A. xylosoxidans* B3 was isolated from sewage sludge<sup>27</sup>; *D. tsuruhatensis* BM90 was



previously isolated from water samples collected at 90 m deep in the Tyrrhenian Sea off the coast of Giglio Island, Grosseto, Italy<sup>28</sup>.

Colonies from each species were used to inoculate 75 ml of AUM. Subsequently, the cultures were incubated overnight (16-18 h) at 37 °C, under agitation (150 rpm). Cell concentration was then assessed by optical density (O.D.) at 620 nm, and each inoculum was diluted in AUM in order to obtain a final concentration of  $10^8$  CFUs.ml<sup>-1</sup> or  $10^2$  CFUs.ml<sup>-1</sup>. AUM was prepared as previously described<sup>26</sup>, using the following formulation in one liter of distilled water: peptone 1 g (Merck, Germany), yeast extract 0.05 g (Liofilchem, Italy), lactic acid 1.1 mmol.l<sup>-1</sup> (Fluka, Portugal), citric acid 0.4 g (VWR, Belgium), sodium bicarbonate 2.1 g (Merck, Germany), urea 10 g (VWR, Belgium), uric acid 0.07 g (VWR, Belgium), creatinine 0.8 g (Merck, Germany), calcium chloride.2H<sub>2</sub>O 0.37 g (Merck, Germany), sodium chloride 5.2 g (Merck, Germany), iron II sulphate.7H<sub>2</sub>O 0.0012 g (Merck, Germany), magnesium sulphate.7H<sub>2</sub>O 0.49 g (Merck, Germany), sodium sulphate.10H<sub>2</sub>O 3.2 g (Merck, Germany), potassium dihydrogen phosphate 0.95 g (Merck, Germany), di-potassium hydrogen phosphate 1.2 g (Merck) and ammonium chloride 1.3 g (Merck, Germany) (pH was adjusted to 6.5).

Single- and dual-species biofilms (*E. coli* CECT 434 / *A. xylosoxidans* B3; *E. coli* CECT 434 / *D. tsuruhatensis* BM90) were formed as described below.

### 2.2.2 Biofilm formation assays

First, single-species biofilms were formed to study the biofilm-forming ability of each species. For this, 200 µl of each inoculum in AUM ( $10^8$  CFUs.ml<sup>-1</sup> of initial concentration) were transferred into each well of a 96-well tissue culture plate (Orange Scientific, Belgium). An additional experiment at an initial inoculum concentration of  $10^6$  CFUs.ml<sup>-1</sup> was performed in order to evaluate the influence of initial inoculation level on the biofilm formation of the three species under study (results are presented in Supplemental material).

In order to understand how *E. coli* biofilm-formation is affected in the presence of the uncommon bacteria, a total of 2 species combinations (*E. coli* / *A. xylosoxidans*; *E. coli* / *D. tsuruhatensis*) at the same initial concentration ( $10^8$  CFUs.ml<sup>-1</sup>) were also studied. For dual-species biofilms, equal volumes of each single culture (100 µl) at an initial concentration of  $2 \times 10^8$  CFUs.ml<sup>-1</sup> were used. Tissue culture plates were then

placed in an incubator (FOC 225I - VELP Scientifica, Italy) at 37 °C, under static conditions, during 8 days. Every 48 h the medium was carefully replaced by fresh AUM. Wells containing sterile AUM were used as a control. These assays were performed in triplicate.

In order to test how a pre-formed single-species biofilm affects the subsequent adhesion of a second colonizer, pre-colonization experiments were performed.

- (i) *Pre-colonization with uncommon bacteria*: Wells of a 96-well tissue culture plate were pre-colonized with uncommon bacteria (initial concentration of  $10^8$  CFUs.ml<sup>-1</sup>). After 24 h, the medium was removed, biofilm was washed twice with 0.85% (v/v) sterile saline and 200 µl of *E. coli* suspension (initial inoculum concentration of  $10^2$  CFUs.ml<sup>-1</sup>) were added. The same assay was performed but with initial concentrations of  $10^2$  CFUs.ml<sup>-1</sup> for the uncommon bacteria and  $10^8$  CFUs.ml<sup>-1</sup> for *E. coli*.
- (ii) *Pre-colonization with E. coli*: The experiments described in i) were repeated but microorganisms were added in reverse sequence.
- (iii) *Single-species biofilms*: Single-species biofilms were developed to study biofilm-forming ability at low initial concentration ( $10^2$  CFUs.ml<sup>-1</sup>). These assays were used as controls to compare the results obtained in biofilm experiments i) and ii).

At selected time points (24 h, 48 h, 96 h and 192 h), formation of single- and dual-species biofilms was assessed by CV (crystal violet) staining (for quantification of biomass formed), CFU (colony-forming units) counts (for cultivable cells counts) and DAPI (4'-6-Diamidino-2-phenylindole) staining (for total cells counts), as described below.

### **2.2.3 Cultivability assesement**

The number of cultivable biofilm cells was determined by CFUs. Briefly, at each time point the biofilm was washed twice in 0.85% (v/v) sterile saline to remove loosely attached cells. Subsequently, 200 µl of 0.85% (v/v) sterile saline were transferred into each well of a 96-well plate. Biofilm was sonicated during 4 min (70 W, 35 kHz, Ultrasonic Bath T420, Elma, Germany) and then resuspended by pipetting up and down three times. The sonication step was previously optimized to ensure that all cells were detached from the wells of the microtiter plate, while avoiding cell disruption.

Subsequently, 100 µl of the disrupted biofilm were serially diluted (1:10) in saline solution, and plated in triplicate on TSA. The plates were incubated at 37 °C for 12-16 h (*E. coli*), 24 h (*D. tsuruhatensis*) and 48 h (*A. xylosoxidans*). For dual-species biofilms, different selective agar media were used for a better discrimination between the two species. MacConkey agar (Liofilchem, Italy) was used to assess *E. coli* counts. MacConkey agar is a selective/differential medium, based on lactose fermentation, commonly used to discriminate Enterobacteriaceae. *D. tsuruhatensis* and *A. xylosoxidans* presented a slow growth in this medium, but were easily distinguished due to their non-lactose fermenting phenotype. The other media used include: Cetrimide agar (Liofilchem, Italy) for *A. xylosoxidans* and Simmons Citrate agar (ammonium dihydrogen phosphate 1 g.l<sup>-1</sup> [Merck, Germany]; di-potassium hydrogen phosphate 1 g.l<sup>-1</sup> [Merck, Germany]; sodium chloride 5 g.l<sup>-1</sup> [Merck, Germany]; tri-sodium citrate 2 g.l<sup>-1</sup> [Sigma, USA]; magnesium sulfate 0.2 g.l<sup>-1</sup> [Merck, Germany]; bromothymol blue 0.08 g.l<sup>-1</sup> [Sigma, USA]; agar 13 g.l<sup>-1</sup> [Merck, Germany]) for *D. tsuruhatensis* discrimination. None of these two media were able to recover *E. coli* cells. Afterwards, selective agar plates were incubated at 37 °C during 12-16 h (*E. coli*), 48 h (*A. xylosoxidans*) and 72 h (*D. tsuruhatensis*). The number of cultivable bacterial cells in biofilms was determined and expressed per area of well in contact with AUM (Log CFU.cm<sup>-2</sup>).

As a control test, the selective medium recovery capacity for each microorganism was compared with TSA. With this purpose, one of the experiments in pure culture for each species was performed in the corresponding selective/differential medium and in TSA. No significant differences between the CFU counts in TSA and in the selective/differential media used, were found.

#### **2.2.4 Biomass quantification by the CV assay**

Biomass of single- and dual-species biofilms was quantified by CV staining method<sup>29</sup>. Briefly, the washed biofilm was fixed with 250 µl of 99% (v/v) ethanol for 15 min. Subsequently, ethanol was removed and plates were allowed to air-dry. Then, fixed biofilms were stained with 250 µl of CV (Merck, Germany) for 5 min. The wells were then washed three times with water. The plates were air dried and the dye bound to the adherent cells was resuspended by adding 200 µl of 33% (v/v) glacial acetic acid (Merck, Germany). Finally, plates were placed in agitation up to two minutes and the

O.D. was measured at 570 nm using a microtiter plate reader (Spectra Max M2, Molecular Devices, USA).

### **2.2.5 DAPI staining**

To assess total bacteria cell counts in single- and dual-species biofilms, 100 µl of the sonicated cell suspensions were filtered in a black Nucleopore polycarbonate membrane (Ø 25 mm) with a pore size of 0.2 µm (Whatman, UK). Subsequently the membrane was stained with DAPI (0.2 mg.ml<sup>-1</sup>) (Merck, Germany) and let for 10 min in the dark. Then, the membrane was placed in a microscope slide. Finally, a drop of immersion oil (Merck, Germany) was added and the membrane covered with a coverslip. Cells were analyzed using a Leica DM LB2 epifluorescence microscope connected to a Leica DFC300 FX camera (Leica Microsystems GmbH, Germany). The optical filter combination for optimal viewing of stained preparations (Chroma 61000-V2), consisted of a 545/30 nm excitation filter combined with a dichromatic mirror at 565 nm and suppression filter 610/75. For image capture, Leica IM50 Image Manager, was used. For each sample, a total of 15 fields with an area of 6.03×10<sup>-5</sup> cm<sup>2</sup> were counted and the average was used to calculate the total cells per cm<sup>2</sup>.

### **2.2.6 Determination of bacterial growth rates**

The growth rate for each species at 37 °C on AUM was determined. For this, cells were grown overnight (16-18 h). Subsequently, cells were diluted in order to obtain a final O.D. at 620 of 0.1, incubated at 37 °C and 150 rpm. The growth was monitored by measuring the O.D. at 620 nm every 30 min until the stationary stage. The experiment was performed in duplicate.

### **2.2.7 Siderophores production**

Siderophore production by the studied microorganisms was assessed by using the chrome azurol S solid medium assay, prepared as described by Schwyn and Neilands<sup>30</sup>. Following incubation at 37 °C for 24 h, plates were analyzed for the presence of growth and orange halos.

### 2.2.8 Antimicrobial activity of biofilm supernatants

The presence of antimicrobial activity on biofilm supernatants was assessed on lawns of *E. coli* and the two species of uncommon bacteria. In order to collect the biofilm supernatants, single- and dual-species biofilms were prepared according to the methodology described above. After 72 h, supernatants were recovered, filtered (0.22 µm filter, Frilabo, Portugal) and kept at -20 °C. In order to test for possible contaminations, 10 µl of these supernatants were placed on TSA for 24 h at 37 °C. Lawns of each of the microorganisms were laid onto TSA, using cotton swabs and allowed to air-dry. Then, 10 µl of each supernatant were applied onto the lawns, and left to air-dry. Afterwards, the plates were incubated for 24 h at 37 °C. The formation of halos is indicative of the presence of antimicrobial activity.

### 2.2.9 Determination of the fitness and Malthusina parameter

The fitness of *E. coli* relative to the uncommon bacteria ( $W_{E. coli}$ ), determined for each dual-species biofilms, was estimated as the ratio of the Malthusian parameter ( $m$ ) of each population<sup>31</sup>. The  $m$  parameter is defined as the average rate of increase and was calculated for both species over the time,

$$m = \frac{\ln[N(t_{\text{final}})/N(t_{\text{initial}})]}{t_{\text{final}}} \quad (\text{eq. 2.1})$$

where  $N$  is the value of CFUs.cm<sup>-2</sup> present in the biofilm at initial time and final time points.  $W_{E. coli}$  was determined as,

$$W_{E. coli} = m_{E. coli} / m_{\text{uncommon bacteria}} \quad (\text{eq. 2.2})$$

resulting in a fitness of 1 when competing species are equally fit.

For pre-colonization experiments, in order to understand the effect of a pre-colonized surface on the initial adhesion of a second species, the  $m$  parameter of the added microorganism was calculated after 48 h of its addition.

### 2.2.10 Statistical analysis and data accommodation

Results were compared using One-Way analysis of variance (ANOVA) by applying Levene's test of homogeneity of variance and the Tukey multiple-comparisons

test, using SPSS software (SPSS - Statistical Package for the Social Sciences, Chicago, USA). All tests were performed with a confidence level of 95%. All raw data derived from this study are stored at the 'BioOmics' platform (<http://biofomics.org>)<sup>32</sup>.

## 2.3 Results and discussion

### 2.3.1 Single- and dual-species biofilm experiments

It is now known that CAUTIs-associated biofilms often involve more than one microbial species, causing what can be defined as a polymicrobial disease<sup>17-19</sup>. As *E. coli* is one of the main pathogens involved in these infections<sup>33-36</sup>, it would be expectable that the biofilm forming ability of this microorganism would surpass the ones exhibited by uncommon bacteria. Actually, the assessment of the bacteria growth rate in AUM has shown that uncommon bacteria were found to be slow-growing (values of growth rates: 0.374 h<sup>-1</sup> for *D. tsuruhatensis*; 0.311 h<sup>-1</sup> for *A. xylosoxidans*) when compared to *E. coli* (0.484 h<sup>-1</sup>).

Interestingly, this behavior was not observed for single-species biofilms, either in terms of biofilm biomass (Figure 2.1-a), cultivable cells (Figure 2.1-b) or total cells (Supplemental material - Figure S2.1). In fact, higher biomass values were observed for *A. xylosoxidans*, which reached an O.D. of ~5 at 192 h, when compared with *D. tsuruhatensis* and *E. coli* (O.D. ~1.4 and ~2.4 at 192 h, respectively). Moreover, for *A. xylosoxidans* values, this biomass difference was statistically significant at 192 h ( $p < 0.05$ ).

Regarding cultivability, no significant differences were found for *E. coli*, *A. xylosoxidans* or *D. tsuruhatensis*, with CFU counts ranging between Log 6.61 and Log 7.25 CFUs.cm<sup>-2</sup> ( $p > 0.05$ ) (Figure 2.1-b). All species presented similar values for total cells for the different time points (between Log 6.76 and Log 7.50 cells.cm<sup>-2</sup>) (Figure S2.1).

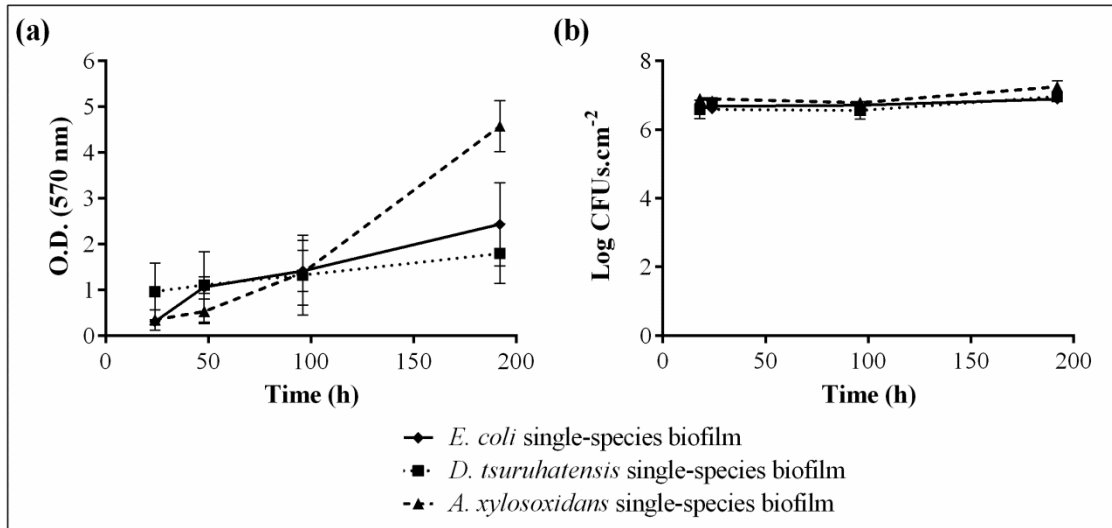


**Figure 2.1** - Biofilm formation for single-species biofilms. Values for (a) total biomass and (b) cultivability. Three independent experiments were performed for each condition. Error bars represent standard deviation.

Regarding the species interaction in dual-species biofilms, to better summarize the results (Supplemental material – Figure S2.2) and visualize the influence of the uncommon bacteria in *E. coli* biofilm formation, we have determined the  $W_{E.coli}$  in dual-species biofilms (Figure 2.2). In the presence of *D. tsuruhatensis* and *A. xylosoxidans*, the  $W_{E.coli}$  slightly increases over the time, reaching a value of 1.12 and 1.07, respectively, after 192 h ( $p < 0.05$ ).

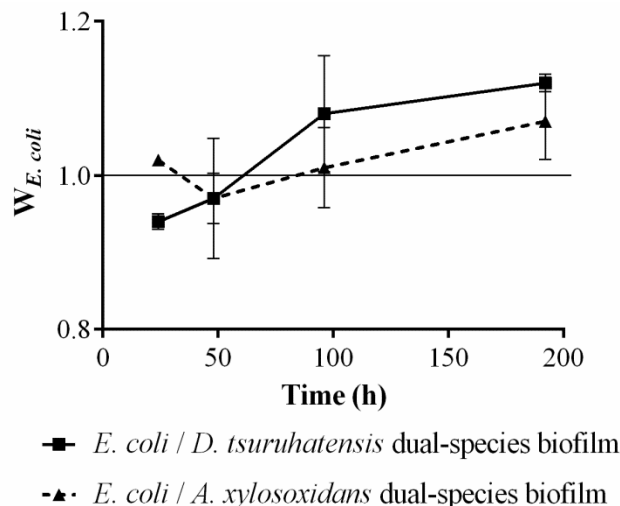


**Figure 2.2** - Relative fitness of *E. coli* in dual-species. Fitness of *E. coli* was determined in the presence of uncommon bacteria (*D. tsuruhatensis* and *A. xylosoxidans*) with simultaneous addition of the bacteria at the same initial concentration ( $10^8$  CFUs.ml<sup>-1</sup>). Data are means of three independent experiments and error bars represent standard deviation.

These conclusions can be observed in more detail in the CV and cultivability graphs (Figure S2.2). CV assays for dual-species biofilms showed that when *E. coli* was co-cultured with the uncommon bacteria the total biomass profiles tend to be more similar to the one of *E. coli* single-species biofilm (Figure S2.2-a,b). In fact, the data of cultivability assays in dual-species biofilms confirmed that *E. coli* ability to form biofilms does not seem to be influenced by the presence of the other species (Figure S2.2-e,f). In addition, dual-species biofilms present similar values for total cells for the different time points (Supplemental material - Figure S2.3) and, as expected, the CFU counts were always lower than the DAPI counts. However, it should be mentioned that the observations here described might be limited to the inoculum concentrations used in this study. To clarify this issue, the influence of initial inoculation level ( $10^6$  CFUs.ml<sup>-1</sup> vs.  $10^8$  CFUs.ml<sup>-1</sup>) on the biofilm formation, was evaluated (Supplemental material - Figure S2.4). No significant differences were found for *E. coli* ( $p > 0.05$  for each point); which indicates that initial inoculum concentration does not seem to have influence in *E. coli* attachment and accumulation over time (Figure S2.4-a). On the other hand, for *D. tsuruhatensis* and *A. xylosoxidans* single-species biofilm formed at an initial concentration of  $10^6$  CFUs.ml<sup>-1</sup>, lower cultivability values were observed for up to 24 h and up to 48 h, respectively. It reflects a delay on its biofilm formation. However, it did not affect the final biofilm concentration, which reached similar values (Figure S2.4-b,c).

It is well known that, in polymicrobial biofilms, the interactions may encourage the coexistence (synergistic interaction) or confer advantage to one species, inhibiting the growth of others (antagonistic interaction)<sup>37-39</sup>. In order to explain the possible interaction between *E. coli* and uncommon bacteria in dual-species biofilm, four additional features were analyzed: antimicrobial activity of biofilm supernatants in single- and dual-species biofilms, siderophores production, growth rate of each species and effect of a pre-formed biofilm on *E. coli* biofilm formation.

### ***2.3.2 Antimicrobial activity of biofilm supernatants and siderophores production***

An important factor in determining the dominant species within a polymicrobial biofilm is the antimicrobial compounds production, which might provide an advantage to the producer species by interfering or killing the neighbor microorganisms<sup>38</sup>.



However, in the present work, examination of antimicrobial compounds in biofilm supernatants, either from single- or dual-species biofilms, suggested that none of the microorganisms secreted compounds able to clearly influence the growth of the others. It might be possible that antimicrobial compounds are present in very low concentrations, as it usually happens for most part of secondary metabolites; which would also appear as a negative result. Also, some other molecules, that interfere with non-essential processes (e.g. quorum sensing molecules), are not detected in this type of assay. Nonetheless, the complete absence of any inhibitory signal suggests that the observed decrease of the uncommon bacteria when co-cultured with *E. coli*, is probably not due to the production of antimicrobial compounds by *E. coli*.

Other type of competitive interaction can be observed in polymicrobial biofilms, in which one microorganism can sequester a limited and essential nutrient, facilitating its dominance over the other species<sup>38</sup>. An example of this competitive behavior involves the iron sequestration by the production, release and uptake of siderophores<sup>38, 40-43</sup>. Siderophores are molecules secreted under low iron availability and are used by microorganisms to sequester the iron available in the medium<sup>38, 44, 45</sup>. The importance of iron acquisition has been reported for the survival of uropathogenic *E. coli* during CAUTIs development<sup>10, 46</sup>. Considering the low iron concentration in urine and its importance for the growth and survival of microorganisms during CAUTIs<sup>10, 47</sup>, this nutrient is expected to be consumed by microorganisms with high ability to produce or utilize siderophores, limiting it to the other microorganisms. Results indicated that *E. coli* produces high levels of siderophores. *A. xylosoxidans* and *D. tusurhatensis* produced siderophores at lower levels (Figure 2.3). Thereby, when *E. coli* is co-cultured with these uncommon bacteria in AUM it can sequester, at a higher extent, iron molecules providing an advantage in iron-depleted conditions, such as in conditions found in CAUTIs.

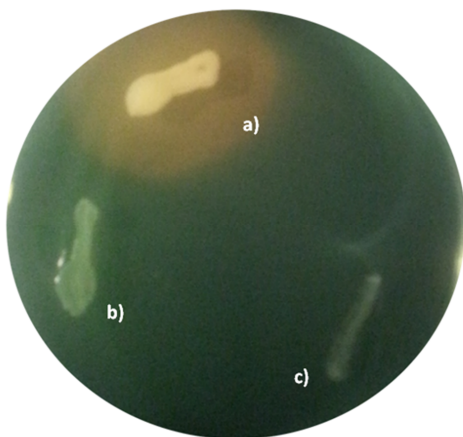


**Figure 2.3** - Screening for siderophores production using the chrome azurol S solid medium assay. (a) An orange halo surrounding the colony indicates that *E. coli* produces high levels of siderophores. The presence of growth without an orange halo indicates that (b) *D. tusurhatensis* and (c) *A. xylosoxidans* produce siderophores at less extent.

### 2.3.3 Pre-colonization assays

Dual-species biofilm experiments suggested that *E. coli* predominates over the co-cultured species. However, nothing is known about the ability of this bacterium to adhere to a pre-colonized surface by the two uncommon bacteria. To confirm whether *A. xylosoxidans* or *D. tusuruhatensis* biofilms affect *E. coli* colonization, 24 h biofilms of *A. xylosoxidans* or *D. tusuruhatensis* were formed and then *E. coli* was added. These experiments were performed with different inoculum concentrations ( $10^8$  CFU.ml<sup>-1</sup> and  $10^2$  CFU.ml<sup>-1</sup>) to see if the inoculation level has influence in the adhesion of a second species to the biofilm.

The addition of *E. coli* to a pre-formed biofilm did not lead to significant changes of total biomass compared to experiments with synchronized addition of species. When *E. coli* was added to 24 h biofilms of the uncommon bacteria, the biomass profile was similar to experiments with synchronized addition of species, no matter the inoculation proportion between the two species. Also, in dual-species biofilms, the concentration of initial inoculum did not seem to have a great influence on biomass production over time (Supplemental material - Figure S2.5 and Figure S2.6). To better understand the possible role that a pre-colonized surface has on the rate at which species adhere and grow, the *m* parameter of the microorganism added to a pre-formed biofilm was determined. This parameter reflects the average rate of increase of each species<sup>31</sup>. Interestingly, the results showed that when a low initial concentration ( $10^2$  CFUs.ml<sup>-1</sup>) of any of the microorganisms was added to a pre-formed biofilm, the population of this species increased more rapidly when compared with the corresponding single-species biofilm (Figure 2.4 and Supplemental material - Figure S2.7 and Figure S2.8).

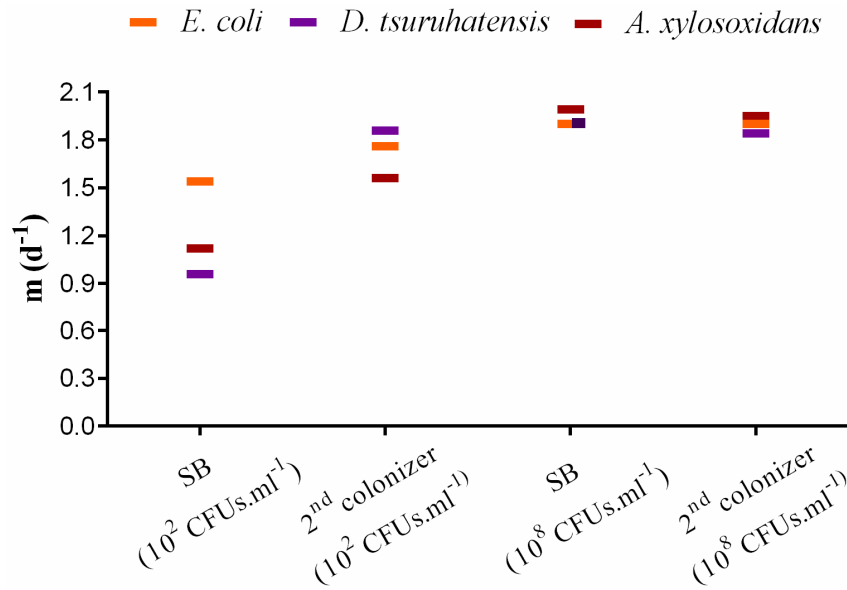


**Figure 2.4** - Values of the Malthusian parameter for pre-colonization experiments. The Malthusian parameter of the second microorganism added to a pre-formed biofilm was determined between time 0 and 48 hours. Values of the Malthusian parameter for single-species biofilms were determined for comparative purpose. SB – Single-species biofilm.

Several biofilms found in both environmental and clinical settings are recognized as polymicrobial structures<sup>2</sup>, and this fact suggests that this diversity provides some advantages for these communities. In fact, it is known that diversity generally protects communities from unstable environmental conditions and, thus, it is likely that bacteria favor the development of polymicrobial structures<sup>14</sup>. Why the apparent induction of polymicrobial populations happens in the specific case of our study remains unclear. It may be, for instance, that the maintenance of uncommon bacteria, even in low densities, might be beneficial for *E. coli* if any environmentally-challenging condition occurs.

Alternatively, or in addition, some of these uncommon bacteria are able to degrade certain components of plastics<sup>24, 25</sup>, which means that the products of their metabolism might be able to feed *E. coli*, explaining why *E. coli* benefit when is co-cultured with uncommon bacteria. However, despite the suitability of the 96-well microtiter plates to simulate the conditions found in catheter-associated urinary tract biofilms<sup>48</sup>, the results of the present work should be replicated using catheter-like materials (eg silicones, latex rubber, etc.). This would allow confirmation if these uncommon bacteria are able to degrade certain components of catheters under conditions found in biofilms associated with CAUTIs.

Taken together, this data seems to indicate that species behavior in dual-species biofilm is also dependent on the population size and physical space available. When cellular concentrations in biofilm were low, competition was not observed; instead, species might benefit from the presence of another colonizer (Figure 2.4). In fact, the adhesion of a second colonizer added at low concentration was accelerated. In opposition, when cellular concentrations reached higher values, the population of uncommon bacteria slightly decreased (Figure S2.2-c,d; and Figure S2.7-d), which suggests that competition has taken place.

A good example of polymicrobial biofilm advantages is provided in the work of Lopes *et al.*<sup>22</sup>. They have studied the role of two novel microorganisms isolated from cystic fibrosis specimens. When *P. aeruginosa* was co-cultured with uncommon bacteria (*I. limosus* and *D. pigrum*), an increase in the tolerance of the dual-species biofilms to most antibiotics was observed<sup>49</sup>. In another study, Sibley *et al.*<sup>50</sup> reported that an avirulent species in combination with *P. aeruginosa* isolated from cystic fibrosis flora has the ability to enhance the pathogenicity of this microorganism and, consequently, to influence the outcome of the infection<sup>50</sup>. In addition, other studies also reported the importance of uncommon pathogens (e.g. *Burkholderia cepacia*, *Stenotrophomonas maltophilia*, *A. xylosoxidans*) in clinical outcome of cystic fibrosis<sup>51, 52</sup>.

Concerning *D. tusurhatensis* and *A. xylosoxidans*, they have been isolated from diverse clinical sources<sup>52-56</sup>, including CAUTIs<sup>18</sup>. Thus, it is expected that these unusual species interact with pathogenic agents and have an important role on biofilm architecture and physiology.

## 2.4 Conclusions

By combining the results obtained in this work, a schematic representation of the dual-species biofilm formation showing the main factors involved on the predominance and coexistence of *E. coli* with uncommon bacteria is proposed (Figure 2.5).

*E. coli* presented a greater ability to form biofilm in conditions mimicking CAUTIs, whatever the pre-existing microbiota, which helps explain the high prevalence of *E. coli* in CAUTIs. Nonetheless, despite the probable non-pathogenic nature of the

two uncommon bacteria, they were also good biofilm producers on abiotic surfaces. Additionally, *E. coli* coexistence with the two uncommon bacteria within dual-species biofilm structures was proved; and, actually, pre-colonization with these species seems to promote the pathogen adhesion.

Results also suggest that species behavior in dual-species biofilm might be dependent on the population size and space to grow. Since diversity within the biofilm population usually represents higher chances to persist in detrimental conditions, coexistence seems to be preferred. But, for mature stages of biofilm formation, competition might take place and then the higher fitness of *E. coli* in this environment becomes evident. In fact, the high *E. coli* rate growth in AUM, in association with high levels of siderophores production, helps explaining the *E. coli* ability to outcompete uncommon bacteria.

In the future, further insights into the resistance profile of these structures might provide an adequate treatment for each patient with an accurate selection of antibiotic and dosage necessary to treat a particular infection originated from a mixed biofilm<sup>18</sup>.

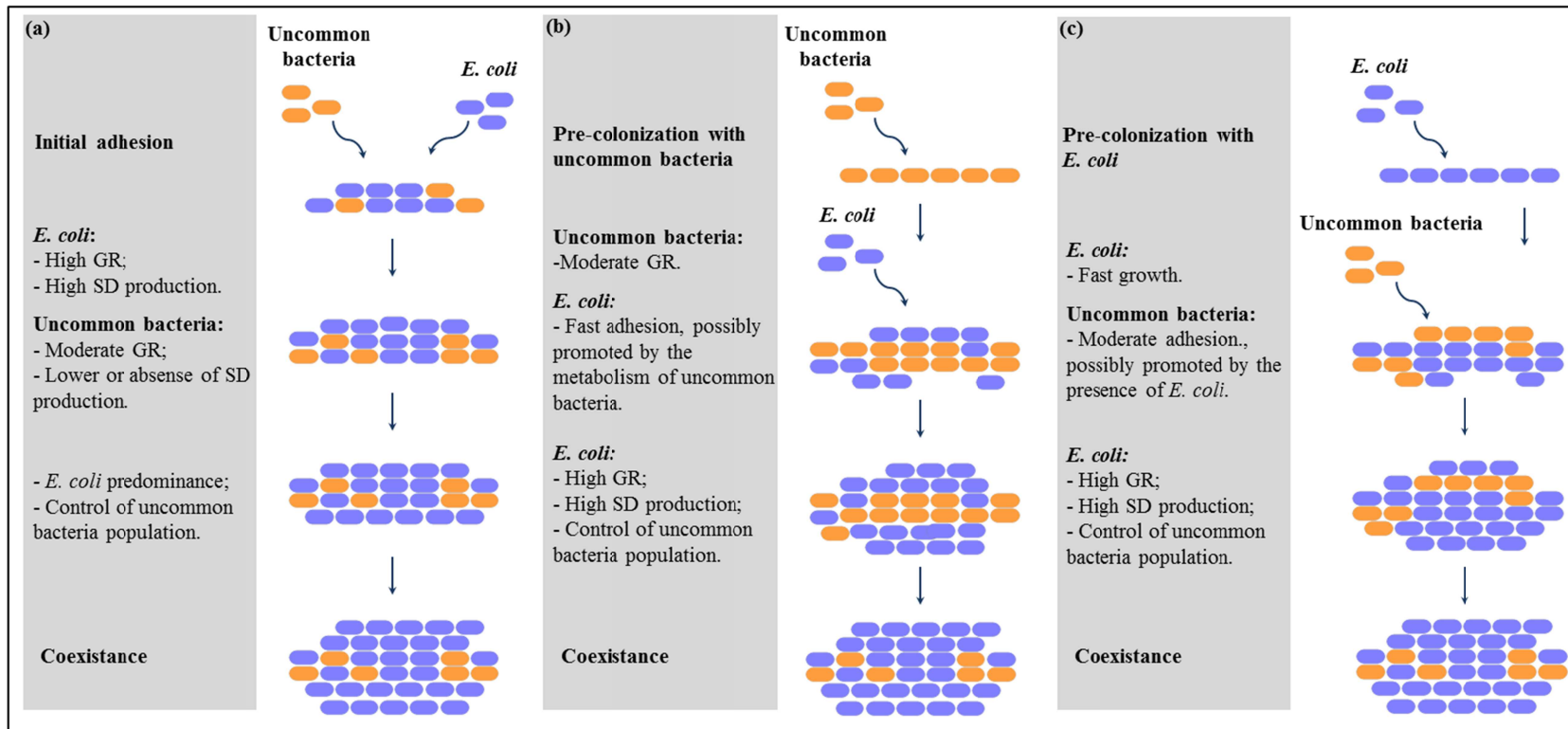


**Figure 2.5** - Schematic representation of the dual-species biofilm formation showing the main factors involved on the predominance and coexistence of *E. coli* with uncommon bacteria. (a) Representation of the interaction between *E. coli* and uncommon bacteria in dual-species biofilm with simultaneous addition of the species; (b) in dual-species biofilm subjected to a pre-colonization step with the uncommon bacteria, followed by the addition of the *E. coli*; and (c) in dual-species biofilms subjected to a pre-colonization step with the *E. coli*, followed by the addition of the uncommon bacteria. Regardless of the initial conditions, the dual-species biofilm tends to a final state of coexistence where *E. coli* predominates over the uncommon bacteria (GR – growth rate; SD – siderophores).

## 2.5 References

1. **S. Silva, M. Negri, M. Henriques, R. Oliveira, D. Williams, J. Azeredo.** Silicone colonization by non-*Candida albicans* *Candida* species in the presence of urine. *J Med Microbiol* **59**, 747-754 (2010).
2. **L. Hall-Stoodley, J.W. Costerton, P. Stoodley.** Bacterial biofilms: from the natural environment to infectious diseases. *Nat Rev Microbiol* **2**, 95-108 (2004).
3. **N.S. Morris, D.J. Stickler.** Encrustation of indwelling urethral catheters by *Proteus mirabilis* biofilms growing in human urine. *J Hosp Infect* **39**, 227-234 (1998).
4. **D. Campoccia, L. Montanaro, C.R. Arciola.** The significance of infection related to orthopedic devices and issues of antibiotic resistance. *Biomaterials* **27**, 2331-2339 (2006).
5. **P. Tenke, B. Kovacs, M. Jackel, E. Nagy.** The role of biofilm infection in urology. *World J Urol* **24**, 13-20 (2006).
6. **L. Ferrieres, V. Hancock, P. Klemm.** Biofilm exclusion of uropathogenic bacteria by selected asymptomatic bacteriuria *Escherichia coli* strains. *Microbiology* **153**, 1711-1719 (2007).
7. **L.T. Curtis.** Prevention of hospital-acquired infections: review of non-pharmacological interventions. *J Hosp Infect* **69**, 204-219 (2008).
8. **R.M. Klevens, J.R. Edwards, C.L. Richards, Jr., T.C. Horan, R.P. Gaynes, D.A. Pollock, D.M. Cardo.** Estimating health care-associated infections and deaths in U.S. hospitals, 2002. *Public Health Rep* **122**, 160-166 (2007).
9. **B. Doyle, Z. Mawji, M. Horgan, P. Stillman, A. Rinehart, J. Bailey, E. Mullin, Jr.** Decreasing nosocomial urinary tract infection in a large academic community hospital. *Lippincotts Case Manag* **6**, 127-136 (2001).
10. **S.M. Jacobsen, D.J. Stickler, H.L. Mobley, M.E. Shirtliff.** Complicated catheter-associated urinary tract infections due to *Escherichia coli* and *Proteus mirabilis*. *Clin Microbiol Rev* **21**, 26-59 (2008).
11. **L. Ganderton, J. Chawla, C. Winters, J. Wimpenny, D. Stickler.** Scanning electron microscopy of bacterial biofilms on indwelling bladder catheters. *Eur J Clin Microbiol Infect Dis* **11**, 789-796 (1992).
12. **P.S. Stewart, M.J. Franklin.** Physiological heterogeneity in biofilms. *Nat Rev Microbiol* **6**, 199-210 (2008).
13. **J.W. Costerton, K.J. Cheng, G.G. Geesey, T.I. Ladd, J.C. Nickel, M. Dasgupta, T.J. Marrie.** Bacterial biofilms in nature and disease. *Annu Rev Microbiol* **41**, 435-464 (1987).
14. **R.M. Donlan, J.W. Costerton.** Biofilms: survival mechanisms of clinically relevant microorganisms. *Clin Microbiol Rev* **15**, 167-193 (2002).
15. **K. Lewis.** Persister cells, dormancy and infectious disease. *Nat Rev Microbiol* **5**, 48-56 (2007).
16. **J.W. Costerton.** Introduction to biofilm. *Int J Antimicrob Agents* **11**, 217-221; discussion 237-219 (1999).
17. **V. Hola, F. Ruzicka, M. Horka.** Microbial diversity in biofilm infections of the urinary tract with the use of sonication techniques. *FEMS Immunol Med Microbiol* **59**, 525-528 (2010).
18. **D.N. Frank, S.S. Wilson, A.L. St Amand, N.R. Pace.** Culture-independent microbiological analysis of foley urinary catheter biofilms. *PLoS One* **4**, e7811 (2009).
19. **S.M. Macleod, D.J. Stickler.** Species interactions in mixed-community crystalline biofilms on urinary catheters. *J Med Microbiol* **56**, 1549-1557 (2007).
20. **M. Matsukawa, Y. Kunishima, S. Takahashi, K. Takeyama, T. Tsukamoto.** Bacterial colonization on intraluminal surface of urethral catheter. *Urology* **65**, 440-444 (2005).
21. **L. Cerqueira, J.A. Oliveira, A. Nicolau, N.F. Azevedo, M.J. Vieira.** Biofilm formation with mixed cultures of *Pseudomonas aeruginosa/Escherichia coli* on silicone using artificial urine to mimic urinary catheters. *Biofouling* **29**, 829-840 (2013).
22. **S.P. Lopes, H. Ceri, N.F. Azevedo, M.O. Pereira.** Antibiotic resistance of mixed biofilms in cystic fibrosis: impact of emerging microorganisms on treatment of infection. *Int J Antimicrob Agents* **40**, 260-263 (2012).

23. **S.P. Lopes, N.F. Azevedo, M.O. Pereira.** Microbiome in cystic fibrosis: Shaping polymicrobial interactions for advances in antibiotic therapy. *Crit Rev Microbiol* **41**, 353-365 (2015).
24. **N.K. Patil, R. Kundapur, Y.S. Shouche, T.B. Karegoudar.** Degradation of plasticizer di-n-butylphthalate by *Delftia* sp. TBKNP-05. *Curr Microbiol* **52**, 369-374 (2006).
25. **N. Wan, J.D. Gu, Y. Yan.** Degradation of p-nitrophenol by *Achromobacter xylosoxidans* Ns isolated from wetland sediment. *Int Biodeter Biodegr* **59**, 90-96 (2007).
26. **T. Brooks, C.W. Keevil.** A simple artificial urine for the growth of urinary pathogens. *Lett Appl Microbiol* **24**, 203-206 (1997).
27. **F. Reinecke, T. Groth, K.P. Heise, W. Joentgen, N. Muller, A. Steinbuchel.** Isolation and characterization of an *Achromobacter xylosoxidans* strain B3 and other bacteria capable to degrade the synthetic chelating agent iminodisuccinate. *FEMS Microbiol Lett* **188**, 41-46 (2000).
28. **M. Fenice, A. Gallo, B. Juarez-Jimenez, J. Gonzalez-Lopez.** Screening for extracellular enzyme activities by bacteria isolated from samples collected in the Tyrrhenian Sea. *Ann Microbiol* **57**, 93-99 (2007).
29. **S. Stepanovic, D. Vukovic, I. Dakic, B. Savic, M. Svabic-Vlahovic.** A modified microtiter-plate test for quantification of staphylococcal biofilm formation. *J Microbiol Methods* **40**, 175-179 (2000).
30. **B. Schwyn, J.B. Neilands.** Universal chemical assay for the detection and determination of siderophores. *Anal Biochem* **160**, 47-56 (1987).
31. **R.E. Lenski, M.R. Rose, S.C. Simpson, S.C. Tadler.** Long-term experimental evolution in *Escherichia coli*. I. Adaptation and divergence during 2,000 generations. *Am Nat* **138**, 1315-1341 (1991).
32. **A. Lourenco, A. Ferreira, N. Veiga, I. Machado, M.O. Pereira, N.F. Azevedo.** BioOmics: a Web platform for the systematic and standardized collection of high-throughput biofilm data. *PLoS One* **7**, e39960 (2012).
33. **S. Niveditha, S. Pramodhini, S. Umadevi, S. Kumar, S. Stephen.** The isolation and the biofilm formation of uropathogens in the patients with catheter associated urinary tract infections (UTIs). *J Clin Diagn Res* **6**, 1478-1482 (2012).
34. **M. Hedlund, R.D. Duan, A. Nilsson, M. Svensson, D. Karpman, C. Svanborg.** Fimbriae, transmembrane signaling, and cell activation. *J Infect Dis* **183**, S47-50 (2001).
35. **C. Svanborg, G. Godaly.** Bacterial virulence in urinary tract infection. *Infect Dis Clin North Am* **11**, 513-529 (1997).
36. **A. Ronald.** The etiology of urinary tract infection: traditional and emerging pathogens. *Am J Med* **113**, 14-19 (2002).
37. **S. Elias, E. Banin.** Multi-species biofilms: living with friendly neighbors. *FEMS Microbiol Rev* **36**, 990-1004 (2012).
38. **M.E. Hibbing, C. Fuqua, M.R. Parsek, S.B. Peterson.** Bacterial competition: surviving and thriving in the microbial jungle. *Nat Rev Microbiol* **8**, 15-25 (2010).
39. **F. Harrison.** Microbial ecology of the cystic fibrosis lung. *Microbiology* **153**, 917-923 (2007).
40. **F. Joshi, G. Archana, A. Desai.** Siderophore cross-utilization amongst rhizospheric bacteria and the role of their differential affinities for Fe<sup>3+</sup> on growth stimulation under iron-limited conditions. *Curr Microbiol* **53**, 141-147 (2006).
41. **V.B. Weaver, R. Kolter.** *Burkholderia* spp. alter *Pseudomonas aeruginosa* physiology through iron sequestration. *J Bacteriol* **186**, 2376-2384 (2004).
42. **A.S. Griffin, S.A. West, A. Buckling.** Cooperation and competition in pathogenic bacteria. *Nature* **430**, 1024-1027 (2004).
43. **E.E. Smith, D.G. Buckley, Z. Wu, C. Saenphimmachak, L.R. Hoffman, D.A. D'Argenio, S.I. Miller, B.W. Ramsey, D.P. Speert, S.M. Moskowitz, J.L. Burns, R. Kaul, M.V. Olson.** Genetic adaptation by *Pseudomonas aeruginosa* to the airways of cystic fibrosis patients. *Proc Natl Acad Sci U S A* **103**, 8487-8492 (2006).
44. **S.C. Andrews, A.K. Robinson, F. Rodriguez-Quinones.** Bacterial iron homeostasis. *FEMS Microbiol Rev* **27**, 215-237 (2003).



45. **C. Ratledge, L.G. Dover.** Iron metabolism in pathogenic bacteria. *Annu Rev Microbiol* **54**, 881-941 (2000).
46. **J.A. Snyder, B.J. Haugen, E.L. Buckles, C.V. Lockett, D.E. Johnson, M.S. Donnenberg, R.A. Welch, H.L. Mobley.** Transcriptome of uropathogenic *Escherichia coli* during urinary tract infection. *Infect Immun* **72**, 6373-6381 (2004).
47. **G.H. Shand, H. Anwar, J. Kadurugamuwa, M.R. Brown, S.H. Silverman, J. Melling.** *In vivo* evidence that bacteria in urinary tract infection grow under iron-restricted conditions. *Infect Immun* **48**, 35-39 (1985).
48. **J.M.R. Moreira, L.C. Gomes, J.D.P. Araújo, J.M. Miranda, M. Simões, L.F. Melo, F.J. Mergulhão.** The effect of glucose concentration and shaking conditions on *Escherichia coli* biofilm formation in microtiter plates. *Chem Eng Sci* **94**, 192-199 (2013).
49. **A.R. Oliveira, A.G. Costa, V.E. Sousa, T.L. Araujo, V.M. Silva, M.V. Lopes, M.V. Cardoso.** Scales for evaluation of the overload of caregivers of patients with stroke. *Rev Bras Enferm* **65**, 839-843 (2012).
50. **C.D. Sibley, K. Duan, C. Fischer, M.D. Parkins, D.G. Storey, H.R. Rabin, M.G. Surette.** Discerning the complexity of community interactions using a *Drosophila* model of polymicrobial infections. *PLoS Pathog* **4**, e1000184 (2008).
51. **A.M. de Vrankrijker, T.F. Wolfs, C.K. van der Ent.** Challenging and emerging pathogens in cystic fibrosis. *Paediatr Respir Rev* **11**, 246-254 (2010).
52. **V. Waters.** New treatments for emerging cystic fibrosis pathogens other than *Pseudomonas*. *Curr Pharm Des* **18**, 696-725 (2012).
53. **A. Lambiase, M.R. Catania, M. Del Pezzo, F. Rossano, V. Terlizzi, A. Sepe, V. Raia.** *Achromobacter xylosoxidans* respiratory tract infection in cystic fibrosis patients. *Eur J Clin Microbiol Infect Dis* **30**, 973-980 (2011).
54. **B. Preiswerk, S. Ullrich, R. Speich, G.V. Bloemberg, M. Hombach.** Human infection with *Delftia tsuruhatensis* isolated from a central venous catheter. *J Med Microbiol* **60**, 246-248 (2011).
55. **L. Amoureux, J. Bador, E. Siebor, N. Taillefumier, A. Fanton, C. Neuwirth.** Epidemiology and resistance of *Achromobacter xylosoxidans* from cystic fibrosis patients in Dijon, Burgundy: first French data. *J Cyst Fibros* **12**, 170-176 (2013).
56. **O. Ciofu, C.R. Hansen, N. Hoiby.** Respiratory bacterial infections in cystic fibrosis. *Curr Opin Pulm Med* **19**, 251-258 (2013).

## 2.6 Supplemental material

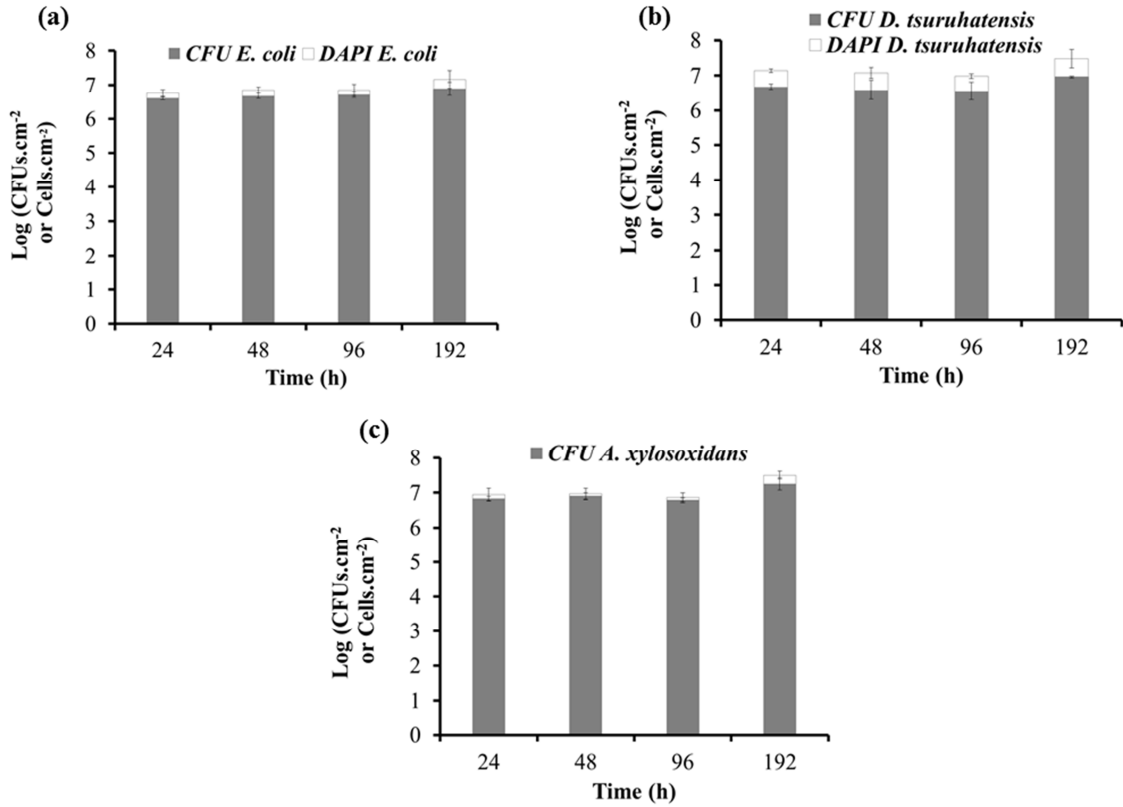


**Figure S2.1** - Total cells and cultivability values for single-species biofilm of (a) *E. coli*, (b) *D. tsuruhatensis* and (c) *A. xylosoxidans*. Three independent experiments were performed for each condition. Error bars represent standard deviation.

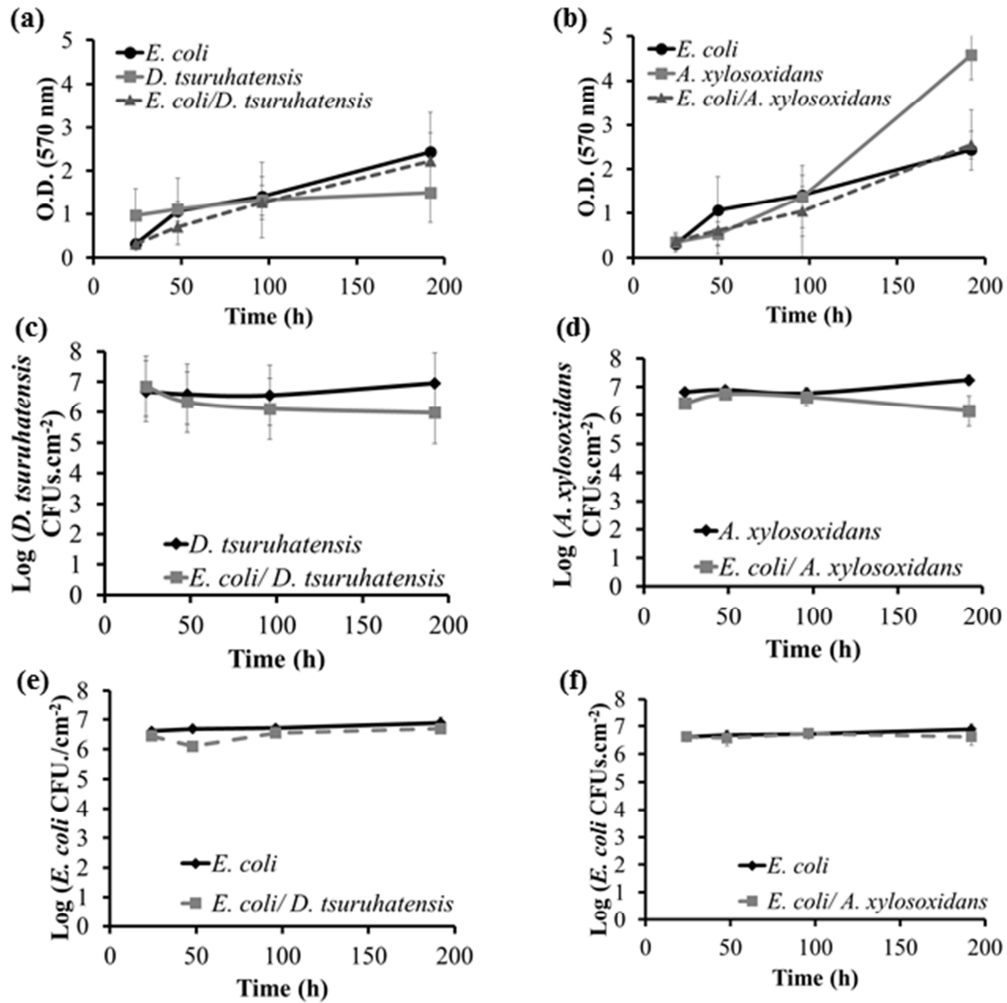


**Figure S2.2** - Biofilm formation for dual-species biofilms, with simultaneous addition of the bacteria at the same concentration ( $10^8$  CFUs.ml<sup>-1</sup>). For all combinations values for (a-b) total biomass and (c-f) cultivability, can be visualized. Pure culture of each microorganism was used for comparative purpose. Three independent experiments were performed for each condition. Error bars represent standard deviation.

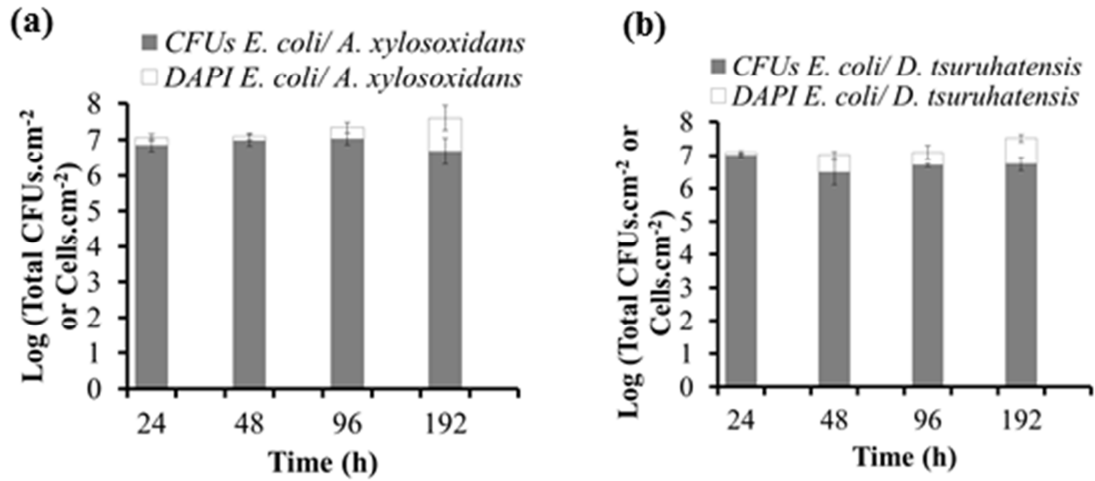


**Figure S2.3** - Total cells and cultivability values for (a) *E. coli* / *D. tsuruhatensis* and (b) *E. coli* / *A. xylosoxidans* dual-species biofilms (synchronized addition of both species). Three independent experiments were performed for each condition. Error bars represent standard deviation.

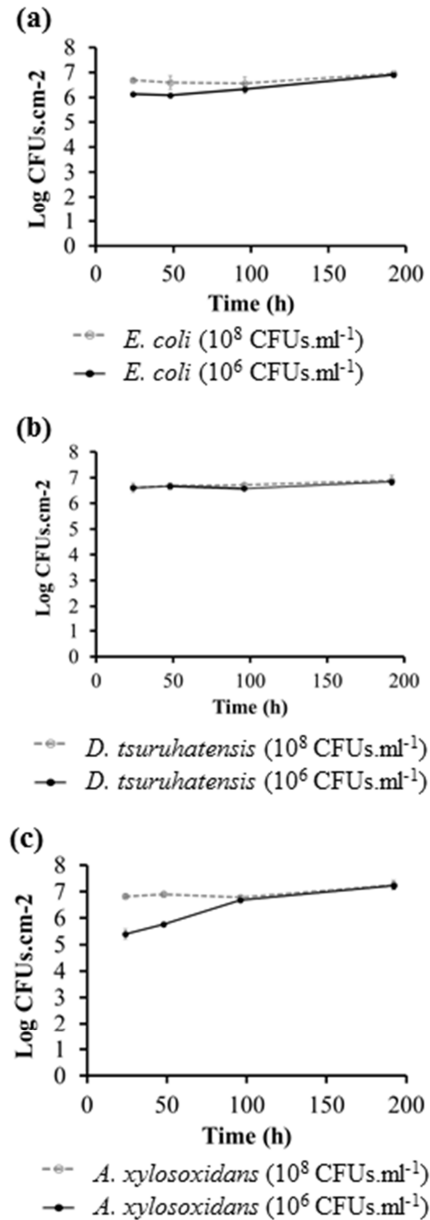


**Figure S2.4** - Effect of the initial inoculum concentration in single-species biofilms. Initial concentrations of  $10^8$  CFUs.ml<sup>-1</sup> and  $10^6$  CFUs.ml<sup>-1</sup> were evaluated for (a) *E. coli*, (b) *D. tsuruhatensis* and (c) *A. xylosoxidans*. Two and three independent experiments were performed for  $10^6$  CFUs.ml<sup>-1</sup> and  $10^8$  CFUs.ml<sup>-1</sup> initial inoculum concentrations, respectively. Error bars represent standard deviation.

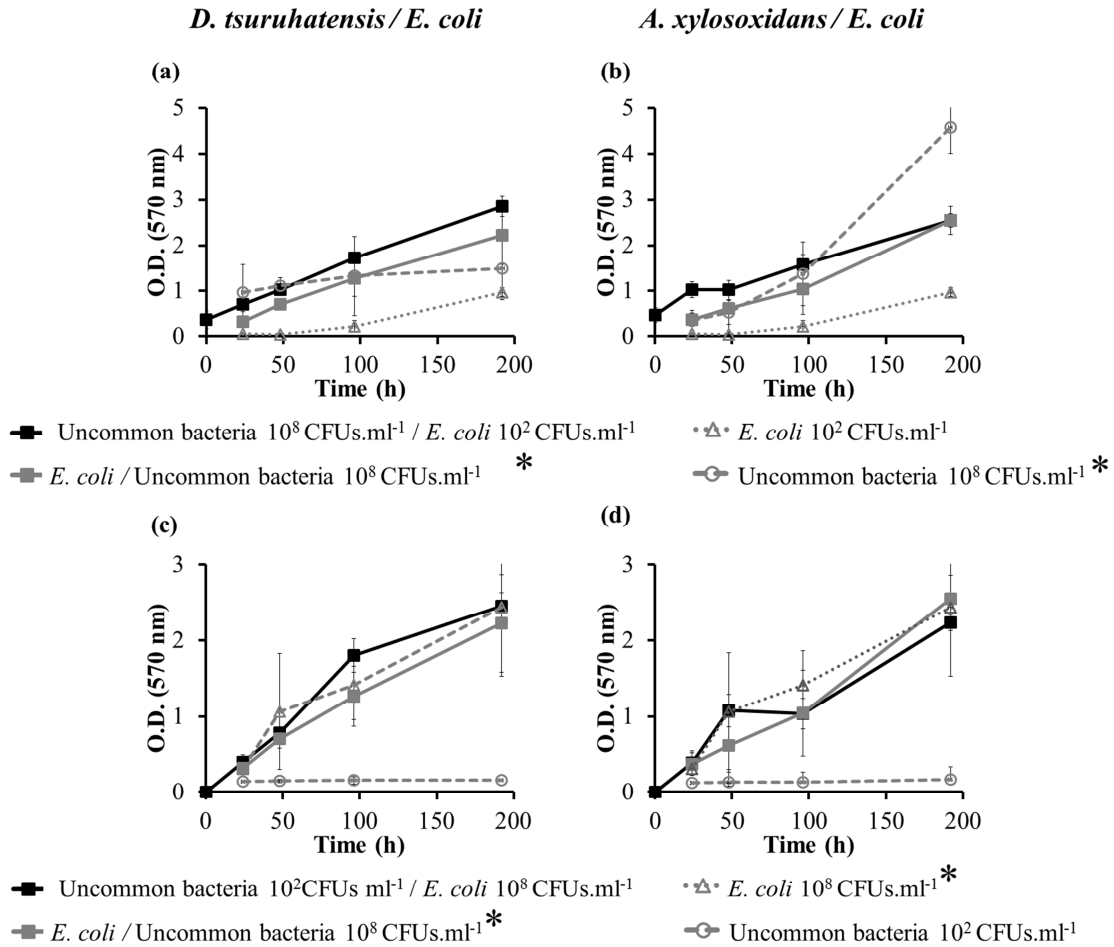


**Figure S2.5** - Total biomass values for dual-species biofilms subjected to a pre-colonization step with the uncommon bacteria, followed by the addition of the *E. coli*. The biofilm data marked with asterisk (\*) are the same represented in Figure 2.1 and Figure 2.2 and were included for comparative purposes. a) and b) present assays with inoculum concentrations of  $10^8$  (uncommon bacteria) and  $10^2$  (*E. coli*) CFUs.ml $^{-1}$ ; while c) and d) present inoculum concentrations of  $10^2$  (uncommon bacteria) and  $10^8$  (*E. coli*) CFUs.ml $^{-1}$ .

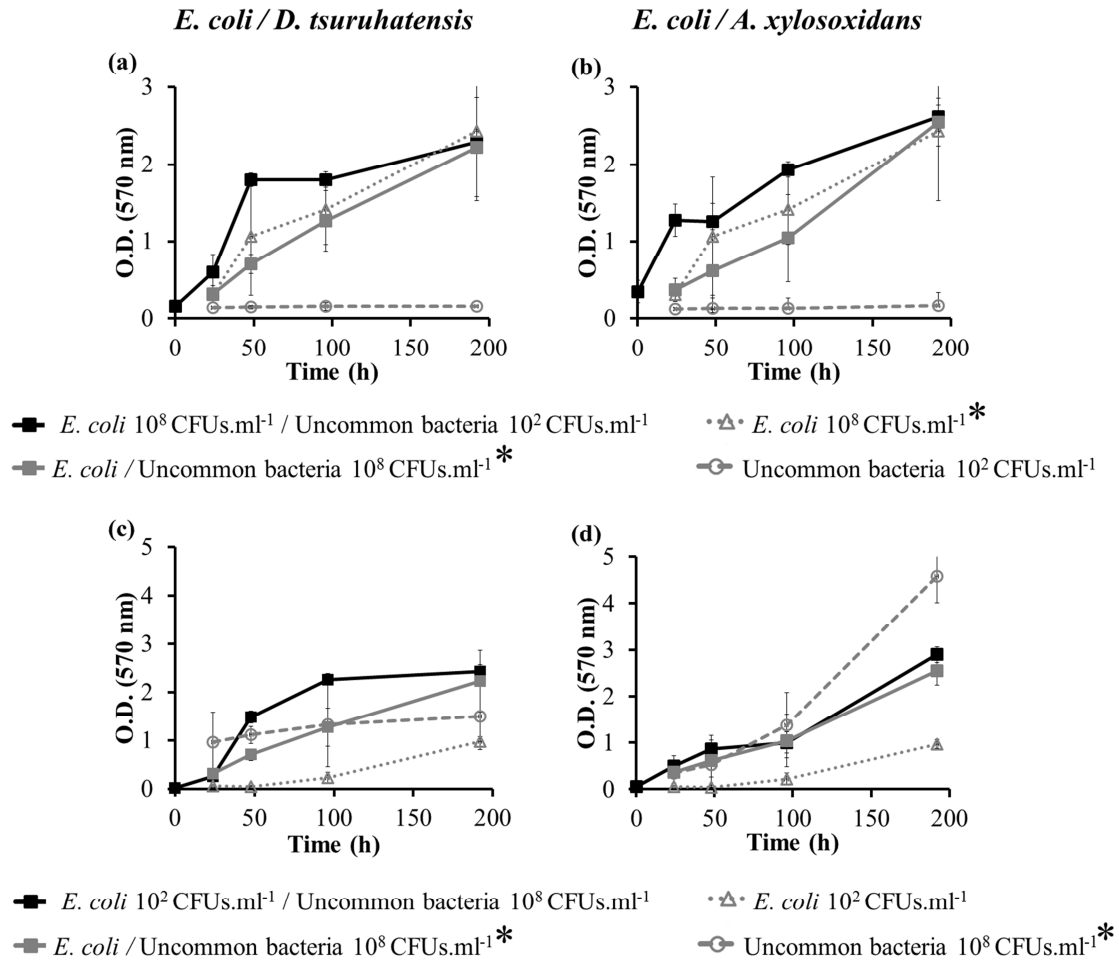


**Figure S2.6** - Values for total biomass for dual-species pre-colonized with *E. coli* during 24h; followed by the addition of the uncommon bacteria. The biofilm data marked with asterisk (\*) are the same represented in Figure 2.1 and Figure 2.2 and were included for comparative purposes. a) and b) present assays with inoculum concentrations of  $10^8$  (*E. coli*) and  $10^2$  (uncommon bacteria) CFUs.ml<sup>-1</sup>; while c) and d) present inoculum concentrations of  $10^2$  (*E. coli*) and  $10^8$  (uncommon bacteria) CFUs.ml<sup>-1</sup>.

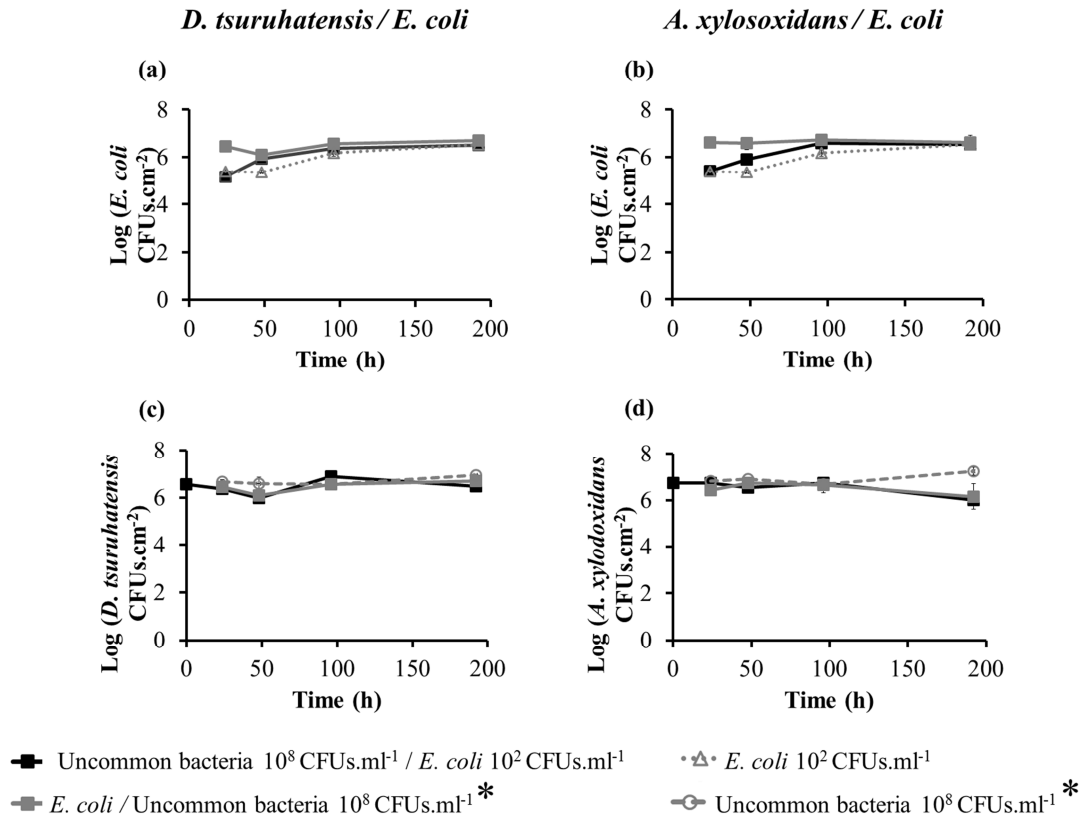


**Figure S2.7** - Cultivability values for (a, c) *E. coli* / *D. tsuruhatensis* and (b, d) *E. coli* / *A. xylosoxidans* dual-species biofilms subjected to a pre-colonization step with uncommon bacteria (10<sup>8</sup> CFUs.ml<sup>-1</sup>), followed by the addition of the *E. coli* (10<sup>2</sup> CFUs.ml<sup>-1</sup>). The biofilm data marked with asterisk (\*) are the same represented in Figure 2.1 and Figure 2.2 and were included for comparative purposes.



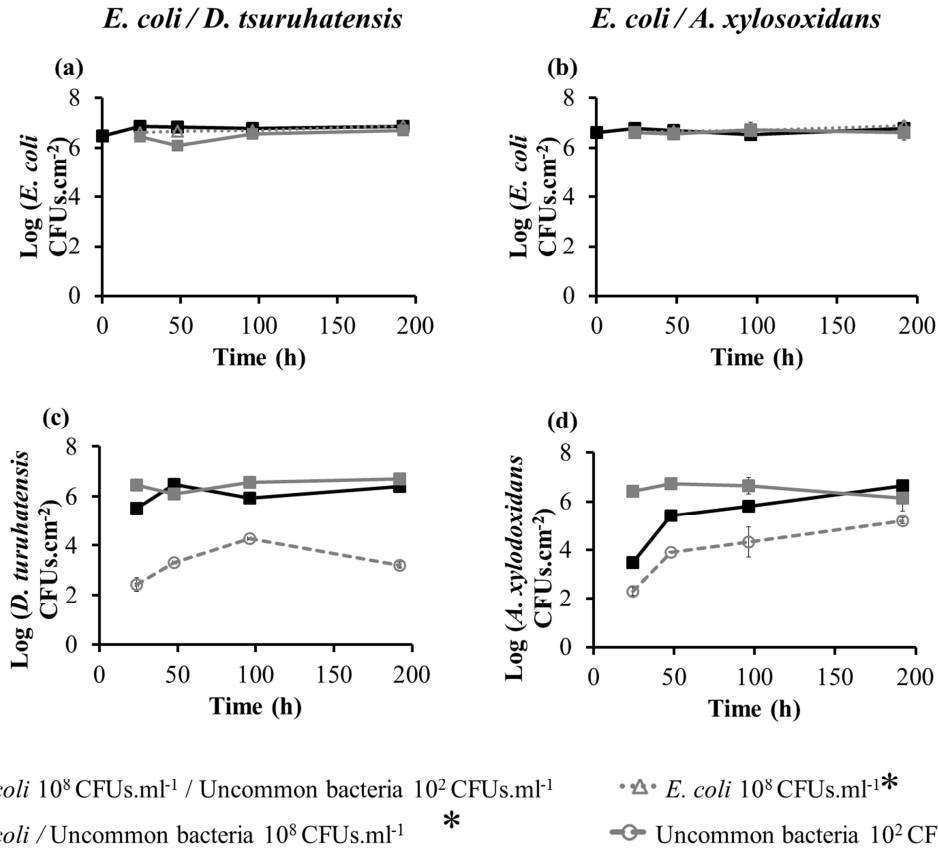


**Figure S2.8** - Cultivability values for (a, c) *E. coli* / *D. tsuruhatensis* and (b, d) *E. coli* / *A. xylosoxidans* dual-species biofilms pre-colonized with *E. coli* (10<sup>8</sup> CFUs ml<sup>-1</sup>) during 24h, followed by the addition of the uncommon bacteria (10<sup>2</sup> CFUs ml<sup>-1</sup>). The biofilm data marked with asterisk (\*) are the same represented in Figure 2.1 and Figure 2.2 and were included for comparative purposes.

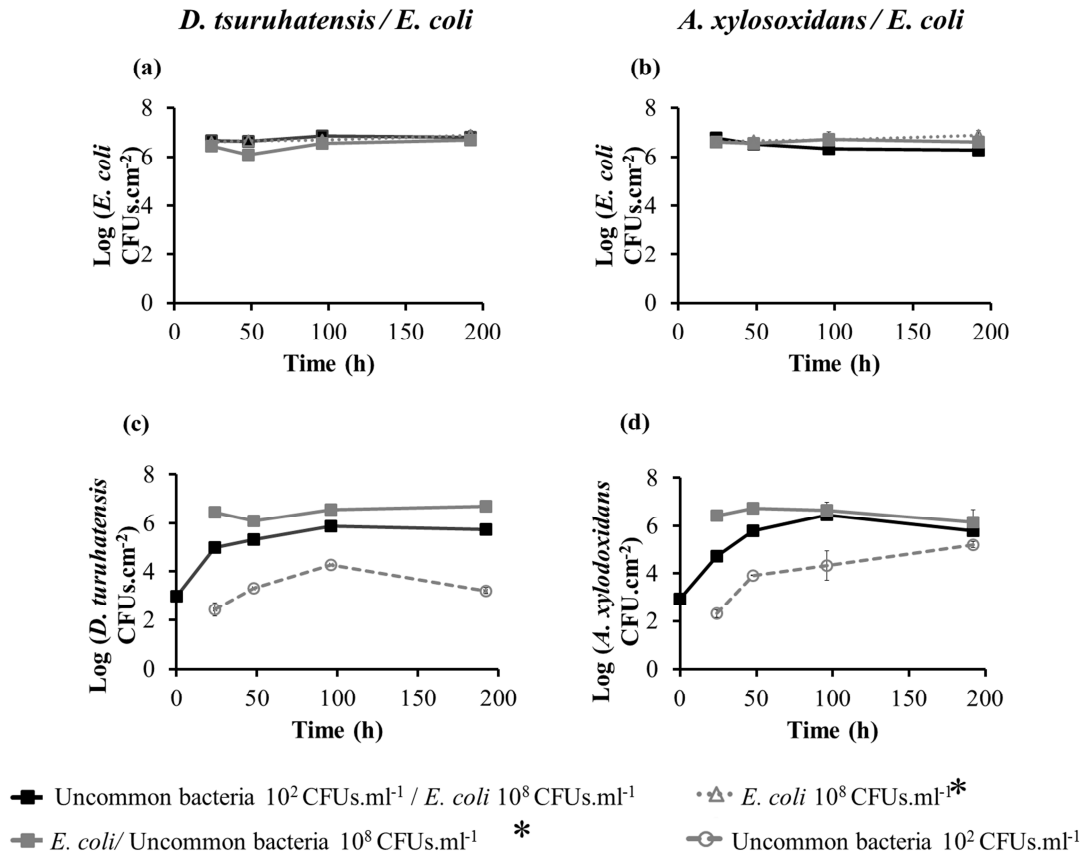


**Figure S2.9** - Cultivability values for (a, c) *E. coli* / *D. tsuruhatensis* and (b, d) *E. coli* / *A. xylooxidans* dual-species biofilms subjected to a pre-colonization step by the uncommon bacteria (10<sup>2</sup> CFUs ml<sup>-1</sup>), followed by the addition of the *E. coli* (10<sup>8</sup> CFUs ml<sup>-1</sup>). The biofilm data marked with asterisk (\*) are the same represented in Figure 2.1 and Figure 2.2 and were included for comparative purposes.

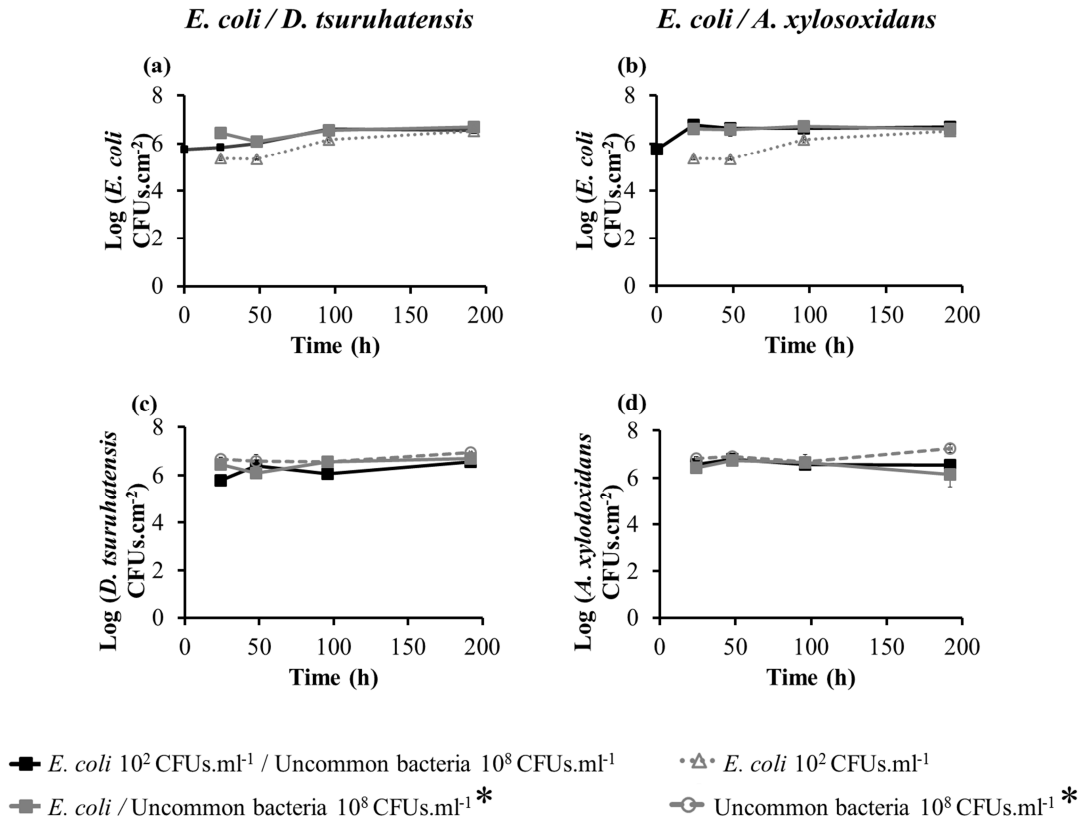


**Figure S2.10** - Cultivability values for (a, c) *E. coli* / *D. tsuruhatensis* and (b, d) *E. coli* / *A. xylosoxidans* dual-species biofilms pre-colonized with *E. coli* (10<sup>2</sup> CFUs ml<sup>-1</sup>) followed by the addition of the uncommon bacteria (10<sup>8</sup> CFUs ml<sup>-1</sup>). The biofilm data marked with asterisk (\*) are the same represented in Figure 2.1 and Figure 2.2 and were included for comparative purposes.



# Chapter 3

---

## Detection and discrimination of biofilm populations using locked nucleic acid/2'-O-methyl-RNA fluorescence *in situ* hybridization (LNA/2'OMe-FISH)

Andreia S. Azevedo, Carina Almeida, Bruno Pereira, Pedro Madureira, Jesper Wengel, Nuno F. Azevedo.

---

*Biochemical Engineering Journal*. 2015.104:64-73. doi:[10.1016/j.bej.2015.04.024](https://doi.org/10.1016/j.bej.2015.04.024).

### Abstract

Polymicrobial biofilms are the dominant form in nature. The application of FISH-based techniques to the discrimination of biofilm populations might contribute to the understanding of microorganism interactions in these structures, and might allow the development of efficient strategies to prevent or minimize biofilm-associated diseases. This work presents the first study that develops, optimizes and validates a multiplex FISH procedure using LNA and 2'OMe oligonucleotides probes for the *in vitro* discrimination within mixed populations. As a case study, *E. coli*, the major cause of UTIs, and three other uncommon colonizers of urinary catheters (*D. tsuruhatensis*, *A. xylosoxidans* and *B. fungorum*) with unproven pathogenic potential, were selected. Specific probes for these species were designed and optimized for specific hybridization in multiplex experiments. Results showed that the LNA/2'OMe-FISH method performed well in multiplex experiments and presented a good correlation with total and cultivability counts, regardless of the cells physiological state. In fact, the method was also able to report variations of viable but non-cultivable populations. Further analysis of mixed biofilm structures by CLSM provided a clear discrimination in three dimensions between the localization of the different populations.

**Keywords:** Biofilms, DNA, Microbial Growth, RNA, LNA/2'OMe-FISH, confocal laser scanning microscopy.



### 3.1 Introduction

In Nature, it is well established that the microorganisms form biofilm structures in response to hostile environmental conditions. In this mode of life, bacteria live predominantly adhered to abiotic or biotic surfaces embedded within a self-produced matrix of EPS<sup>1, 2</sup>. Typically, the bacterial biofilms are mostly polymicrobial and are responsible for most public health (e.g. device-related infections, persistent and recurrent infections)<sup>3-5</sup>, industrial (e.g. food processing)<sup>6</sup> and environmental (e.g. drinking water distribution)<sup>7</sup> problems.

Biofilm dynamics and interactions have received little attention as most studies have assessed single-species adhesion and biofilm formation<sup>8-10</sup>, due to the lack of adequate methodologies to discriminate the populations *in situ*<sup>11, 12</sup>. Recent advances in fluorescence-based techniques and in molecular biology allow *in situ* studies of the spatial organization and the species interactions in bacterial biofilms<sup>13-15</sup>. For instance, the Green fluorescence protein (GFP) has been applied to monitor the development of polymicrobial biofilms *in situ*<sup>15, 16</sup>. However, this technique requires the construction of strains that express GFP and is thus not applicable to natural biofilm samples. Alternatively, researchers have been using a different molecular biology approach, namely FISH<sup>17</sup>. FISH is used for the identification/detection of microorganisms based on its phylogenetic markers at 16S or 23S rRNA, particularly abundant in viable cells<sup>17</sup>. It is based on the hybridization of a fluorescent oligonucleotide probe with a conserved rRNA sequences, and subsequent detection by epifluorescence microscopy, CLSM or flow cytometry. FISH in combination with CLSM is being increasingly used to visualize/study the co-localization of each species in biofilm, and can be useful to quantify the microbial populations without disturbing biofilm structure (see examples<sup>11, 18</sup>).

Taking advantage of progress within nucleic acid mimics development, notably PNA, LNA, and 2'OMe, we were aiming at improving FISH efficiency<sup>19-22</sup>. Despite the potential of the different nucleic acid mimics, studies regarding the application of FISH to assess the spatial species organization in biofilm samples have been limited to rather few PNA probes (some examples<sup>11, 18, 23-25</sup>). These studies have shown that the PNA-FISH method is a robust technique able to discriminate and locate the species within biofilms. Despite the absence of studies applying other mimics to biofilm

characterization, the properties of other molecules are promising. For instance, the use of LNA probes offers several advantages compared to DNA probes, including a greater affinity toward DNA/RNA targets, a higher bio-stability (resistance to nuclease degradation), a better signal-to-noise ratio, and a better sensitivity and specificity<sup>26-28</sup>. In addition, LNA probes are highly soluble in water and were found to hybridize with RNA (and DNA) more efficiently than PNA probes. Thus, for at least some FISH applications, the use of LNA would be advantageous comparing to PNA<sup>29-31</sup>.

LNA is a RNA analogue which contains a ribose ring locked by an O2'-C4'-methylene linkage resulting in a *N*-type (C3'-*endo*) furanose ring conformation<sup>32, 33</sup>. The 2'OMe is another RNA mimic which – though not locked – preferentially displays a C3'-*endo* furanose ring conformation, enhancing its affinity for RNA targets<sup>34</sup>. It was reported that the introduction of LNA nucleotides at every third position in a 2'OMe probe increases the target affinity with a concomitant increase in sensitivity<sup>22</sup>. In fact, the remarkable hybridization properties of LNA-modified probes enable the use of these molecules in FISH experiments<sup>20</sup>. For example, LNA-modified probes might be used for therapeutic (e.g. via inhibition of gene expression)<sup>35, 36</sup> and for diagnostic (e.g. for the detection of microRNAs and for single nucleotide polymorphism genotyping)<sup>37, 38</sup> purposes. However, there are no available studies regarding their application for the detection/identification of bacterial populations within a biofilm. As such, this article describes the first development and validation of FISH method to assess the biofilm spatial organization and the species distribution/discrimination without disturbing the biofilm structure, using the LNA technology (LNA/2'OMe probes) in combination with CLSM.

As a case study, we selected *E. coli*, the major cause of urinary tract infections<sup>39-41</sup>, and three other uncommon colonizers of urinary catheters (*D. tsuruhatensis*, *A. xylosoxidans* and *B. fungorum*). Despite their unproven pathogenic potential, it was reported that these microorganisms can coexist on the catheter surface with pathogenic bacteria (e.g. *E. coli*)<sup>42</sup>. In fact, CAUTIs are the most common nosocomial infection, but there is a lack of knowledge about the impact that polymicrobial biofilms have on CAUTIs outcome and, particularly, on the role that these uncommon bacteria have on outcome of this type of infection. The ability of LNA/2'OMe oligonucleotide probes to discriminate the biofilm populations would give insights on the type of interactions (e.g. symbiotic, antagonistic, and synergistic) that might occur between different species, and



thus could provide valuable knowledge on how to prevent, minimize or treat these infections.

## 3.2 Material and methods

### 3.2.1 Culture of bacterial strains

The bacterial strains, *E. coli* CECT 434, *A. xylosoxidans* B3, *D. tsuruhatensis* BM90 and *B. fungorum* DSM 17061, were maintained on TSA (Merck, Germany) and incubated at 37 °C. Single colonies were streaked onto fresh plates at 37 °C for 20-24 h (for *E. coli*, *A. xylosoxidans*, *D. tsuruhatensis*) or 48 h (for *B. fungorum*) prior to the experiments.

### 3.2.2 Design and theoretical evaluation of oligonucleotide probes

Oligonucleotide probes with different sizes (13 bp and 16 bp) were designed and synthesized to increase the chances of finding oligonucleotide probes that work at the same temperature (Table 3.1). The oligonucleotide probe design and the theoretical specificity and sensitivity assessment were performed as described in Almeida *et al.*<sup>43</sup>.

**Table 3.1** - Sequence of LNA/2'OMe oligonucleotide probes synthesized in this study.

Bacteria	Name	Sequence (5'Label-3')
<i>E. coli</i>	Ec1505_LNA/2'OMe_13	FAM-IGmCmCITmCmAIGmCmCITmUmGIA
	Ec1505_LNA/2'OMe_16	FAM-ICmAmCIGmCmCITmCmAIGmCmCITmUmGIA
<i>D. tsuruhatensis</i>	Dt404_LNA/2'OMe_13	CY3-IGmAmGICmUmUITmUmUICmGmUIT
	Dt404_LNA/2'OMe_16	CY3-IGmAmGICmUmUITmUmUICmGmUITmCmCIG
<i>B. fungorum</i>	Bf411_LNA/2'OMe_13	CY3-ITmAmUITmAmAICmCmAICmGmGIC
	Bf411_LNA/2'OMe_16	CY3-IGmGmUAmUmUAmAmCICmAmCIGmGmCIG
<i>A. xylosoxidans</i>	Ax590_LNA/2'OMe_13	CY3-IAmAmAITmGmCIAmGmUITmCmCIA
	Ax590_LNA/2'OMe_16	CY3-IAmAmAITmGmCIAmGmUITmCmCIAmAmAIG

LNA nucleotide monomers are represented with "l"; 2'-OMe-RNA monomers are represented with "m". Labels: FAM - Fluorescein; Cy3 - Cyanine 3.

### 3.2.3 Synthesis and purification of LNA/2'OMe oligonucleotide probes

Based on previous studies<sup>20, 22</sup>, LNAs were incorporated at every third 2'OMe monomer. The LNA/2'OMe oligonucleotide probes included a PS backbone instead of

a phosphodiester. The PS monomers include replacement of one of the two non-bridging oxygen atoms by a sulfur atom at each internucleotide linkage<sup>44</sup>. The choice of this type of modifications was also based on a previous work of our group<sup>20</sup>, which demonstrated that LNA/2'OMe oligonucleotide probes with a PS linkage are good candidate probes to be used in FISH experiments. Oligonucleotide synthesis was carried out on an automated nucleic acid synthesizer (PerSpective Biosystems Expedite 8909 instrument) under anhydrous conditions in 1.0  $\mu\text{mol}$  scale, according to Fontenete *et al.*<sup>20</sup>.

#### **3.2.4 Melting temperature analysis**

In order to predict optimal hybridization temperatures for each oligonucleotide probe, the Kierzek website (<http://rnachemlab.ibch.poznan.pl/calculator2.php>) was used. Here, the thermodynamic parameters are calculated for a  $10^{-4}$  M oligonucleotide probe concentration. A lower concentration, 200 nM, was used in our FISH experiments. Thus, as the probe concentration affects the  $T_m$  and as it is also the case for the denaturant agent, the data provided by this software was only used as an indicative value. To address this problem, the  $T_m$  values were also experimentally determined as described by Fontenete *et al.*<sup>20</sup>.

#### **3.2.5 FISH protocol development**

Standard hybridization procedures on glass slides were performed in order to determine the optimal hybridization temperature of each oligonucleotide probe on pure cultures. Nonetheless, since flow cytometry is the easiest way to quantify the bacterial populations, FISH signals at selected hybridization temperatures were confirmed by performing the hybridizations in suspension.

Hybridization on slides and in suspension was performed as previously described<sup>19, 43, 45</sup>, with a few modifications. Briefly, cellular suspensions from each species were prepared at approximately  $10^8$  CFU.ml<sup>-1</sup> and then 20  $\mu\text{l}$  samples were spread on epoxy-coated microscope glass slides (Thermo Scientific, USA). The slides were air-dried. Then, smears of each species were immersed in 4% (v/v) paraformaldehyde and 50% (v/v) ethanol for 15 min each at room temperature followed by air drying. Subsequently, 20  $\mu\text{l}$  of hybridization buffer (0.5 M of urea [VWR BHD Prolabo, Belgium], 50 mM Tris-HCl [Fisher Scientific, USA], 0.9 M NaCl [Panreac,

Spain]; pH 7.5) with 200 nM of the respective probe, were added. The samples were covered with coverslips and incubated in moist chambers at the hybridization temperature under analysis (from 51 °C to 59 °C) during 90 min. Next, the coverslips were removed and the slides were washed in a pre-warmed washing solution (5 mM Tris Base [Fisher Scientific, USA], 15 mM NaCl [Panreac, Spain] and 1% Triton X [Panreac, Spain]; pH 10) for 30 min at the hybridization temperature. Finally, the glass slides were allowed to air dry before microscopic visualization. The FISH procedure in suspension was also performed as previously described<sup>19, 20, 43</sup>. Briefly, cellular suspensions from each species (and also mixtures of the different species) were centrifuged (10.000 x g, 5 min) and fixed in 400 µl of 4% (v/v) paraformaldehyde for 1 h at room temperature. After centrifugation, fixed cells were resuspended in 500 µl of 50% (vol/vol) ethanol and incubated at -20 °C for 30 min. Then, 100 µl of fixed cells were mixed in 100 µl of 2 × concentrated hybridization solution (as described above) with 400 nM of probe and incubated at the optimal hybridization temperature for 90 min. Afterwards, samples were centrifuged, resuspended in 500 µl of washing solution (as described above) and incubated at the optimal hybridization temperature for 30 min. Subsequently, the suspension was pelleted by centrifugation and resuspended in sterile water. Finally, 20 µl of the suspension was spread on a microscope slide which was allowed to air dry before microscopy visualization. Three independent experiments were performed at the optimal temperatures of the oligonucleotide probes selected for subsequent experiments. All samples were visualized with other available filters to check for autofluorescence. Additionally, for each experiment, a negative control was performed simultaneously, without the addition of the oligonucleotide probe. The samples were stored at 4 °C in the dark for a maximum of 24 h before microscopy analysis.

The specificity of each oligonucleotide probe was evaluated in a culture smear of the remaining species selected for this study, at the optimal hybridization temperature. In addition, since probes are intended to work in multiplex experiments, it is important to confirm the ability of the oligonucleotide probes to discriminate between the species. A mixture of two probes was applied simultaneously in a mixed smear of the two corresponding species. For this, 10 µl of the final suspension from each species were mixed, spread on glass slides and hybridization was performed as described above.

### **3.2.6 Microscopic visualization and image quantification**

For image acquisition a Leica DM LB2 epifluorescence microscope (Leica Microsystems GmbH, Germany) equipped with Leica DFC300 FX camera (Leica Microsystems GmbH, Germany) and filters capable of detecting the LNA/2'OMe oligonucleotide probes (BP 450-490, FT 510, LP 515 for FAM-labelling and BP 570/20, FT 590, LP 640/40 for Cy3-labelling) was used. For image capture, Leica IM50 Image Manager, was used and the fluorescence intensity of each oligonucleotide probe (at different temperatures) was quantified in the microscopy images using the ImageJ program<sup>46</sup>. The quantification by ImageJ software was performed in order to determine the average fluorescence intensity of each image obtained by epifluorescence microscopy. Data was plotted as mean of arbitrary fluorescence units (AFU) which represented the mean fluorescence intensity.

### **3.2.7 LNA/2'OMe-FISH correlation with cultivability and PI staining**

In order to determine whether the LNA/2'OMe-FISH method is able to detect bacteria in different physiological states, the correlation between LNA/2'OMe-FISH counts, CFUs counts (for cultivable counts assessment) and propidium iodide (PI) staining (for total cells counts assessment) was performed at selected time points of the bacterial growth (lag phase, exponential phase, early stationary phase and late stationary phase).

Bacterial growth curves were previously assessed in Tryptic Soy Broth (TSB) (Merck, Germany) as described in sub-section 2.2.6 (Chapter 2). Cells were harvested at different growth stages for cultivability, LNA/2'OMe-FISH and total cells assessments. The quantification of cells by LNA/2'OMe-FISH was performed in suspension as described above (sub-section 3.2.5). The number of cultivable cells was determined by standard CFU counts as described in sub-section 2.2.3 (Chapter 2). The plates were incubated at 37 °C for 16 h (*E. coli*), 24 h (*D. tsuruhatensis*) and 48 h (*A. xylosoxidans* and *B. fungorum*). For PI staining, 100 µl of fixed cells (prepared as described in sub-section 3.2.5) were centrifuged at 10.000 x g for 5 min, and resuspended in 100 µl of PI (Invitrogen, Portugal; 50 µg.ml<sup>-1</sup>). After 10 min in the dark at room temperature, the cell suspension was centrifuged and the cells were resuspended in saline solution.

The counting of the stained cells (by PI or LNA/2'OMe-FISH) was performed by flow cytometry. Flow cytometry analysis was performed using an EPICS XL flow

cytometer containing a low-power air-cooled 15 mW blue (488 nm) argon laser. Data analyses were performed with the EXPO32ADC software (Beckman Coulter, Brea, USA). All experiments were repeated in triplicate and negative controls without probe were included in every analysis. Flow cytometric analyses of samples were performed based on both scattering signals (forward scatter and side scatter), FL-1 and FL-3. FAM fluorescence was detected on the FL-1 channel (BP530/30) and PI fluorescence was detected on the FL-3 channel (LP650). For all detected parameters, amplification was carried out using logarithmical scales. For the FISH and PI counts, 10  $\mu$ l of the microsphere suspension (6  $\mu$ m; Life Technologies, USA) was added to 200 ml of phosphate buffered saline containing 10  $\mu$ l of the stained cell suspension. The mixture was vortexed and analyzed by flow cytometry.

All the data from CFU, LNA/2'OMe-FISH and PI counts values were Log transformed and used to calculate the Pearson correlation coefficient for each species (LNA/2'OMe-FISH vs. CFU counts; and LNA/2'OMe-FISH vs. PI counts); a linear regression model was also used to adjust the data. These experiments were performed in duplicate.

### 3.2.7.1 Resazurin assay

Resazurin is a blue fluorescent dye which is reduced by viable cell bacteria to a pink colored resofurin. The amount of conversion from blue to pink is proportional to the number of viable cells<sup>47</sup>. The resazurin assay was performed in order to check the viability of *B. fungorum* during the growth curve in TSB medium. At selected time points of the growth of the bacterium (lag phase, exponential phase, early stationary phase and late stationary phase), 190  $\mu$ l of *B. fungorum* suspension was dispensed into wells (8 wells) of a 96-well microtiter plate (Orange Scientific, Belgium) followed by the addition of 10  $\mu$ l of 0.1 g.l<sup>-1</sup> resazurin (Sigma-Aldrich, USA) solution<sup>48</sup>. Plates were incubated during 90 min in darkness at 37 °C<sup>49</sup>. Afterwards, the fluorescence was measured ( $\lambda_{\text{excitation}}=570$  nm and  $\lambda_{\text{emission}}=590$  nm) using a microtiter plate reader (SpectraMax M2E, Molecular Devices, UK)<sup>48</sup>. Wells containing sterile TSB were used as a control. The experiment was performed in duplicate.

### 3.2.8 Spatial discrimination of biofilm population using LNA/2'OMe-FISH

In other to evaluate whether LNA/2'OMe-FISH would be useful to discriminate and elucidate the spatial organization of the biofilm populations without disturbing the

biofilm structure, CLSM was used to visualize *in situ* hybridized single- and dual-species biofilm samples. Single- (*B. fungorum*) and dual-species biofilms (*E. coli* / *B. fungorum*) were formed as previously described<sup>11, 25</sup>. Briefly, the strains were grown overnight in AUM and then the inoculum was diluted in AUM in order to obtain a final concentration of  $1 \times 10^5$  CFUs.ml<sup>-1</sup>. AUM was prepared as previously described<sup>50</sup>. For single-species biofilms, 6 ml of each inoculum were transferred to 6-well tissue culture plate (Orange Scientific, Belgium) containing coupons of silicone, prepared as previously described<sup>51</sup>. For dual-species biofilms, equal volumes of two-fold concentrated solutions were mixed. Plates were incubated (FOC 225I - VELS Scientifica, Italy) at 37 °C, under static conditions, during 192 h. Every 48 h the medium was carefully replaced by fresh AUM. FISH protocol was applied to biofilms formed on silicone coupons at 192 h. Before hybridization, coupons were washed in 0.85% (v/v) sterile saline, dried at ~60 °C for 15 minutes and fixed with 100% methanol for 20 min to prevent the detachment of biofilm during hybridization. After this, the FISH procedure was similar to the one applied for slides (sub-section 3.2.5). After hybridization, the silicone coupons were allowed to air dry, mounted with 1 drop of mounting oil and covered with a coverslip. The experiment was performed in triplicate.

### 3.2.9 Confocal laser scanning microscopy

The biofilm CSLM images were acquired in a FluoView FV1000 microscope (Olympus). Biofilms were observed using a 60x water-immersion objective (60x/1.2 W). Multichannel simulated fluorescence projection images and vertical cross sections through the biofilm were generated by using the FluoView application Software package (Olympus). *E. coli* cells were identified as green fluorescent rods and the uncommon bacteria as bright red fluorescent rods.

## 3.3 Results and discussion

Previous studies have demonstrated that uncommon bacteria might enhance the pathogenicity of virulent bacteria, increase the overall resistance of the biofilm to antibiotics, and influence the clinical outcome of the infection<sup>52-55</sup>. Thus, it is crucial to

have a better knowledge about the formation of biofilms and the contribution of each population in polymicrobial infections.

The FISH methodology has been shown to be a valuable technique to discriminate and to analyze the spatial distribution of the individual species *in situ* without disturbing the biofilm structure<sup>11, 18, 25</sup>. The characterization of biofilms has been limited to PNA molecules, despite the well-known advantages of other molecules, such as LNA and 2'OMe. As such, was developed a procedure, based on a multiplex LNA/2'OMe FISH and CLSM, for the analysis of the spatial organization of *in vitro* biofilms.

### 3.3.1 Analysis of LNA/2'OMe oligonucleotide probes

#### 3.3.1.1 Probe design and theoretical evaluation

For the selection of useful oligonucleotides, conserved regions for the 23S rRNA (*E. coli*) and 16S rRNA (*D. tsuruhatensis*, *A. xylooxidans* and *B. fungorum*) sequences were identified using ClustalW. The sequences selected for *E. coli* hybridize between the position 1505 and 1520 (Ec1505\_LNA/2'OMe\_13 and Ec1505\_LNA/2'OMe\_16 probes) of the 23S rRNA gene sequence (accession number: X80724). The other probes target the 16S rRNA sequences with target positions between 404 and 419 (Dt404\_LNA/2'OMe\_13 and Dt404\_LNA/2'OMe\_16) for *D. tsuruhatensis* (accession number: EU779949); 411 and 426 (Bf411\_LNA/2'OMe\_13 and Bf411\_LNA/2'OMe\_16) for *B. fungorum* (accession number: AF215705); and 590 to 605 (Ax590\_LNA/2'OMe\_13 and Ax590\_LNA/2'OMe\_16) on *A. xylooxidans* (accession number: AF225979).

The theoretical specificity and sensitivity of each selected oligonucleotide probe was evaluated using the probeCheck program coupled to the large subunit (LSU) database for *E. coli* probes, or using ProbeMatch coupled with the RDP II database for the other three bacteria (Table 3.2). According to the LSU database, the *E. coli* probes (Ec1505\_LNA/2'OMe\_13 and Ec1505\_LNA/2'OMe\_16) detected 3260 out of 4619 *E. coli* sequences present in the database which corresponds to a sensitivity of 70.6% (last accession, September 2014). The sensitivity value shows that the *E. coli* probes are not able to detect all *E. coli* strains; however, these oligonucleotides are suitable to be used in this study since both detected the *E. coli* strain CECT 434. According to the ProbeMatch from RDP II database (isolates with good quality and sequence size > 1200 bp), theoretical sensitivities of 97.82%, 90.47% and 97.80% were obtained for *D.*

*tsuruhatensis*, *B. fungorum*, and *A. xylosoxidans*, respectively. In addition, as shown in Table 3.2, all oligonucleotide probes display high specificity. While the specificity and sensitivity values are good indications of probe performance, especially for species identification purposes, this is in this particular case not the most important feature. As the intention is to form dual-species biofilms (*E. coli* co-cultured with uncommon bacteria), the absence of cross-hybridization with the other species under study is the most important criterion. In fact, none of the non-target sequences were detected by the probes belong to the other species under study. As such, the *in silico* analyses indicated that the oligonucleotide probes are able to detect specifically each target species, with no cross-complementarity observed with the other species to be used in the biofilm experiments. These are actually the first LNA/2'OMe oligonucleotide probes specifically designed for *E. coli*, *D. tsurusurhatensis*, *A. xylosoxidans* and *B. fungorum* detection.

**Table 3.2** - Theoretical sensitivity and specificity of each LNA/2'OMe oligonucleotide probe tested in this study.

Name	<sup>a</sup> No. of strains detected	<sup>a</sup> No. of non-strains detected	<sup>a</sup> Sensitivity (%)	<sup>a</sup> Specificity (%)
Ec1505_LNA/2'OMe_13	3260	130	70.6	97.2
Ec1505_LNA/2'OMe_16	3260	130	70.6	99.2
Dt404_LNA/2'OMe_13	45	42	97.8	99.9
Dt404_LNA/2'OMe_16	45	42	97.8	99.9
Bf411_LNA/2'OMe_13	38	19	90.5	99.9
Bf411_LNA/2'OMe_16	38	19	90.5	99.9
Ax590_LNA/2'OMe_13	223	19	97.8	99.9
Ax590_LNA/2'OMe_16	223	19	97.8	99.9

<sup>a</sup>Calculated by the TestProbe program (for *E. coli* oligonucleotide probes) coupled to the LSU database with the following data set options: sequence length > 1900 bp; sequence quality > 90% (last accession, September 2014); or ProbeMatch from RDP II database (for the other three bacteria) with the following data set options: strain - both; source - both; size > 1200 bp; quality - good (last accession, May 2014).

### 3.3.2 Thermodynamic parameters

The  $T_m$  value for each oligonucleotide probe was predicted using the LNA-2'OMeRNA/RNA calculator (<http://rnachemlab.ibch.poznan.pl/calculator2.php>) and was furthermore experimentally determined (Table 3.3). These experiments showed  $T_m$ -values in the range of 76-88 °C for all oligonucleotide probes. The theoretical  $T_m$ -



values are higher (between 100 and 129 °C) since this estimation does not consider the presence of the denaturing agent. Nonetheless, the correlation coefficient observed between the theoretical and the experimental  $T_m$  values presented an acceptable value of 0.85 ( $p < 0.05$ ) (Supplemental material - Figure S3.1).

The affinity to the target is also affected by several other factors like target accessibility and probe size<sup>56</sup>. The oligonucleotide probe affinity is defined as  $\Delta G^\circ$ , and a threshold  $\Delta G^\circ$  of -13 kcal.mol<sup>-1</sup> has been recommended for the design of DNA probes to guarantee a good hybridization efficiency<sup>56</sup>. However, for LNA/2'OMe oligonucleotide probes there is no information about the recommended threshold  $\Delta G^\circ$ . It is known that the introduction of LNA monomers increases the target affinity by having a positive and additive effect on the  $T_m$  (one LNA substitution increases  $T_m$  between 1 and 10 °C against RNA)<sup>57-59</sup>.

Also the Na<sup>+</sup> concentration has an important effect on the  $\Delta G^\circ$  values. Positive ions promote rRNA folding by reducing the repulsion between phosphates groups which could reduce accessibility<sup>60-63</sup>. However, positive ions are also essential to stabilize the hybrid duplex<sup>64</sup>. Thus, for the  $\Delta G^\circ$  and theoretical  $T_m$  calculations at Na<sup>+</sup> concentration of 0.9 M was used, which corresponds to the NaCl concentration used in the hybridization solution. This high concentration has a strong impact on the  $\Delta G^\circ$  values that can be reduced in average -10 kcal.mol<sup>-1</sup> ( $\pm 1.1$ ), when compared to values obtained with no NaCl. In general, analysis of the data in Table 3.3 showed the lower  $\Delta G^\circ$  values (between -32 and -42 kcal.mol<sup>-1</sup>) for the 16 nucleotide probes. The shorter ones displayed  $\Delta G^\circ$  values between -26 and -33 kcal.mol<sup>-1</sup>, which suggest a lower affinity. Nonetheless, too much affinity might be undesirable for those situations where a one mismatch distinction is required, which means that hybridization might occur with sequences that are not 100% complementary.

**Table 3.3** - Theoretical melting temperature, Gibbs free energy and results of thermal denaturation experiments performed in urea buffer for each LNA/2'OMe oligonucleotide probe.

Name	<sup>a</sup> Theoretical T <sub>m</sub> (°C)	<sup>b</sup> ΔG° (kcal.mol <sup>-1</sup> )	%GC	<sup>c</sup> RNA complement T <sub>m</sub> (°c)
Ec1505_LNA/2'OMe_13	117.2	-33.08	61.54	88.20 (±0.71)
Ec1505_LNA/2'OMe_16	128.6	-41.56	62.50	88.20 (±0.14)
				Ref. 68.70 (±0.28)*
Dt404_LNA/2'OMe_13	105.2	-26.01	38.46	76.15 (±0.49)
Dt404_LNA/2'OMe_16	116.9	-36.78	50.00	87.15 (±0.07)
				Ref. 64.10 (±0.00)*
Bf411_LNA/2'OMe_13	110.1	-27.69	46.15	79.35 (±0.35)
Bf411_LNA/2'OMe_16	124.2	-37.71	56.25	87.25 (±0.35)
				Ref. 63.80 (±0.57)*
Ax590_LNA/2'OMe_13	101.6	-26.40	38.46	77.45 (±0.35)
Ax590_LNA/2'OMe_16	100.6	-31.99	37.50	81.15 (±0.07)
				Ref. 55.70 (±0.42)*

The RNA complementary oligonucleotide has the following sequence: 5' - AAUCAAGGCUGAGGCGUGAU - 3' (for *E. coli* probes); 5' - TACGGAACGAAAAAGCTCCT - 3' (for *D. tsuruhatensis* probes); 5' - AACGCCGUGGUUAAUACCCG - 3' (for *B. fungorum* probes); 5' - AACUUUGGAACTGCAUUUUU - 3' (for *A. xylosoxidans* probes).

\*The DNA oligonucleotide probe reference (Ref.) has the following sequence: 5' - ATCACGCCTCAGCCTTGATT - 3' (for *E. coli* probes); 5' - AGGAGCTTTTCGTTCCGTA - 3' (for *D. tsuruhatensis* probes); 5' - CGGGTATTAACCACGGCGTT - 3' (for *B. fungorum* probes); 5' - AAAAATGCAGTTCCAAAGTT - 3' (for *A. xylosoxidans* probes).

<sup>a, b</sup> Determined on <http://rnachemlab.ibch.poznan.pl/calculator2.php> at 0.9 M NaCl.

<sup>c</sup> Determined experimentally on a temperature-controlled UV-vis spectrophotometer.

### 3.3.3 Optimization of hybridization conditions

Different hybridization temperatures, between 51 °C and 59 °C, were tested using the FISH method in glass slides for each oligonucleotide probe to achieve the best FISH signals. The results demonstrated that the strongest fluorescence intensity was obtained at 55 °C (Figure 3.1) for most of the oligonucleotide probes. The exception was for the *A. xylosoxidans* probes (Ax590\_LNA/2'OMe\_13 and Ax590\_LNA/2'OMe\_16) that presented a peak of fluorescence at 53 °C.

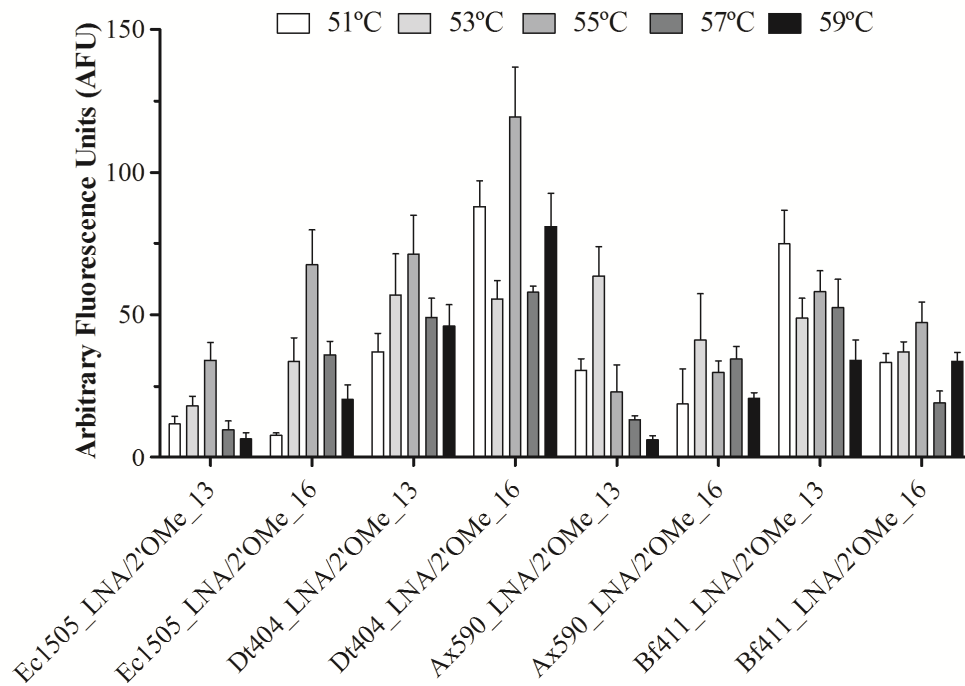


**Figure 3.1** - Fluorescence intensity of *E. coli* (Ec1505\_LNA/2'OMe\_13 and Ec1505\_LNA/2'OMe\_16), *D. tsuruhatensis* (Dt404\_LNA/2'OMe\_13 and Dt404\_LNA/2'OMe\_16), *A. xylosoxidans* (Ax590\_LNA/2'OMe\_13 and Ax590\_LNA/2'OMe\_16), and *B. fungorum* (Bf411\_LNA/2'OMe\_13 and Bf411\_LNA/2'OMe\_1). Hybridizations were performed in pure culture smears on glass slides. Fluorescence signal intensity, determined using ImageJ software, was expressed in arbitrary fluorescence units. All images were acquired at equal exposure conditions. Error bars represent standard deviation.

Concerning the specificity of each probe against the non-target strains, a slight cross-hybridization was observed for some of the oligonucleotide probes at 55 °C, especially for the *E. coli* / *D. tsuruhatensis* and *E. coli* / *A. xylosoxidans* combinations (Figure 3.2). As observed in columns for 57 °C, this problem was solved by increasing the hybridization temperature 2 °C. No cross-hybridization between the two LNA/2'OMe oligonucleotide probes was observed and, thus, an accurate discrimination between the two species involved was obtained. In addition, the signal-to-noise ratio was also optimal at 57 °C. Therefore, to achieve an appropriate specificity, 57 °C was used for all subsequent experiments. As such, for each bacterium, the LNA/2'OMe oligonucleotide probes that presented the best signal at 57 °C was selected for further experiments. For *E. coli*, *D. tsuruhatensis* and *A. xylosoxidans*, the 16 nucleotide probes (Ec1505\_LNA/2'OMe\_16, Ax590\_LNA/2'OMe\_16 and Dt404\_LNA/2'OMe\_16, respectively) were selected, while for *B. fungorum* the 13 nucleotide probe (Bf411\_LNA/2'OMe\_13) was chosen.

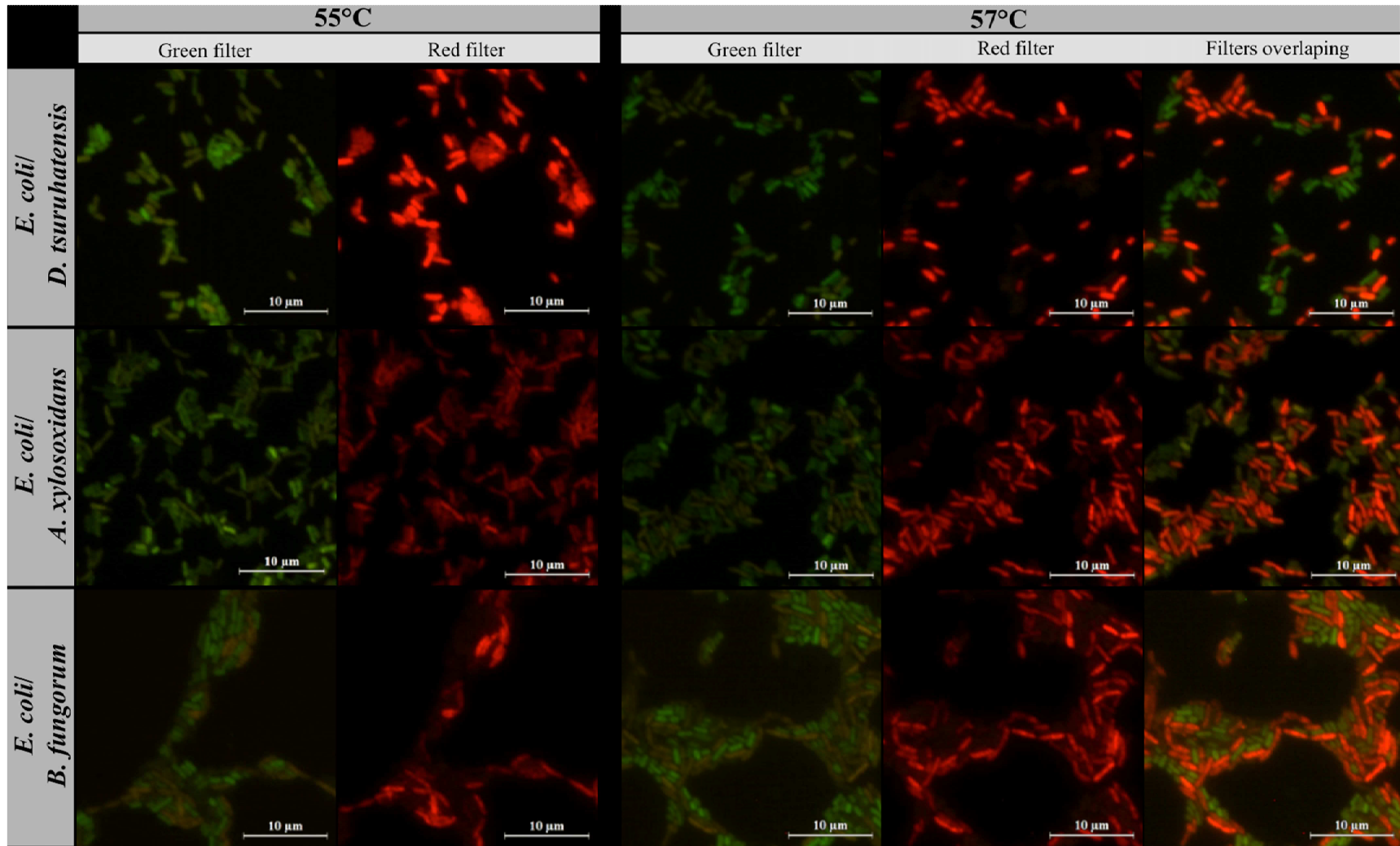


**Figure 3.2** - Epifluorescence microscopy images of a multiplex LNA/2'OMe-FISH assay for dual-species smears.

**Figure 3.2 (continuation)** - In the first two columns is possible observe some degree of cross-hybridization between the two LNA/2'OMe oligonucleotide probes at 55 °C, especially for the *E. coli* / *D. tsuruhatensis* and *E. coli* / *A. xylosoxidans* combinations. Columns for 57 °C of hybridization show no cross-hybridization and, thus, an accurate discrimination between the two species involved.

As described above, hybridization in suspension is the easiest way to quantify the bacterial population by subsequent flow cytometry or epifluorescence microscopy analysis, and it is important to ensure that the signal obtained on a standard glass slide test is maintained in suspension. For these, the FISH procedure in suspension was also performed for the probes selected at 57 °C. Comparing the values of fluorescence signal intensity, the results showed that the signals obtained in hybridizations performed in suspension were similar or higher than those obtained in standard smears (hybridization procedures performed in glass slides) (Figure 3.3).

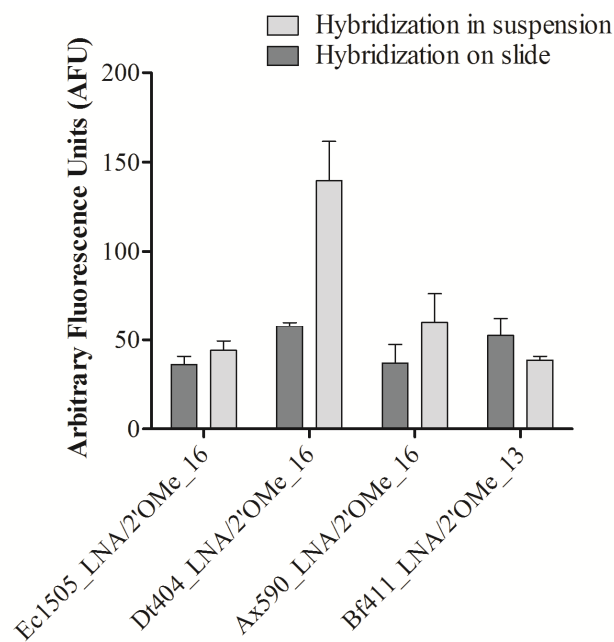


**Figure 3.3** - Comparison of the average fluorescence intensity of the selected LNA/2'OMe oligonucleotide probes obtained in standard smears (hybridization procedures performed in glass slides) and in suspension at 57 °C. Fluorescence signal intensity is expressed in arbitrary fluorescence units and was quantified using ImageJ software. All images were acquired at equal exposure conditions. Data are means of three independent experiments and error bars represent standard deviation.

Once the hybridization temperature had been optimized and the probes for subsequent experiments were selected, multiplex FISH was tested against a smear of two species mixed together (*E. coli* in combination with the uncommon bacteria). The results showed that both hybridization protocols (on slides and in suspension) provided an accurate discrimination between the two species at 57 °C. We have shown that the LNA/2'OMe oligonucleotide probes selected for subsequent experiments are able to successfully hybridize with the target microorganisms at 57 °C providing a species-specific hybridization signal. The results thus confirmed the potential applicability of the selected oligonucleotide probes to a multiplex LNA/2'OMe-FISH experiment.

### **3.3.4 LNA/2'OMe-FISH validation**

With the intended application of the FISH method here developed in mind, and considering that LNA/2'OMe-FISH application to biofilms are inexistent so far, it is important to establish the scope and limits of this methodology. As the rRNA is usually the target for the oligonucleotide probes used in FISH, the fluorescence signal is expected to be affected by the cell rRNA content. Microbial cells with a high metabolic activity have a rRNA content sufficient to generate a strong FISH signal<sup>63, 65</sup>. However, it is well established that the physiological state of biofilm cells vary spatially and temporally<sup>1</sup>. Therefore, changes in the number of rRNA molecules occur, and consequently, a low hybridization rate can be observed. In an early biofilm, the cells are metabolically active and have all requisites to divide and grow, due to the presence and rapid diffusion of the nutrients. In a mature biofilm, different physiological states are observed, namely active, dormant or dead cells<sup>1</sup>.

#### **3.3.4.1 LNA/2'OMe-FISH correlation with cultivability and PI staining**

For each species under study, cells at different physiological states (lag phase, exponential phase, early stationary phase and late stationary phase) were collected and evaluated using CFU counts; PI staining and LNA/2'OMe-FISH staining, for further correlation purposes. CFU is a conventional method for viability assessment, since only actively growing cells (cultivable cells) will be measured, while a general fluorescent nucleic acid dye is usually used for total cell quantifications<sup>66, 67</sup>. The PI binds to DNA and is commonly used in combination with SYTO9 to discriminate live and dead cells, but it can also be used to count the total cells in previously fixed samples. The LNA/2'OMe-FISH allows the identification and quantification of cells with intact or

significant rRNA content; which might eventually correlates with viability since RNA content is rapidly degraded after cell dead<sup>68</sup>.

Linear regression and Pearson correlation analysis for each species was performed to compare the CFU and PI counts against LNA/2'OMe-FISH counts (Table 3.4 and Supplemental material - Figure S3.2). As shown in Table 3.4, the Pearson correlations were significant for all pairs of methods (LNA/2'OMe-FISH counts vs. CFU counts and LNA/2'OMe-FISH counts vs. PI counts) with  $p < 0.05$ . *E. coli*, *A. xylosoxidans*, and *D. tsuruhatensis* presented strong and similar correlation values between the LNA/2'OMe-FISH vs. CFU and LNA/2'OMe-FISH vs. PI counts. The comparison between LNA/2'OMe-FISH and CFU counts showed a correlation coefficient of 0.95, 0.88, and 0.83 for *E. coli*, *D. tsuruhatensis*, and *A. xylosoxidans*, respectively. Correlation coefficient values of 0.93 (for *E. coli*), 0.84 (for *D. tsuruhatensis*), and 0.99 (for *A. xylosoxidans*) were found for the comparison of LNA/2'OMe-FISH vs. PI counts. For *B. fungorum*, as expected, a good correlation was observed between the LNA/2'OMe-FISH and PI counts ( $r=0.83$ ). However, a negative correlation was obtained LNA/2'OMe-FISH vs. CFU counts ( $r=-0.92$ ).

**Table 3.4** - Linear regression equations and Pearson correlations between LNA/2'OMe-FISH counts and CFU or PI counts for each species under study.

Bacteria		CFU counts vs.	PI counts vs.
		LNA/2'OMe-FISH counts	LNA/2'OMe-FISH counts
<i>E. coli</i>	Regression equation	$y = 0.63x + 3.61$	$y = 0.70x + 2.67$
	$R^2$	0.90	0.86
	Pearson correlation	<b>0.95</b> ( $p < 0.0003^*$ )	<b>0.93</b> ( $p < 0.0009$ )
<i>D. tsuruhatensis</i>	Regression equation	$y = 0.73x + 3.18$	$y = 0.5846x + 3.79$
	$R^2$	0.78	0.71
	Pearson correlation	<b>0.88</b> ( $p < 0.0036^*$ )	<b>0.84</b> ( $p < 0.0086$ )
<i>A. xylosoxidans</i>	Regression equation	$y = 1.05x + 0.32$	$y = 0.87x + 1.556$
	$R^2$	0.69	0.98
	Pearson correlation	<b>0.83</b> ( $p < 0.0106^*$ )	<b>0.99</b> ( $p < 0.0001$ )
<i>B. fungorum</i>	Regression equation	$y = -0.35x + 11.25$	$y = 0.71x + 2.09$
	$R^2$	0.85	0.69
	Pearson correlation	<b>-0.92</b> ( $p < 0.0012^*$ )	<b>0.83</b> ( $p < 0.0101$ )

\*Significant correlation with  $p < 0.05$  (two-sided).

In order to explain this result, the *B. fungorum* growth curve was analyzed in terms of CFU and LNA/2'OMe-FISH counts. The CFU assessment showed a decrease

in the cultivable population, which was inconsistent with the LNA/2'OMe-FISH counts that increased over time (Figure 3.4-a). Therefore, the negative correlation obtained in LNA/2'OMe-FISH vs. CFU counts was due to the decrease of CFU counts during the *B. fungorum* growth. However, the O.D. measurement (Figure 3.4-b) seemed to indicate that the cells are viable and metabolically active, since the O.D. is increasing as a result of active cellular division. This result corroborated the data obtained by LNA/2'OMe-FISH counts. To further investigate this issue, the resazurin assay was performed at selected time points during the growth of *B. fungorum*. The resazurin assay is commonly used for the assessment of bacterial viability with the fluorescence output being proportional to the number of viable cells. Despite the decrease in CFU counts, resazurin and O.D. data showed that cellular viability increased until the stationary phase (Figure 3.4-b). The decrease observed in the cultivable population might be the result of a transition to a non-cultivable/dormant state of the bacteria, which is activated when growth condition are not optimal.

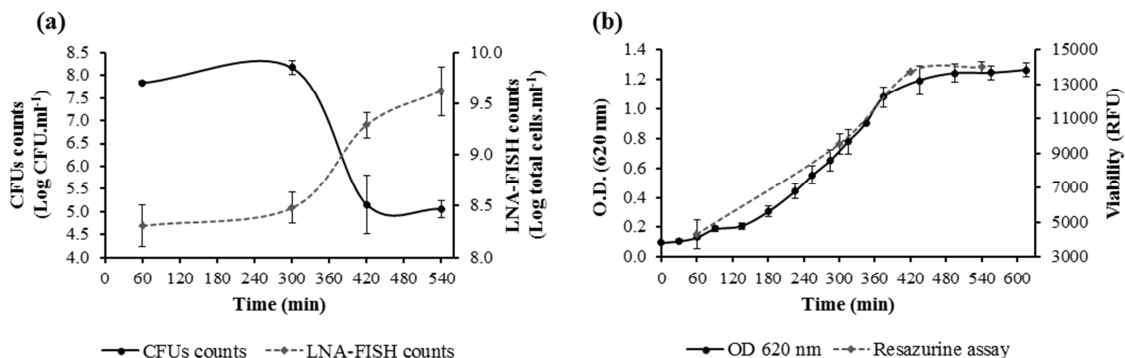


**Figure 3.4** - Evaluation of the *B. fungorum* growth curve by (a) CFU and LNA/2'OMe-FISH counts and by (b) O.D. and the resazurine assay. The CFU assessment shows a decrease in the cultivable population, which is inconsistent with the LNA/2'OMe-FISH counts that increase over time. O.D. measurements and viability assessment using resazurine assay, showed active growth over time, which corroborate the results obtained with the LNA/2'OMe-FISH counts. Data are means of two independent experiments and error bars represent standard deviation.

Overall, the values produced by LNA/2'OMe-FISH correlated well with viable and total cells counts for all species under study. The only exception was noticed for *B. fungorum*, which seems to present a non-cultivable state that renders CFU unable to correctly estimate changes in the population. In fact, this particular result showed the potential of FISH techniques for species with known dormant stages or unknown physiological behavior. To our knowledge no study has so far analyzed the correlation



between LNA/2'OMe-FISH and CFU and total cell counts. The results provided evidences of the utility of this technique for studies of population dynamics, especially for biofilms which present a variety of cellular fractions at different metabolic stages.

#### **3.3.4.2 Characterization of biofilm three-dimensional structures using multiplex LNA/2'OMe-FISH**

While our results have provided evidence of the suitability of LNA/2'OMe-FISH for characterization of heterogeneous populations, analysis of biofilms requires that probes are able to penetrate over the complex matrix that surrounds the cells. A biofilm matrix is rich in extracellular nucleic acid, proteins, and exopolysaccharides<sup>69, 70</sup>, which might hinder the LNA/2'OMe oligonucleotide probe diffusion (also negatively charged). To evaluate the ability of the method to provide an *in situ* three-dimensional characterization of biofilm populations, biofilms were formed in artificial urine for 8 days. Samples from single- and dual-species biofilms were taken, fixed, *in situ* hybridized and then evaluated by CLSM. As an example, Figure 3.5 showed that the LNA/2'OMe oligonucleotide probes were able to penetrate over the biofilm matrix, providing a complete staining of the biofilm surface and a strong signal, even in a thicker biofilm with 40  $\mu\text{m}$  (Figure 3.5-a). This clearly demonstrated that the probes, despite their negative charge, did not face any diffusion barrier within the biofilm structure. Unlike their DNA counterparts, for which diffusion problems have been attributed to the negative charge and size of the probes<sup>11, 17</sup>, the LNA/2'OMe probes apparently present a different behavior. It might be possible that the size of the oligonucleotides might be more determinant than the charge with respect to assuring an efficient diffusion through the biofilm matrix. Regarding the multiplex assay, it was also possible to analyze an 8-days dual-species biofilm of *E. coli* / *B. fungorum* (Figure 3.5-b), where the discrimination and localization of the two populations was evident. In this case, the transversal biofilm image showed both species mixed together, which corresponds to a typical co-aggregation organization of the bacteria in polymicrobial biofilms. This distribution is commonly associated with cooperation or synergetic interaction within biofilms<sup>71</sup>. This might suggest that, in this particular case, these species might benefit from the mixed consortium; or, at least, they are not negatively affected by each other presence.

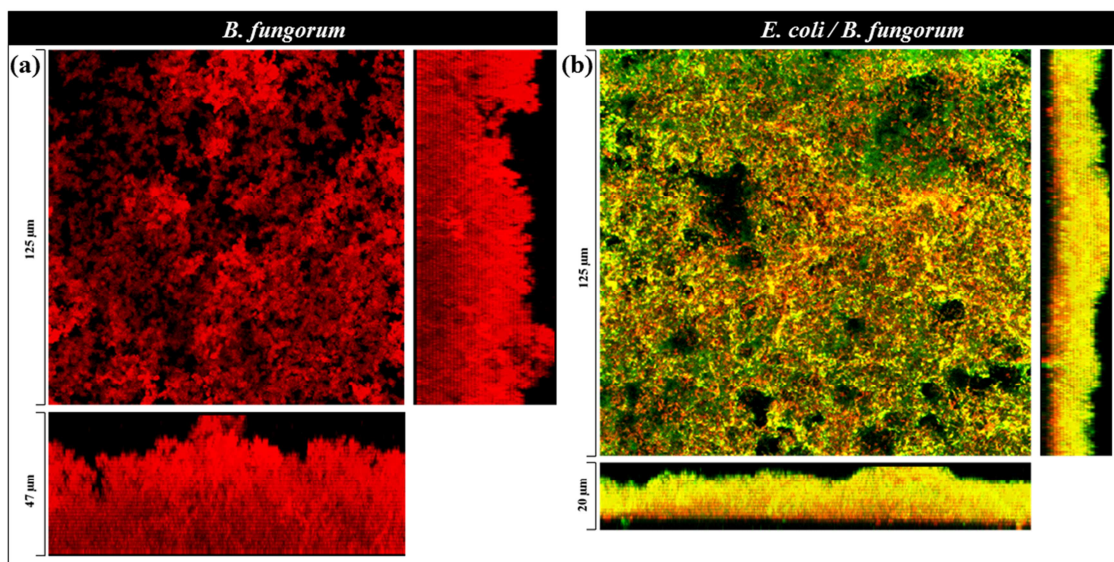


**Figure 3.5** - An example of LNA/2'OMe-FISH combined with CLSM analysis. CLSM images for (a) *B. fungorum* single-species biofilm and for (b) *E. coli* / *B. fungorum* dual-species biofilm, showing the localization of species in the biofilm formed in conditions mimicking the CAUTIs for 8 days on silicone coupons. For dual-species biofilms, the transverse biofilm image shows both species mixed together in the direction of the z-axis. Green fluorescent cells represent *E. coli*; red fluorescent cells represent *B. fungorum*.

### 3.4 Conclusions

Multiplex FISH methodology in combination with CLSM is becoming common in biofilm experiments providing a simple way to analyze *in situ* the spatial distribution of natural biofilm populations. While the potential of DNA or PNA probes have already been proven for biofilm studies, the potential application of LNA-modified probes have been studied for the first time with this report. We have herein developed and validated a multiplex LNA/2'OMe-FISH procedure which, in combination with CLSM, is capable of discriminating among bacterial species providing spatial localization data of complex biofilm populations, in conditions mimicking the CAUTIs.

### 3.5 References

1. **P.S. Stewart, M.J. Franklin.** Physiological heterogeneity in biofilms. *Nat Rev Microbiol* **6**, 199-210 (2008).
2. **J.W. Costerton, K.J. Cheng, G.G. Geesey, T.I. Ladd, J.C. Nickel, M. Dasgupta, T.J. Marrie.** Bacterial biofilms in nature and disease. *Annu Rev Microbiol* **41**, 435-464 (1987).
3. **T.S. Murray, M. Egan, B.I. Kazmierczak.** *Pseudomonas aeruginosa* chronic colonization in cystic fibrosis patients. *Curr Opin Pediatr* **19**, 83-88 (2007).
4. **J.D. Bryers.** Medical biofilms. *Biotechnol Bioeng* **100**, 1-18 (2008).
5. **C.A. Fux, J.W. Costerton, P.S. Stewart, P. Stoodley.** Survival strategies of infectious biofilms. *Trends Microbiol* **13**, 34-40 (2005).
6. **C.G. Kumar, S.K. Anand.** Significance of microbial biofilms in food industry: a review. *Int J Food Microbiol* **42**, 9-27 (1998).
7. **H.C. Flemming.** Biofouling in water systems-cases, causes and countermeasures. *Appl Microbiol Biotechnol* **59**, 629-640 (2002).
8. **D.G. Desai, K.S. Liao, M.E. Cevallos, B.W. Trautner.** Silver or nitrofurazone impregnation of urinary catheters has a minimal effect on uropathogen adherence. *J Urol* **184**, 2565-2571 (2010).
9. **D.J. Stickler.** Bacterial biofilms in patients with indwelling urinary catheters. *Nat Clin Pract Urol* **5**, 598-608 (2008).
10. **D.J. Stickler, S.D. Morgan.** Observations on the development of the crystalline bacterial biofilms that encrust and block Foley catheters. *J Hosp Infect* **69**, 350-360 (2008).
11. **C. Almeida, N.F. Azevedo, S. Santos, C.W. Keevil, M.J. Vieira.** Discriminating multi-species populations in biofilms with peptide nucleic acid fluorescence *in situ* hybridization (PNA FISH). *PLoS One* **6**, e14786 (2011).
12. **R.M. Donlan, J.W. Costerton.** Biofilms: survival mechanisms of clinically relevant microorganisms. *Clin Microbiol Rev* **15**, 167-193 (2002).
13. **A. Bridier, E. Tischenko, F. Dubois-Brissonnet, J.M. Herry, V. Thomas, S. Daddi-Oubekka, F. Waharte, K. Steenkeste, M.P. Fontaine-Aupart, R. Briandet.** Deciphering biofilm structure and reactivity by multiscale time-resolved fluorescence analysis. *Adv Exp Med Biol* **715**, 333-349 (2011).
14. **F. Gu, R. Lux, L. Du-Thumm, I. Stokes, J. Kreth, M.H. Anderson, D.T. Wong, L. Wolinsky, R. Sullivan, W. Shi.** *In situ* and non-invasive detection of specific bacterial species in oral biofilms using fluorescently labeled monoclonal antibodies. *J Microbiol Methods* **62**, 145-160 (2005).
15. **A.C. Rodrigues, S. Wuertz, A.G. Brito, L.F. Melo.** Three-dimensional distribution of GFP-labeled *Pseudomonas putida* during biofilm formation on solid PAHs assessed by confocal laser scanning microscopy. *Water Sci Technol* **47**, 139-142 (2003).
16. **A. Bridier, R. Briandet, T. Bouchez, F. Jabot.** A model-based approach to detect interspecific interactions during biofilm development. *Biofouling*, 761-771 (2014).
17. **R. Amann, B.M. Fuchs.** Single-cell identification in microbial communities by improved fluorescence *in situ* hybridization techniques. *Nat Rev Microbiol* **6**, 339-348 (2008).
18. **S. Malic, K.E. Hill, A. Hayes, S.L. Percival, D.W. Thomas, D.W. Williams.** Detection and identification of specific bacteria in wound biofilms using peptide nucleic acid fluorescent *in situ* hybridization (PNA FISH). *Microbiology* **155**, 2603-2611 (2009).
19. **C. Almeida, N.F. Azevedo, C. Iversen, S. Fanning, C.W. Keevil, M.J. Vieira.** Development and application of a novel peptide nucleic acid probe for the specific detection of *Cronobacter genomospecies* (*Enterobacter sakazakii*) in powdered infant formula. *Appl Environ Microbiol* **75**, 2925-2930 (2009).
20. **S. Fontenete, N. Guimaraes, M. Leite, C. Figueiredo, J. Wengel, N. Filipe Azevedo.** Hybridization-based detection of *Helicobacter pylori* at human body temperature using advanced locked nucleic acid (LNA) probes. *PLoS One* **8**, e81230 (2013).
21. **M. Petersen, J. Wengel.** LNA: a versatile tool for therapeutics and genomics. *Trends Biotechnol* **21**, 74-81 (2003).

22. **M.J. Soe, T. Moller, M. Dufva, K. Holmstrom.** A sensitive alternative for microRNA *in situ* hybridizations using probes of 2'-O-methyl RNA + LNA. *J Histochem Cytochem* **59**, 661-672 (2011).
23. **T. Thurnheer, R. Gmur, B. Guggenheim.** Multiplex FISH analysis of a six-species bacterial biofilm. *J Microbiol Methods* **56**, 37-47 (2004).
24. **N.F. Azevedo, M.J. Vieira, C.W. Keevil.** Establishment of a continuous model system to study *Helicobacter pylori* survival in potable water biofilms. *Water Sci Technol* **47**, 155-160 (2003).
25. **L. Cerqueira, J.A. Oliveira, A. Nicolau, N.F. Azevedo, M.J. Vieira.** Biofilm formation with mixed cultures of *Pseudomonas aeruginosa/Escherichia coli* on silicone using artificial urine to mimic urinary catheters. *Biofouling* **29**, 829-840 (2013).
26. **A. Silaharoglu, H. Pfundheller, A. Koshkin, N. Tommerup, S. Kauppinen.** LNA-modified oligonucleotides are highly efficient as FISH probes. *Cytogenet Genome Res* **107**, 32-37 (2004).
27. **R. Thomsen, P.S. Nielsen, T.H. Jensen.** Dramatically improved RNA *in situ* hybridization signals using LNA-modified probes. *RNA* **11**, 1745-1748 (2005).
28. **R.N. Veedu, J. Wengel.** Locked nucleic acid as a novel class of therapeutic agents. *RNA Biol* **6**, 321-323 (2009).
29. **K.L. Robertson, D.C. Thach.** LNA flow-FISH: a flow cytometry-fluorescence *in situ* hybridization method to detect messenger RNA using locked nucleic acid probes. *Anal Biochem* **390**, 109-114 (2009).
30. **A.N. Elayadi, D.A. Braasch, D.R. Corey.** Implications of high-affinity hybridization by locked nucleic acid oligomers for inhibition of human telomerase. *Biochemistry* **41**, 9973-9981 (2002).
31. **D.A. Braasch, D.R. Corey.** Locked nucleic acid (LNA): fine-tuning the recognition of DNA and RNA. *Chem Biol* **8**, 1-7 (2001).
32. **S. K. Singh, A. A. Koshkin, J. Wengel, P. Nielsen.** LNA (locked nucleic acids): synthesis and high-affinity nucleic acid recognition. *Chem Commun*, 455-456 (1998).
33. **A.A. Koshkin, S.K. Singh, P. Nielsen, V.K. Rajwanshi, R. Kumar, M. Meldgaard, C.E. Olsen, J. Wengel.** LNA (Locked Nucleic Acids): Synthesis of the adenine, cytosine, guanine, 5-methylcytosine, thymine and uracil bicyclonucleoside monomers, oligomerisation, and unprecedented nucleic acid recognition. *Tetrahedron* **54**, 3607-3630 (1998).
34. **M. Majlessi, N.C. Nelson, M.M. Becker.** Advantages of 2'-O-methyl oligoribonucleotide probes for detecting RNA targets. *Nucleic Acids Res* **26**, 2224-2229 (1998).
35. **D.A. Braasch, Y. Liu, D.R. Corey.** Antisense inhibition of gene expression in cells by oligonucleotides incorporating locked nucleic acids: effect of mRNA target sequence and chimera design. *Nucleic Acids Res* **30**, 5160-5167 (2002).
36. **J. Kurreck, E. Wyszko, C. Gillen, V.A. Erdmann.** Design of antisense oligonucleotides stabilized by locked nucleic acids. *Nucleic Acids Res* **30**, 1911-1918 (2002).
37. **A.N. Silaharoglu, D. Nolting, L. Dyrskjot, E. Berezikov, M. Moller, N. Tommerup, S. Kauppinen.** Detection of microRNAs in frozen tissue sections by fluorescence *in situ* hybridization using locked nucleic acid probes and tyramide signal amplification. *Nat Protoc* **2**, 2520-2528 (2007).
38. **A. Simeonov, T.T. Nikiforov.** Single nucleotide polymorphism genotyping using short, fluorescently labeled locked nucleic acid (LNA) probes and fluorescence polarization detection. *Nucleic Acids Res* **30**, e91 (2002).
39. **S. Niveditha, S. Pramodhini, S. Umadevi, S. Kumar, S. Stephen.** The isolation and the biofilm formation of uropathogens in the patients with catheter associated urinary tract infections (UTIs). *J Clin Diagn Res* **6**, 1478-1482 (2012).
40. **A. Ronald.** The etiology of urinary tract infection: traditional and emerging pathogens. *Am J Med* **113**, 14-19 (2002).
41. **C. Svanborg, G. Godaly.** Bacterial virulence in urinary tract infection. *Infect Dis Clin North Am* **11**, 513-529 (1997).
42. **D.N. Frank, S.S. Wilson, A.L. St Amand, N.R. Pace.** Culture-independent microbiological analysis of foley urinary catheter biofilms. *PLoS One* **4**, e7811 (2009).

43. **C. Almeida, N.F. Azevedo, R.M. Fernandes, C.W. Keevil, M.J. Vieira.** Fluorescence *in situ* hybridization method using a peptide nucleic acid probe for identification of *Salmonella* spp. in a broad spectrum of samples. *Appl Environ Microbiol* **76**, 4476-4485 (2010).
44. **P. Guga, M. Koziolkiewicz.** Phosphorothioate nucleotides and oligonucleotides - recent progress in synthesis and application. *Chem Biodivers* **8**, 1642-1681 (2011).
45. **S. Fontenete, M. Leite, N. Guimarães, P. Madureira, R.M. Ferreira, C. Figueiredo, J. Wengel, N.F. Azevedo.** Towards fluorescence *in vivo* hybridization (FIVH) detection of *H. pylori* in gastric mucosa using advanced LNA probes. *PLoS ONE* **10**, e0125494 (2015).
46. **S. Fontenete, D. Carvalho, A. Lourenço, N. Guimarães, P. Madureira, C. Figueiredo, N.F. Azevedo.** FISHji: New ImageJ macros for the quantification of fluorescence in epifluorescence images. *Biochem Eng J* **112**, 61-69 (2016).
47. **R.K. Pettit, C.A. Weber, G.R. Pettit.** Application of a high throughput Alamar blue biofilm susceptibility assay to *Staphylococcus aureus* biofilms. *Ann Clin Microbiol Antimicrob* **8**, 28 (2009).
48. **A. Borges, L.C. Simões, M.J. Saavedra, M. Simões.** The action of selected isothiocyanates on bacterial biofilm prevention and control. *Int Biodeter Biodegr* **86, Part A**, 25-33 (2014).
49. **K. Tote, D. Vanden Berghe, S. Levecque, E. Benere, L. Maes, P. Cos.** Evaluation of hydrogen peroxide-based disinfectants in a new resazurin microplate method for rapid efficacy testing of biocides. *J Appl Microbiol* **107**, 606-615 (2009).
50. **T. Brooks, C.W. Keevil.** A simple artificial urine for the growth of urinary pathogens. *Lett Appl Microbiol* **24**, 203-206 (1997).
51. **N.F. Azevedo, A.P. Pacheco, C.W. Keevil, M.J. Vieira.** Adhesion of water stressed *Helicobacter pylori* to abiotic surfaces. *J Appl Microbiol* **101**, 718-724 (2006).
52. **A.M. de Vrankrijker, T.F. Wolfs, C.K. van der Ent.** Challenging and emerging pathogens in cystic fibrosis. *Paediatr Respir Rev* **11**, 246-254 (2010).
53. **V. Waters.** New treatments for emerging cystic fibrosis pathogens other than *Pseudomonas*. *Curr Pharm Des* **18**, 696-725 (2012).
54. **C.D. Sibley, K. Duan, C. Fischer, M.D. Parkins, D.G. Storey, H.R. Rabin, M.G. Surette.** Discerning the complexity of community interactions using a *Drosophila* model of polymicrobial infections. *PLoS Pathog* **4**, e1000184 (2008).
55. **S.P. Lopes, N.F. Azevedo, M.O. Pereira.** Emergent bacteria in cystic fibrosis: *in vitro* biofilm formation and resilience under variable oxygen conditions. *Biomed Res Int* **2014**, 678301 (2014).
56. **L.S. Yilmaz, D.R. Noguera.** Mechanistic approach to the problem of hybridization efficiency in fluorescent *in situ* hybridization. *Appl Environ Microbiol* **70**, 7126-7139 (2004).
57. **K. Bondensgaard, M. Petersen, S.K. Singh, V.K. Rajwanshi, R. Kumar, J. Wengel, J.P. Jacobsen.** Structural studies of LNA:RNA duplexes by NMR: conformations and implications for RNase H activity. *Chemistry* **6**, 2687-2695 (2000).
58. **E. Kierzek, A. Ciesielska, K. Pasternak, D.H. Mathews, D.H. Turner, R. Kierzek.** The influence of locked nucleic acid residues on the thermodynamic properties of 2'-O-methyl RNA/RNA heteroduplexes. *Nucleic Acids Res* **33**, 5082-5093 (2005).
59. **B. Vester, J. Wengel.** LNA (locked nucleic acid): high-affinity targeting of complementary RNA and DNA. *Biochemistry* **43**, 13233-13241 (2004).
60. **B.M. Fuchs, K. Syutsubo, W. Ludwig, R. Amann.** *In situ* accessibility of *Escherichia coli* 23S rRNA to fluorescently labeled oligonucleotide probes. *Appl Environ Microbiol* **67**, 961-968 (2001).
61. **B.M. Fuchs, G. Wallner, W. Beisker, I. Schwiippel, W. Ludwig, R. Amann.** Flow cytometric analysis of the *in situ* accessibility of *Escherichia coli* 16S rRNA for fluorescently labeled oligonucleotide probes. *Appl Environ Microbiol* **64**, 4973-4982 (1998).
62. **L.S. Yilmaz, H.E. Okten, D.R. Noguera.** Making all parts of the 16S rRNA of *Escherichia coli* accessible *in situ* to single DNA oligonucleotides. *Appl Environ Microbiol* **72**, 733-744 (2006).
63. **M. Wagner, M. Horn, H. Daims.** Fluorescence *in situ* hybridisation for the identification and characterisation of prokaryotes. *Curr Opin Microbiol* **6**, 302-309 (2003).

64. **S. Herzer, D.F. Englert** in *Molecular Biology Problem Solver*. (ed. A.S. Gerstein) 399-460 (John Wiley & Sons, Inc., 2002).
65. **Y. Odaa, S. Slagmana, W.G. Meijerb, L.J. Forneya, J.C. Gottschala**. Influence of growth rate and starvation on fluorescent *in situ* hybridization of *Rhodopseudomonas palustris*. *FEMS Microbiol Ecol* **32**, 205-213 (2000).
66. **J.D. Oliver**. The viable but nonculturable state in bacteria. *J Microbiol* **43**, 93-100 (2005).
67. **F. Cerca, G. Trigo, A. Correia, N. Cerca, J. Azeredo, M. Vilanova**. SYBR green as a fluorescent probe to evaluate the biofilm physiological state of *Staphylococcus epidermidis*, using flow cytometry. *Can J Microbiol* **57**, 850-856 (2011).
68. **K. Piir, A. Paier, A. Liiv, T. Tenson, U. Maivali**. Ribosome degradation in growing bacteria. *EMBO Rep* **12**, 458-462 (2011).
69. **H.C. Flemming, J. Wingender**. The biofilm matrix. *Nat Rev Microbiol* **8**, 623-633 (2010).
70. **G. Carlson, J. Silverstein**. Effect of molecular size and charge on biofilm sorption of organic matter. *Water Res* **32**, 1580-1592 (1998).
71. **S. Elias, E. Banin**. Multi-species biofilms: living with friendly neighbors. *FEMS Microbiol Rev* **36**, 990-1004 (2012).

### 3.6 Supplemental material

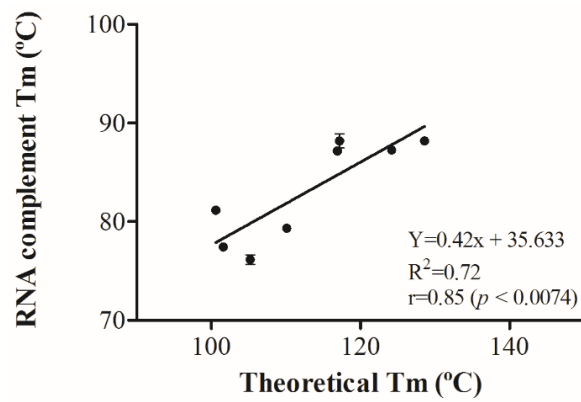


**Figure S3.1** - Representation of the linear regression equations and correlations values of theoretical melting temperature and RNA complement melting temperature for all LNA/2'OMe oligonucleotide probes.

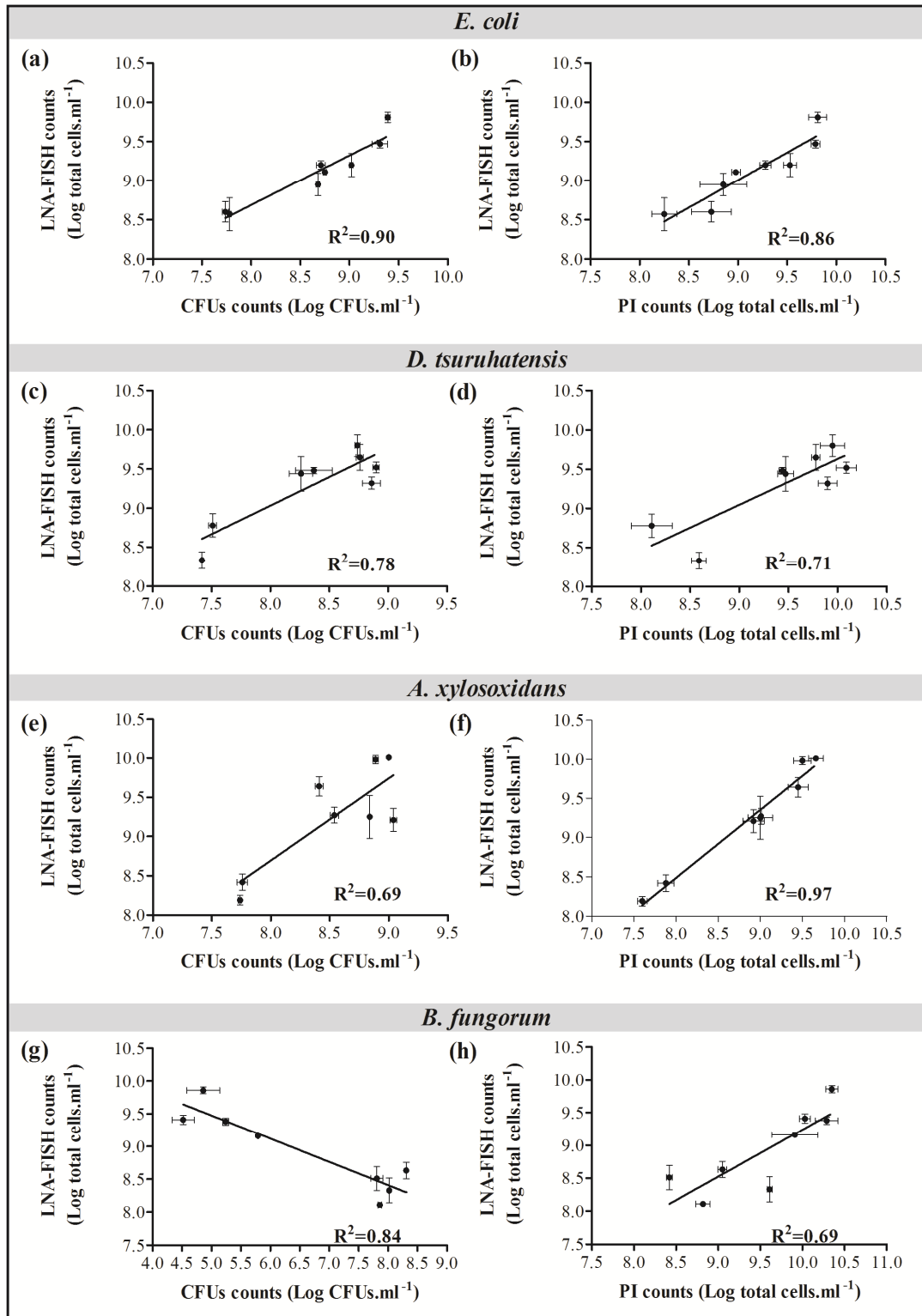


**Figure S3.2** - Representation of the linear regression equations and correlations values of (a, c, e, g) LNA/2'OMe-FISH counts vs. CFU counts and (b, d, f, h) LNA/2'OMe-FISH counts vs. PI counts assessed in different physiological states for each species under study. Data are means of two independent experiments and error bars represent standard deviation.



# Chapter 4

---

## **Impact of *Delftia tsuruhatensis* and *Achromobacter xylosoxidans* on *Escherichia coli* dual-species biofilms treated with antibiotic agents**

**Andreia S. Azevedo**, Carina Almeida, Bruno Pereira, Luís F. Melo, Nuno F. Azevedo.  
*Biofouling*. 2016. 32(3):227-41. doi: [10.1080/08927014.2015.1124096](https://doi.org/10.1080/08927014.2015.1124096).

---

### **Abstract**

Recently it was demonstrated that UTIs species with a lower or unproven pathogenic potential, such as *D. tsuruhatensis* and *A. xylosoxidans*, might interact with conventional pathogenic agents as such *E. coli*. Here, single- and dual-species biofilms of these bacteria were characterized in terms of the microbial composition over time, the average fitness of *E. coli*, the spatial organization and the biofilm antimicrobial profile. Results revealed a positive impact of these species on *E. coli* fitness and a greater tolerance to the antibiotic agents. Surprisingly, in dual-species biofilms exposed to antibiotics, *E. coli* was able to dominate the microbial consortia in spite of being the most sensitive strain. This is the first study demonstrating the protective effect of uncommon bacteria over *E. coli* under adverse conditions imposed by the use of antibiotic agents.

**Keywords:** polymicrobial biofilms, catheter-associated urinary tract infections, antibiotics, *Escherichia coli*, uncommon bacteria, LNA/2'OMe-FISH.



## 4.1 Introduction

Healthcare-associated infections include UTIs<sup>1</sup>, cystic fibrosis lung disease<sup>2</sup>, and device-related infections<sup>3-6</sup> (e.g. urinary catheters). Concerning CAUTIs, *E. coli* is typically one of the most prevailing bacteria<sup>7, 8</sup>. Advances in molecular technologies have disclosed that in short-term catheterization, the surface of the urinary catheter is frequently colonized by a single species; while, in the long-term catheterization, a diverse microbial community inhabiting the urinary catheter surface can be observed, with a predominance of Gram-negative bacteria<sup>6, 9, 10</sup>. Nonetheless, only a few studies have examined mixed-species structures (e.g.<sup>11</sup> and study reported in Chapter 2), and hence, our current knowledge about interspecies dynamic within polymicrobial biofilms, such as microbe-microbe interactions, remains scarce<sup>12</sup>.

Two of the bacteria uncommonly found on the surface of urinary catheters are *D. tsuruhatensis* and *A. xylosoxidans*<sup>5</sup>. As addressed in Chapter 2, these bacteria have been shown to be able to coexist with *E. coli* in biofilms, and a pre-colonization of the surface with these bacteria seemed to promote *E. coli* adhesion. While only a limited number of studies have investigated the behavior and the role of *E. coli* in catheter-associated polymicrobial biofilms (e.g.<sup>11, 13</sup>), a previous work with uncommon bacteria suggests that *E. coli* interacts synergistically with those uncommon species (Chapter 2). Similar results were reported for cystic fibrosis associated species, where two other uncommon bacteria, *I. limosus* and *D. pigrum*, were able to interact synergistically with *P. aeruginosa*<sup>14</sup>. This type of interaction also resulted into an increased tolerance of the overall consortia to a wide range of antibiotics. Although the pathogenic nature of these uncommon bacteria remains unknown, these studies suggest that some species might cooperate with conventional microorganisms (e.g. *E. coli*, *P. aeruginosa*) to form mixed biofilms in order to protect them from environmentally challenging condition such as antibiotic exposure.

The present study aimed to assess the effect that the uncommon bacteria might have on the fitness and antimicrobial profile of *E. coli* biofilms. *E. coli* and two uncommon bacteria, *D. tsuruhatensis* and *A. xylosoxidans*, were used to form single- and dual-species biofilms on silicone surfaces. Then, the single- and dual-species biofilms were characterized in terms of the microbial composition over time, the average fitness of *E. coli*, the spatial organization and the biofilm antimicrobial profile.

The interactions, synergetic or antagonistic, among the species within the biofilm have been demonstrated to have a crucial role in the process of biofilm development, architecture and resistance to several antimicrobial agents<sup>15-18</sup>. This information might provide data to model microbial behavior on polymicrobial communities and might also be the base for new personalized treatment strategies<sup>19</sup>.

## **4.2 Material and methods**

### **4.2.1 Culture conditions and preparation of inoculum**

For each experiment, *E. coli* CECT 434, *A. xylosoxidans* B3 and *D. tsuruhatensis* BM90 were streaked from a frozen stock (-80 °C) on TSA (Merk, Germany) and grown overnight at 37 °C.

For the preparation of each inoculum, cells were subcultured (16-18 h) at 37 °C and 150 rpm, in AUM. AUM was prepared as previously described<sup>20</sup>. Cell concentration was assessed by O.D. at 620 nm, and the inoculum was diluted in AUM in order to obtain a final concentration of  $10^5$  CFUs.ml<sup>-1</sup>.

### **4.2.2 Single- and dual-species biofilm formation**

Single-species biofilms were formed to study the biofilm-forming ability of each species on silicone material, which is frequently used in urinary catheters<sup>4, 21</sup>. In order to understand the interactions that occur between *E. coli* and the uncommon microorganisms, 2 species combinations (*E. coli*  $10^5$  CFU.ml<sup>-1</sup> / *D. tsuruhatensis*  $10^5$  CFU.ml<sup>-1</sup>; *E. coli*  $10^5$  CFU.ml<sup>-1</sup> / *A. xylosoxidans*  $10^5$  CFU.ml<sup>-1</sup>) were studied.

Coupons of silicone (Neves & Neves Lda, Portugal) were cut (dimensions of 2 × 2 cm or 1 × 1 cm), cleaned and sterilized according to the procedure described by Azevedo *et al.*<sup>22</sup>. Each coupon of silicone was placed in the bottom of the wells of the 6-well tissue culture plates (Orange Scientific, Belgium).

Cell suspension cultures prepared in AUM at  $10^5$  CFUs.ml<sup>-1</sup> were used as an inoculum for biofilm formation. Single- and dual-species biofilms were formed as described in sub-section 2.2.2 (Chapter 2). Two independent experiments were performed for each condition. At specific times (2, 4, 6, 24, 48, 96 and 192 h), the

biofilm formation was assessed by CFU counts. The spatial organization of dual-species biofilm was also performed using LNA/2'OMe-FISH at 192 h.

### 4.2.3 CFU counts for quantification of biofilm cells

At each time point, the silicone coupons with biofilm were washed twice in 10 ml of 0.85% (v/v) sterile saline solution to remove loosely attached cells. After washing, coupons were placed in a new well of the tissue plate containing 9 ml of 0.85% (v/v) sterile saline; subsequently, the biofilms were sonicated (Sonopuls HD 2070, Bandelin Electronics, Germany) for 10 seconds with 25 % amplitude. The sonication conditions were previously optimized to guarantee that the cells were detached from the silicone coupons, avoiding the bacteria lysis. Afterwards, the CFU counts were performed. For this, as described in sub-section 2.2.3 (Chapter 2), 100  $\mu$ l of the disrupted biofilm were serially diluted (1:10) in saline solution, and plated in triplicate on TSA (for the single-species biofilms). The plates were incubated at 37 °C for 12–16 h (*E. coli*), 24 h (*D. tsuruhatensis*) and 48 h (*A. xylosoxidans*). For discrimination of the bacteria involved on the dual-species biofilms, different selective agar media were used, as stated in sub-section 2.2.3 (Chapter 2).

The number of CFU in biofilms was determined and expressed per unit area of silicone coupon in contact with AUM (Log CFUs.cm<sup>-2</sup>). These values were used for the determination of the  $W_{E.coli}$  as previously described in equations 2.1 and 2.2 of sub-section 2.2.9 (Chapter 2).

### 4.2.4 Antibiotic stock solutions

Four relevant antibiotics commonly used in the treatment of UTIs and CAUTIs<sup>9, 23-25</sup>, with distinct modes of action, were selected, namely: ciprofloxacin (Sigma-Aldrich, Portugal), ampicillin (AppliChem, Germany), gentamicin (AppliChem, Germany), amoxicillin/clavulanic acid (Sigma-Aldrich, Portugal). Stock solution of antibiotics were prepared at 100 000 mg.l<sup>-1</sup>. Working solutions were prepared on the day of use at 1024 mg.l<sup>-1</sup>, and from these two-fold serial dilutions were made in AUM. The antibiotic concentrations tested ranged from 0.5 to 1024 mg.l<sup>-1</sup>.

#### **4.2.5 Antibiotic susceptibility testing**

The antibiotic susceptibility of single- and dual-species biofilms pre-formed on silicone coupons was evaluated according to Ceri *et al.*<sup>26</sup> with slight modifications. Briefly, silicone coupons (1 × 1 cm) were placed on the bottom of the wells of the 24-well tissue culture plates (Orange Scientific, Belgium). The biofilm formation was performed as described above. After 48 h, silicone coupons with biofilm were washed twice in 3 ml of 0.85% (v/v) sterile saline and placed in a new well of the tissue culture plate. Then, two-fold serial dilutions of the antibiotic in AUM were applied in the pre-established biofilms and the plates were incubated for 24 h at 37 °C, under static conditions. It is important to notice that, at 48 h, the biofilms are mature and the species involved in dual-species biofilms are equally fit.

After the antibiotic exposure, the coupons with biofilms were washed and placed in a new well of the 24-well tissue culture plate containing 1.5 ml of 0.85% (v/v) sterile saline. Subsequently, biofilms were sonicated, according the conditions stated above (sub-section 4.2.3), and the suspension of each biofilm was spotted onto TSA plates. The plates were incubated at 37 °C for CFU enumeration. These counts allowed to determine the minimum biofilm eradication concentration (MBEC) values, which corresponded to the lower concentration of antibiotic required to eradicate 99% of the sessile bacteria.

#### **4.2.6 Determination of the species relative composition after antibiotic exposure**

To determine the effect of sub-MBEC concentrations of antibiotics on the species composition in the dual-species biofilms, the CFU enumeration was performed for the concentration close to the MBEC and 8× and 64× lower concentrations. Then, population compositions after and before antibiotic exposure, were compared. A good correlation between LNA/2'OMe-FISH procedure and CFU counts was shown in Chapter 3; therefore, it was considered that the CFU enumeration reflects the population involved in the dual-species biofilms.

#### ***4.2.7 Effect of inoculum size on the species relative composition after antibiotic exposure***

To understand the effect of inoculum size on the species relative composition in antibiotic treated dual-species biofilms, two conditions were tested: i) the antibiotic susceptibility of *E. coli*  $10^5$  CFU.ml<sup>-1</sup> / *D. tsuruhatensis*  $10^2$  CFU.ml<sup>-1</sup> and *E. coli*  $10^5$  CFU.ml<sup>-1</sup> / *A. xylosoxidans*  $10^2$  CFU.ml<sup>-1</sup> dual-species biofilms to four antibiotic agents; ii) the susceptibility to ampicillin and amoxicillin/clavulanic acid was tested for the *E. coli*  $10^2$  CFU.ml<sup>-1</sup> / *D. tsuruhatensis*  $10^5$  CFU.ml<sup>-1</sup> and *E. coli*  $10^2$  CFU.ml<sup>-1</sup> / *A. xylosoxidans*  $10^5$  CFU.ml<sup>-1</sup> dual-species biofilms. These experiments were performed as described above (sub-section 4.2.5). The CFU enumeration was also performed for the concentration close to the MBEC and 8× and 64× lower concentrations to determine the species relative composition of each dual-species biofilm.

#### ***4.2.8 Spatial organization of biofilm populations***

In order to assess the biofilm spatial organization and the species distribution, the LNA/2'OMe-FISH procedure in combination with CLSM analysis was performed directly on single- and dual-species biofilms formed on silicone coupons at 192 h and on ampicillin treated-biofilms, according to a protocol already stated in sub-section 3.2.8 (Chapter 3).

Finally, the biofilm CSLM images were acquired in a FluoViewFV1000 microscope (Olympus) as described in sub-section 3.2.9 (Chapter 3).

#### ***4.2.9 Statistical analysis***

Results were compared using ANOVA by applying Levene's test of homogeneity of variance and the Tukey multiple-comparisons test, using the SPSS software. All tests were performed with a confidence level of 95%.

### **4.3 Results and discussion**

Typically, in ecological and clinical environments, biofilm communities are dominated by the species that is better fitted to the environmental conditions<sup>27, 28</sup>.

However, other pathogenic species, or even, species with an unknown pathogenic potential (e.g. *D. tsuruhatensis* and *A. xylosoxidans*) are also present at a lesser extent<sup>5</sup>.

Previous work (Chapter 2) on *D. tsuruhatensis* and *A. xylosoxidans* bacteria provided relevant information about the type of interactions between these species and *E. coli*, as well as on their impact on biofilm formation and development. While the uncommon bacteria are not directly involved in the pathogenesis of the biofilm, they seemed to help the establishment of the predominant species in the microbial consortium<sup>14, 29</sup>. As the results presented in Chapter 2 were performed in a 96-well plate model, with surfaces that are composed by polystyrene, the first experiments of the present chapter intended to clarify if this behavior is maintained on silicone surfaces. As such, two consortia composed by the *E. coli* and the uncommon bacteria (*E. coli* / *D. tsuruhatensis* and *E. coli* / *A. xylosoxidans*), formed on silicone surfaces in AUM at 37 °C were studied.

#### ***4.3.1 Single- and dual-species biofilms growth and spatial organization of the species on silicone material***

First, we assessed the ability of these species to form biofilm on silicone coupons in single- and dual-species biofilms. In single-species biofilms, from 2 h up to 48 h, the CFU counts significantly increased for all species ( $p < 0.05$ ). Then, all species stabilized with CFU counts ranging between Log 7.3 CFUs.cm<sup>-2</sup> and Log 7.8 CFUs.cm<sup>-2</sup>. These results corroborated the one previously obtained in Chapter 2. In addition, the CLSM images for *E. coli*, *D. tsuruhatensis* and *A. xylosoxidans* single-species biofilms are available in Supplemental material (Figure S4.1).

To study the influence of the uncommon bacteria on the  $W_{E.coli}$ , *E. coli* was co-cultured with each uncommon bacterium (Figure 4.1-a). It was clear that at early stages of biofilm formation the  $W_{E.coli}$  increased significantly in the presence of both uncommon bacteria ( $p < 0.05$ ). For the *E. coli* / *D. tsuruhatensis* biofilm, this fitness increase was also noticed at 192 h ( $p < 0.05$ ). Overall, these results were similar to the results of Chapter 2 obtained in polystyrene 96-well tissue culture plates, where the uncommon bacteria and *E. coli* coexisted within the dual-species biofilms at high cell concentrations, with a positive effect on *E. coli* fitness.

The elucidation of the bacterial interactions can be supported by the spatial distribution of the species within the polymicrobial biofilms. It has been shown that



particular interactions are associated with specific spatial organizations<sup>12</sup>. As such, a multiplex LNA/2'OMe-FISH technique previously validated (Chapter 3) on biofilm samples was combined with CLSM to assess the spatial organization of the species in 192 h-dual-species biofilms (Figure 4.1-b,c). The information allowed to infer the type of interaction that occurs between *E. coli* and the uncommon bacteria. Images show that the dual-species biofilms were composed by both species mixed together in a typical co-aggregation structure. This spatial organization occurs commonly when the species within the biofilm cooperate or interact synergistically<sup>12</sup>. Relating this information with data described in present Chapter, it becomes clear that *E. coli* might benefit from the presence of the *D. tsuruhatensis* and *A. xylosoxidans* or, at least, *E. coli* and these uncommon bacteria are not negatively affected by each other's presence, coexisting in the biofilm.

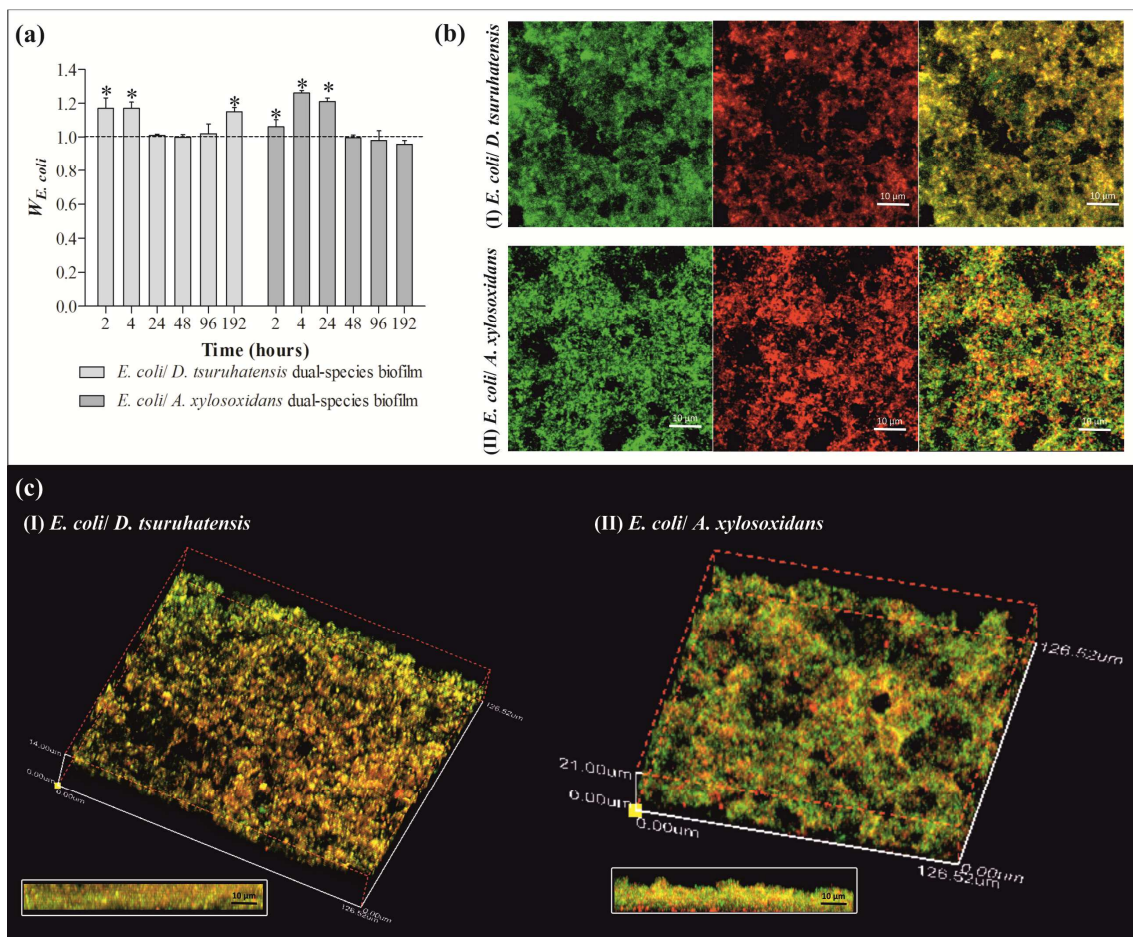


**Figure 4.1** - Single- and dual-species biofilm growth in silicone material. The three species were individually cultured or co-cultured at 37 °C, on silicone coupons, under static conditions. Two independent experiments were performed for each condition.

**Figure 4.1 (continuation)** - Error bars represent the standard deviation. (a) Representation of the relative fitness of *E. coli* when co-cultured with the uncommon bacteria (*D. tsuruhatensis* and *A. xylosoxidans*). The dashed line represents the relative fitness of 1, which means that the species are equally fit. The asterisk symbol (\*) placed over the bars indicates a statistically significant difference between the relative fitness of *E. coli* in dual-species biofilms and 1 ( $p < 0.05$ ). (b) CLSM images of *E. coli*  $10^5$  CFU.ml<sup>-1</sup> / *D. tsuruhatensis*  $10^5$  CFU.ml<sup>-1</sup> (I) and *E. coli*  $10^5$  CFU.ml<sup>-1</sup> / *A. xylosoxidans*  $10^5$  CFU.ml<sup>-1</sup> (II), distinguishing each bacteria in two different fluorescence channels and the superposition of the two fields. (c) CLSM showing the biofilm spatial organization of *E. coli*  $10^5$  CFU.ml<sup>-1</sup> / *D. tsuruhatensis*  $10^5$  CFU.ml<sup>-1</sup> (I) and *E. coli*  $10^5$  CFU.ml<sup>-1</sup> / *A. xylosoxidans*  $10^5$  CFU.ml<sup>-1</sup> (II) 192 h dual-species biofilms. The bottom images represent the transversal planes.

In the synergetic interactions, microorganisms acquire a beneficial phenotype which can result in the development of a stable biofilm, metabolic cooperation, increased resistance to antibiotics and host immune responses<sup>12</sup>. Several studies have demonstrated that the polymicrobial consortia are more resistant to antibiotic treatment than the corresponding mono-species biofilms<sup>15, 17, 30, 31</sup>. This demonstrated that under challenging conditions imposed by the use of antibacterial agents, the species within the biofilm can cooperate metabolically in order to protect themselves<sup>12, 31</sup>. In fact, the population proportion might be adjusted in order to reach a new balance better suited to the new environmental conditions.

#### ***4.3.2 Antibiotic effects on the relative composition and spatial organization of biofilms formed by E. coli and uncommon bacteria***

Assuming that the uncommon bacteria might cooperate with *E. coli* and that this cooperation might have an impact on the antimicrobial profile of the overall microbial consortia, the antibiotic resistance profiles of dual-species biofilms were characterized.

Four relevant antibiotics/antibiotic combinations with different modes of action were applied in a 48 h pre-established dual-species biofilms; and, the more prevalent species was determined for the three different antibiotic concentrations below the MBEC. The antibiotics selected, including ciprofloxacin, gentamicin, ampicillin and amoxicillin/clavulanic acid (from the fluoroquinolone, aminoglycoside and  $\beta$ -lactam drug-class, respectively), are widely used in the treatment of UTIs and CAUTIs<sup>9, 23-25</sup>.

The MBECs were evaluated for the single- and dual-species biofilms. Results are listed on Table 4.1.

For the dual-species biofilms (*E. coli* 10<sup>5</sup> CFU.ml<sup>-1</sup> / *D. tsuruhatensis* 10<sup>5</sup> CFU.ml<sup>-1</sup>; *E. coli* 10<sup>5</sup> CFU.ml<sup>-1</sup> / *A. xylosoxidans* 10<sup>5</sup> CFU.ml<sup>-1</sup>), it was also expected that higher concentrations of antibiotics were needed to eradicate the consortia than those required to eradicate single-species biofilms; or, at least, an antibiotic concentration equal to the one needed to eradicate the more resistant species which, in this case, were *D. tsuruhatensis* and *A. xylosoxidans*. As expected, in general the MBEC results showed that behavior. An exception was observed for the *E. coli* / *D. tsuruhatensis* dual-species biofilm where the ciprofloxacin was able to eradicate the biofilm at very low concentration (0.5 mg.l<sup>-1</sup>). While individually the single-species biofilms were highly resistance to ciprofloxacin; when combined the resulting mixed biofilm was highly susceptible to the antibiotic. This result reflects how urgent it is to understand the composition and the species interactions in mixed biofilms in order to select a therapy directed to the species involved.

**Table 4.1** - MBEC values for *E. coli*, *D. tsuruhatensis* and *A. xylosoxidans* single- and dual-species biofilms, exposed to four relevant antibiotics. An initial inoculum concentration of 10<sup>5</sup> CFU.ml<sup>-1</sup> was used for these experiments.

	Antibiotics (mg.l <sup>-1</sup> )			
	Ciprofloxacin	Ampicillin	Gentamicin	Amoxicillin/ Clavulanic acid*
<i>E. coli</i>	256	128	2	64/9.15
<i>D. tsuruhatensis</i>	256	>1024	256	>1024/146.29
<i>A. xylosoxidans</i>	256	>1024	32	>1024/146.29
<i>E. coli</i> / <i>D. tsuruhatensis</i>	0.50	>1024	64	>1024/146.29
<i>E. coli</i> / <i>A. xylosoxidans</i>	256	>1024	64	>1024/146.29

\*ratio 1/7 used in clinical treatments.

While it was apparent that, in general, the presence of the uncommon bacteria highly increased the *E. coli* odds of surviving in the presence of antibiotic agents, it was unclear if the exposure to these agents results in a new repositioning of the population

balance. To further investigate this, the dual-species biofilm cells were quantified after exposure to antibiotic concentration near or below the MBEC (the CFU.cm<sup>-2</sup> values are present in Supplemental material on Table S4.1, Table S4.2 and Table S4.3). Figure 4.2 shows which species was more prevalent after the introduction of specific antibiotic agents. Before antibiotic exposure, the proportions of the species were similar in both dual-species biofilms with a slight prevalence of *E. coli* (Figure 4.2-a, b). After antibiotic exposure, results showed that, in general, the relative bacteria composition of the dual-species biofilms was dependent of the antibiotic and concentration applied. For ciprofloxacin, the 3 bacteria presented high MBEC and, thus, the percentages of each population were more balanced. For the other 3 antibiotics, for which MBEC values of the uncommon bacteria were much higher than those obtained for the *E. coli*, a different behavior was observed. It would be expectable that the more resistant species would dominate the microbial consortia. This, in fact, happened for gentamycin-exposed dual-species biofilms, where the percentage of the uncommon species increased with the antibiotic concentration. However, the opposite happened for the ampicillin and amoxicillin/clavulanic acid-exposed biofilms. While the uncommon bacteria biofilm cells were much more resistant, surprisingly the *E. coli* population dominated the consortia. Both ampicillin and amoxicillin/clavulanic acid belong to the same antibiotic class, the  $\beta$ -lactam class, which might explain the similar results obtained for both antibiotics. The  $\beta$ -lactam antibiotics are able to inhibit the cell wall biosynthesis in the bacterial cell, which ultimately might lead to the cell lysis<sup>32</sup>. Interestingly, biofilms resistance was observed even in the presence of clavulanic acid, which is an inhibitor of the  $\beta$ -lactamase production.

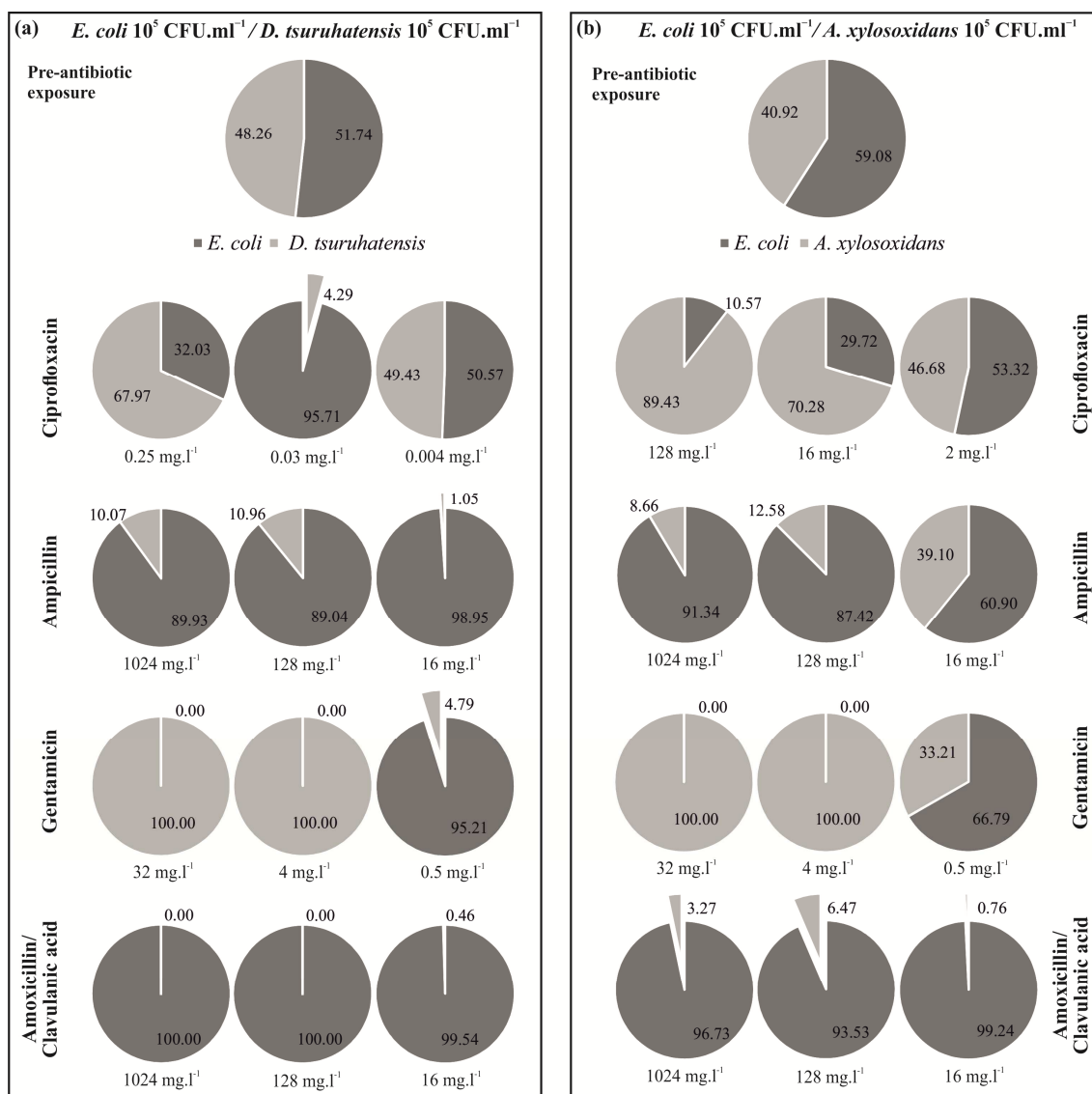


**Figure 4.2** - Relative bacteria composition of the dual-species biofilms after antibiotic exposure. For each antibiotic, the (a) *E. coli* / *D. tsuruhatensis* and (b) *E. coli* / *A. xylosoxidans* 48 h dual-species biofilms were exposed to three different concentrations below the MBEC; then, the CFU counts were determined after 24 h of exposure. An initial inoculum concentration of 10<sup>5</sup> CFU.ml<sup>-1</sup> was used for these experiments. Two independent experiments were performed for each condition.

These results suggested that a small relative percentage of the *D. tsuruhatensis* and *A. xylosoxidans* was sufficient to introduce some protective changes on the *E. coli* physiology, promoting its resistance and survival against the ampicillin and amoxicillin/clavulanic acid treatment. To determine if this protective effect exhibited by *D. tsuruhatensis* and *A. xylosoxidans* is maintained in the presence of low initial ratios

of the species, the initial inoculum concentration of these species was lowered ( $10^2$  CFU.ml<sup>-1</sup>) when co-cultured with *E. coli* ( $10^5$  CFU.ml<sup>-1</sup>).

In general, while the MBEC values decreased due, in part, to a low initial inoculum concentration of *D. tsuruhatensis* and *A. xylosoxidans* (Table 4.2), *E. coli* population dominated the consortia after the antibiotic treatment (Figure 4.3). The exception was for the ciprofloxacin action on the *E. coli*  $10^5$  CFU ml<sup>-1</sup> / *A. xylosoxidans*  $10^2$  CFU ml<sup>-1</sup> (Figure 4.3-b). Concerning the gentamycin-treated dual-species biofilms, as previously observed, the results also showed that the *E. coli* population only survived when the antibiotic concentration was below the MBEC of *E. coli* single-species biofilms (Figure 4.3-a, b).

**Table 4.2** - Effect of a low *D. tsuruhatensis* or *A. xylosoxidans* initial inoculum concentration ( $10^2$  CFUs.ml<sup>-1</sup>) on the *in vitro* susceptibility of the dual-species biofilms to four relevant antibiotics.

	Antibiotics (mg.l <sup>-1</sup> )			
	Ciprofloxacin	Ampicillin	Gentamicin	Amoxicillin/ Clavulanic acid*
<i>E. coli</i> $10^5$ CFU.ml <sup>-1</sup> / <i>D. tsuruhatensis</i> $10^2$ CFU.ml <sup>-1</sup>	0.5	512	16	512
<i>E. coli</i> $10^5$ CFU.ml <sup>-1</sup> / <i>A. xylosoxidans</i> $10^2$ CFU.ml <sup>-1</sup>	128	256	16	128

\*ratio 1/7 used in clinical treatments.

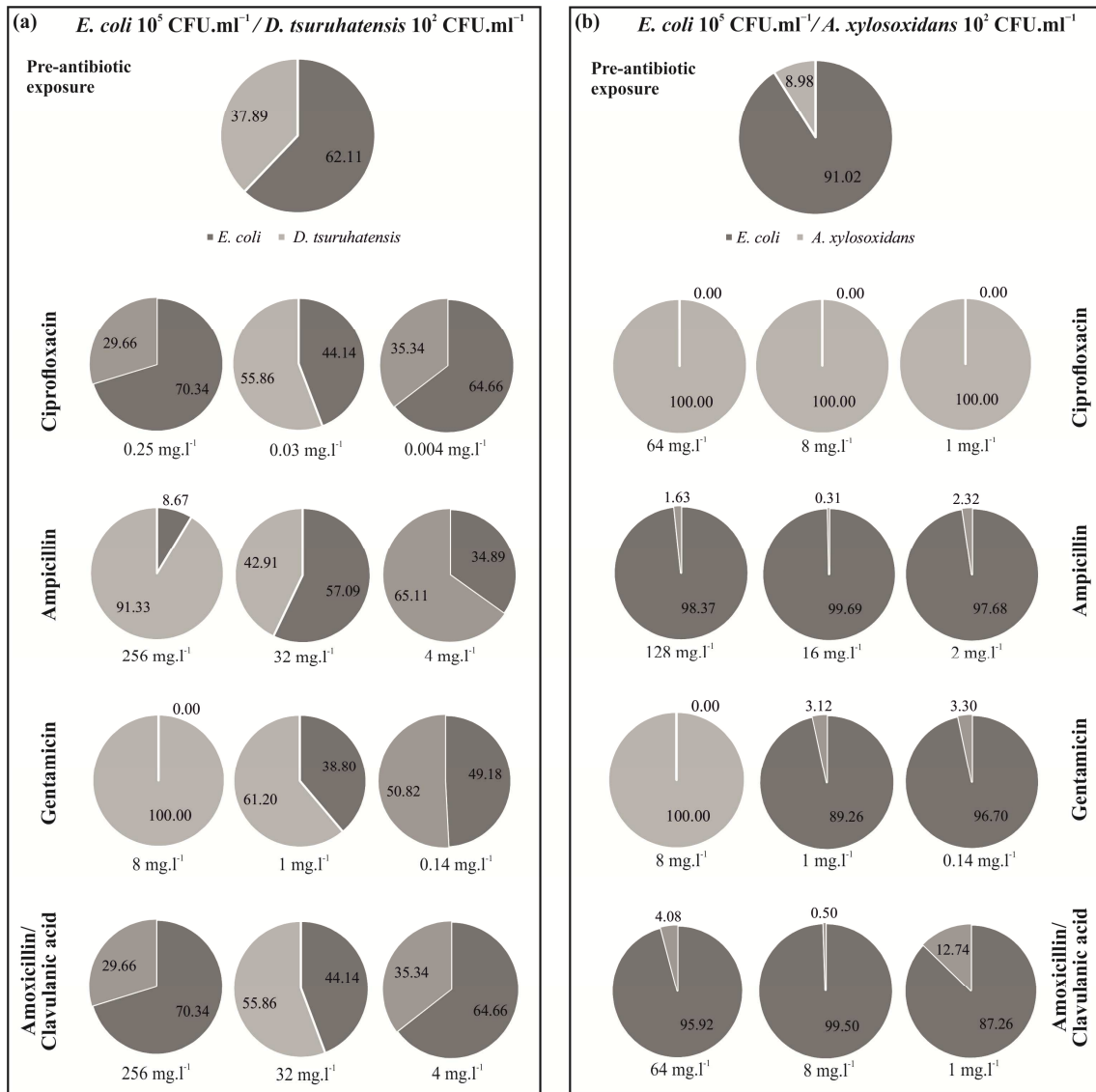


**Figure 4.3** - Effect of a lower *D. tsuruhatensis* or *A. xylosoxidans* initial inoculum concentration ( $10^2$  CFU.ml<sup>-1</sup>) on the *E. coli* population after antibiotic exposure. For each antibiotic, the (a) *E. coli* / *D. tsuruhatensis* and (b) *E. coli* / *A. xylosoxidans* 48 h dual-species biofilms were exposed to three different concentrations below the MBEC, then, the CFU counts were determined after 24 h of exposure. An *E. coli* initial inoculum concentration of  $10^5$  CFU.ml<sup>-1</sup> was used for these experiments. Two independent experiments were performed for each condition.

Next, it was also important to understand whether the *E. coli* population is able to dominate the ampicillin and amoxicillin/clavulanic acid treated biofilms even lowering significantly its initial inoculum concentration ( $10^2$  CFU.ml<sup>-1</sup>). The results showed that a lower initial inoculum concentration of *E. coli* did not affect the MBEC value to ampicillin and amoxicillin/clavulanic acid of dual-species biofilms (Supplemental material – Table S4.4). *E. coli* lost its dominance when co-cultured with

*D. tsuruhatensis*, but in general, was able to persist within the consortia (~20% of the total population) (Figure 4.4-a). When co-cultured with *A. xylosoxidans*, *E. coli* maintained its dominance (Figure 4.4-b).

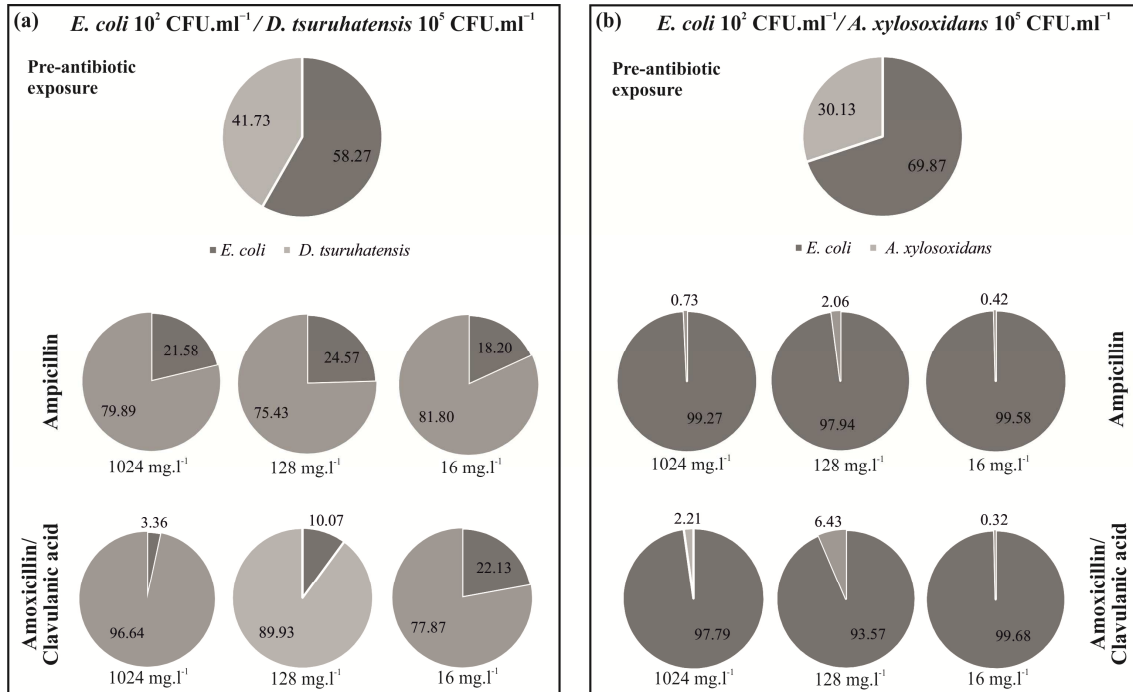


**Figure 4.4** - Effect of a lower *E. coli* initial inoculum concentration (10<sup>2</sup> CFU.ml<sup>-1</sup>) on the relative bacteria composition of the dual-species biofilms after ampicillin and amoxicillin/alavulanic acid exposure. For each antibiotic, the (a) *E. coli* / *D. tsuruhatensis* and (b) *E. coli* / *A. xylosoxidans* 48 h dual-species biofilms were exposed to three different concentrations below the MBEC, then, the CFU counts were determined after 24 h of exposure. An initial inoculum concentration of 10<sup>5</sup> CFU.ml<sup>-1</sup> for *D. tsuruhatensis* and *A. xylosoxidans* was used for these experiments. Two independent experiments were performed for each condition.

The images captured by CLSM revealed that the dual-species biofilms maintain the same structure after treatment with ampicillin (Figure 4.5). The species are closely associated with a dominance of *E. coli* population (Figure 4.5-II, VI, VII, VIII). Collectively, these results suggested that the uncommon bacteria seem to offer a shared resistance to the *E. coli* population, independently of its initial inoculum concentration. In fact, Lee *et al.*<sup>33</sup> have reported that the role of the species in a consortium is not necessarily related with this abundance; the less abundant species might have a protective effect over the other members involved in the consortia.



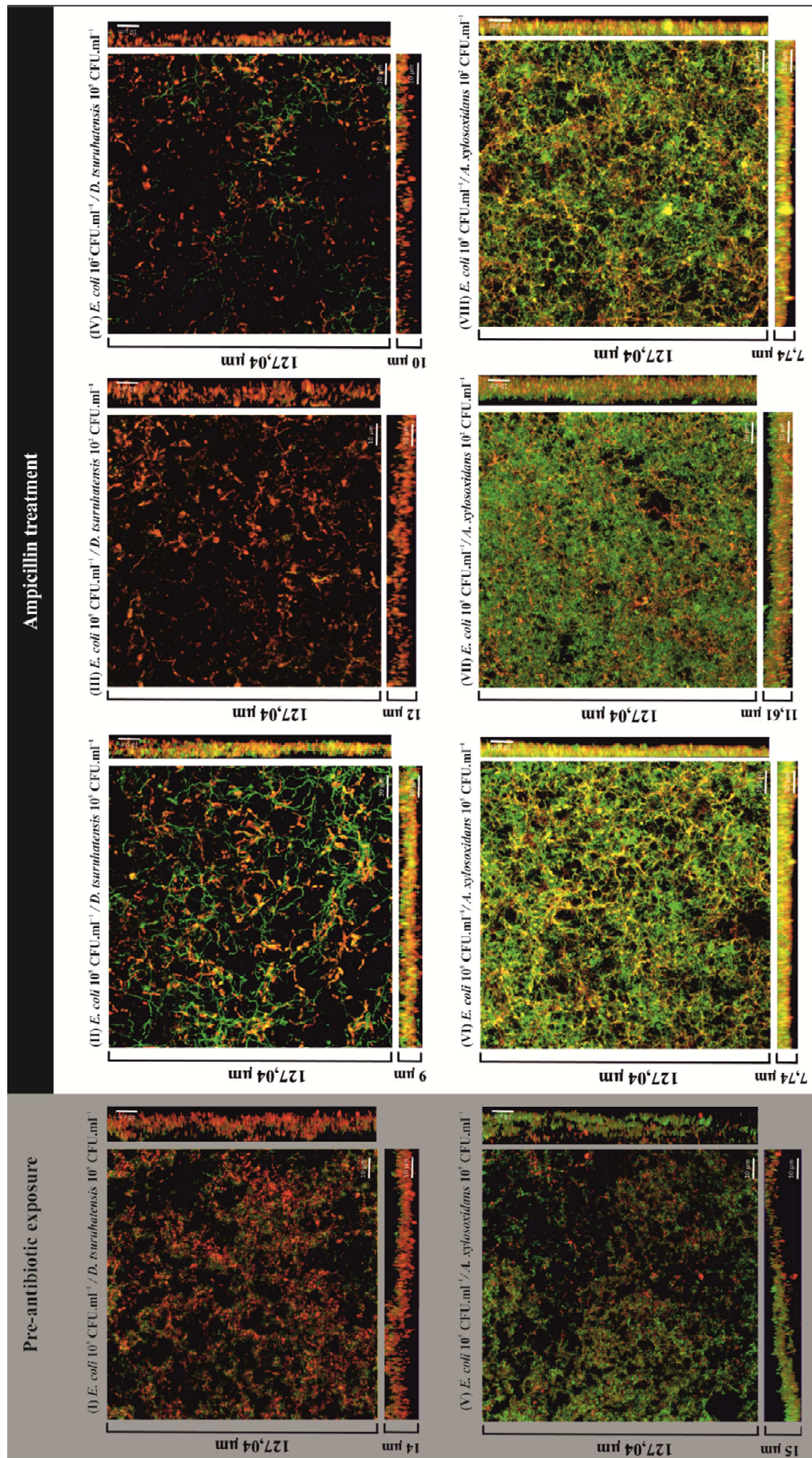


Figure 4.5 - Spatial localization and structure of dual-species biofilms exposed to ampicillin.

**Figure 4.5 (continuation)** - The CLSM showing the biofilm spatial organization of (I) *E. coli*  $10^5$  CFU ml<sup>-1</sup>/ *D. tsuruhatensis*  $10^5$  CFU.ml<sup>-1</sup> before the ampicillin exposure; and, (II) *E. coli*  $10^5$  CFU ml<sup>-1</sup>/ *D. tsuruhatensis*  $10^5$  CFU.ml<sup>-1</sup>, (III) *E. coli*  $10^5$  CFU.ml<sup>-1</sup>/ *D. tsuruhatensis*  $10^2$  CFU.ml<sup>-1</sup>, (IV) *E. coli*  $10^2$  CFU.ml<sup>-1</sup>/ *D. tsuruhatensis*  $10^5$  CFU.ml<sup>-1</sup> after ampicillin treatment; (V) *E. coli*  $10^5$  CFU.ml<sup>-1</sup>/ *A. xylosoxidans*  $10^5$  CFU.ml<sup>-1</sup> before the ampicillin exposure; and, (VI) *E. coli*  $10^5$  CFU.ml<sup>-1</sup>/ *A. xylosoxidans*  $10^5$  CFU.ml<sup>-1</sup>, (VII) *E. coli*  $10^5$  CFU ml<sup>-1</sup>/ *A. xylosoxidans*  $10^2$  CFU.ml<sup>-1</sup>, (VIII) *E. coli*  $10^2$  CFU.ml<sup>-1</sup>/ *A. xylosoxidans*  $10^5$  CFU.ml<sup>-1</sup> after ampicillin treatment. The bottom and side images of each panel represent the transversal planes.

Recently, several studies have demonstrated a new phenomenon of antibiotic resistance based on the “shared resistance” by some members of the microbial consortia<sup>33-35</sup>. However, the mechanism underlying this shared resistance is unknown. For the results presented here, three hypotheses are formulated to explain the dominance of the more antibiotic-sensitive species in a polymicrobial biofilm (Figure 4.6): 1) the transfer of genetic material from the uncommon bacteria to *E. coli*; 2) the induction of a different physiological state in *E. coli* due to antibiotic uptake; 3) the degradation of the antibiotic in the biofilm matrix, through the action of the  $\beta$ -lactamases produced by the uncommon bacteria.

Horizontal gene transfer of antibiotic resistance genes is a way by which some bacteria become resistant to antibiotic agents<sup>36</sup>. Recent data have also been provided for the occurrence of this mechanism in biofilms<sup>36-40</sup> which may result, in part, from the close cell-to-cell contact occurring in the biofilm<sup>38</sup>. For instance, the horizontal transfer of specific genes coding for  $\beta$ -lactamases, is not new. May *et al.*<sup>37</sup> reported that the resistance to  $\beta$ -lactam antibiotics is mainly due to the localization of the  $\beta$ -lactamase genes on plasmids, which can spread rapidly among bacteria.

Regarding the induction of a different physiological state, Kara *et al.*<sup>31</sup> have suggested this type of interaction for *Streptococcus mutans* and *Veillonella parvula*. When *S. mutans* was co-cultured with *V. parvula*, the latter species induced changes in the gene expression of *S. mutans* allowing its survival under challenging conditions caused by the use of different antibacterial compounds. Another study reported that the sub-inhibitory concentrations of  $\beta$ -lactam antibiotics promote alterations into the biofilm phenotype, such as a loss of viable bacteria and an increase in biofilm biomass, which can protect and allow the survival of the bacteria exposed to antibiotic agents<sup>41</sup>.

Regarding the last hypothesis, it was demonstrated that the presence of  $\beta$ -lactamases in the biofilms matrix might inactivate  $\beta$ -lactam antibiotics<sup>42</sup>. Lee *et al.*<sup>33</sup> suggested that *Pseudomonas protegens* was able to protect all species involved in the microbial consortia (*P. aeruginosa* and *K. pneumonia*) when exposed to tobramycin, probably due to the ability of the resistant species to produce enzymes that degrade or modify the antibiotics.

In the present chapter, as previously reported by Lee *et al.*<sup>33</sup>, there was no selection of the more resistant species (*D. tsuruhatensis* and *A. xylosoxidans*) over the *E. coli* (the less resistant species). The presence of resistant species, even in low concentration, seemed to offer a protection, allowing the survival and dominance of *E. coli* within microbial consortia under lethal antibiotic concentrations. While the uncommon bacteria (the resistant species) might have their metabolism directed to the secretion of  $\beta$ -lactamases, *E. coli* (the susceptible cells) might gain benefit from the action of  $\beta$ -lactamases secreted. In this situation, *E. coli* does not expend energy in producing enzymes and may redirect that energy to promote its growth and survival without paying the cost. A similar scenario, described by Foster *et al.*<sup>43</sup>, reports that the resistant cells, through the production of enzymes that break down the antibiotic agents, promote the growth of susceptible cells without cost, conferring a competitive disadvantage to the resistant cells.

Finally, it is important to note that to ensure the reproducibility of results the use of an established formula of artificial urine was preferred. In fact, human urine varies significantly in terms of pH and compositions according the type of food intake and the health of the individual<sup>44</sup>. The formula used in this study was reported as a suitable replacement for normal urine and may be used in a wide range of experiments (e.g. for modelling the growth and attachment of urinary pathogens in the clinical environment)<sup>11, 20, 45-47</sup>. Also, the use of a dynamic biofilm system might allow better mimicking of the urine flow that occurs in the urinary catheter, but the experiments were performed in static conditions using the well plates. These platforms offer the possibility of providing a larger amount of data<sup>48, 49</sup>.

## 4.4 Conclusions

Interactions between *E. coli* and uncommon bacteria in CAUTIs can promote *E. coli* survival under challenging conditions, such as those imposed by the antibiotic agents. A residual concentration of these uncommon bacteria appears to be sufficient to protect *E. coli* population. In fact, for certain situations where *E. coli* was more sensitive to the antibiotics than the other microorganisms, it was, nonetheless, able to predominate within the dual-species biofilms. Combining the results obtained in this chapter, Figure 4.6 shows a schematic representation of the hypothesis proposed to explain the predominance of a certain species (*E. coli*, in this case) when a dual-species biofilm is exposed to antibiotics agents or other molecules.

While synergistic interactions between the *E. coli* and the uncommon bacteria might significantly contribute to the development of well-organized and resistant biofilm structures, it also became clear that some particular species-combination might induce metabolic processes that decrease the resistance mechanism.

In conclusion, this study suggested that there are new aspects about the role of uncommon bacteria that should be investigated such as, how the protection offered by these species contribute to the survival and dominance of sensitive species under lethal antibiotic concentrations. More experiments involving this type of bacteria should be carried out, and the mechanisms involved in evolution of antibiotic resistance should be taken into consideration. In addition, it is suggested that the microbial composition and environmental conditions present in the polymicrobial biofilms should be considered in the development and validation of novel antimicrobial strategies.

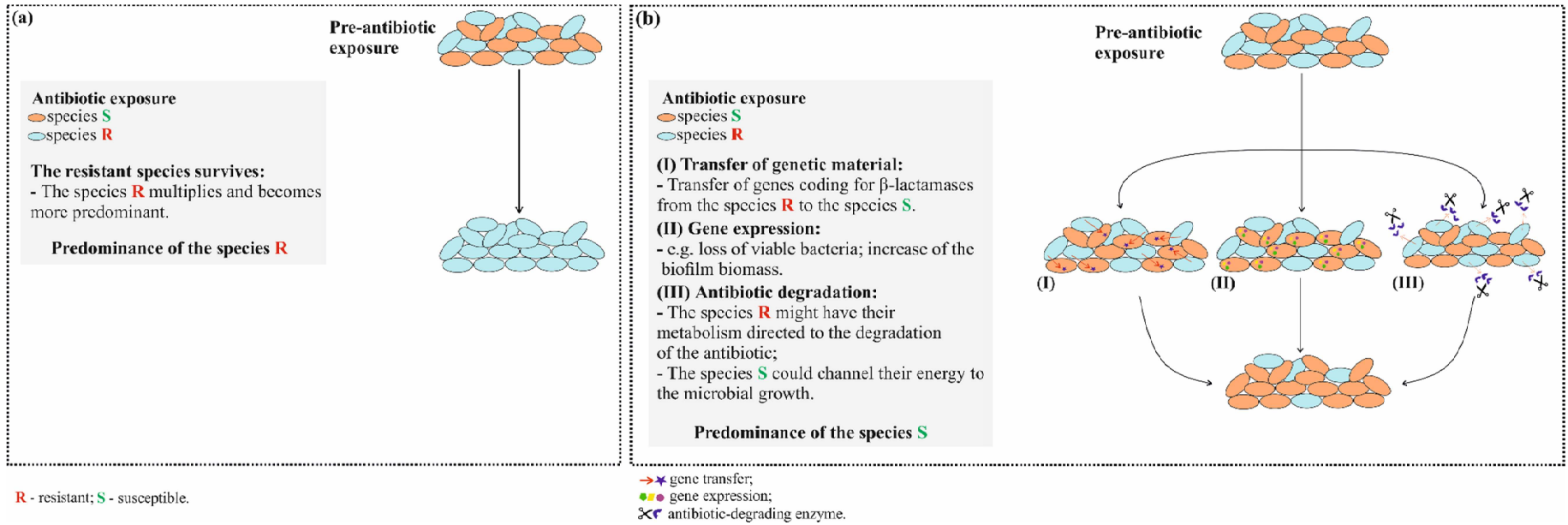


**Figure 4.6** - Schematic representation of the hypothesis proposed in the present work to explain the predominance of a certain species when a dual-species biofilm is exposed to antibiotic. After antibiotic exposure, (a) typically the species more resistant survives and dominates the microbial consortia; (b) however, the opposite can occur, and, the more susceptible species resists and dominates. Some hypothesis to explain that observation include, I) transfer of genetic material from the resistant species to the susceptible species; II) induction of a different physiological state in the susceptible species due to the antibiotic uptake; III) degradation of the antibiotic in the biofilm matrix, through the action of the enzymes produced by the resistant species.

## 4.5 References

1. **K.A. Kline, D.J. Schwartz, N.M. Gilbert, S.J. Hultgren, A.L. Lewis.** Immune modulation by group B *Streptococcus* influences host susceptibility to urinary tract infection by uropathogenic *Escherichia coli*. *Infect Immun* **80**, 4186-4194 (2012).
2. **R. Baldan, C. Cigana, F. Testa, I. Bianconi, M. De Simone, D. Pellin, C. Di Serio, A. Bragonzi, D.M. Cirillo.** Adaptation of *Pseudomonas aeruginosa* in cystic fibrosis airways influences virulence of *Staphylococcus aureus in vitro* and murine models of co-infection. *PLoS One* **9**, e89614 (2014).
3. **C.E. Armbruster, S.N. Smith, A. Yep, H.L. Mobley.** Increased incidence of urolithiasis and bacteremia during *Proteus mirabilis* and *Providencia stuartii* coinfection due to synergistic induction of urease activity. *J Infect Dis* **209**, 1524-1532 (2014).
4. **D.J. Stickler.** Bacterial biofilms in patients with indwelling urinary catheters. *Nat Clin Pract Urol* **5**, 598-608 (2008).
5. **D.N. Frank, S.S. Wilson, A.L. St Amand, N.R. Pace.** Culture-independent microbiological analysis of foley urinary catheter biofilms. *PLoS One* **4**, e7811 (2009).
6. **V. Hola, F. Ruzicka, M. Horka.** Microbial diversity in biofilm infections of the urinary tract with the use of sonication techniques. *FEMS Immunol Med Microbiol* **59**, 525-528 (2010).
7. **A. Ronald.** The etiology of urinary tract infection: traditional and emerging pathogens. *Am J Med* **113 Suppl 1A**, 14S-19S (2002).
8. **S. Niveditha, S. Pramodhini, S. Umadevi, S. Kumar, S. Stephen.** The isolation and the biofilm formation of uropathogens in the patients with catheter associated urinary tract infections (UTIs). *J Clin Diagn Res* **6**, 1478-1482 (2012).
9. **T.M. Hooton, S.F. Bradley, D.D. Cardenas, R. Colgan, S.E. Geerlings, J.C. Rice, S. Saint, A.J. Schaeffer, P.A. Tambayh, P. Tenke, L.E. Nicolle, A. Infectious Diseases Society of.** Diagnosis, prevention, and treatment of catheter-associated urinary tract infection in adults: 2009 International Clinical Practice Guidelines from the Infectious Diseases Society of America. *Clin Infect Dis* **50**, 625-663 (2010).
10. **L.E. Nicolle.** Catheter-related urinary tract infection. *Drugs Aging* **22**, 627-639 (2005).
11. **L. Cerqueira, J.A. Oliveira, A. Nicolau, N.F. Azevedo, M.J. Vieira.** Biofilm formation with mixed cultures of *Pseudomonas aeruginosa/Escherichia coli* on silicone using artificial urine to mimic urinary catheters. *Biofouling* **29**, 829-840 (2013).
12. **S. Elias, E. Banin.** Multi-species biofilms: living with friendly neighbors. *FEMS Microbiol Rev* **36**, 990-1004 (2012).
13. **J.T. Spadafino, B. Cohen, J. Liu, E. Larson.** Temporal trends and risk factors for extended-spectrum beta-lactamase-producing *Escherichia coli* in adults with catheter-associated urinary tract infections. *Antimicrob Resist Infect Control* **3**, 39 (2014).
14. **S.P. Lopes, H. Ceri, N.F. Azevedo, M.O. Pereira.** Antibiotic resistance of mixed biofilms in cystic fibrosis: impact of emerging microorganisms on treatment of infection. *Int J Antimicrob Agents* **40**, 260-263 (2012).
15. **M. Burmolle, J.S. Webb, D. Rao, L.H. Hansen, S.J. Sorensen, S. Kjelleberg.** Enhanced biofilm formation and increased resistance to antimicrobial agents and bacterial invasion are caused by synergistic interactions in multispecies biofilms. *Appl Environ Microbiol* **72**, 3916-3923 (2006).
16. **M. Kostaki, N. Chorianopoulos, E. Braxou, G.J. Nychas, E. Giaouris.** Differential biofilm formation and chemical disinfection resistance of sessile cells of *Listeria monocytogenes* strains under monospecies and dual-species (with *Salmonella enterica*) conditions. *Appl Environ Microbiol* **78**, 2586-2595 (2012).
17. **V. Leriche, R. Briandet, B. Carpentier.** Ecology of mixed biofilms subjected daily to a chlorinated alkaline solution: spatial distribution of bacterial species suggests a protective effect of one species to another. *Environ Microbiol* **5**, 64-71 (2003).
18. **M. Simões, L.C. Simões, M.J. Vieira.** Species association increases biofilm resistance to chemical and mechanical treatments. *Water Res* **43**, 229-237 (2009).

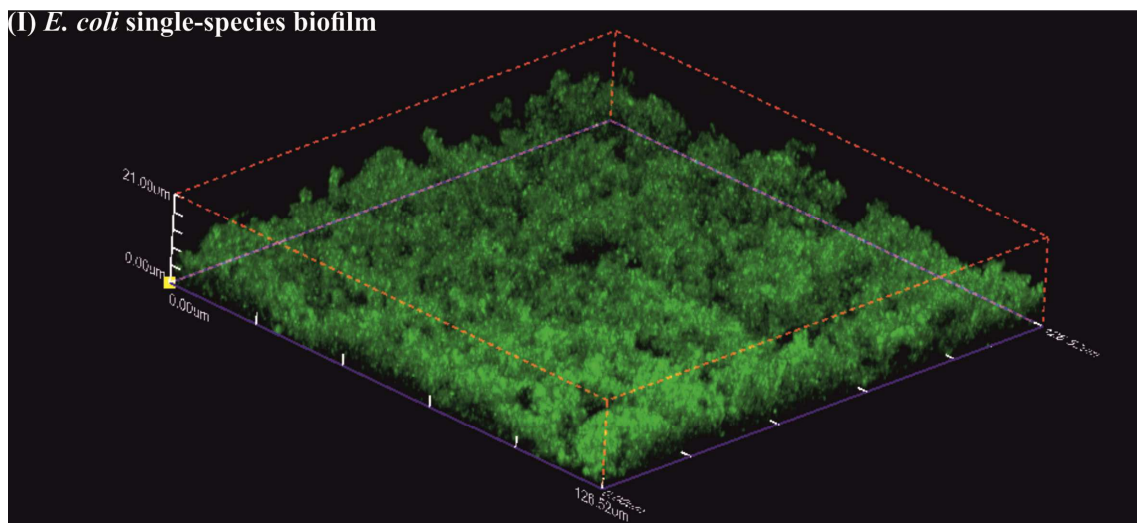
19. **S.P. Lopes, N.F. Azevedo, M.O. Pereira.** Microbiome in cystic fibrosis: Shaping polymicrobial interactions for advances in antibiotic therapy. *Crit Rev Microbiol* **41**, 353-365 (2015).
20. **T. Brooks, C.W. Keevil.** A simple artificial urine for the growth of urinary pathogens. *Lett Appl Microbiol* **24**, 203-206 (1997).
21. **E.L. Lawrence, I.G. Turner.** Materials for urinary catheters: a review of their history and development in the UK. *Med Eng Phys* **27**, 443-453 (2005).
22. **N.F. Azevedo, A.P. Pacheco, C.W. Keevil, M.J. Vieira.** Adhesion of water stressed *Helicobacter pylori* to abiotic surfaces. *J Appl Microbiol* **101**, 718-724 (2006).
23. **K.H. Dellimore, A.R. Helyer, S.E. Franklin.** A scoping review of important urinary catheter induced complications. *J Mater Sci Mater Med* **24**, 1825-1835 (2013).
24. **G.G. Zhanel, J.A. Karlowsky, G.K. Harding, A. Carrie, T. Mazzulli, D.E. Low, D.J. Hoban.** A Canadian national surveillance study of urinary tract isolates from outpatients: comparison of the activities of trimethoprim-sulfamethoxazole, ampicillin, mecillinam, nitrofurantoin, and ciprofloxacin. The Canadian Urinary Isolate Study Group. *Antimicrob Agents Chemother* **44**, 1089-1092 (2000).
25. **M.A. Steinman, R. Gonzales, J.A. Linder, C.S. Landefeld.** Changing use of antibiotics in community-based outpatient practice, 1991-1999. *Ann Intern Med* **138**, 525-533 (2003).
26. **H. Ceri, M.E. Olson, C. Stremick, R.R. Read, D. Morck, A. Buret.** The Calgary Biofilm Device: new technology for rapid determination of antibiotic susceptibilities of bacterial biofilms. *J Clin Microbiol* **37**, 1771-1776 (1999).
27. **J.B. Lyczak, C.L. Cannon, G.B. Pier.** Lung infections associated with cystic fibrosis. *Clin Microbiol Rev* **15**, 194-222 (2002).
28. **S.M. Jacobsen, D.J. Stickler, H.L. Mobley, M.E. Shirtliff.** Complicated catheter-associated urinary tract infections due to *Escherichia coli* and *Proteus mirabilis*. *Clin Microbiol Rev* **21**, 26-59 (2008).
29. **S.P. Lopes, N.F. Azevedo, M.O. Pereira.** Emergent bacteria in cystic fibrosis: *in vitro* biofilm formation and resilience under variable oxygen conditions. *Biomed Res Int* **2014**, 678301 (2014).
30. **A.G. Al-Bakri, P. Gilbert, D.G. Allison.** Influence of gentamicin and tobramycin on binary biofilm formation by co-cultures of *Burkholderia cepacia* and *Pseudomonas aeruginosa*. *J Basic Microbiol* **45**, 392-396 (2005).
31. **D. Kara, S.B. Luppens, J.M. Cate.** Differences between single-and dual-species biofilms of *Streptococcus mutans* and *Veillonella parvula* in growth, acidogenicity and susceptibility to chlorhexidine. *Eur J Oral Sci* **114**, 58-63 (2006).
32. **M.A. Kohanski, D.J. Dwyer, J.J. Collins.** How antibiotics kill bacteria: from targets to networks. *Nature reviews. Microbiology* **8**, 423-435 (2010).
33. **K.W. Lee, S. Periasamy, M. Mukherjee, C. Xie, S. Kjelleberg, S.A. Rice.** Biofilm development and enhanced stress resistance of a model, mixed-species community biofilm. *ISME J* **8**, 894-907 (2014).
34. **M.H. Perlin, D.R. Clark, C. McKenzie, H. Patel, N. Jackson, C. Kormanik, C. Powell, A. Bajorek, D.A. Myers, L.A. Dugatkin, R.M. Atlas.** Protection of *Salmonella* by ampicillin-resistant *Escherichia coli* in the presence of otherwise lethal drug concentrations. *Proc Biol Sci* **276**, 3759-3768 (2009).
35. **E.A. Yurtsev, H.X. Chao, M.S. Datta, T. Artemova, J. Gore.** Bacterial cheating drives the population dynamics of cooperative antibiotic resistance plasmids. *Mol Syst Biol* **9**, 683 (2013).
36. **M. Broszat, E. Grohmann** in *Antibiofilm Agents*, Vol. 8. (eds. K.P. Rumbaugh, I. Ahmad) 67-95 (Springer Berlin Heidelberg, 2014).
37. **T. May, A. Ito, S. Okabe.** Induction of multidrug resistance mechanism in *Escherichia coli* biofilms by interplay between tetracycline and ampicillin resistance genes. *Antimicrob Agents Chemother* **53**, 4628-4639 (2009).
38. **V.J. Savage, I. Chopra, A.J. O'Neill.** *Staphylococcus aureus* biofilms promote horizontal transfer of antibiotic resistance. *Antimicrob Agents and Chemother* **57**, 1968-1970 (2013).
39. **J.M. Ghigo.** Natural conjugative plasmids induce bacterial biofilm development. *Nature* **412**, 442-445 (2001).

40. **N. Hoiby, T. Bjarnsholt, M. Givskov, S. Molin, O. Ciofu.** Antibiotic resistance of bacterial biofilms. *Int J Antimicrob Agents* **35**, 322-332 (2010).
41. **S. Wu, X. Li, M. Gunawardana, K. Maguire, D. Guerrero-Given, C. Schaudinn, C. Wang, M.M. Baum, P. Webster.** Beta-lactam antibiotics stimulate biofilm formation in non-typeable *Haemophilus influenzae* by up-regulating carbohydrate metabolism. *PLoS One* **9**, e99204 (2014).
42. **O. Ciofu, N. Høiby** in *Antibiotic Policies: Fighting Resistance*. (eds. I.M. Gould, J.W.M. Meer) 149-174 (Springer US, Boston, MA; 2008).
43. **K.R. Foster.** The secret social lives of microorganisms. *Microbe* **6**, 183-186 (2011).
44. **R. Siener, A. Jahnen, A. Hesse.** Influence of a mineral water rich in calcium, magnesium and bicarbonate on urine composition and the risk of calcium oxalate crystallization. *Eur J Clin Nutr* **58**, 270-276 (2004).
45. **C. Almeida, N.F. Azevedo, J.C. Bento, N. Cerca, H. Ramos, M.J. Vieira, C.W. Keevil.** Rapid detection of urinary tract infections caused by *Proteus* spp. using PNA-FISH. *Eur J Clin Microbiol Infect Dis* **32**, 781-786 (2013).
46. **J.E. Klinth, M. Castelain, B.E. Uhlin, O. Axner.** The influence of pH on the specific adhesion of P piliated *Escherichia coli*. *PLoS One* **7**, e38548 (2012).
47. **H.S. Raffi, J.M. Bates, D.J. Flournoy, S. Kumar.** Tamm-Horsfall protein facilitates catheter associated urinary tract infection. *BMC Res Notes* **5**, 532 (2012).
48. **W.A. Duetz.** Microtiter plates as mini-bioreactors: miniaturization of fermentation methods. *Trends Microbiol* **15**, 469-475 (2007).
49. **S. Kumar, C. Wittmann, E. Heinzle.** Review: Minibioreactors. *Biotechnol Lett* **26**, 1-10 (2004).

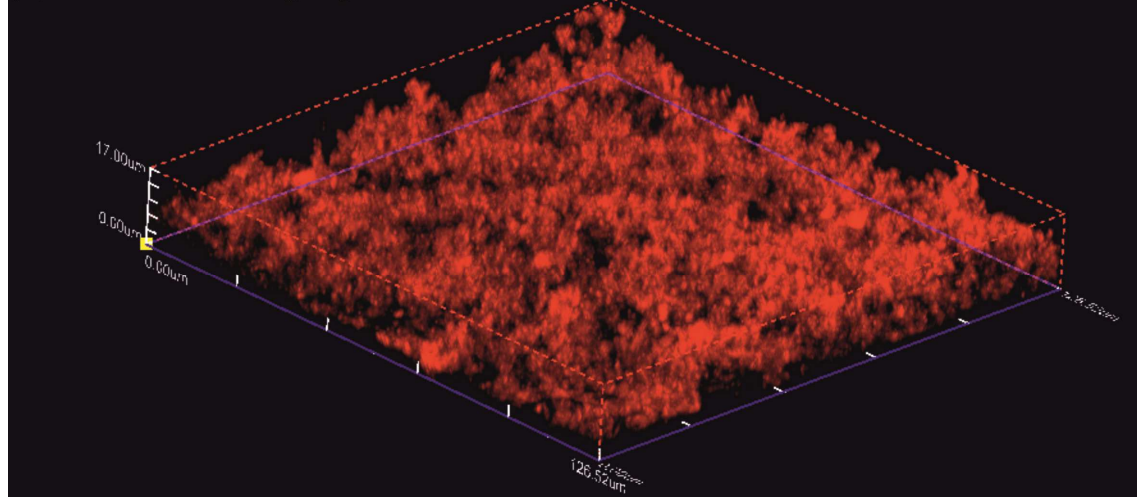


## 4.6 Supplemental material

(I) *E. coli* single-species biofilm



(II) *D. tsuruhatensis* single-species biofilm



(III) *A. xylosoxidans* single-species biofilm

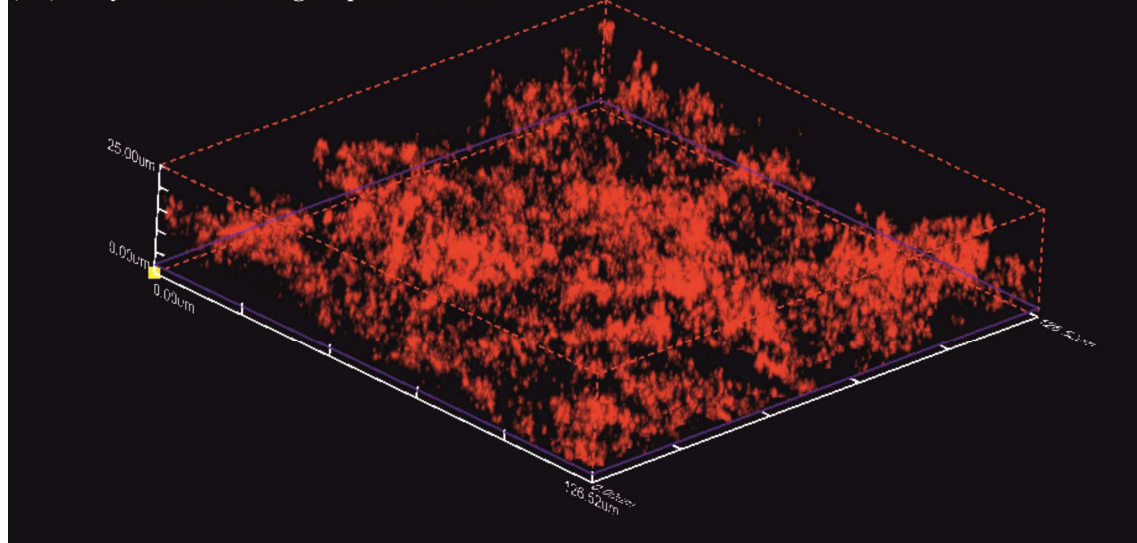


**Figure S4.1** - CLSM images of *E. coli* (I), *D. tsuruhatensis* (II) and *A. xylosoxidans* (III) single-species biofilms.

**Table S4.1** - CFU.cm<sup>2</sup> counts for the *E. coli* / *D. tsuruhatensis* and *E. coli* / *A. xylosoxidans* 48 h dual-species biofilms exposed to three different concentrations below the MBEC. These counts were determined after 24 h of exposure. An initial inoculum concentration of 10<sup>5</sup> CFU.ml<sup>-1</sup> for both species was used for these experiments.

	Antibiotic	Antibiotic concentration (mg.l <sup>-1</sup> )	Bacteria	CFU.cm <sup>-2</sup>	Standard deviation
<i>E. coli</i> 10 <sup>5</sup> CFU.ml <sup>-1</sup> / <i>D. tsuruhatensis</i> 10 <sup>5</sup> CFU.ml <sup>-1</sup>	Ciprofloxacin	0.25	<i>E. coli</i>	1.70E+05	7.42E+03
			<i>D. tsuruhatensis</i>	3.62E+05	5.20E+04
		0.03	<i>E. coli</i>	1.73E+05	3.71E+04
			<i>D. tsuruhatensis</i>	3.87E+06	8.17E+05
		0.004	<i>E. coli</i>	4.67E+06	2.20E+06
			<i>D. tsuruhatensis</i>	4.31E+06	1.98E+05
	Ampicillin	1024	<i>E. coli</i>	5.95E+05	6.93E+04
			<i>D. tsuruhatensis</i>	6.72E+04	1.68E+04
		128	<i>E. coli</i>	6.08E+05	4.39E+05
			<i>D. tsuruhatensis</i>	4.25E+04	2.10E+04
		16	<i>E. coli</i>	2.99E+06	7.18E+05
			<i>D. tsuruhatensis</i>	3.15E+04	5.44E+03
	Gentamicin	32	<i>E. coli</i>	0.00E+00	0.00E+00
			<i>D. tsuruhatensis</i>	6.55E+05	5.44E+04
		4	<i>E. coli</i>	0.00E+00	0.00E+00
<i>D. tsuruhatensis</i>			7.18E+05	1.29E+05	
0.5		<i>E. coli</i>	8.26E+06	5.15E+06	
		<i>D. tsuruhatensis</i>	4.06E+05	2.28E+05	
Amoxicillin/ Clavulanic acid	1024	<i>E. coli</i>	1.02E+06	1.48E+05	
		<i>D. tsuruhatensis</i>	0.00E+00	0.00E+00	
	128	<i>E. coli</i>	7.77E+05	7.33E+05	
		<i>D. tsuruhatensis</i>	0.00E+00	0.00E+00	
	16	<i>E. coli</i>	6.27E+06	2.13E+06	
		<i>D. tsuruhatensis</i>	2.98E+04	1.39E+04	
<i>E. coli</i> 10 <sup>5</sup> CFU.ml <sup>-1</sup> / <i>A. xylosoxidans</i> 10 <sup>5</sup> CFU/ml <sup>-1</sup>	Ciprofloxacin	128	<i>E. coli</i>	5.50E+05	6.58E+04
			<i>A. xylosoxidans</i>	3.82E+05	4.01E+05
		16	<i>E. coli</i>	2.75E+05	2.47E+03
			<i>A. xylosoxidans</i>	6.53E+05	7.18E+04
		2	<i>E. coli</i>	6.86E+06	2.00E+06
			<i>A. xylosoxidans</i>	4.97E+06	0.00E+00
	Ampicillin	1024	<i>E. coli</i>	3.52E+05	3.34E+05
			<i>A. xylosoxidans</i>	1.63E+04	6.68E+03
		128	<i>E. coli</i>	3.651E+06	4.64E+06
			<i>A. xylosoxidans</i>	7.18E+04	2.47E+03
		16	<i>E. coli</i>	4.03E+05	2.47E+04
			<i>A. xylosoxidans</i>	2.59E+05	3.96E+04
	Gentamicin	32	<i>E. coli</i>	2.99E+06	1.24E+05
			<i>A. xylosoxidans</i>	2.28E+04	3.96E+03
		4	<i>E. coli</i>	0.00E+00	0.00E+00
<i>A. xylosoxidans</i>			6.60E+05	1.81E+05	
0.5		<i>E. coli</i>	0.00E+00	0.00E+00	
		<i>A. xylosoxidans</i>	2.29E+06	2.47E+04	
Amoxicillin/ Clavulanic acid	1024	<i>E. coli</i>	5.18E+05	1.58E+05	
		<i>A. xylosoxidans</i>	1.66E+05	7.42E+02	
	128	<i>E. coli</i>	4.80E+05	3.96E+04	
		<i>A. xylosoxidans</i>	3.31E+04	2.47E+02	
	16	<i>E. coli</i>	2.99E+06	1.24E+05	
		<i>A. xylosoxidans</i>	2.28E+04	3.96E+03	

**Table S4.2** - The CFU.cm<sup>-2</sup> counts for the *E. coli* 10<sup>5</sup> CFUs.ml<sup>-1</sup> / *D. tsuruhatensis* 10<sup>2</sup> CFUs.ml<sup>-1</sup> and *E. coli* 10<sup>5</sup> CFUs.ml<sup>-1</sup> / *A. xylosoxidans* 10<sup>2</sup> CFUs.ml<sup>-1</sup> 48 h dual-species biofilms exposed to three different concentrations below the MBEC. These counts were determined after 24 h of exposure.

	Antibiotic	Concentration (mg.l <sup>-1</sup> )	Bacteria	CFU.cm <sup>-2</sup>	Standard deviation
<i>E. coli</i> 10 <sup>5</sup> CFU.ml <sup>-1</sup> / <i>D. tsuruhatensis</i> 10 <sup>2</sup> CFU.ml <sup>-1</sup>	Ciprofloxacin	0.25	<i>E. coli</i>	6.07E+05	4.33E+05
			<i>D. tsuruhatensis</i>	2.19E+05	5.69E+04
		0.03	<i>E. coli</i>	2.66E+06	4.95E+05
			<i>D. tsuruhatensis</i>	3.34E+06	1.24E+05
		0.004	<i>E. coli</i>	1.56E+07	6.19E+05
			<i>D. tsuruhatensis</i>	8.54E+06	2.97E+05
	Ampicillin	256	<i>E. coli</i>	4.26E+05	5.85E+05
			<i>D. tsuruhatensis</i>	1.68E+05	4.45E+04
		32	<i>E. coli</i>	6.76E+05	1.15E+05
			<i>D. tsuruhatensis</i>	5.06E+05	7.67E+04
		4	<i>E. coli</i>	1.84E+05	6.68E+04
			<i>D. tsuruhatensis</i>	3.45E+05	7.67E+04
	Gentamicin	8	<i>E. coli</i>	0.00E+00	00E+00
			<i>D. tsuruhatensis</i>	6.41E+05	5.79E+05
		1	<i>E. coli</i>	1.07E+06	9.18E+05
			<i>D. tsuruhatensis</i>	1.79E+06	1.68E+06
		0.14	<i>E. coli</i>	5.25E+06	1.39E+06
			<i>D. tsuruhatensis</i>	5.39E+06	1.41E+06
Amoxicillin/ Clavulanic acid	256	<i>E. coli</i>	2.70E+04	3.96E+03	
		<i>D. tsuruhatensis</i>	5.65E+05	2.72E+04	
	32	<i>E. coli</i>	2.80E+06	2.55E+06	
		<i>D. tsuruhatensis</i>	4.67E+06	2.00E+06	
	4	<i>E. coli</i>	2.43E+06	1.21E+06	
		<i>D. tsuruhatensis</i>	3.69E+06	7.18E+05	
<i>E. coli</i> 10 <sup>5</sup> CFU.ml <sup>-1</sup> / <i>A. xylosoxidans</i> 10 <sup>2</sup> CFU.ml <sup>-1</sup>	Ciprofloxacin	64	<i>E. coli</i>	0.00E+00	0.00E+00
			<i>A. xylosoxidans</i>	1.31E+05	7.42E+03
		8	<i>E. coli</i>	0.00E+00	0.00E+00
			<i>A. xylosoxidans</i>	5.29E+05	3.56E+05
		1	<i>E. coli</i>	0.00E+00	00E+00
			<i>A. xylosoxidans</i>	3.78E+06	1.68E+06
	Ampicillin	128	<i>E. coli</i>	2.36E+05	4.70E+04
			<i>A. xylosoxidans</i>	4.10E+03	2.43E+03
		16	<i>E. coli</i>	1.45E+06	2.00E+04
			<i>A. xylosoxidans</i>	2.24E+03	9.90E+02
		2	<i>E. coli</i>	4.59E+06	1.98E+05
			<i>A. xylosoxidans</i>	1.11E+05	6.64E+04
	Gentamicin	8	<i>E. coli</i>	0.00E+00	0.00E+00
			<i>A. xylosoxidans</i>	2.87E+05	2.23E+05
		1	<i>E. coli</i>	4.55E+06	5.44E+05
			<i>A. xylosoxidans</i>	1.59E+05	6.19E+04
		0.14	<i>E. coli</i>	4.92E+06	2.47E+04
			<i>A. xylosoxidans</i>	1.68E+05	4.95E+04
Amoxicillin/ Clavulanic acid	64	<i>E. coli</i>	8.02E+05	3.46E+04	
		<i>A. xylosoxidans</i>	3.62E+04	4.54E+04	
	8	<i>E. coli</i>	3.45E+06	1.61E+06	
		<i>A. xylosoxidans</i>	1.56E+04	2.47E+02	
	1	<i>E. coli</i>	4.92E+06	1.11E+06	
		<i>A. xylosoxidans</i>	7.11E+05	9.40E+04	

**Table S4.3** - The CFU.cm<sup>-2</sup> counts for the *E. coli* 10<sup>2</sup> CFUs.ml<sup>-1</sup> / *D. tsuruhatensis* 10<sup>5</sup> CFUs.ml<sup>-1</sup> and *E. coli* 10<sup>2</sup> CFUs.ml<sup>-1</sup> / *A. xylosoxidans* 10<sup>5</sup> CFUs.ml<sup>-1</sup> 48 h dual-species biofilms exposed to three different concentrations below the MBEC. These counts were determined after 24 h of exposure.

	Antibiotic	Antibiotic concentration (mg.l <sup>-1</sup> )	Species	CFU.cm <sup>-2</sup>	Standard deviation
<i>E. coli</i> 10 <sup>2</sup> CFU.ml <sup>-1</sup> / <i>D. tsuruhatensis</i> 10 <sup>5</sup> CFU.ml <sup>-1</sup>	Ampicillin	1024	<i>E. coli</i>	4.88E+05	4.21E+04
			<i>D. tsuruhatensis</i>	1.86E+06	3.96E+05
		128	<i>E. coli</i>	1.22E+06	1.19E+06
			<i>D. tsuruhatensis</i>	3.05E+05	4.45E+04
		16	<i>E. coli</i>	3.76E+05	2.00E+05
			<i>D. tsuruhatensis</i>	1.63E+06	5.69E+05
	Amoxicillin/ Clavulanic acid	1024	<i>E. coli</i>	1.75E+04	2.47E+03
			<i>D. tsuruhatensis</i>	5.09E+05	1.21E+05
		128	<i>E. coli</i>	3.06E+05	1.96E+05
			<i>D. tsuruhatensis</i>	2.61E+06	3.22E+05
		16	<i>E. coli</i>	9.50E+05	6.86E+05
			<i>D. tsuruhatensis</i>	3.10E+06	2.23E+05
<i>E. coli</i> 10 <sup>2</sup> CFU.ml <sup>-1</sup> / <i>A. xylosoxidans</i> 10 <sup>5</sup> CFU.ml <sup>-1</sup>	Ampicillin	1024	<i>E. coli</i>	2.17E+05	5.94E+04
			<i>A. xylosoxidans</i>	1.56E+03	1.24E+02
		128	<i>E. coli</i>	3.45E+05	1.61E+05
			<i>A. xylosoxidans</i>	6.55E+03	2.97E+02
		16	<i>E. coli</i>	1.82E+06	6.43E+05
			<i>A. xylosoxidans</i>	7.32E+03	3.46E+02
	Amoxicillin/ Clavulanic acid	1024	<i>E. coli</i>	4.10E+05	4.45E+04
			<i>A. xylosoxidans</i>	9.26E+03	7.67E+02
		128	<i>E. coli</i>	2.89E+05	4.21E+04
			<i>A. xylosoxidans</i>	1.98E+04	1.73E+03
		16	<i>E. coli</i>	1.94E+06	6.19E+05
			<i>A. xylosoxidans</i>	6.32E+03	2.25E+03

**Table S4.4** - Effect of a low *E. coli* initial inoculum concentration (10<sup>2</sup> CFUs.ml<sup>-1</sup>) on the *in vitro* susceptibility of the dual-species biofilms to ampicillin and amoxicillin/clavulanic acid.

	Antibiotics (mg.l <sup>-1</sup> )	
	Ampicillin	Amoxicillin/ clavulanic acid*
<i>E. coli</i> 10 <sup>2</sup> CFU.ml <sup>-1</sup> / <i>D. tsuruhatensis</i> 10 <sup>5</sup> CFU.ml <sup>-1</sup>	>1024	>1024
<i>E. coli</i> 10 <sup>2</sup> CFU.ml <sup>-1</sup> / <i>A. xylosoxidans</i> 10 <sup>5</sup> CFU.ml <sup>-1</sup>	>1024	>1024

# Chapter 5

---

## **An *in vitro* model of catheter-associated urinary tract infections to investigate the role of uncommon bacteria on the *Escherichia coli* microbial consortium**

**Andreia S. Azevedo**, Carina Almeida, Luciana C. Gomes, Filipe J. Mergulhão, Luís F. Melo, Nuno F. Azevedo.

---

(submitted)

### **Abstract**

Urinary catheters are a common niche for polymicrobial biofilms, leading to CAUTIs development. Uncommon bacteria, such as *D. tsuruhatensis* have been isolated from CAUTIs in combination with well-established pathogenic bacteria such as *E. coli*. Nonetheless, the reason why *E. coli* coexists with other bacteria instead of outcompeting and completely eliminating them is unknown. As such, a flow cell reactor simulating the hydrodynamic conditions found in CAUTIs (shear rate of  $15 \text{ s}^{-1}$ ) was used to characterize the microbial physiology of *E. coli* and *D. tsuruhatensis* individually and in consortium, in terms of the growth kinetics and the substrate uptake. Single-species biofilms showed that up to 48 h the cultivable cell counts significantly increased for both species ( $p < 0.05$ ). After 48 h, both species stabilized with similar cultivable cell values reaching  $\text{Log } 6.24 \text{ CFU.cm}^{-2}$  for *E. coli* and  $\text{Log } 6.31 \text{ CFU.cm}^{-2}$  for *D. tsuruhatensis* ( $p > 0.05$ ). When in dual-species biofilm, *E. coli* outnumbered *D. tsuruhatensis* up to 16 h and then *D. tsuruhatensis* gained fitness advantage. However, the assessment of the spatial distribution of the dual-species biofilm by LNA/2'OMe-FISH revealed that *E. coli* and *D. tsuruhatensis* coexist and tend to co-aggregate over time, which suggests that both bacteria are able to cooperate synergistically. Substrate uptake measurements revealed that in AUM both bacteria metabolized lactic acid and uric acid, while *D. tsuruhatensis* was also able to use citric acid. In the consortium, *D. tsuruhatensis* metabolized citric acid more rapidly, presumably leaving more uric acid available in the medium to be used by *E. coli*. In conclusion, *E. coli* and uncommon bacteria seem to cooperate metabolically, when sharing the same environment under

dynamic conditions, leading to the persistence of both bacteria in a stable microbial community.

**Keywords:** *Escherichia coli*, *Delftia tsuruhatensis*, uncommon bacteria, flow cell, urine flow.

## 5.1 Introduction

In hospitals and nursing homes, there is a regular occurrence of infections, of which about 9% are attributed to CAUTIs<sup>1</sup>. Urinary catheters are medical devices used in patients to control the urine drain due to incontinence problems or post-operative urine retention<sup>2</sup>. Unfortunately, most patients experience long-term catheterization, which is frequently associated with polymicrobial infections<sup>3-6</sup>. In fact, with time microorganisms end up forming polymicrobial biofilms on the surface of urinary catheters<sup>7-9</sup>.

A biofilm is a community of microorganisms adhered to a biotic or abiotic surface, which is enclosed in an EPS matrix. Compared to planktonic microorganisms, they have an altered phenotype associated with a reduced growth rate, a high tolerance to antimicrobial agents and to host immune system, and an altered expression of specific genes<sup>10-13</sup>. Typically, microbial biofilms display a coordinated and cooperative behavior<sup>14</sup>, where the concentration of individual populations is adjusted according to the conditions found in the environment as shown in Chapter 4.

Recently, uncommon bacteria such as *D. tursorhatensis* have been isolated and identified in nosocomial infections involving polymicrobial biofilms<sup>7, 15</sup>, including CAUTIs<sup>7</sup>. The pathogenic potential of these uncommon bacteria is undefined. Nonetheless, this type of bacteria appears in catheter-associated biofilms in combination with well-established pathogenic bacteria (e.g. *E. coli*, *K. pneumoniae* and *P. aeruginosa*)<sup>7</sup>. As reported in Chapters 2 and 4, *E. coli* and uncommon bacteria are good biofilm producers on abiotic surfaces (e.g. silicone, polystyrene), and when in co-culture they are able to form a stable microbial consortia, where both bacteria coexist, even when inoculated at different proportions. Also, the analysis of ecological interactions between *E. coli* and uncommon bacteria has revealed that these bacteria tend to interact either synergistically or, at least, display a neutralism behavior. These previous studies have only described the possible synergistic interactions assessing bacterial adhesion, biofilm formation and overall antibiotic resistance of mixed-species consortia in static conditions. Nonetheless, knowledge about the microbial physiology of *E. coli* and *D. tursorhatensis* under dynamic conditions, especially when concerning nutritional requirements, remains unknown. Hence, a pressing need exists for research

directed toward understanding microbial interactions that drive CAUTIs biofilm communities involving uncommon and pathogenic bacteria under dynamic conditions.

As biofilms in urinary catheters are exposed to hydrodynamic shear forces, a flow cell system simulating the shear strain rate found in urinary catheters ( $15 \text{ s}^{-1}$ )<sup>16-18</sup> was used. Species behavior was then evaluated individually and in consortium, when exposed to AUM flow and to the silicone material. The physiology of each bacterium was characterized in terms of the growth kinetics and the substrate's uptake (lactic acid, urea, citric acid, creatinine and uric acid) under dynamic conditions.

## **5.2 Material and methods**

### **5.2.1 Strains and culture media**

Culture conditions were similar to those previously described in Chapters 2 and 4. Briefly, for each experiment, *E. coli* CECT 434 and *D. tsuruhatensis* BM90 were recovered from a frozen stock ( $-80 \text{ }^{\circ}\text{C}$ ), streaked on TSA (Merck, Germany) and grown overnight at  $37 \text{ }^{\circ}\text{C}$ . For the inoculum preparation, each bacterium was inoculated in 250 ml of AUM and the cultures were placed in an incubator (AGITORB 200, Aralab, Portugal) during 16-18 h at  $37 \text{ }^{\circ}\text{C}$  and 150 rpm. AUM was prepared as previously described<sup>19</sup>, but as yeast extract and peptone are a mixture of polypeptides and amino acids, they were not added to the medium to enable the measurement of substrate's uptake. Then, cell concentration was assessed by O.D. at 620 nm and each inoculum was diluted in AUM in order to obtain a final concentration of  $10^8 \text{ CFU.ml}^{-1}$ . A diluted inoculum was used to inoculate the reactor system during 1 h at a flow rate ( $Q$ ) of  $0.5 \text{ ml.min}^{-1}$ .

### **5.2.2 Determination of bacterial growth rates**

The growth rate for each bacterium was determined in AUM (without yeast extract and peptone) in a batch culture as described in sub-section 2.2.6 (Chapter 2).

### **5.2.3 Flow cell reactor setup**

The reactor system used in this work (Figure 5.1) consists of a vertical flow cell, water bath at  $37 \text{ }^{\circ}\text{C}$ , peristaltic (B1) and centrifuge pumps (B2), vessel containing the



nutrients, recirculating silicone tubes and a waste vessel. The flow cell used is a rectangular Perspex column with 10 apertures in removable rectangular pieces of Perspex where silicone coupons were placed. All specifications of the flow cell reactor are provided in Table S5.1 (Supplemental material).

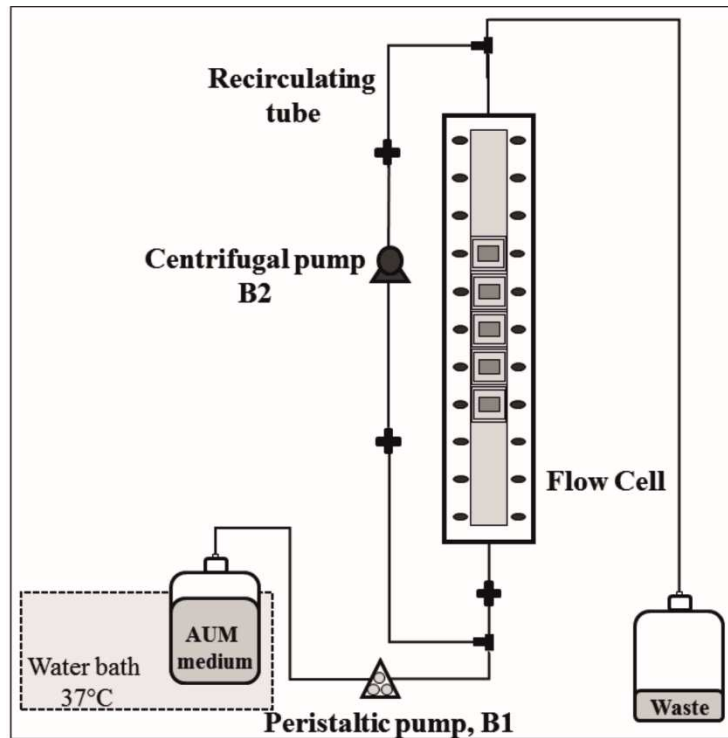


**Figure 5.1** - Schematic representation of the flow cell reactor. Pumps B1 and B2 controlled the flow rate of AUM ( $0.5 \text{ ml}\cdot\text{min}^{-1}$ ) and the velocity of recirculating fluid ( $300 \text{ ml}\cdot\text{min}^{-1}$ ), respectively.

Important aspects involved in CAUTIs were simulated such as the composition of the AUM, which was reported as suitable to mimic the urine in a wide range of microbial studies<sup>19-23</sup>. The temperature of AUM was kept at  $37 \text{ }^{\circ}\text{C}$ , corresponding to the human body temperature. Considering that the normal daily range for an adult urinary output is between 800 to 2000 ml of urine<sup>24</sup>, a AUM flow rate of  $0.5 \text{ ml}\cdot\text{min}^{-1}$ <sup>25-27</sup> was used for feeding the system. In addition, the recirculating system allowed adjusting the flow rate ( $300 \text{ ml}\cdot\text{min}^{-1}$ ) inside the flow cell independently of the AUM flow rate. This value was determined based on the shear strain rate ( $8, \text{ in } \text{s}^{-1}$ ) reported for the urinary catheter ( $15 \text{ s}^{-1}$ )<sup>16, 17</sup>. The shear stress ( $\tau_w$ , in Pa) was firstly obtained by multiplying the 8 value by the fluid viscosity ( $\mu$ , in  $\text{kg}\cdot\text{m}^{-1}\cdot\text{s}^{-1}$ ) of the fluid involved<sup>17</sup>:

$$\tau_w = 8\mu \quad (\text{eq.5.1})$$

Then, to calculate the resulting  $Q$ , a mathematical model<sup>28</sup> assuming a Newtonian fluid was used, in which the  $\tau_w$  is calculated as a function of the  $Q$ ,

$$\tau_w = \frac{6\mu Q}{bh^2} \quad (\text{eq.5.2})$$

where  $b$  is the width of the chamber and  $h$  is the distance between plates.

Under these conditions, a Reynolds number (Re) of 346 was obtained according to the e.q. 5.3<sup>28</sup>,

$$\text{Re} = \frac{Q\rho}{\mu b} \quad (\text{eq.5.3})$$

where  $\rho$  is the fluid density (in  $\text{kg}\cdot\text{m}^{-3}$ ).

Silicone (Neves & Neves Lda, Portugal) was used to assess biofilm formation. Coupons of silicone (1 x 0.5 cm) were glued onto the rectangular pieces of Perspex and placed in contact with the bacterial suspension circulating in the system. Each silicone coupon could be removed without disturbing the biofilms formed on the others coupons<sup>29</sup>. Before each experiment, the system was properly cleaned with water and diluted bleach. Before inoculation, water with bleach was totally removed and the system was rinsed with sterile water in aseptic conditions<sup>30</sup>. Feed tubes from flasks containing sterile AUM were fitted with anti-reflux valves to prevent upstream migration of bacteria and subsequent contamination of the AUM. Flasks and tubes were autoclaved at 120 °C during 20 min. Then, the complete system was assembled aseptically.

#### **5.2.4 Flow cell reactor operation and biofilm formation**

Firstly, single-species biofilm experiments were performed in order to evaluate the biofilm dynamics each bacterium individually. For this, 500 ml of each inoculum

diluted in AUM ( $10^8$  CFU.ml<sup>-1</sup> of cell concentration) were used to inoculate the reactor system during 1 h<sup>25, 31, 32</sup> at a flow rate of 0.5 ml.min<sup>-1</sup><sup>25</sup>. In order to understand how the behavior of each bacterium in co-culture, a dual-species biofilm (*E. coli* / *D. tsuruhatensis*) at the same initial concentration ( $10^8$  CFU.ml<sup>-1</sup>) was also studied. For dual-species biofilm formation, equal volumes of each single-culture (250 ml) at an initial concentration of  $2 \times 10^8$  CFUs.ml<sup>-1</sup> were used.

After 1 h, the system was stopped and the bacterial inoculum was drained out from the flow cell. Pre-warmed and sterile AUM was pumped at a flow rate of 0.5 ml.min<sup>-1</sup> to fill the reactor system without disturbing the cells already adhered to the silicone coupons. Once the reactor system was filled, the recirculating flow rate (300 ml.min<sup>-1</sup>) was gently established and the system was continuously fed with sterile AUM (at a flow rate of 0.5 ml.min<sup>-1</sup>) for 72 h at 37 °C.

### 5.2.5 Sampling

Sampling was performed at three time points (16, 48 and 72 h) for the cultivable cell counts of biofilms and quantification of the overall consumed substrates (lactic acid, uric acid, urea, citric acid and creatinine). The spatial organization of single- and dual-species biofilms was also assessed using LNA/2'OMe-FISH in combination with CLSM.

At each time point, the system was stopped to allow silicone coupon removal and carefully started again maintaining the same flow conditions in order to guarantee that the biofilms formed on other coupons were not disturbed. This sampling step was made from the top to the bottom of the flow cell and each removed coupon was substituted with a new one that was previously cleaned and kept in ethanol. Afterwards, biofilms were immediately prepared for further analysis.

### 5.2.6 Biofilm analysis

For quantification of biofilm cultivable cells, silicone coupons with biofilms were washed twice in 10 ml of 0.85% (v/v) sterile saline solution to remove loosely attached cells. Then, coupons were placed in wells of a 24-well tissue culture plate containing 1.5 ml of 0.85% (v/v) sterile saline. Subsequently, biofilms were sonicated and the cultivable cell counts were performed as described in sub-section 4.2.3 (Chapter 4). Cultivable cell counts were determined and expressed per unit area of the silicone

coupon in contact with AUM (Log CFUs.cm<sup>-2</sup>). Cultivable cell counts for the bulk liquid were also performed according to the same methodology. To assess the biofilm spatial organization and the species distribution, the LNA/2'OMe-FISH procedure in combination with CLSM analysis was performed directly on single- and dual-species biofilms as described in sub-section 3.2.8 (Chapter 3).

The concentration of each substrate was determined enzymatically according to the manufacturer instructions provided in the lactic acid assay Kit (MAK064, Sigma-Aldrich, USA), uric acid assay Kit (MAK077, Sigma-Aldrich, USA), urea assay Kit (MAK006, Sigma-Aldrich, USA), citric acid assay Kit (MAK057, Sigma-Aldrich, USA) and creatinine assay Kit (MAK080, Sigma-Aldrich, USA).

### **5.2.7 Fitness and Malthusian parameters calculation**

$W$  and  $m$  parameters were determined as previously described in equations 2.1 and 2.2 of sub-section 2.2.9 (Chapter 2). When the value of  $W$  is 1, it means that both bacteria are equally fit.

### **5.2.8 Statistical analysis**

For each parameter, the average and standard deviation were calculated. Results were compared using ANOVA by applying Levene's test of homogeneity of variance and the Tukey multiple-comparisons test, using the SPSS software. Statistical tests were carried out at a significance level of 0.05.

## **5.3 Results and discussion**

Microbial infections in catheterized patients are usually composed by a dominant pathogenic bacterium (e.g. *E. coli*) which might interact and coexist with other pathogens (e.g. *P. aeruginosa*, *E. faecalis* and *P. mirabilis*)<sup>9, 33, 34</sup>, or even, with uncommon bacteria with a poorly understood role such as *D. tsuruhatensis*<sup>7</sup>. Hence, a polymicrobial community is established on the surface of an urinary catheter, in particular when the urinary catheter remains in the patient for several weeks or months<sup>3-6</sup>. Similarly to the observations of Chapters 2 and 4, Lopes *et al.*<sup>35, 36</sup> have studied the

role of some uncommon bacteria in clinical infections and have highlighted their role in shaping the overall behavior of the microbial biofilm.

In this work, the physiology of *E. coli* and the uncommon bacteria *D. tsuruhatensis* under dynamic conditions similar to those found in catheterized urinary tract was evaluated, both in terms of the microbial growth and the nutritional requirements, in order to better understand how these bacteria might persist in a microbial community and start disclosing the potential role of uncommon bacteria on *E. coli*. In fact, despite uncommon bacteria appear at lesser extent in CAUTIs, the microbial interactions between uncommon bacteria and pathogenic bacteria are likely to occur.

### ***5.3.1 Characterization of E. coli and D. tsuruhatensis single-species biofilm growth under dynamic conditions***

First, the development of *E. coli* and *D. tsuruhatensis* single-species biofilm was assessed. As *E. coli* is one of the most frequently detected microorganisms in CAUTIs<sup>37, 38</sup>, it would be expectable that *E. coli* presents a higher ability to grow under dynamic conditions in AUM. However, this was not observed in terms of cultivable cell counts (Figure 5.2-a). Single-species biofilms showed that up to 48 h the cultivable cell counts significantly increased for both species ( $p < 0.05$ ) with a notorious higher growth for *D. tsuruhatensis* biofilms. In fact, the assessment of the bacterial growth rate in AUM (without yeast extract and peptone) showed that *D. tsuruhatensis* grew faster ( $0.4879 \text{ h}^{-1}$ ) when compared to *E. coli* ( $0.2831 \text{ h}^{-1}$ ). After 48 h, both species stabilized with similar cultivable cell values ( $\text{Log } 6.24 \text{ CFU.cm}^{-2}$  for *E. coli* and  $\text{Log } 6.31 \text{ CFU.cm}^{-2}$  for *D. tsuruhatensis*,  $p > 0.05$ ). These growth profiles were similar to those obtained in results presented in Chapter 4 where biofilms of both bacteria were formed in silicone coupons in AUM under static conditions. Nonetheless, the higher  $m$  values for single-species biofilms grown under static conditions indicated that, in these conditions, bacteria form more biofilm than under dynamic conditions (Figure 5.2-b).

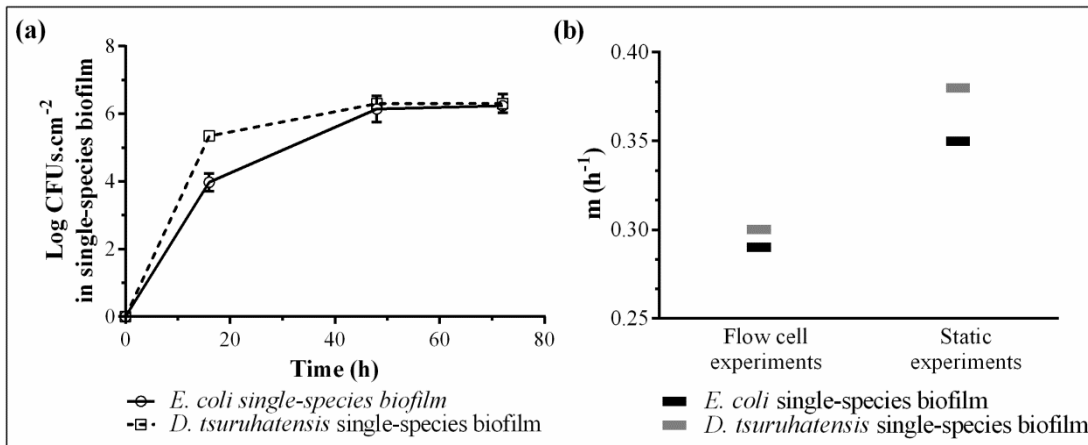


**Figure 5.2** - Formation of *E. coli* and *D. tsuruhatensis* single-species biofilms. (a) Cultivable cell values for biofilms in silicone coupons under dynamic conditions; (b) Comparison of Malthusian parameter values for *E. coli* and *D. tsuruhatensis* single-species biofilms grown in silicone coupons under dynamic and under static conditions (results of static conditions were from Chapter 4). The Malthusian parameter was determined between time 0 and 48 h, before the biofilm stabilization. Error bars represent standard deviations.

Indeed, the assessment of the spatial distribution of biofilm populations by LNA/2'OMe-FISH in combination with CLSM revealed that single-species biofilms in static conditions presented higher thickness values (21  $\mu\text{m}$  for *E. coli* and 17  $\mu\text{m}$  for *D. tsuruhatensis*; Supplemental material - Figure S4.1) compared to single-species biofilms formed under dynamic conditions (6  $\mu\text{m}$  for both bacteria; Supplemental material - Figure S5.1). These data suggested that the absence of yeast extract and peptone and the hydrodynamic conditions that biofilms are subjected to when cultured in dynamic conditions, affect negatively the cell concentration. In fact, it is well established that the hydrodynamic conditions and the nutrients availability have a crucial impact in the adhesion process of the microorganisms, structure and behavior of microbial biofilms<sup>39-44</sup>.

### 5.3.2 How uncommon bacterium might impact on *E. coli* population under dynamic conditions

To understand the potential role of *D. tsuruhatensis* on *E. coli* physiology, the fitness of *E. coli* and *D. tsuruhatensis* was determined and the spatial localization of the biofilm populations in *E. coli* / *D. tsuruhatensis* dual-species biofilm was analyzed (Figure 5.3).

It was speculated that *D. tsuruhatensis* would dominate the microbial consortium since it grows faster compared with *E. coli*. However, the data only showed this behavior at 72 h with cultivable cell values reaching Log 5.27 CFU.cm<sup>-2</sup> for *E. coli* and Log 6.27 CFU.cm<sup>-2</sup> for *D. tsuruhatensis* ( $p < 0.05$ ) (Figure 5.3-a). On the other hand,  $W_{E. coli}$  results showed that *E. coli* presented a higher advantage up to 16 h ( $W_{E. coli} > 1$  and  $W_{D.tsuruhatensis} < 1$ , with a  $p < 0.05$ ). Then, the  $W_{E. coli}$  decreased ( $W_{E. coli} < 1$ ) and *D. tsuruhatensis* gained fitness advantages ( $W_{D.tsuruhatensis} > 1$ ). However, for 48 h there are no statistically significant differences between  $W_{E. coli}$  and  $W_{D.tsuruhatensis}$  ( $p > 0.05$ ). Part of these data might be corroborated with the previous study performed in silicone coupons under static conditions (Chapter 4), where an advantage for *E. coli* when co-cultured with uncommon species was reported, especially for the early stages of biofilm development.

The assessment of the spatial distribution of biofilm populations by LNA/2'OMe-FISH in combination with CLSM revealed that *E. coli* and *D. tsuruhatensis* coexist and tend to co-aggregate over time (Figure 5.3-c). This spatial organization is also similar to a study performed in static conditions (Chapter 4). This suggests that the presence of flow and absence of yeast extract and peptone did not influence the spatial distribution of biofilm populations. This only affected the thickness of biofilms which was lower under dynamic conditions (6.38  $\mu\text{m}$  at 72 h under dynamic conditions [Figure 5.3-cIII] and 14  $\mu\text{m}$  at 48 h [Figure 4.5-I] and 192 h [Figure 4.1-cI] under static conditions).

Despite a slight decrease of  $W_{E. coli}$  values for the last time points, this spatial organization typically means that both species are able to cooperate or interact synergistically<sup>45</sup>, as discussed in Chapter 4. In fact, as *E. coli* and *D. tsuruhatensis* might co-inhabit the same urinary catheter<sup>7</sup>, it would be expectable that both species might cooperate and benefit from the presence of each other.

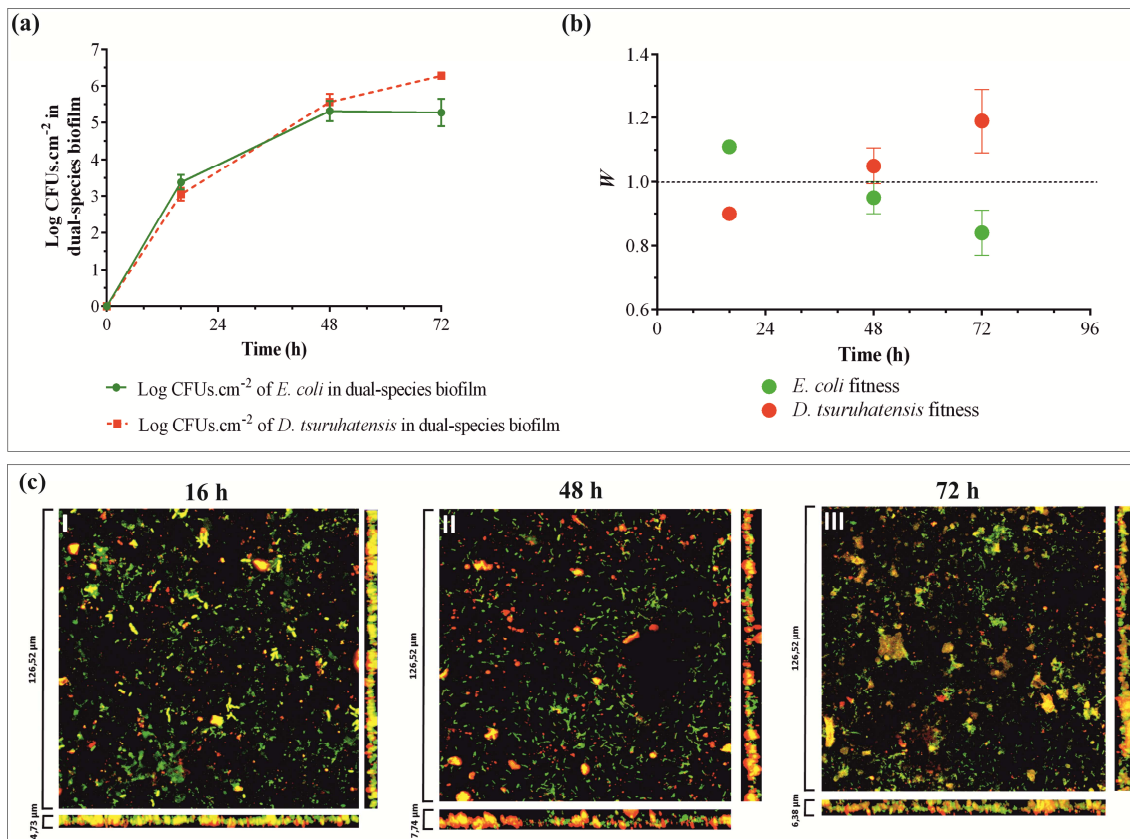


**Figure 5.3** - Single- and dual-species biofilm growth in silicone material under dynamic conditions. (a) Cultivable cell values of each bacterium overtime; (b) Representation of the relative fitness of *E. coli* and *D. tsuruhatensis*. The dashed line represents a relative fitness of 1, which means that the species are equally fit within biofilms. Error bars represent standard deviations; (c) Images of LNA/2'OMe-FISH in combination with CLSM, showing the spatial organization of the *E. coli* / *D. tsuruhatensis* dual-species biofilm at (I) 16 h, (II) 48 h and (III) 72 h. The bottom and side images represent the transverse planes. Green cells correspond to *E. coli* and red cells correspond to *D. tsuruhatensis*.

Two of the previous studies included in this thesis (Chapters 2 and 4) have suggested that the uncommon bacteria have a positive impact on *E. coli* fitness and under adverse conditions these bacteria seem to offer a protective effect over *E. coli*, increasing the tolerance of the overall microbial consortia to antibiotic agents. Nonetheless, there are no studies reporting how substrate uptake is affected when both bacteria are present simultaneously. Thus, analysis of nutritional requirements of *E. coli* and *D. tsuruhatensis* when growing under dynamic conditions might explain why *E. coli* coexists with uncommon bacteria rather than alone.



### 5.3.3 Substrate uptake by *E. coli* and *D. tsuruhatensis* in single- and dual-species biofilms

The concentration profiles of lactic acid, uric acid, citric acid, urea and creatinine concentrations *E. coli*, *D. tsuruhatensis* and *E. coli* / *D. tsuruhatensis* are presented in Figure 5.4. Both bacteria had preference for organic acids like lactic acid, uric acid (*E. coli* and *D. tsuruhatensis*) and citric acid (*D. tsuruhatensis*).

A higher uptake of lactic acid was observed up to 16 h by *E. coli* and *D. tsuruhatensis* which means that this substrate was clearly the primary carbon source for both bacteria when grown individually (Figure 5.4-a). Then, as the amount of lactic acid decreased substantially, *E. coli* started to uptake uric acid gradually until 72 h. On the other hand, *D. tsuruhatensis* consumed a higher amount of uric acid up to 48 h (Figure 5.4-b). At this point, *E. coli* was not able to uptake other substrate; but, *D. tsuruhatensis* was able to uptake the citric acid (Figure 5.4-c). When in consortium, *E. coli* and *D. tsuruhatensis* consumed more rapidly lactic acid and citric acid, but not uric acid.

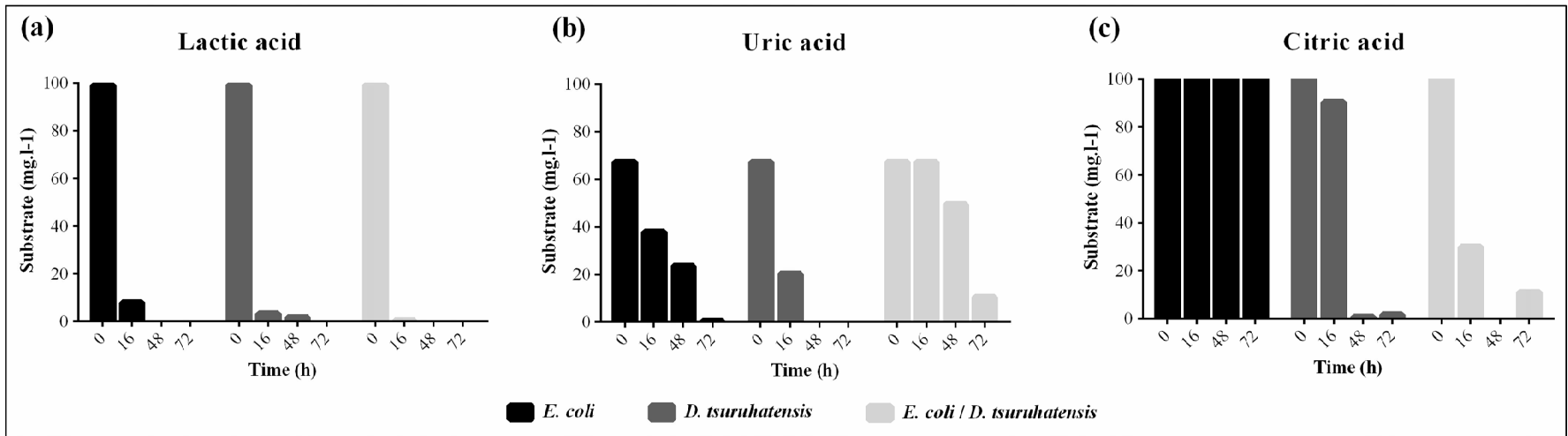


**Figure 5.4** - The evolution of (a) lactic acid, (b) uric acid and (c) citric acid concentrations for *E. coli*, *D. tsuruhatensis* and *E. coli* / *D. tsuruhatensis*. Citric acid was not consumed by *E. coli*. Two other carbon sources present in artificial urine medium, creatinine and urea, were not consumed by *E. coli* and *D. tsuruhatensis*.

## 5.4 Conclusions

The flow cell system allowed studying how *D. tsuruhatensis* influences the physiology of *E. coli* in conditions similar to those found in CAUTIs, providing data about the growth kinetics and the carbon sources that are preferentially consumed by each bacterium individually and in consortium. Under flow conditions, *E. coli* and *D. tsuruhatensis* are able to persist and survive within biofilm community. Concerning their ability to consume urine substrates, *E. coli* and *D. tsuruhatensis* seem to cooperate in order to obtain the maximum nutritional benefit. Indeed, *D. tsuruhatensis* co-cultured with *E. coli* preferred the consumption of citric acid instead of uric acid, leaving more uric acid available to be used by *E. coli*. This hints at a cooperative interaction between *E. coli* and uncommon bacteria when these species share the same environment in order to guarantee their persistence and survival within microbial community.

## 5.5 References

1. **S.S. Magill, J.R. Edwards, W. Bamberg, Z.G. Beldavs, G. Dumyati, M.A. Kainer, R. Lynfield, M. Maloney, L. McAllister-Hollod, J. Nadle, S.M. Ray, D.L. Thompson, L.E. Wilson, S.K. Fridkin, I.A.U.P.S. Emerging Infections Program Healthcare-Associated, Team.** Multistate point-prevalence survey of health care-associated infections. *N Engl J Med* **370**, 1198-1208 (2014).
2. **J.W. Warren.** Catheter-associated urinary tract infections. *Infect Dis Clin North Am* **11**, 609-622 (1997).
3. **J.W. Warren.** The catheter and urinary tract infection. *Med Clin North Am* **75**, 481-493 (1991).
4. **J.W. Warren.** Catheter-associated urinary tract infections. *Int J Antimicrob Agents* **17**, 299-303 (2001).
5. **S.M. Jacobsen, D.J. Stickler, H.L. Mobley, M.E. Shirtliff.** Complicated catheter-associated urinary tract infections due to *Escherichia coli* and *Proteus mirabilis*. *Clin Microbiol Rev* **21**, 26-59 (2008).
6. **L.E. Nicolle.** The chronic indwelling catheter and urinary infection in long-term-care facility residents. *Infect Control Hosp Epidemiol* **22**, 316-321 (2001).
7. **D.N. Frank, S.S. Wilson, A.L. St Amand, N.R. Pace.** Culture-independent microbiological analysis of foley urinary catheter biofilms. *PLoS One* **4**, e7811 (2009).
8. **S.M. Macleod, D.J. Stickler.** Species interactions in mixed-community crystalline biofilms on urinary catheters. *J Med Microbiol* **56**, 1549-1557 (2007).
9. **V. Hola, F. Ruzicka, M. Horka.** Microbial diversity in biofilm infections of the urinary tract with the use of sonication techniques. *FEMS Immunol Med Microbiol* **59**, 525-528 (2010).
10. **J.W. Costerton, K.J. Cheng, G.G. Geesey, T.I. Ladd, J.C. Nickel, M. Dasgupta, T.J. Marrie.** Bacterial biofilms in nature and disease. *Annu Rev Microbiol* **41**, 435-464 (1987).
11. **P.S. Stewart, M.J. Franklin.** Physiological heterogeneity in biofilms. *Nat Rev Microbiol* **6**, 199-210 (2008).
12. **R.M. Donlan, J.W. Costerton.** Biofilms: survival mechanisms of clinically relevant microorganisms. *Clin Microbiol Rev* **15**, 167-193 (2002).
13. **R.M. Donlan.** Biofilms: microbial life on surfaces. *Emerg Infect Dis* **8**, 881-890 (2002).
14. **C.D. Nadell, J.B. Xavier, K.R. Foster.** The sociobiology of biofilms. *FEMS Microbiol Rev* **33**, 206-224 (2009).
15. **B. Preiswerk, S. Ullrich, R. Speich, G.V. Bloemberg, M. Hombach.** Human infection with *Delftia tsuruhatensis* isolated from a central venous catheter. *J Med Microbiol* **60**, 246-248 (2011).
16. **M.M. Velraeds, B. van de Belt-Gritter, H.C. van der Mei, G. Reid, H.J. Busscher.** Interference in initial adhesion of uropathogenic bacteria and yeasts to silicone rubber by a *Lactobacillus acidophilus* biosurfactant. *J Med Microbiol* **47**, 1081-1085 (1998).
17. **D.P. Bakker, A. van der Plaats, G.J. Verkerke, H.J. Busscher, H.C. van der Mei.** Comparison of velocity profiles for different flow chamber designs used in studies of microbial adhesion to surfaces. *Appl Environ Microbiol* **69**, 6280-6287 (2003).
18. **L. Gomes, J. Moreira, J. Teodósio, J. Araújo, J. Miranda, M. Simões, L. Melo, F. Mergulhão.** 96-well microtiter plates for biofouling simulation in biomedical settings. *Biofouling* **30**, 535-546 (2014).
19. **T. Brooks, C.W. Keevil.** A simple artificial urine for the growth of urinary pathogens. *Lett Appl Microbiol* **24**, 203-206 (1997).
20. **J.E. Klinth, M. Castelain, B.E. Uhlin, O. Axner.** The influence of pH on the specific adhesion of P piliated *Escherichia coli*. *PLoS One* **7**, e38548 (2012).
21. **H.S. Raffi, J.M. Bates, D.J. Flournoy, S. Kumar.** Tamm-Horsfall protein facilitates catheter associated urinary tract infection. *BMC Res Notes* **5**, 532 (2012).
22. **C. Almeida, N.F. Azevedo, J.C. Bento, N. Cerca, H. Ramos, M.J. Vieira, C.W. Keevil.** Rapid detection of urinary tract infections caused by *Proteus* spp. using PNA-FISH. *Eur J Clin Microbiol Infect Dis* **32**, 781-786 (2013).

23. **L. Cerqueira, J.A. Oliveira, A. Nicolau, N.F. Azevedo, M.J. Vieira.** Biofilm formation with mixed cultures of *Pseudomonas aeruginosa/Escherichia coli* on silicone using artificial urine to mimic urinary catheters. *Biofouling* **29**, 829-840 (2013).
24. **MedlinePlus** (U.S. National Library of Medicine, 2016).
25. **V. Levering, Q. Wang, P. Shivapooja, X. Zhao, G.P. Lopez.** Soft robotic concepts in catheter design: an on-demand fouling-release urinary catheter. *Adv Healthc Mater* **3**, 1588-1596 (2014).
26. **B.V. Jones, E. Mahenthiralingam, N.A. Sabbuba, D.J. Stickler.** Role of swarming in the formation of crystalline *Proteus mirabilis* biofilms on urinary catheters. *J Med Microbiol* **54**, 807-813 (2005).
27. **S.M. Lehman, R.M. Donlan.** Bacteriophage-mediated control of a two-species biofilm formed by microorganisms causing catheter-associated urinary tract infections in an *in vitro* urinary catheter model. *Antimicrob Agents Chemother* **59**, 1127-1137 (2015).
28. **R.G. Bacabac, T.H. Smit, S.C. Cowin, J.J. Van Loon, F.T. Nieuwstadt, R. Heethaar, J. Klein-Nulend.** Dynamic shear stress in parallel-plate flow chambers. *J Biomech* **38**, 159-167 (2005).
29. **M.O. Pereira, P. Morin, M. Vieira, L. Melo.** A versatile reactor for continuous monitoring of biofilm properties in laboratory and industrial conditions. *Lett Appl Microbiol* **34**, 22-26 (2002).
30. **J.S. Teodósio, M. Simões, L.F. Melo, F.J. Mergulhão.** Flow cell hydrodynamics and their effects on *E. coli* biofilm formation under different nutrient conditions and turbulent flow. *Biofouling* **27**, 1 - 11 (2011).
31. **L. Ferrieres, V. Hancock, P. Klemm.** Biofilm exclusion of uropathogenic bacteria by selected asymptomatic bacteriuria *Escherichia coli* strains. *Microbiology* **153**, 1711-1719 (2007).
32. **R.J. Broomfield, S.D. Morgan, A. Khan, D.J. Stickler.** Crystalline bacterial biofilm formation on urinary catheters by urease-producing urinary tract pathogens: a simple method of control. *J Med Microbiol* **58**, 1367-1375 (2009).
33. **M. Matsukawa, Y. Kunishima, S. Takahashi, K. Takeyama, T. Tsukamoto.** Bacterial colonization on intraluminal surface of urethral catheter. *Urology* **65**, 440-444 (2005).
34. **M. Ohkawa, T. Sugata, M. Sawaki, T. Nakashima, H. Fuse, H. Hisazumi.** Bacterial and crystal adherence to the surfaces of indwelling urethral catheters. *J Urol* **143**, 717-721 (1990).
35. **S.P. Lopes, H. Ceri, N.F. Azevedo, M.O. Pereira.** Antibiotic resistance of mixed biofilms in cystic fibrosis: impact of emerging microorganisms on treatment of infection. *Int J Antimicrob Agents* **40**, 260-263 (2012).
36. **S.P. Lopes, N.F. Azevedo, M.O. Pereira.** Emergent bacteria in cystic fibrosis: *in vitro* biofilm formation and resilience under variable oxygen conditions. *Biomed Res Int* **2014**, 678301 (2014).
37. **H. Wu, C. Moser, H.-Z. Wang, N. Høiby, Z.-J. Song.** Strategies for combating bacterial biofilm infections. *Int J Oral Sci* **7**, 1-7 (2015).
38. **S. Niveditha, S. Pramodhini, S. Umadevi, S. Kumar, S. Stephen.** The isolation and the biofilm formation of uropathogens in the patients with catheter associated urinary tract infections (UTIs). *J Clin Diagn Res* **6**, 1478-1482 (2012).
39. **L.F. Melo, M.J. Vieira.** Physical stability and biological activity of biofilms under turbulent flow and low substrate concentration. *Bioprocess Eng* **20**, 363-368 (1999).
40. **L. Hall-Stoodley, P. Stoodley.** Developmental regulation of microbial biofilms. *Curr Opin Biotechnol* **13**, 228-233 (2002).
41. **Y.P. Tsai.** Impact of flow velocity on the dynamic behaviour of biofilm bacteria. *Biofouling* **21**, 267-277 (2005).
42. **M.J. Chen, Z. Zhang, T.R. Bott.** Effects of operating conditions on the adhesive strength of *Pseudomonas fluorescens* biofilms in tubes. *Colloid Surface B* **43**, 61-71 (2005).
43. **N. Mohamed, T.R. Rainier, Jr., J.M. Ross.** Novel experimental study of receptor-mediated bacterial adhesion under the influence of fluid shear. *Biotechnol Bioeng* **68**, 628-636 (2000).
44. **J.S. Teodosio, M. Simoes, L.F. Melo, F.J. Mergulhao.** Flow cell hydrodynamics and their effects on *E. coli* biofilm formation under different nutrient conditions and turbulent flow. *Biofouling* **27**, 1-11 (2011).

45. **S. Elias, E. Banin.** Multi-species biofilms: living with friendly neighbors. *FEMS Microbiol Rev* **36**, 990-1004 (2012).

## 5.6 Supplemental material

**Table S5.1** - Specifications of the flow cell reactor.

Length of the column	42 cm
Height of the column	2 cm
Depth of the column	1 cm
Total surface area of the Flow Cell	252 cm <sup>2</sup>
Total volume of the Flow Cell	84 ml
Total surface area of tubes	709.64 cm <sup>2</sup>
Total volume of tubes	177.41 ml
Total surface area of the Flow Cell reactor	965.64 cm <sup>2</sup>
Total volume of the Flow Cell reactor	261.41 ml

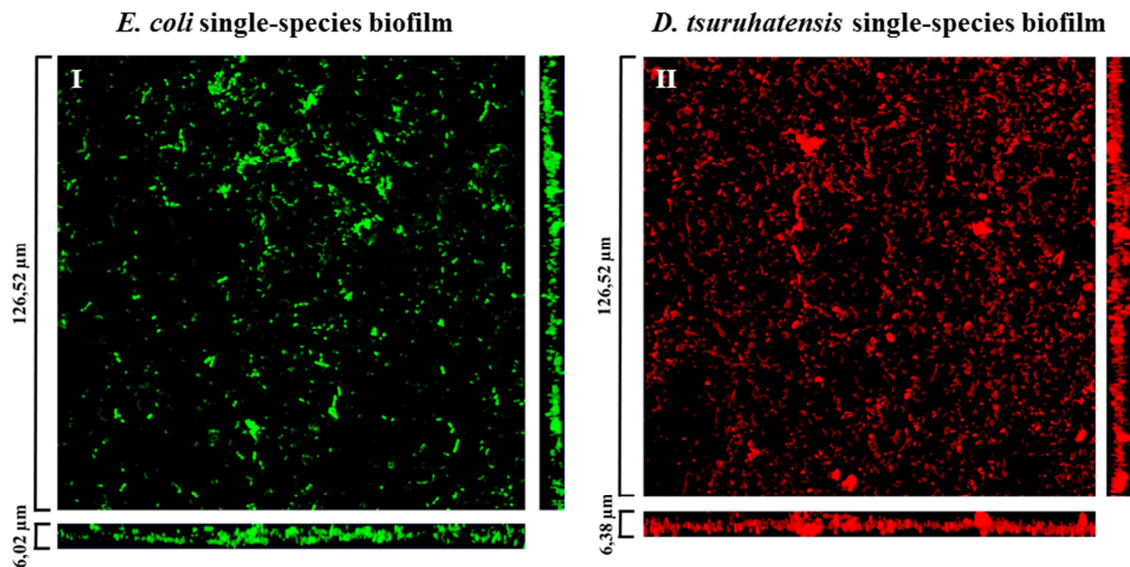


**Figure S5.1** - CLSM images of *E. coli* (I) and *D. tsuruhatensis* (II) single-species biofilms.





# Chapter 6

---

## Concluding remarks and Future perspectives

---

This chapter summarizes the major conclusions obtained in the thesis. Proposals for future work are also addressed.



## 6.1 Concluding remarks

The ultimate goal of this thesis was to understand how the presence of uncommon bacteria affects the development, structure and functions of polymicrobial biofilms in urinary catheters. While most polymicrobial biofilms involved in CAUTIs are dominated by pathogenic bacteria (e.g. *E. coli*, *K. pneumoniae*, *P. aeruginosa*), uncommon bacteria (e.g. *D. tsuruhatensis*, *A. xylosoxidans*) can also co-inhabit the same urinary catheter. Little was known about the effect that uncommon bacteria have on the ability of *E. coli* to adhere and grow, as well as on the overall biofilm formation and resistance. As *E. coli* and uncommon bacteria are able to occupy the same urinary catheter, microbial interactions among these bacteria are likely to occur. This might mean that both types of bacteria prefer to cooperate rather than compete, and, consequently bacteria may benefit from joining polymicrobial biofilms. Hence, a pressing need existed for research directed toward understanding dynamics of such communities and which forces drive the coexistence of *E. coli* and uncommon bacteria in biofilm communities formed on the surface of urinary catheters.

The first results of this work, presented in Chapter 2, led to conclude that despite the probable non-pathogenic nature of *D. tsuruhatensis* and *A. xylosoxidans*, they were good biofilm producers on abiotic surfaces. When co-cultured with *E. coli*, their ability to form a biofilm appeared to be hampered by the presence of *E. coli*. In addition, a pre-colonization with uncommon bacteria seemed to promote adhesion of *E. coli*. These results proved that *E. coli* and uncommon bacteria are able to coexist within dual-species biofilm structures. However, it is important to note that for more mature stages of biofilm formation, competition might take place. Indeed, a higher fitness of *E. coli* was evident in later stages of biofilm formation. In part, this might be explained by the higher growth rate of *E. coli* in AUM associated with higher levels of siderophore production. However, the uncommon bacteria were not completely eliminated, and the coexistence seems to be preferred. To explain the benefits of *E. coli* and uncommon bacteria coexistence under conditions mimicking CAUTIs, two different scenarios were hypothesized: (1) the maintenance of uncommon bacteria, even at low densities, might be beneficial for *E. coli* if any environmentally challenging condition occurs; and (2) uncommon bacteria might be able to degrade certain components of plastics, and, the resulting products might be used by *E. coli*.

Another important part of the present thesis has involved the *in silico* design, development, optimization and validation of a multiplex FISH technique using LNA/2'OMe probes (LNA/2'OMe-FISH) (Chapter 3). When combined with CLSM, this new approach provides a clear 3D image of the biofilm organization, allowing a better understanding of biofilm dynamics and ecology. This spatial information provides some insights on the type of microbial interactions present in the biofilm. For instance, when microorganisms are in separate microcolonies or arranged in layers, this suggests that they may interact antagonistically; on the other hand, synergetic interactions are commonly associated with a co-aggregation organization or a layered-biofilm structure.

To perform LNA/2'OMe-FISH, a set of probes were designed and developed specifically for each bacterium. The probes worked well in a multiplex experiment and showed a good correlation between LNA/2'OMe-FISH and total cells and cultivability counts. These results confirmed that LNA/2'OMe-FISH is a robust technique, able to discriminate and locate the bacteria in conditions mimicking the CAUTIs without disturbing the biofilm structure. Taking advantage of LNA/2'OMe-FISH, the next stage consisted to evaluate the two hypothesis proposed above to better understand how the bacteria behave and interact with each other when in polymicrobial consortia formed in silicone coupons.

To know if a polymicrobial consortium has influence on the overall resistance of biofilm population, single- and dual-species biofilms were exposed to different antibiotic agents (Chapter 4). If a synergistic interaction mode is present, it might result in an increased antibiotic resistance. In fact, results showed that dual-species biofilms involving *E. coli* and uncommon bacteria were highly resistant to antibiotic agents typically used in the treatment of CAUTIs (ciprofloxacin, gentamycin, ampicillin and amoxicillin/clavulanic acid). An exception was observed for ciprofloxacin, where dual-species biofilms involving *E. coli* and *D. tsuruhatensis* were highly susceptible to this antibiotic agent. Also, the microbial relative composition revealed that, as expected, for gentamycin treatment, the most resistance bacteria (uncommon bacteria) predominated within the consortia. For ciprofloxacin-exposed dual-species biofilms, the microbial composition was balanced. Surprisingly, for ampicillin and amoxicillin/clavulanic acid treatment, *E. coli* (sensitive bacteria) was able to dominate within consortia. These results suggested that uncommon bacteria could protect the *E. coli* population, even

when its initial inoculum concentration was lowered. In fact, the function of bacteria within biofilm community is not related with its abundance.

Another important observation was the maintenance of the co-aggregation distribution of the dual-species biofilm after antibiotic treatment (*i.e.*, the bacteria remain closely associated). All these data seemed to demonstrate that *E. coli* and uncommon bacteria adjust their cell concentration in order to form well-organized and resistant biofilm structures. Here, a residual concentration of uncommon bacteria was found to be enough to contribute for *E. coli* survival. The specific mechanism of this shared protection is currently unknown; however, three theories were proposed: (1) transfer of genetic material from the uncommon bacteria to *E. coli*; (2) induction of a different physiological state in the susceptible species reducing antibiotic uptake; (3) degradation of the antibiotic in the biofilm matrix, through the action of the enzymes produced by uncommon bacteria. In this case, the cell concentration of uncommon bacteria might decrease because they have their metabolism directed to the secretion of, for instance,  $\beta$ -lactamases. On the other hand, *E. coli* (the susceptible cells) would benefit, without any energy cost, from the action of those enzymes in the microbial consortium.

In parallel to all these studies, considering the hydrodynamic shear forces inside of urinary catheters, it was also relevant to understand if the behavior of uncommon bacteria and *E. coli* is maintained under dynamic conditions (Chapter 5). The other studies (Chapters 2 and 4), reported in this thesis, were performed in 96-well plates and silicone coupons inserted in 6- or 24-well plates, because these platforms allowed studying several conditions simultaneously. However, when studying the microbial physiology of *E. coli* and *D. tsuruhatensis*, especially concerning nutritional requirements, a dynamic biofilm system mimicking the hydrodynamic conditions based on the shear strain rate found inside of urinary catheter ( $15 \text{ s}^{-1}$ ) was considered more suitable. For single-species biofilms the results corroborated the ones obtained in silicone coupons under static conditions (Chapter 4), but with lower values of cultivable cells and biofilm thickness. On the other hand, the dual-species biofilm behaved slightly differently. In fact, under dynamic conditions, *E. coli* only outnumbered *D. tsuruhatensis* up to 16 h. In addition, the dual-species biofilm thickness was also lower. However, as demonstrated under static conditions, the spatial distribution revealed that both bacteria might maintain synergistic interactions. The findings in Chapter 5 led to conclude that, under dynamic and static conditions, *E. coli* and uncommon bacteria, when occupying the same environment, tend to cooperate. In terms of nutritional

requirements, *D. tsuruhatensis* seemed opt to use citric acid instead uric acid, probably leaving uric acid available in the medium to be used by *E. coli*.

In conclusion, the observation presented in this thesis suggested that the surface of urinary catheter and urine is a favorable habitat for polymicrobial biofilms involving *E. coli* and uncommon bacteria. In these conditions, *E. coli* and uncommon bacteria, with a previous unrecognized role, appear to be able to persist and survive, adjusting their cell concentrations and metabolism to get maximum benefits from living together. The presence of uncommon bacteria showed to have a protective impact on the whole community. For instance, this could be crucial if any stress condition (e.g. use of antibiotic agents) occurs. Hence, this work allowed to identify possible contributions of uncommon bacteria to the development of CAUTIs (Figure 6.1).

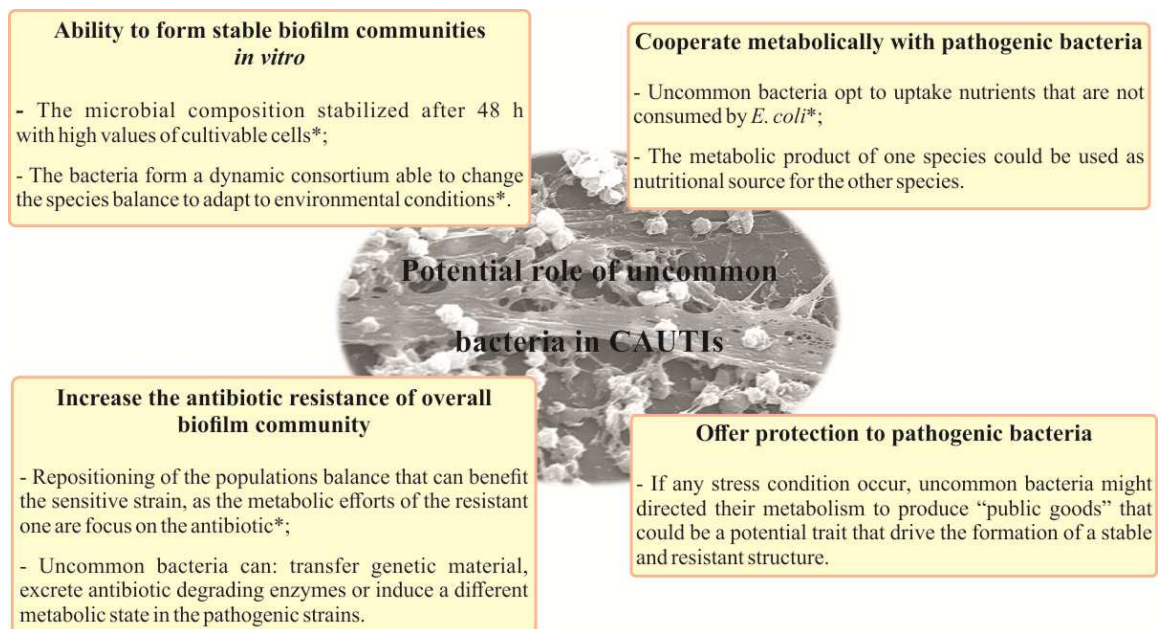


**Figure 6.1** - Potential contribution of uncommon bacteria to a more stable polymicrobial biofilms development in CAUTIs. The hypothesis marked with asterisk (\*) were observed in the present thesis.

Understanding how polymicrobial biofilm communities behave and how uncommon bacteria interact with conventional bacteria might have further implications in the control and treatment of CAUTIs, since bacterial behavior cannot be predicted from studies of single-species biofilms. In addition, it is also important to note that the role of uncommon bacteria is underestimated probably due to the absence of commercial media and kits to detect these bacteria in hospitals. However, the present

study shows that there are new lessons in polymicrobial infections that should be taken into consideration. In this way, if the clinicians know the biofilm composition, a more adequate therapy might be selected for an effective prevention or treatment of infections.

## 6.2 Future perspectives

Being the bacterium most commonly isolated from urine, it is not surprising that *E. coli* virulence and fitness factors are much more characterized than those of uncommon bacteria. Fimbrial adhesins, autotransporter proteins, capsular structures, flagella, exopolysaccharides, hemolysin or cytotoxic necrotizing factor 1, are all factors with reported influence on *E. coli* adhesion and biofilm formation/persistence<sup>1-4</sup>. For uncommon bacteria, there is a lack of information that needs to be filled. In this way, the assessment of gene expression pattern for uncommon bacteria biofilms would be the first step towards this knowledge. Simultaneously, the co-culture with *E. coli*, or other pathogenic bacteria, could help to identify potential virulence factors that drive the development of more resistant biofilm communities.

While the knowledge on uncommon bacteria is essential for this field evolve, the fact is that any *in vitro* behavior should be validated in *in vivo* to assure that host factor will not change the biological response. If the main goal is to establish some type of guideline on interactions/biofilms compositions and their potential clinical outcome, *in vivo* testing would be mandatory. This would be the bases for a new approach that would use urine/catheter microbiome to establish personalized clinical practices. For instance: should an asymptomatic infection be treated? Is this consortium indicative of a potential harmful biofilm? Which antibiotic should be prescribed for this particular consortium? A rat model of CAUTI, in which urinary catheter is inserted in the bladder, was validated to reproduce the host environment and mimic the host immune system<sup>5</sup>. The use of such a model could be the first step in this attempt to validate those biological responses. The ability of the catheter population to trigger an inflammatory reaction in the host or the time to blockage of the catheters (especially for consortia forming crystalline biofilms), would be important aspects to evaluate on this model.

For instance, crystalline biofilms formation is frequently responsible for the blockage of the urine flow inside of urinary catheters, since there are no effective procedures available for its control and prevention<sup>6-8</sup>. Hence, it would also be interesting to investigate if uncommon bacteria are able to produce crystalline biofilms or if they are able to interact with bacteria that are responsible for the crystalline biofilms such as *P. mirabilis*<sup>8,9</sup>. In fact, until the moment, only one study has reported the effect of other bacteria (*P. aeruginosa*, *E. coli*, *K. pneumoniae*, *M. morgani*, *E. cloacae*) on the rate at which *P. mirabilis* encrusts urinary catheters<sup>10</sup>. Again, an *in vivo* model would be important to provide evidences in whether a specific consortium would be effective on block/delay crystalline biofilm formation, or instead would promote that biofilm.

Other important factors that can model the biofilm consortium are urine properties (such as pH or glucose concentration) and exposure to antibiotic agents. For instance, it is well know that patients with diabetes have a risk factor for the development of UTIs/CAUTIs<sup>11-13</sup>. Hence, simulating the urine of a diabetic patient would give additional information about the behavior and role of uncommon bacteria when a diabetic patient is subject to a urinary catheter. Similarly, as shown in this thesis, the biofilm population can adjust its composition to the presence of antibiotics. For that reason, the study presented in Chapter 4 should be expanded to other antibiotics prescribed in the treatment of CAUTIs/UTIs (e.g. levofloxacin, nitrofurantoin, norfloxacin<sup>14</sup>) or combination of antibiotics (e.g. clarithromycin plus vancomycin, roxithromycin plus imipenem, trimethoprim plus sulfamethoxazole), natural antimicrobial compounds or even combination of antibiotics and natural compounds. In fact, the antibiotic combination has revealed the ability to eradicate the biofilms formed *in vitro* and *in vivo* conditions<sup>15,16</sup>. Alternatively to antibiotics, some natural substances from plants and marine species have showed antibacterial properties<sup>17,18</sup>. Several plant derived antimicrobials have been also tested in the treatment and control of patients with UTIs<sup>19,20</sup>. Also, natural compounds used in combination with less effective antibiotics have also demonstrated higher efficiency on biofilm inhibition<sup>21-23</sup>.

Another important study still to be done, and perhaps the most important, would involve the characterization of more complex consortia. While in here consortia of two species have been studied, those conditions are still a step away from the real natural composition of CAUTI biofilms. Hola and colleagues have shown that most of the catheters are infected by three or more microorganisms (only 12.5% showed monomicrobial infection)<sup>24</sup>. In that sense, it would be also interesting to expand this



study into other combinations of pathogenic bacteria that are frequently found in catheterized patients (e.g. *K. pneumoniae*, *P. aeruginosa*, *E. faecalis* and *P. mirabilis*<sup>25</sup>). Other uncommon bacteria (Figure 1.2 - Chapter 1) can also be studied in this context in order to start understanding the real role of other microorganisms over pathogenesis of CAUTIs.

The use of clinically relevant species combinations found in catheterized patients would improve the potential impact of the results obtained; but it is important to bear in mind that traditional culture techniques can underestimate the diversity of the populations<sup>26, 27</sup> and, thus, culture-independent approaches are important to accurately study biofilms diversity. Metagenomic approaches, based on 16S sequencing, could be applied to real clinical biofilms to better characterize natural consortia. Then, those compositions could be simulated *in vitro* and *in vitro* to evaluate the clinical significant of each combination. For an accurate evaluation, the development of expedite alternative technique allowing an *in situ* visualization and a culture-independent multiplex approach, would be essential. A combinatorial labeling methodology based on FISH has been developed to allow the discrimination of up to 15 microorganisms simultaneously, using a combination of 6 fluorochromes<sup>28</sup>. While this technology is still taking the first steps, the number of fluorochromes can be easily increased to discrimination even a higher number of microorganism/characteristics. Its application to biofilms would certainly revolutionize microbial ecology studies.

All this information together highlights the need for: (1) *in vivo* models reproducing the consortia and conditions found in CAUTI to validate the data obtained; (2) additional studies with more complex consortia and conditions; (3) characterization techniques that can accurately estimate the microbial diversity. Altogether, these studies could constitute the basis for a new strategy in the control and treatment of CAUTIs that uses the knowledge on the microbiome of each patient for a personalized therapy selection.

### 6.3 References

1. **V. Hancock, P. Klemm.** Global gene expression profiling of asymptomatic bacteriuria *Escherichia coli* during biofilm growth in human urine. *Infect Immun* **75**, 966-976 (2007).
2. **V. Roos, P. Klemm.** Global gene expression profiling of the asymptomatic bacteriuria *Escherichia coli* strain 83972 in the human urinary tract. *Infect Immun* **74**, 3565-3575 (2006).
3. **E.C. Hagan, A.L. Lloyd, D.A. Rasko, G.J. Faerber, H.L. Mobley.** *Escherichia coli* global gene expression in urine from women with urinary tract infection. *PLoS Pathog* **6**, e1001187 (2010).
4. **A. Reisner, M. Maierl, M. Jorger, R. Krause, D. Berger, A. Haid, D. Tesic, E.L. Zechner.** Type 1 fimbriae contribute to catheter-associated urinary tract infections caused by *Escherichia coli*. *J Bacteriol* **196**, 931-939 (2014).
5. **H.Y. Kim, H.-S. Choe, D.S. Lee, J.M. Yoo, S.-J. Lee.** A novel rat model of catheter-associated urinary tract infection. *Int Urol Nephrol* **47**, 1259-1263 (2015).
6. **P. Tenke, B. Kovacs, M. Jäckel, E. Nagy.** The role of biofilm infection in urology. *World J Urol* **24**, 13-20 (2006).
7. **J. Hatt, P. Rather** in *Bacterial Biofilms*. (ed. T. Romeo) 163-192 (Springer Berlin Heidelberg, Heidelberg; 2008).
8. **D.J. Stickler.** Bacterial biofilms in patients with indwelling urinary catheters. *Nature clinical practice urology* **5**, 598-608 (2008).
9. **D. Stickler, S. Morgan.** Observations on the development of the crystalline bacterial biofilms that encrust and block Foley catheters. *J Hosp Infect* **69**, 350-360 (2008).
10. **S.M. Macleod, D.J. Stickler.** Species interactions in mixed-community crystalline biofilms on urinary catheters. *J Med Microbiol* **56**, 1549-1557 (2007).
11. **E.J. Boyko, S.D. Fihn, D. Scholes, L. Abraham, B. Monsey.** Risk of urinary tract infection and asymptomatic bacteriuria among diabetic and nondiabetic postmenopausal women. *Am J Epidemiol* **161**, 557-564 (2005).
12. **B.R. Shah, J.E. Hux.** Quantifying the risk of infectious diseases for people with diabetes. *Diabetes care* **26**, 510-513 (2003).
13. **D.G. Maki, P.A. Tambyah.** Engineering out the risk for infection with urinary catheters. *Emerg Infect Dis* **7**, 342 (2001).
14. **K. Dellimore, A. Helyer, S. Franklin.** A scoping review of important urinary catheter induced complications. *J Mater Sci Mater Med* **24**, 1825-1835 (2013).
15. **S. Fujimura, T. Sato, T. Kikuchi, J. Zaini, K. Gomi, A. Watanabe.** Efficacy of clarithromycin plus vancomycin in mice with implant-related infection caused by biofilm-forming *Staphylococcus aureus*. *J Orthop Sci* **14**, 658-661 (2009).
16. **M. Tré-Hardy, F. Vanderbist, H. Traore, M.J. Devleeschouwer.** *In vitro* activity of antibiotic combinations against *Pseudomonas aeruginosa* biofilm and planktonic cultures. *Int J Antimicrob Agents* **31**, 329-336 (2008).
17. **M. Salta, J.A. Wharton, S.P. Dennington, P. Stoodley, K.R. Stokes.** Anti-biofilm performance of three natural products against initial bacterial attachment. *Int J Mol Sci* **14**, 21757-21780 (2013).
18. **S. Gibbons.** Anti-staphylococcal plant natural products. *Nat Prod Rep* **21**, 263-277 (2004).
19. **F.R. Pérez-López, J. Haya, P. Chedraui.** *Vaccinium macrocarpon*: an interesting option for women with recurrent urinary tract infections and other health benefits. *J Obstet Gynaecol Res* **35**, 630-639 (2009).
20. **D.T. Bailey, C. Dalton, F.J. Daugherty, M.S. Tempesta.** Can a concentrated cranberry extract prevent recurrent urinary tract infections in women? A pilot study. *Phytomedicine* **14**, 237-241 (2007).

21. **V.B. Maisuria, Z. Hosseinidoust, N. Tufenkji.** Polyphenolic extract from maple syrup potentiates antibiotic susceptibility and reduces biofilm formation of pathogenic bacteria. *Appl Environ Microbiol* **81**, 3782-3792 (2015).
22. **N.C. Cady, K.A. McKean, J. Behnke, R. Kubec, A.P. Mosier, S.H. Kasper, D.S. Burz, R.A. Musah.** Inhibition of biofilm formation, quorum sensing and infection in *Pseudomonas aeruginosa* by natural products-inspired organosulfur compounds. *PLoS One* **7**, e38492 (2012).
23. **M.J. Søre, T. Møller, M. Dufva, K. Holmstrøm.** Effect of combinations of antibiotics and gallates on biofilm formation in *Staphylococcus aureus*. *Lett Drug Des Discov* **7**, 160-164 (2010).
24. **V. Hola, F. Ruzicka, M. Horka.** Microbial diversity in biofilm infections of the urinary tract with the use of sonication techniques. *FEMS Immunol Med Microbiol* **59**, 525-528 (2010).
25. **European Centre for Disease Prevention and Control. Antimicrobial resistance surveillance in Europe 2014.** Annual Report of the European Antimicrobial Resistance Surveillance Network (EARS-Net). (2015).
26. **O. Aspevall, B. Osterman, R. Dittmer, L. Sten, E. Lindback, U. Forsum.** Performance of four chromogenic urine culture media after one or two days of incubation compared with reference media. *J Clin Microbiol* **40**, 1500-1503 (2002).
27. **H.A. D'Souza, M. Campbell, E.J. Baron.** Practical bench comparison of BBL CHROMagar Orientation and standard two-plate media for urine cultures. *J Clin Microbiol* **42**, 60-64 (2004).
28. **A.M. Valm, J.L. Mark Welch, G.G. Borisy.** CLASI-FISH: principles of combinatorial labeling and spectral imaging. *Syst Appl Microbiol* **35**, 496-502 (2012).

